All-India Survey of Photovoltaic Module Reliability: 2014

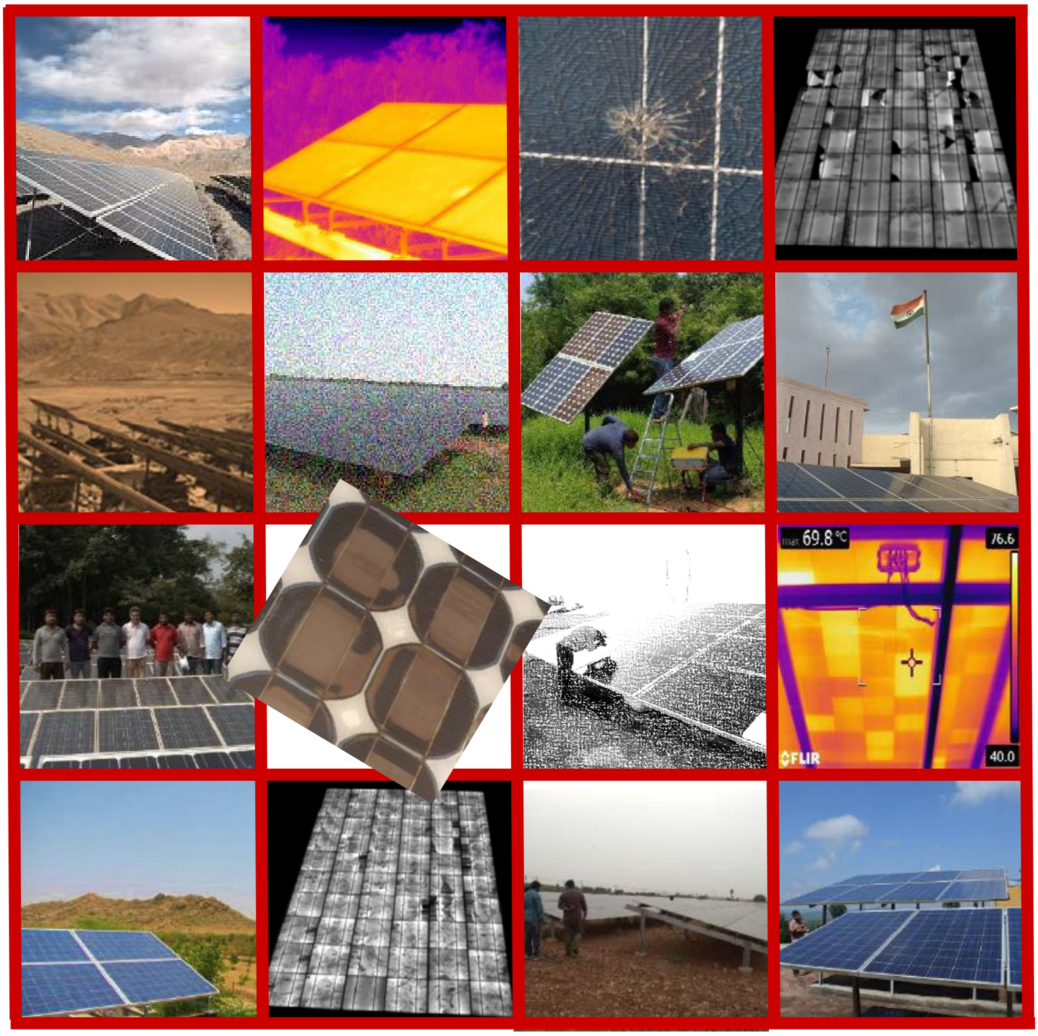

National Centre for Photovoltaic Research and Education (NCPRE), IIT Bombay

&

National Institute of Solar Energy (NISE), Gurgaon

NCPRE

NISE
National Institute of Solar Energy

September-November 2014

All-India Survey of Photovoltaic Module Reliability: 2014

Rajiv Dubey, Shashwata Chattopadhyay, Vivek Kuthanazhi,
Jim John, Firoz Ansari, S. Rambabu, B. M. Arora,
Anil Kottantharayil, K. L. Narasimhan and Juzer Vasi

National Centre for Photovoltaic Research and Education
Indian Institute of Technology Bombay
Powai, Mumbai 400076, India

and

Birinchi Bora, Yogesh Kumar Singh, Kamlesh Yadav,
Manander Banger, Ramayan Singh and O. S. Sastry

National Institute of Solar Energy
Gwalpahari, Gurgaon, Haryana 122003, India

Survey in September-November 2014
(plus a few sites in September 2015)

Report dated March 2016

rev. 2

Contents

Acknowledgments

The 2014 All-India Survey of Photovoltaic Module Reliability is the second in the series of such surveys conducted to assess the reliability and durability of photovoltaic (PV) modules in different parts of India. It was conducted between September and November 2014, with some isolated visits in 2015. The suggestion that such surveys be conducted came from a meeting in March 2013 of the "High Powered Task Force under JNNSM for Solar Photovoltaics". As in the case of the 2013 Survey, the 2014 Survey was also conducted jointly by the National Centre for Photovoltaic Research and Education (NCPRE) at the Indian Institute of Technology Bombay (IITB) and the National Institute of Solar Energy (NISE).

NCPRE and NISE would like to thank the various participants in the 2014 survey at various levels (PV system owners, state Renewable Energy nodal agencies, private EPC contractors and local installers) who have helped us in multiple ways to bring the survey to fruition. Their names and organizations are not individually mentioned in order to preserve anonymity of the sites.

Thanks are due to many people at NCPRE and NISE who have helped in making the Survey possible. We thank Dr. Praveen Saxena and Dr. Rajesh Kumar of NISE and Prof. B. G. Fernandes, Prof. Chetan Singh Solanki and Mr. Vaman Kuber of NCPRE for their support of the survey. We also thank Ms. Smita Bhattacharjee, Dr. Diksha Makwani, Ms. Mallika Moolya, Mr. Vikrant Sharma, Mr. Rahul Rawat, Mr. Mithlesh Kumar, Ms. Renu, Ms. Rashmi Singh and Ms. Supriya Rai for logistic and other support. We thank Dr. K. Chalapathi, Ms. Namrata Pandey and Dr. Diksha Makwani for help in proof reading and preparation of the report. The team also wishes to thank Mr. Ajit Singh who made the arrangements for the vehicles for the cross-country travel, and the drivers Mr. Raj Kumar and Mr. Ram Pati Gupta, who drove the 18,000 plus km safely in sometimes difficult terrain.

We are also thankful to several persons who have given advice and feedback on the Survey. Mr. Hemant Lamba gave the initial suggestion at the Task Force meeting which launched the surveys, and has continued to be actively involved over the years. Thanks are also due to Dr. S. P. Gonchaudhuri and Dr. B. Bhargava for their support and encouragement. We are also thankful to Dr. Sarah Kurtz and Dr. Lawrence Kazmerski of the National Renewable Energy Laboratory (NREL) for discussions held with them on several occasions, and Dr. G. Tamizhmani of the Arizona State University (ASU) and Dr. Dirk Jordan (NREL) for their inputs. Preliminary results of the survey were presented at the Workshop on *PV Module Reliability in Hot Climates* held at IIT Bombay in October 2015, and we received valuable inputs from many participants.

Finally, both NCPRE and NISE would like to thank the Ministry of New and Renewable Energy (MNRE), Government of India, for funding which enabled this survey to be undertaken.

Executive Summary

The All-India PV Survey of Photovoltaic Module Reliability: 2014 is the second in a series of such surveys conducted to assess the health, reliability and durability of photovoltaic (PV) modules put up in different parts of India. It was conducted between September and November 2014 (with some isolated measurements made in 2015), and followed the first survey which was conducted during May to June 2013. The suggestion that such surveys be conducted came from a meeting in March 2013 of the "High Powered Task Force under JNNSM for Solar Photovoltaics". As in the case with the 2013 Survey, the 2014 Survey was also conducted jointly by the National Centre for Photovoltaic Research and Education (NCPRE) at the Indian Institute of Technology Bombay (IITB) and the National Institute of Solar Energy (NISE).

The 2014 Survey was a much-expanded version of the 2013 Survey. A total of 1148 modules were checked at 51 sites in all the 6 climatic zones of India. The age of the modules varied from 1 year to more than 25 years, and 6 different technology types were represented. The sites visited are shown in Fig. 1. The types of inspection undertaken in 2014 were also more extensive than in 2013, and included: visual inspection, measurement of *I-V* characteristics under light and dark conditions, infra-red (IR) thermography under light and dark conditions, electroluminescence (EL) imaging, interconnect integrity test, insulation resistance test, measurement of irradiance and ambient and module temperatures, and a "socio-economic" survey.

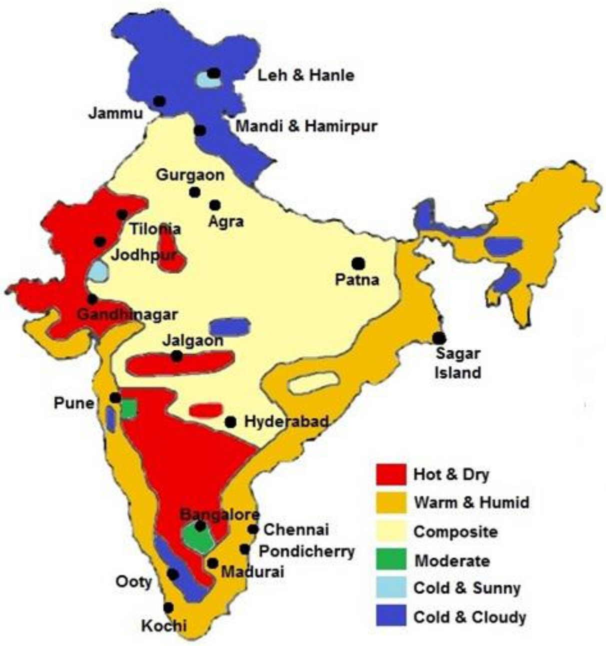

Fig. 1: Climatic zones of India and sites visited during the 2014 All-India Survey

The distribution of the 1148 modules surveyed in the 51 sites was as follows. Of the 51 sites, 6 sites containing 146 modules had 'large' installations of size greater than 100 kW, and 45 sites containing 1002 modules fell in the 'small/medium' category of installations of size less than 100 kW. The distribution of modules in the various climatic zones was: Hot & Dry – 194, Warm & Humid – 333, Composite – 308, Moderate – 135, Cold & Sunny – 56, and Cold & Cloudy – 122. The technology distribution was: mono c-Si – 431, multi c-Si – 552, a-Si – 74, CdTe – 72, CIGS – 12, and HIT – 7. The age distribution of the modules was: 0-5 years – 757, 5-10 years – 83, 10-20 years – 268, and 20-30 years – 40. At each site, about 15 to 35 modules were typically taken up for the survey.

One of the most notable outcomes of the survey was that there was a *wide distribution* in the performance of the modules. Some modules (221 in number) showed degradation rates of more than 6%/year, and these modules, termed 'outliers', were not taken up for further analysis as there appeared to be serious quality and other extraneous issues, such as over-rating, with them. Further, 161 modules were measured under low irradiance conditions (less than 500 W/m^2), and these were also not taken further for detailed study. Of the remaining 766 modules, the annual degradation rate, that is, the rate at which the output power P_{max} decreases per year, was measured to vary over a large range, from less than 0.6%/year to more than 4%/year, as shown in Fig. 2(a). An accepted international benchmark is about 0.8 to 1.0%/year.

As can be seen, many of the modules are performing well with good degradation rates, while others are not. To understand and analyze this wide variation among the 766 modules, we have divided the sites surveyed into two categories: Group X sites and Group Y sites. The criterion for the division is that sites whose modules show an *average* degradation rate of less than 2%/year were considered to be 'good' sites, and labelled as Group X; and sites whose modules show an *average* degradation rate of more than 2%/year were considered to be 'problematic' sites, and labelled as Group Y. The 2% criterion was chosen somewhat arbitrarily, but guided by ~ 2% average value seen (Fig. 2(a)) for all modules. This segregation is purely empirical and unbiased, but, as will be seen later, leads to a good appreciation of the reasons for the wide variance. We emphasize that the 2% criterion is based on the *site* average, (since performance appears to depend on both intrinsic module quality and installation procedures), and individual modules in Group X sites may show degradation rates of more than 2%/year, just as individual modules in Group Y sites may show degradation rates of less than 2%/year. The histograms for modules in the Group X and Group Y sites are shown in Figs. 2(b) and 2(c) respectively. The average degradation rate for modules in Group X sites was found to be 1.33%/year, which is quite good, though still somewhat higher than the internationally reported degradation rates. The average degradation rate for modules in Group Y modules was 2.73%/year. We will sometimes refer to modules in Group X sites as 'Group X modules', and similarly for Group Y.

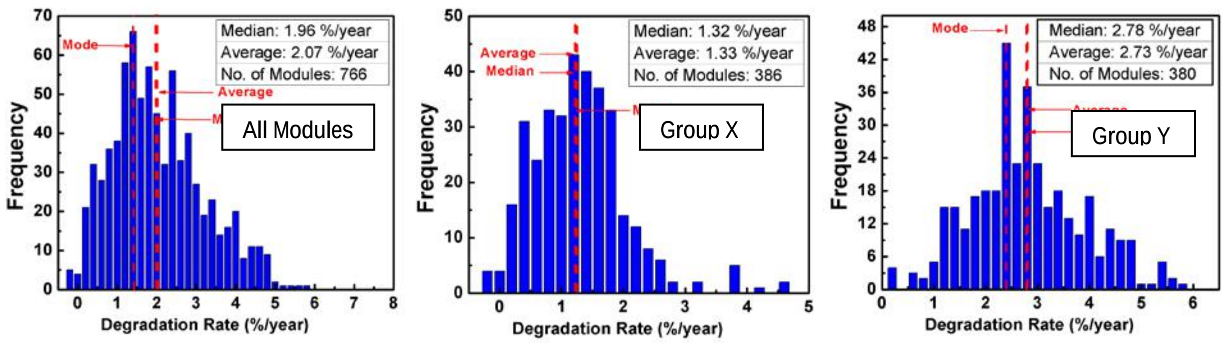

(a) (b) (c)

Fig. 2: Histogram of P_{max} degradation rate of (a) All modules (b) Modules in Group X sites (c) Modules in Group Y sites

The histograms shown in Fig. 2 refer to all the 766 modules which have been analyzed. To see how the large power plants perform, we have looked at the breakup of degradation rates in terms of *size* of the installation. It is comforting to note that modules in large (> 100 kW) sites perform significantly better than modules in small/medium sites, and, as seen in Fig. 3, show an average degradation rate of 0.97%/year. Furthermore, all the large sites fall in the Group X category, indicating good performance. However, the implications for reliability of small/medium sites which are likely to come up on rooftops needs to be examined. Please note that the numbers at the top in parentheses indicate the number of modules in that category. Open and filled symbols differentiate the data on the basis of the age of the module: less than 5 years (open) and more than 5 years (filled). The red horizontal bar represents the average or mean (the value being indicated in brackets). The error bars due to nameplate error (red) and measurement/translation (green) and 95% confidence interval (diamond) are also shown in the plot.

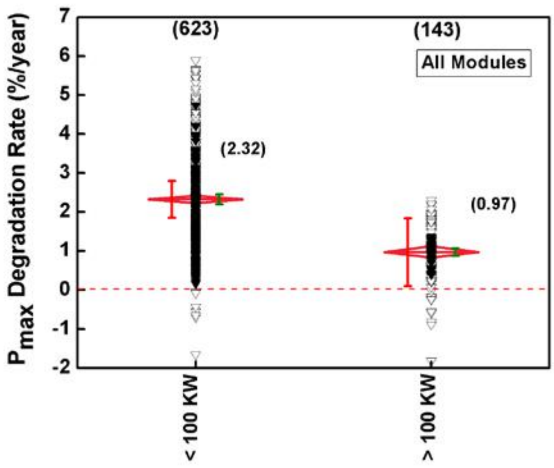

Fig. 3: Effect of installation size on P_{max} degradation for 'All' (Group X + Group Y) modules

The climatic variation is analyzed for modules falling in Group X. This is done since these are the 'good' sites, where extraneous effects are presumably not playing a role, and therefore the effect of the climate itself is being correctly captured. The degradation rates for the Group X modules is shown in Fig. 4. It can be seen that the Warm & Humid climate is worst (1.53%/year), followed by Hot & Dry (1.32%/year). Modules in the Cold & Sunny zone (0.8%/year) perform very well.

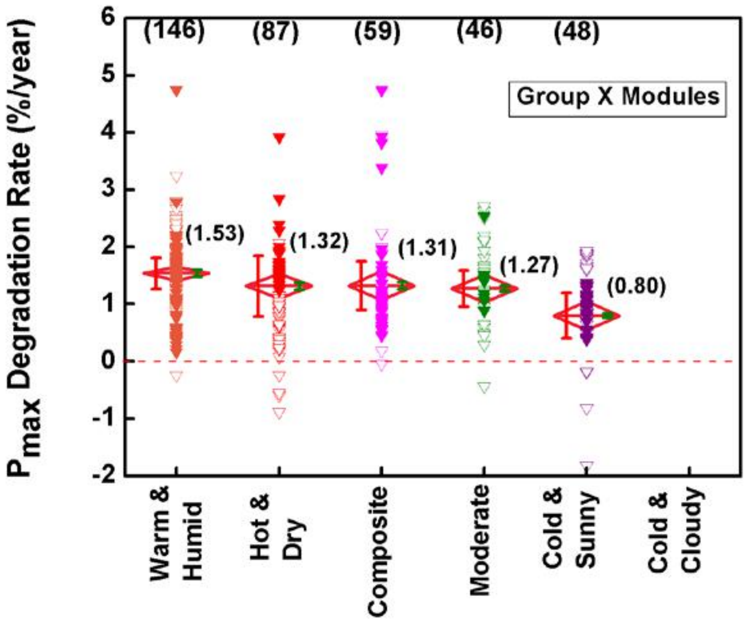

Fig. 4: Comparison of P_{max} degradation rate for Group X modules in different climatic zones. The numbers on top represent the total number of modules in that zone, and the horizontal red bar is the average degradation rate in that zone. Error bars due to nameplate and measurement error are also shown.

The technology-wise distribution of degradation rates for Group X modules shows that c-Si modules degrade somewhat faster (~ 1.4%/year) than thin films (~1.1%/year). This is not unexpected as many thin films like

CdTe are known to have lower degradation rates. However, it should be noted that the number of thin-film modules was small (111), so this should not be taken to be a conclusive finding.

A surprising observation is that young modules (< 5 years) show a higher degradation rate than old modules (> 5 years old). This may reflect the higher initial degradation rate seen for many technologies. However, taken together with the fact that if we consider *only* Group X modules, where young modules degrade slower than old modules, the result also suggests that newer installations have poorer quality of modules and/or installation practices. For the young modules, the main contributor for P_{max} degradation is the fill factor (FF) which is often related to poor quality and cracks, whereas for the old modules, it is short circuit current (I_{sc}) degradation, symptomatic of encapsulant discoloration and delamination, expected to occur with aging.

Another observation which calls for serious consideration relates to the relative performance of roof-mounted versus ground-mounted modules. To make a fair comparison, roof-mounted and ground-mounted modules of only the small/medium size (< 100 kW) were compared, and these show annual degradation rates of 2.76%/year and 1.82 %/year respectively. Infrared (IR) measurements show that modules installed on rooftops, especially in the hot zones, are running hotter than modules installed on the ground. This means special attention is needed for the design and deployment of PV systems for India's 40 GW rooftop target.

We have performed a detailed study of the visual degradation seen on modules, using an enhanced NREL visual checklist. Some of the key results are as follows. Encapsulant discoloration (yellowing or browning), shown in Fig. 5(a), has been observed in all climatic zones and tends to occur in most modules which are in operation for more than 10 years. Modules in 'Hot' climates (comprising the Hot & Dry, Warm & Humid and Composite zones) are seen to discolor faster than modules in 'Non-Hot' climates (comprising the Moderate, Cold & Sunny and Cold & Cloudy zones). Among young modules, discoloration is twice as common in Group Y modules as compared to the Group X modules, which raises questions about the quality of the materials used in the Group Y modules, and is one of the reasons for the poor performance of Group Y modules. Delamination (Fig. 5(b)) is seen to occur most frequently in Warm & Humid climates, and again is more widespread among Group Y modules compared with Group X modules. Snail trails, shown in Fig. 5(c), are seen mainly in humid climates, and many young modules (especially in Group Y modules) show snail trails. Metallization discoloration and corrosion (Fig. 5(d)) are seen in all climatic zones, but the severity is highest in the Warm & Humid zone. Backsheet degradation, including chalking, has been seen in both old and young modules. The latter is surprising, and again points to material quality issues.

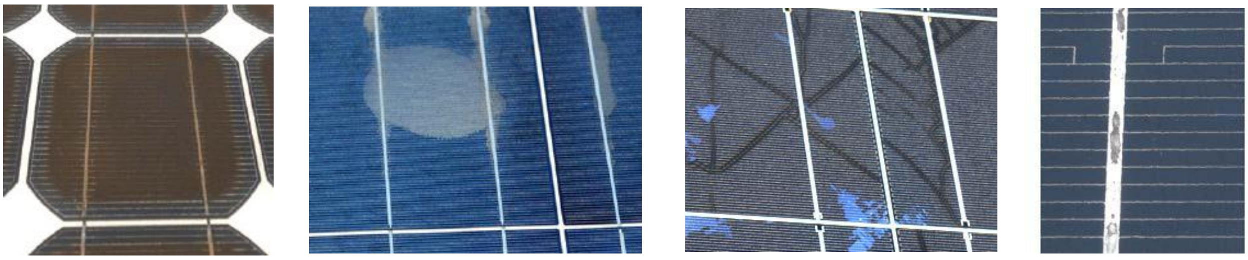

(a) (b) (c) (d)

Fig. 5: (a) Encapsulant browning (b) Delamination (c) Snail trails (d) Metallization discoloration

We have developed a 'Visual Degradation Index' (VDI) which allows us to quantify the amount of visual degradation seen on the basis of three major effects: encapsulant discoloration, delamination, and metallization discoloration. There is a good correlation between the power degradation of a module and its VDI value, as seen in Fig. 6. This is useful, because a visual inspection of the module and a quick calculation of its VDI would allow an estimate of its power loss. Note that in Fig. 6, the y-axis shows the *total* percentage power loss suffered by the module since installation, and not the annual power degradation rate.

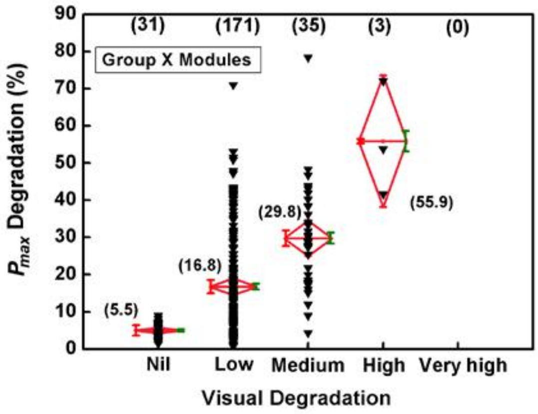

Fig. 6: Plot of total output power degradation versus extent of visual degradation (VDI category)

Using a special daylight electroluminescence (EL) technique developed for the 2014 Survey, EL images of several modules were taken in the field. These images could detect micro-cracks in the modules, and it was seen that there were many more cracks in Group Y modules compared to Group X modules, and also in young modules as compared to old modules. Further, many of the cracks were near the periphery of the modules. These observations lead to the conclusion that one of the problems afflicting the Group Y sites is improper transportation to sites and/or installation at the site. This seems to be especially true for young sites where the pressure of deadlines may have resulted in less-than-ideal procedures being adopted. Cracks in the modules cause enhanced power degradation. Fig. 7(a) shows the EL image of a Group Y module, and Fig. 7(b) shows the correlation between number of cracks and power degradation, where the young/old distinction can also be clearly seen. The field EL imaging also showed that most non-framing type of snail trails are associated with micro-cracks which may not always be visible with the naked eye, as shown in Figs. 7(c) and 7(d). We believe this was the first ever widespread study of module performance in the field, coupled with field-based EL.

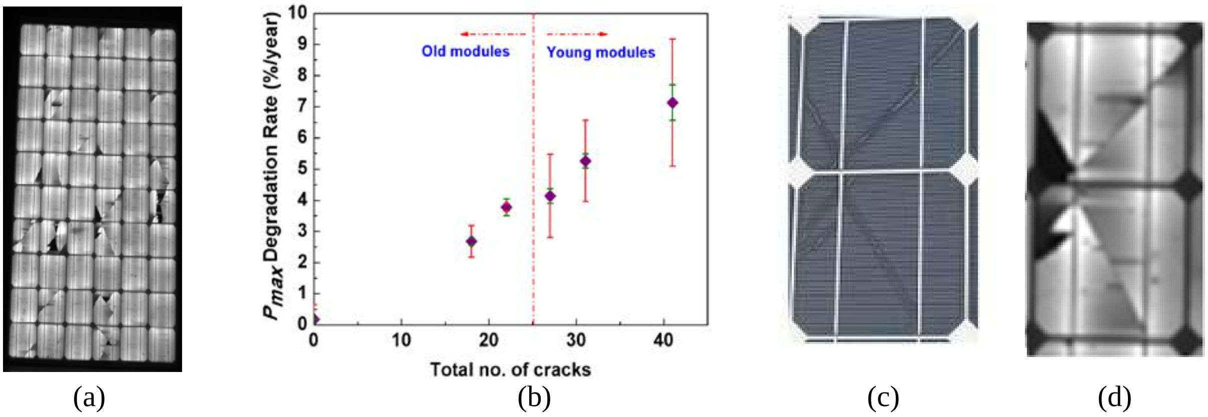

Fig. 7: (a) EL of a Group Y module showing many cracks (b) Correlation of power degradation with number of cracks (c) Visible photograph of snail trail (d) corresponding EL image showing cracks.

Modules were also characterized using infra-red (IR) thermography, which shows the temperature distribution over the module, and is particularly useful for identifying hot spots in the module, which can cause significant long-term degradation. Fig. 8 shows a typical IR image and its temperature histogram. Table 1 shows that hot cells in Hot zones run much hotter than hot cells in Non-Hot zones, with a concomitant increase in power degradation rates (2.02%/year versus 1.7%/year). This can have important repercussions for modules operating in the Hot climates of India, where much of the PV installation is likely to take place.

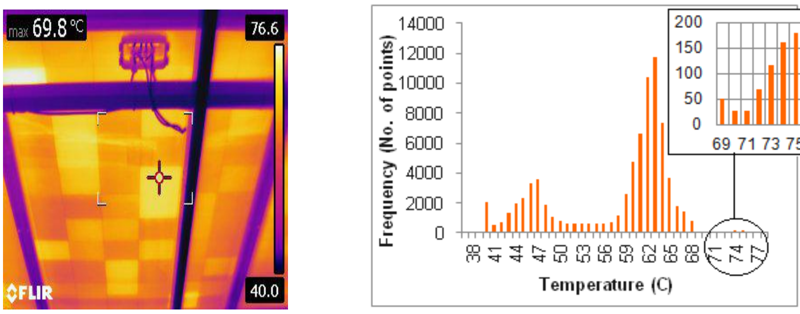

(a) (b)

Fig. 8: (a) IR image of a module in Warm & Humid climate (b) its temperature histogram. The highest temperature in this module is 75°C (shown in inset), and its representative (modal) temperature is 63°C.

Table 1: Effect of hot cells on power degradation rate of PV modules in Hot and Non-Hot zones

Parameter (average of many samples)	**Hot zone**		**Non-Hot zone**	
	without Hot Cells	**with Hot Cells**	**without Hot Cells**	**with Hot Cells**
Power degradation rate (%/year)	1.39	2.02	1.39	1.70
Normalized *module* ΔT (ºC)	6.8	24.7	5.7	18.9
Normalized maximum cell temperature (ºC)	68.8	86.1	50.3	58.6
No. of Samples	10	18	14	17

The 2014 Survey also undertook measurements of dark *I-V* characteristics, dark IR, insulation resistance and interconnect breakage occurrence. The dark *I-V* measurements yield the ideality factor *n* of the diode in the forward bias region. It was seen that *n*, which can be related to series resistance and/or cell quality, increases with age, and shows more degradation in Hot than Non-Hot climates. Further, increasing (worsening) values of *n* correlate well with power loss. The dry insulation resistance test showed that most modules (95%) pass the test, and all (100%) in the large-size category pass. However, there are more young Group Y modules failing the test than other modules. This result again supports the conclusion that Group Y modules have various quality issues. The interconnect breakage (measured by a cell line tester and shown in Fig 9(a)) is most prevalent in the Hot zones, and especially the Warm & Humid zones. It correlates well with increase in series resistance of the module and consequent loss in power output, as shown in Figs. 9(b) and 9(c).

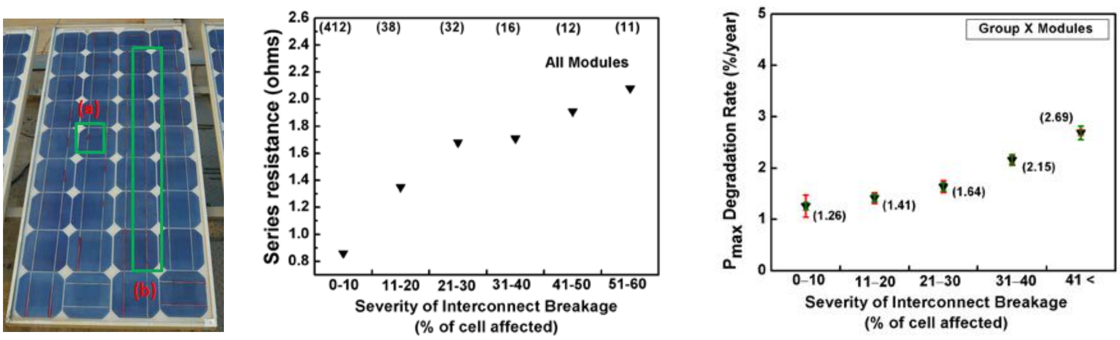

(a) (b) (c)

Fig. 9: (a) Module showing point **(a)** and line **(b)** breakage (b) Series resistance degradation versus severity of interconnect breakage (c) power degradation versus severity of interconnect breakage.

An important question which arises is whether it is possible to identify the *risk* associated with various defects or degradation modes in different climatic zones. If so, it would be possible to check for those defects more regularly, and thus pre-empt both performance and safety failures. The method of assigning a Risk Priority Number (RPN) allows this to be done. The RPN depends on the severity of the defect, its frequency of occurrence and how easily detectable it is. The RPN methodology has been used for analyzing the field data collected for the modules during the survey. Some results of the RPN analysis are presented in Fig. 10, which shows the RPN versus performance failure modes for young modules in different climatic zones (higher numbers indicate more risky). It can be seen that discoloration and solder bond failure have the highest RPNs. For safety failure modes, backsheet degradation and loose junction boxes have the highest RPN in all climatic zones, since both of these defects can potentially give electric shocks to operating and maintenance personnel.

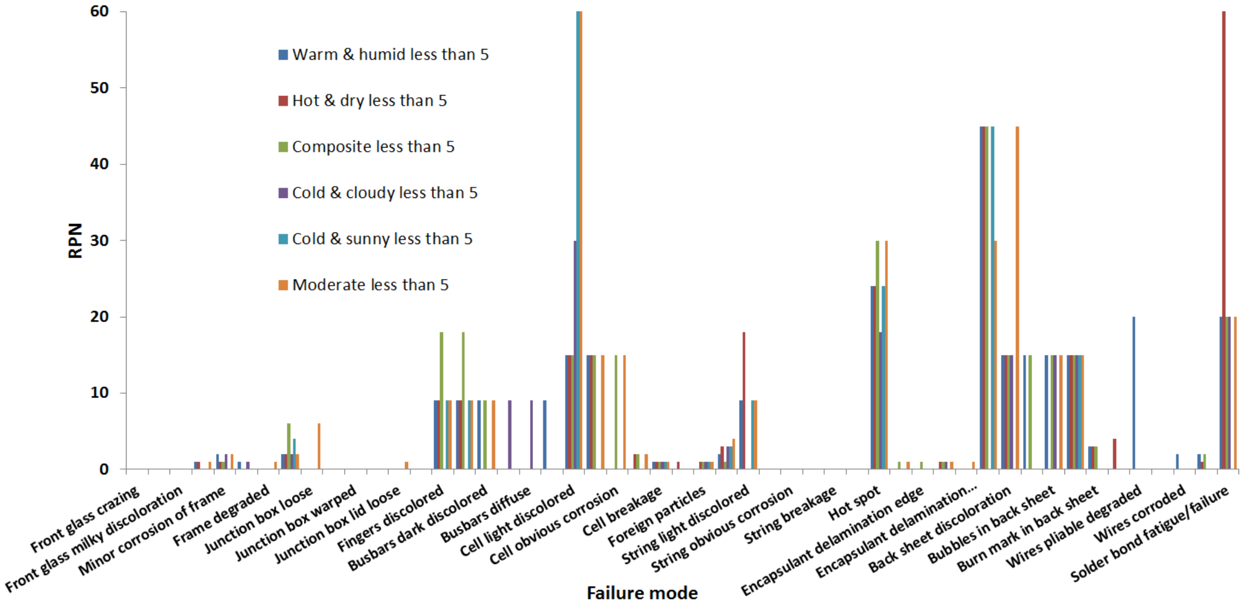

Fig. 10: RPN versus performance failure modes for young modules (less than 5 year outdoor exposure) for different climatic zones

During the Survey, we also performed a 'socio-economic' appraisal which assessed various non-technical aspects of the installation, such as ownership model, financial model, and motivation in installing the PV system. The Survey team also assessed what kind of technicians were employed for installation and maintenance, frequency of maintenance, frequency and type of cleaning, etc. Among the results obtained it was seen that, generally speaking, privately-owned installations are not as well installed as those owned by government or semi-government organizations, but they are usually much better maintained and cared for. We have been able to correlate the performance of the system, in terms of power degradation rates, with care of installation, frequency of cleaning, and type of technicians used. Fig. 11 shows how the degradation rates vary with cleaning cycles and whether the modules have been properly installed (shaded or shade-free). It can be seen that regular cleaning cycles improve the long-term performance (besides the obvious improvement which would be seen in immediate power output). Similarly, shading not only incurs the obvious present loss of power, but also has long-term degradation repercussions.

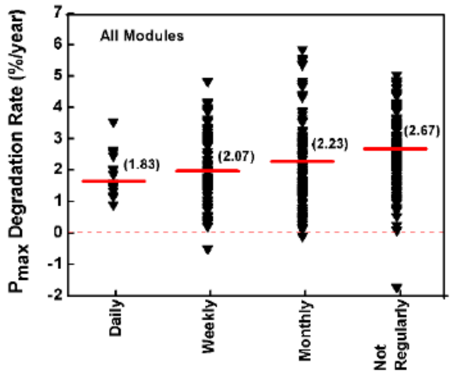

(a)

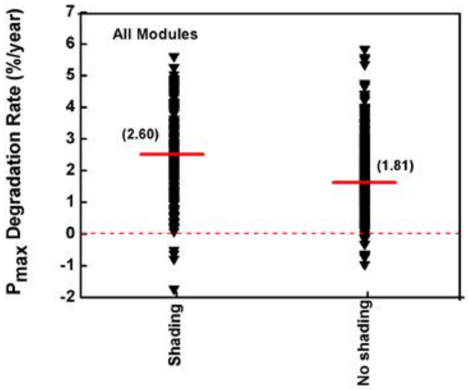

(b)

Fig. 11: (a) P_{max} degradation rate with frequency of cleaning cycle (b) P_{max} degradation rate with module shading indicating care of installation

A broad picture on the health and reliability of PV modules in the country has emerged from the 2014 All-India Survey. One of the important results is that there is wide variability in the quality and degradation rates. Many modules show excellent performance, but there are many others showing high degradation rates. Modules in Group X sites show reasonably good performance with an average degradation rate of 1.33%/year. Modules in Group Y sites show an average degradation rate of 2.73%/year, which is cause for concern. If one looks at only large-size (> 100 kW) installations, the degradation seen is < 1%/year, which is good news, since it shows that most large power plants are performing quite well. All large-size systems are Group X sites. Further, it is seen that ground-mounted systems perform better than roof-mounted systems. This means that due consideration must be given to the long-term durability of small/medium roof-top systems which will be needed for India's 40 GW rooftop solar target. Another important point which emerges is that many of the new installations and especially those in Group Y sites suffer from material quality issues, including encapsulant and backsheet quality, as well as transport/installation procedures which show up as cracks, scratches, etc. These problems have perhaps been caused by the aggressive pricing and deadlines associated with solar PV projects in recent years.

Based on the field observations and results, some high-level recommendations which can be made are the following:

- Due diligence should be exercised while selecting and procuring modules. This may include verifying the antecedents of the manufacturer, and independent checks on the quality of the module(s). Although most modules available in the market carry the IEC certification, it should be noted that the IEC certification is really a certification of the manufacturing process, and does not guarantee that the module will perform adequately through its intended life.
- Materials used in modules are important. EVA and backsheet particularly can be of different qualities, and should be specified by the manufacturer in the datasheet, and also in the tender for procurement.
- An independent audit of modules and installations by a third party is strongly recommended. This may include detailed testing of randomly selected modules before as well as after shipment.
- Some cases of 'over-rating' of modules have been detected during the survey, especially in small/medium sites. Owners and installers should be vigilant about this malpractice.
- Module manufacturers and installers should place more emphasis on proper packaging and handling of the modules during transportation since improper handling can induce cracks in the solar cells and lead to long-term degradation.
- Installation procedures and protocols are important, and standard procedures as recommended should be strictly followed.

- It is recommended that a field-based electroluminescence (EL) study be performed after receiving the modules at site and after installation to reveal micro-cracks which may have been caused during the transport and installation phases.
- It has been noted that the ‘Hot’ climates present a harsh operating environment for PV modules. An intensive study of degradation phenomena in hot climates, which has not been emphasized sufficiently by the PV community so far, is needed. This is particularly important for India, since much of the 100 GW is expected to come up in the resource-rich Hot climatic zones.
- The IEC certification protocols (eg. 61215), and other standards, which are currently being updated, need to take into account the hot climate phenomena, and develop more aggressive test protocols going to higher temperatures. Involvement of India-based R&D organizations and industry in PVQAT (International PV Quality Assurance Task Force) is highly recommended.
- Modules and sites perform very well in the ‘Cold & Sunny’ climate of Ladakh. Power plants set up in this region will enjoy not only low degradation rates, but also excellent irradiance.
- It is felt that some of the quality issues seen especially in the young modules and in Group Y sites are the result of very aggressive pricing and hasty installation.

Many more details on the performance of the modules, and a fuller analysis of the results have been given in the report entitled *All-India Survey of Photovoltaic Module Reliability: 2014*.

1. Introduction

1.1 Introduction to the Survey

India has set ambitious renewable energy generation targets under the Jawaharlal Nehru National Solar Mission (JNNSM) in an effort to avoid over-dependence on fossil fuels for electricity generation. The 22 GW solar energy target by 2022 under the JNNSM was revised in 2015 to 100 GW (40% of which is to come from rooftop projects and rest from ground-mounted large scale solar power plants), which would require rapid growth in solar installations throughout the country in the coming years. The success of the JNNSM in de-carbonizing the power generation sector will depend not just on meeting the 100 GW installation target but also on the satisfactory long-term performance of the photovoltaic systems. The financial success of these projects depends on the total energy generation during the guaranteed lifetime of these systems (usually 25 years). Considering the lack of information with regard to the long-term performance of PV systems in different climatic conditions of India, the High Powered Task Force of MNRE had in March 2013 requested the National Centre for Photovoltaic Research and Education (NCPRE), at the Indian Institute of Technology Bombay (IITB) to survey the performance of older PV systems already installed in the country. NCPRE requested the National Institute of Solar Energy (NISE) to partner in conducting the survey, keeping in view the wide experience which NISE (formerly Solar Energy Centre) had in monitoring PV system performance. Accordingly, a joint team was formed which surveyed 63 visually degraded PV modules spread across the country and submitted their report in March 2014 [1]. This "1st All India Survey of Photovoltaic Module Degradation 2013" showed that the PV modules were degrading at a faster rate in the Hot climates (Hot & Dry and Warm & Humid), where incidentally most of the mega-watt scale PV installations are expected to be concentrated. The primary cause behind the electrical degradation was the discoloration of the encapsulant (due to high annual UV radiation dose and high temperatures) and corrosion of the metallization (due to high humidity/moisture ingress and high temperatures). Since the 2013 survey was performed on a limited set of visually degraded modules, it was deemed necessary to undertake another survey to expand the database to get statistically significant numbers. For the 2014 survey, apart from the small installations which have been in service for about two decades, many new installations with capacities varying between 10 KW to 1 MW were selected in order to understand the initial degradation modes and associated degradation rates. The 2014 survey was conducted jointly by NCPRE and NISE in the months of September to November 2014 and September 2015, in which 1148 modules were surveyed from 51 different sites covering all six climatic zones of India. The assessment included a visual checklist, a detailed electrical characterization of the modules (illuminated *I-V*, dark *I-V*, insulation resistance test, interconnect breakage test, off-grid inverter performance test, electroluminescence imaging), thermal characterization (illuminated IR and dark IR), measurement of the relevant weather and irradiance data, and a survey of socio-economic factors associated with the installation.

The survey methodology and a review of related literature are presented in the forthcoming sections of this chapter, including a discussion on the climatic zones of India. Chapter 2 deals with the survey statistics, where some general information about the survey sites is also presented. Actual analysis of the survey data starts from Chapter 3 onwards. The field data have been collected under various ambient conditions (different irradiance and module temperatures). For the sake of performance comparison and degradation analysis, it is necessary to convert all the data to a standard reference condition. This reference condition is prescribed in international standards as 1000 W/m^2, 25°C and AM1.5G solar spectrum, and this set of conditions is referred to as the standard test condition (STC). Chapter 3 mainly deals with this conversion and assesses the errors associated with such conversions as well as due to other reasons. Chapters 4 to 7 deal with illuminated *I-V* analysis, analysis of dark *I-V*, dark IR and insulation resistance data, visual analysis and analysis of electroluminescence and infra-red thermography data. Risk Priority Number (RPN) is a recent concept in the field of photovoltaic system risk assessment, and the results are presented in Chapter 8. Chapter 9 deals with socio-economic analysis of the survey data, after which we present our concluding remarks in Chapters 10 with recommendations for the PV community. This would help in better decision making for research and economic investment in the Indian PV industry.

1.2 Literature Review

A comprehensive review of the relevant literature has been presented in the report on the All India Survey of Photovoltaic Module Degradation 2013 [1], and the interested reader is referred to that. However, we would like to highlight some important literature relevant to the results of the current Survey. It is worth mentioning here that the first major push to commercial terrestrial photovoltaic systems came in the 1970s, with the Flat Plate Solar Array (FSA) Project of the US Department of Energy [2]. Apart from the introduction of PVB and EVA polymers for encapsulation, the FSA project improved the design of almost every component of the solar module, increasing the module efficiency from 5% to 15% while also bringing in module performance warranty of 10 years (there were no warranties in 1975) [2]. After the FSA project ended in 1985, the work of standardization of the module design continued through research in both USA and Europe, finally leading to the release of the international standard IEC 61215 for design qualification of terrestrial photovoltaic modules in 1993 [3]. For large scale PV power plants that came up in the last part of the 20th century, continuous monitoring of the power plant performance was built-in into the project, but no such provision exists even today for smaller systems (rooftop systems, systems for water pumping, street-lighting, etc.). It is important to evaluate the performance of individual modules (as opposed to string-level or array-level performance which is monitored in large scale PV power plants) so as to establish the reliability of the photovoltaic modules. Several such surveys have been conducted in the past in different parts of the world, which has enhanced the confidence of the module manufacturers to provide 25 year warranties on power output (at least 80% of rated power after 25 years of operation) [4].

1.2.1 Literature on Electrical Performance Degradation

The paper by Jordan *et al.* on "Technology and Climate Trends in PV Module Degradation" [5] throws light on the degradation rates of field-aged PV modules and correlates these degradation rates with technology and climatic zones. They have reported an average degradation rate of 0.7%/year for crystalline silicon and 1.5%/year for thin films modules. In crystalline silicon modules, the decline in the power output is mainly due to the reduction in short circuit current, to a small extent in fill factor and is least dependent on reduction of voltage, whereas for thin film modules it is mainly due to fill factor loss. They have pointed out that discoloration and delamination are common signs of degradation in modules. In a later study, it has been reported that the average degradation rate for crystalline silicon modules is 0.8-0.9%/year whereas it is around 1%/year for thin film modules [6]. They have indicated that hotter climates and mounting configurations may lead to higher degradation in some, but not all, products. Suleske has investigated the degradation of modules installed in a grid-tied power plant in Arizona, for 10 to 17 years, and has reported degradation rates ranging from 0.9%/yr to 1.9%/yr for non-hot spot modules, while for modules with hot spots, the degradation rate was found to be as high as 5%/yr [7]. Sastry *et al.* [8] have also reported that the degradation rates of crystalline silicon PV modules, monitored at their test bed at the National Institute of Solar Energy (NISE) in Gurgaon (near New Delhi) over a time of ten years, are more than the expected level [9]. Furthermore, studies done by NISE on the performance analysis of different photovoltaic technologies (a-Si, multi c-Si and HIT) and found that HIT and a-Si have performed better than multi c-Si [10] [11] [12] [13] [14]. In addition to these studies they have also reported the effect of the seasonal spectral variation on performance on these technologies and for composite zone they have found that HIT is least affected while a-Si is most affected [15] [16]. They have also mentioned that some of the IEC 61215 qualified PV module designs had degraded faster than the guaranteed level in actual field conditions. They finally concluded that the present qualification standards need to be revised in order to ensure reliable field performance of the modules deployed in harsh Indian conditions so as to survive for more than 20 years. It has also been reported that in Hot & Dry type of climate there is a significant increase in the number of modules suffering from solder joint failure. Tamizhmani [17] has shown that modules in the hot climates of USA show a higher degradation rate than in other climatic zones. Studies done by Kuitche *et al.* [18] mentioned that for Hot & Dry type of climatic condition of Arizona, USA, solder bond failure and discoloration are the two dominant failure modes. Jeong *et al.* [19] have done the physical analysis of the solder bonds in degraded modules and they have found cracks in solder to solder and solder to silver paste. They have further mentioned that the main failure mechanism of these cracks in solder interconnection is due to the mismatch in the coefficient of thermal expansion between the module material and the ribbon wire solder. These solder joint failures cause increase in series resistance of the module which impacts the fill factor and eventually reduces the power output. Hence it becomes important to accurately determine the series resistance value of the module. Kaminski *et al.* [20] have developed a new method to extract the series resistance value from the dark *I-V* characteristic. The use of dark *I-V* characteristics can be extended to accurately obtain other critical parameters such as shunt resistance, diode ideality factor, and diode saturation currents that affect the electrical performance of photovoltaic power output [21] [22]. In order to get a good quality photovoltaic module with high efficiency it is necessary to use a good quality solar cell which is free from defects and impurities. These defects act as recombination centres or charge carrier traps which give rise to a high ideality factor ($n > 1$) [23] affecting the efficiency of solar cells. Salinger *et al.* [24] have developed a simple and fast method to obtain these parameters from dark *I-V* characteristic. Furthermore, Spataru *et al.* [25] have proposed a fault identification method which is based on the complementary analysis of light and dark *I-V* characteristics. Degradation modes that lead to the power loss (such as cell interconnects breaks, corrosion, cell microcracks and PID) affect the dark and light *I-V* characteristics in different ways and Spataru’s proposed method identifies these distinct signatures and correlates them with the degradation modes. These degradation modes can also be well indentified through an electroluminescence (EL) image. EL imaging of PV modules has become an important characterization tool in recent times. It is a powerful, quick and reliable inspection technique to get information on defects in solar cells and modules. These defects, particularly cracks and inactive regions, appear as dark parts in the EL image of the PV cell or module [26]. The EL intensity has been found to correlate well with the minority carrier diffusion length of crystalline silicon solar cells, and hence can serve as a tool for diffusion length mapping [27] [28] [29]. A linear relation has been obtained between the number and size of breakages and the power drop in crystalline silicon modules by Mansouri *et al.* [26]. Also, for thin film modules, EL imaging has helped in verifying the reduction in the size of the localized shunts in CdTe modules after light soaking, which explains the increase in the efficiency of these modules after stabilization.

1.2.2 Literature on Module Component Degradation

Often it has been observed that the electrical performance degradation is caused by deterioration in the module components due to weathering in the field. In order to standardize the documentation of the degradation and failure modes noticed in the field, Packard *et al.* [30] have developed a Visual Inspection Data Collection Checklist. A modified version of this checklist has been used for the All-India Survey of Photovoltaic Modules in 2013 and 2014. In the 2013 survey, it has been observed that discoloration of the encapsulant is the most common degradation observed in the field-aged visually degraded modules [1]. This problem of discoloration had been extensively studied in the 1990s, and STR Corporation came out with a report for NREL, wherein they identified certain additives as the primary cause behind discoloration of EVA [31]. The replacement of Lupersol 101 by Lupersol TBEP reduced the susceptibility to discoloration, and the use of cerium oxide containing front glass eliminated it. The curing agent and conditions (time and temperature) also play a role in determining the rate of discoloration during service, with fast cure EVA reported to be less prone to discoloration as compared to slow cure EVA [32]. Also, advanced formulations of High Light Transmission EVA are available nowadays which have almost no discoloration in accelerated UV tests [33]. Besides discoloration, delamination on the front of the solar cell can also reduce the short-circuit current (as the intensity of light reaching the solar cell gets reduced due to increased reflection losses). While discoloration has been seen to be almost uniform in all cells in a PV module, delamination is very non-uniform and hence can cause mismatch in the short-circuit current of the solar cells connected in series. Dhere *et al.* have found that delamination is more common in the Hot & Humid climate [34]. Tsuyoshi Shoida [35] has reported that delamination over a solar cell can reduce the short circuit current by as much as 43%, the decrease being almost proportional to the area of the cell delaminated. Often, high current reduction in the delaminated solar cells gives rise to reverse bias heating of these cells leading to hot spots. Hot spots have been monitored in PV power plants with the goal of determining their impact on the power output of the modules. Moreton *et al.* [36] have suggested that for detection of hot spot related issues, infrared thermography should be performed under a solar irradiance of at least 700 W/m^2. They have defined the hot spot temperature difference (ΔT) as the difference between the hot spot temperature and the module's representative temperature. They have suggested that if the hot spot ΔT (after correcting for variations in irradiance by linearly extrapolating to 1000 W/m^2) exceeds 20^{o}C, then the module should be considered defective and replaced by the installer [36]. Buerhop *et al.* [37] have identified from literature that some of the common causes of hot spots are bypassed sub-strings, broken cells, open solder joints, and shunted cells. Corrosion is one of the causes behind open circuiting of solder joints. Corrosion of interconnects has been found to be the most common degradation observed, after discoloration of EVA, in the 2013 All India survey of PV Module degradation [1]. Corrosion of metallization leads to increase in the series resistance which reduces the Fill Factor of the PV module. The series resistance can also increase in the event of solder bond deterioration/failure between the interconnect ribbon and the busbars due to thermo-mechanical fatigue [38]. The backsheet plays a major role in preventing the entry of the moisture into the module, which can cause corrosion of metallization. Usually backsheets have a 3-layer structure, where the middle layer (usually PET) provides electrical insulation, and the outer layer (usually a PVF film like Tedlar, or PVDF, or hydrolysis-resistant PET) provides resistance against moisture and ultraviolet light [39]. The innermost layer of the backsheet provides good bonding to the encapsulant. PVDF and PET films have been found to degrade significantly in damp heat tests while PVF film has shown "excellent" stability [40]. Some module manufacturers opt to use just a single layer of standard grade PET film as the backsheet, but such modules have been found to degrade in the field within a few years of installation [41]. Apart from the packaging material, there is also a possibility of degradation of the semiconductor material in the solar cell. Light Induced Degradation (LID) is seen in both mono crystalline Si and multi crystalline Si modules within a few hours of exposure to sunlight, causing up to a maximum of 5% reduction in short circuit current [38]. The presence of impurities like oxygen and iron (which associate with boron) is the primary cause behind LID in the crystalline silicon solar cells [42]. For thin film modules, LID can be as high as 10% - 30% and requires a few months to fully develop [43]. A very common visual degradation observed in thin film modules are white spots which are caused due to hot spot shunts in the module [44]. Shunts in the thin film modules may be generated due to presence of impurities embedded during the manufacturing process (Type A shunts) owing to improper cleaning of the superstrate glass, or due to severe hot spot heating (Type B shunt) which may be caused due to partial shading. Some manufacturers provide installation guidelines to avoid partial shading in their modules as a means to prevent white spots [45].

1.2.3 Literature on Socio-economic Aspects of Small Installations

Degradation, underperformance and even failure of PV systems due to improper installation and lack of maintenance are often reported in the literature [46]. A study on PV dissemination trajectories in Ghana, Kenya and Zimbabwe [47] has helped in identifying 'donor driven' implementations as a major mode of PV dissemination. This paper also refers to the analysis of institutional models based on ownership of systems. The paper by Jafar [48] states that the nature of maintenance support and the expenses on maintenance can be studied effectively by categorising the installations based on their ownership. The paper concludes that maintenance activities are more effective if they are done by a third party at a reasonable service charge. Another case study from China shows that promoting a local free market can be more effective than subsidy-driven donor-based programs [49]. A case study on SELCO [50] has revealed that PV systems are better maintained when there is a regular income or cash flow associated with them.

The importance of installing the modules at an easily accessible place has been emphasised in a case study by El-Shobokshy *et al.* [51] in their paper dealing with the degradation of solar cells due to accumulation of dust. The importance of regular cleaning of modules is also highlighted in a study from Algeria [52]. Similarly, shading of single module based rooftop home lighting PV systems was found to be a serious issue resulting from improper installation location [53].

Studies conducted as early as the 1980s concluded that village energy centres are technically and economically more viable than individual rooftop systems. Better maintenance, superior load management and better security are some of the advantages of centralised systems [54]. On the contrary, some studies say that the independence in operational aspects and increased responsibility of users due to individual ownership ensures better maintenance of PV systems [55]. A detailed study by Cust *et al.* [56] provides adequate inputs for designing a framework for analysing renewable energy based rural electrification projects based on the ownership of assets of generation, distribution and end use of the generated power. Based on the insights from the above literature as well as a few other case studies [57] [58] [59] [60] [61] [62], we have developed a framework for analysing the socio-economic aspects based on ownership, financial model and the end purpose of the installation. The parameters which we have compared are the correctness in the design, installation and maintenance of the systems using both quantitative and qualitative values.

1.3 Survey Methodology

A complete understanding of degradation in PV modules is possible only when thorough characterization and analysis of each and every component of the PV modules is carried out. Keeping this in mind, an extensive array of characterization tools was taken to the field for detailed inspection of the modules, as shown in Table 1.1.

The first activity on reaching the site was to collect dust samples from a few modules so that these can be analyzed later in the laboratory. Then the modules were cleaned with water. The module surface was wiped dry before starting the current-voltage (*I-V*) characterization (since any water film on the module surface would interfere with the module performance). Visual inspection, illuminated *I-V* and infrared (IR) thermography, interconnect failure test and insulation resistance test were performed in daylight. In the late afternoon, electroluminescence imaging, using a special daylight EL technique, was performed on selected modules (based on their *I-V* characteristics and other daylight test results), followed by dark *I-V* and dark IR thermography. The methodology adopted for the various tests are briefly explained below.

Table 1.1: Equipment Specifications

Instrument	Make & Model No.	Specifications
I-V Tracer	Solmetric PVA-1000S	Voltage Range (& Accuracy) : 0-1000 V DC, (+/-0.5% +/-0.25V) Current Range (& Accuracy) : 0-20 A DC, (+/-0.5% +/-40mA) Irradiance Sensor Range & accuracy: 0-1500 W/sq.m., (+/-2%)
	PV Engineering PVPM 2540C	Voltage range: 25 V / 50 V / 100 V / 250 V Current: 2 A / 5 A / 10 A / 40 A Accuracy in peak power measurement: +/-5% Temperature: -40°C to +100 °C with Pt1000 Irradiance: 0 – 1300 W/m^2 (Standard sensor)
Infrared Camera	FLIR E60	Temperature Range : -20 ^{o}C to 650 ^{o}C Thermal Sensitivity : <0.05 ^{o}C at 30 ^{o}C Detector Type (& size) : Uncooled Microbolometer, 320 x 240 Pixels
Electroluminescence Camera	Sensovation HR-830	No. of Pixels (& pixel size) : 3326 X 2504, (5.4 um x 5.4 um) Sensor cooling : Thermo-electric cooling to 50 ^{o}C below ambient
Cell Line Checker	Togami SPLC-A-Y1	Voltage range : 15V DC – 1000 V DC (Magnetic field mode), 0-1000V DC (Electric Field mode)
Insulation Resistance Tester	FLUKE 1550C	Insulation test voltage : 250 V / 500 V / 1000 V / 2500 V / 5000 V Leakage current measurement range : 1 nA – 2 mA
DC Power Supply	Aplab VSP8015 ODI	0-80 V, 0-15 A, Variable DC Power Supply
	Aplab VSP12005 ODI	0-120 V, 0-5 A, Variable DC Power Supply
Single Phase Power Analyzer	VOLTEC PM100	Max. measurable voltage : 1000 V Max. measurable current: 20 A
Digital camera	Nikon D3200	Effective Pixels : 24.2 Million Image sensor : 23.2 x 15.4 mm CMOS sensor

a) Visual Inspection

Visual inspection of the modules was done to record the physical degradation visible in various parts of the module. A visual inspection checklist, which is a slightly modified and enhanced version of the NREL Visual Inspection Checklist [30], was filled up. Images of the modules were taken using a high resolution camera for future reference. The high resolution images enable us to magnify the region of interest in the captured image and get a better view of the defect zone. A fully filled sample Checklist sheet is given in Appendix A.

b) Current-voltage (I-V) Measurement under illumination

The current-voltage (*I-V*) characteristic is a major diagnostic tool for determining the electrical performance of a PV module [25]. Two sets of portable *I-V* tracers, which were cross-calibrated earlier, were used in the survey, enabling us to collect data of multiple PV modules in parallel. Both of these equipments had additional accessories for measurement of the Plane of Array (POA) global solar irradiance and module temperature. At least 5 sets of *I-V* readings were taken for each module, at intervals of 1 minute. The ambient temperature and relative humidity were also recorded at the time of *I-V* measurement so as to aid in the spectral correction during STC translation of the field data [63], if required.

c) Infrared Thermography under Illumination

Infra-red (IR) images enable us to detect hot spots in the module which can degrade the module performance significantly [37]. IR images were taken for all inspected modules, from the backside of the module (where possible, else taken from the front), with the module terminals short-circuited. These images should be taken only when the irradiance is above 700 W/m^2, so as to enable proper detection of hot spots. The IR images taken during the survey at irradiances below 700 W/m^2 were not considered for further analysis.

d) Insulation Resistance Measurement

Insulation resistance is an important measure of the quality of insulating materials used in the module, like the encapsulant and backsheet [64]. Low values of insulation resistance can be a cause of concern with regard to the safety of the personnel handling such modules. The insulation resistance of the modules was checked in the field under both dry condition and wet conditions. The insulation resistance was measured between the shorted output terminals and the module frame. A towel was soaked with water and placed on the module for wetting its front glass surface for a modified wet insulation test.

e) Electroluminescence Imaging

Electroluminescence (EL) imaging of modules is an important diagnostic tool that provides information about the extent and nature of cracks and various other defects in the solar cells [26]. An electroluminescence camera, having a silicon CCD sensor, was used to capture the luminescence emitted by the selected PV module, when forward biased to carry 1.3 times of the rated short circuit current using a DC power supply. An innovative image difference technique, developed in-house at IIT Bombay specifically for the Survey, was utilized to capture the EL images in the late afternoon hours, in low irradiance conditions in the field. This technique takes the difference of two images of the module captured by the CCD camera – one taken with, and another without, forward biasing the module [65]. The EL images are later analyzed to find out what fraction of the short circuit current degradation is accounted for by the cracks and inactive areas in the module.

f) Dark I-V Measurement

Spataru *et al.* [25] have explained in detail the utility of the illuminated and dark *I-V* characteristics of a PV module in determining the degradation modes. The dark *I-V* was taken by sweeping the applied terminal voltage from zero to the open circuit voltage of the respective module, using a programmable DC power supply (which was controlled by a custom-made MATLAB code running on a laptop).

g) Dark IR Measurement

Dark IR imaging was done in the evening hours by covering the selected module from the front. The module was forward biased at its rated short circuit current, and it was allowed to heat up (owing to the current flow) for about 1 minute before taking the image using the infrared camera. The image was usually taken from the back side of the module, unless the installation structure prevented access to its back side. These dark IR images were later analyzed and compared with EL to assess whether dark IR can serve as a substitute for EL imaging in the field.

h) Interconnect Failure Test

Interconnect failure is one of the most common failure modes for PV modules installed in Hot & Dry climatic zones [66]. The Cell Line Checker from Togami Corporation is an innovative tool that can detect interconnect failures in PV modules [67]. It consists of 2 units – the transmitter (which is connected to the PV module output terminals) and the receiver (which is swept on the front side of the module over the interconnect ribbons). The receiver unit shows the health of the interconnect connections through flashes of LEDs on a scale of 0 to 10; with no flash meaning complete failure of the associated interconnect ribbon.

i) Performance Test of Off-grid Inverters

In small off-grid installations, people usually prefer to purchase low-cost locally made inverters which may not have good efficiencies. We carried power analyzers to check the various performance parameters of these off-grid inverters like no-load losses, efficiency at maximum connected load, power factor and total harmonic distortion in output voltage. The analysis of the collected data will provide us insights into the quality assurance and testing standards required for such off-grid installations.

j) Socio-economic Survey

Field performance of PV systems is influenced by the appropriateness of design, installation and maintenance activities. In some cases, especially for small and medium installations, the degradation in performance is due to improper system design, faulty installation practices and poor maintenance cycles [1]. These factors can again be linked with the ownership model of the system, the way in which the funds and cash flows are associated with the system, and the main purpose of system installation. We have surveyed, through a questionnaire and discussions, the appropriateness in system design and installation (support structure, orientation and tilt angle, choice of balance of system components, consideration of shading objects, etc.) and the effectiveness of system maintenance cycles (frequency of module cleaning, whether preventive or responsive maintenance, skill level of technicians, response time of the repairers, etc.). The cost of installation and details regarding the savings (in electricity bills) and income generation (through sale of energy) associated with the system were also recorded so as to do an economic analysis.

1.4 Climatic Zones of India

The National Building Code of India [68] divides India into 5 climatic zones based on average annual temperature and humidity – Hot & Dry, Warm & Humid, Composite, Temperate and Cold (refer Table 1.2). This five-zone climate classification has been used in the 1st All-India Survey of Photovoltaic Module Degradation 2013 [1]. In the 2014 survey, we have visited additional sites in and around Ooty in South India and Mandi in the Himalayan foothills, which have a cold climate, but are better classified as Cold & Cloudy (or Cold & Wet), unlike the other cold zone sites of Ladakh, which are Cold & Sunny (or Cold & Dry). It was deemed necessary to capture this climatic difference, and hence, in this report, we use the six-zone classification system of Bansal and Minke [69], the criteria for which are described in Table 1.3.

Table 1.2: Climatic Zone Classification criteria as per National Building Code [68]

Climate	Mean Monthly Maximum Temperature (deg. C)	Mean Relative Humidity (%)
Hot & Dry	>30	<55
Warm & Humid	>30	>55
	>25	>75
Temperate	25 – 30	<75
Cold	<25	All Values
Composite	This applies when six months or more do not fall within any of above categories	

Table 1.3: Climatic Zone Classification criteria as per Bansal and Minke [69]

Climate	Mean Monthly Temperature (deg. C)	Mean Relative Humidity (%)
Hot & Dry	>30	<55
Warm & Humid	>30	>55
Moderate	25 – 30	<75
Cold & Cloudy	<25	>55
Cold & Sunny	<25	<55
Composite	This applies when six months or more do not fall within any of above categories	

As per the six-zone classification, the coastal area of India (like Mumbai, Chennai and Kolkata) fall in the Warm & Humid zone, whereas the central parts of India (including the capital city of New Delhi) fall in Composite zone. Places in the central western part of India like Jaipur, Jodhpur, Jaisalmer and Gandhinagar lie in the Hot & Dry zone. Bangalore falls in the Moderate climatic zone. Sites in Ladakh fall in the Cold & Sunny climatic zone whereas sites in Jammu, Himachal Pradesh and Ooty experience Cold & Cloudy climate. The various climatic zones in India have been shown in Fig. 1.1, along with the sites where the survey has been conducted (in black dots). As evident from the figure, all the zones have been covered in this survey. The number of sites (refer to Table 1.4) is not quite evenly distributed, with many sites falling in the Warm & Humid and Composite zones, but nevertheless there are enough modules in all zones to gauge climatic variations. Further, it has been found that many aspects of module degradation are similar between the 'Hot' zones, that is, Hot & Dry, Warm & Humid and Composite zones. Similarly, the cooler ('Non-Hot') climates, namely Moderate, Cold & Cloudy and Cold & Sunny zones also have similar kind of module degradation. Hence the six climatic zones will sometimes be classified into Hot and Non-Hot zones for the sake of analysis wherever found necessary.

Table 1.4: Survey site statistics

Climatic Zone	No. of Sites	No. of Modules
Warm & Humid	15	333
Composite	10	308
Cold & Cloudy	9	122
Hot & Dry	8	194
Moderate	6	134
Cold & Sunny	3	55

While the six-climate classification of Bansal and Minke is being used for the analysis of the survey data, we have provided some of the important climate-dependent analysis also in terms of the internationally accepted Koppen-Geiger climate classification system, in Appendix B.

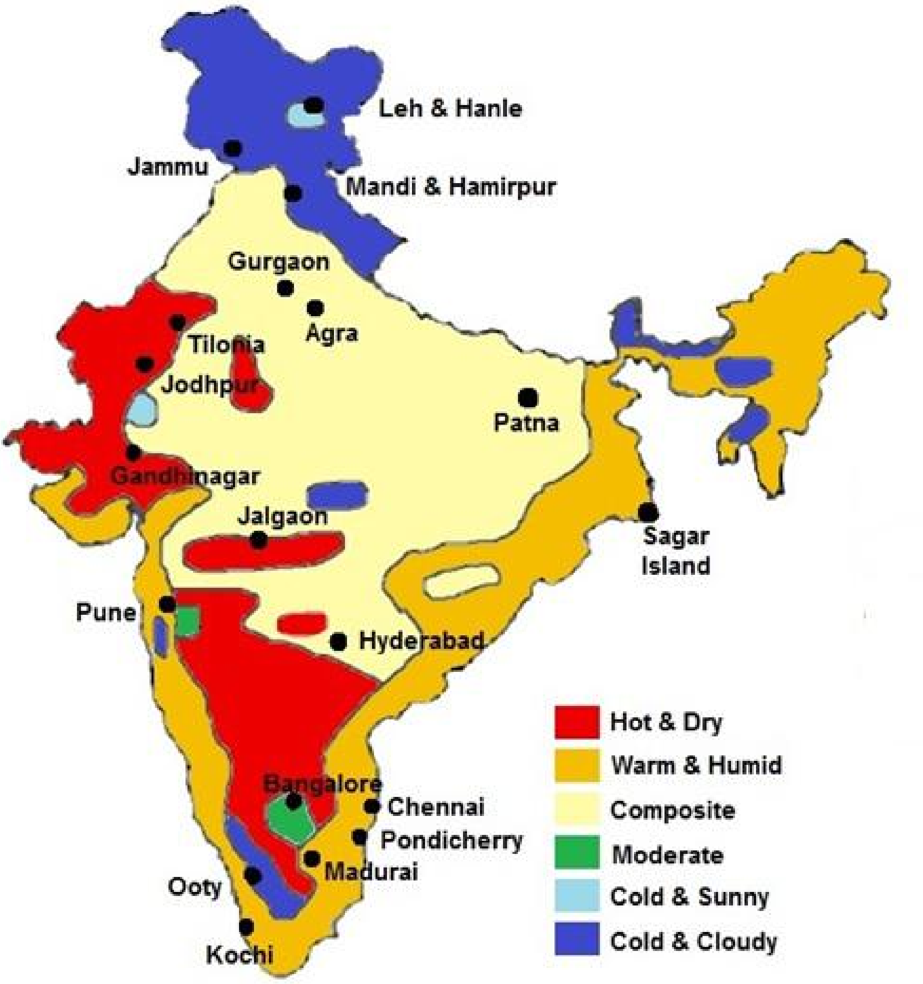

Fig. 1.1: Climatic Zones of India as per Bansal and Minke [69]

1.5 Summary

This chapter has given an overview of All-India Surveys of PV Module Degradation undertaken in 2013 and 2014, together with a brief review of the relevant literature. The survey methodology, types of inspections and measurements undertaken, and the details of the equipment used in the field have been described. Since India experiences a variety of climatic conditions, from extremely hot climates in Rajasthan to cold climates in Ladakh, the climatic zone classification has been described in some detail, particularly since it was decided to use a slightly different classification in the 2014 Survey compared to the 2013 Survey. Before going into the analysis of the survey data, it is important to understand the distribution of the data, in terms of the age, technology and various other aspects. The following chapter discusses some of these vital statistics related to the survey.

2. Information on Modules Surveyed

2.1 Introduction

This chapter presents an overview of the diversity in the modules inspected during this survey, in terms of the technology, climatic zone, power rating, age group, packaging material etc. A total of 1148 modules were examined in the 6 different climatic zones of India, but these were not equally distributed among the various categories. However, each of the categories had a respectable representation in the survey, as will be clear from the data being presented here.

2.2 Statistics of Sites Surveyed

The survey team visited a total of 51 sites from Tamil Nadu to Ladakh, and from Rajasthan to West Bengal, covering all the climatic zones in India (Hot & Dry, Warm & Humid, Moderate, Composite, Cold & Cloudy and Cold & Sunny). Fig. 2.1 shows that 45 of the surveyed sites (having 1002 modules) fall in the small to medium size category (less than 100 kW installed capacity), and 6 sites (having 46 modules) are in the large size category (more than 100 kW installed capacity). As evident from Fig. 2.2, 31 sites were rooftop installations, 5 sites were PV power plants and the rest were small water pumping systems, home lighting systems etc. Some details of these sites are presented in Appendix C.

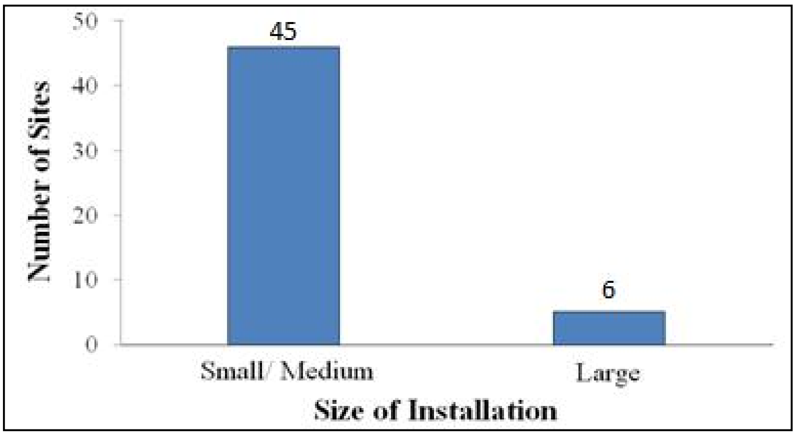

Fig. 2.1: Installed capacity (size) of the sites

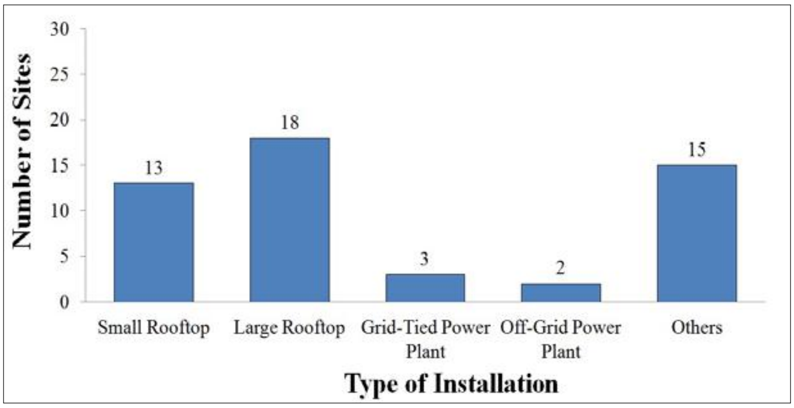

Fig. 2.2: Type of installation

2.3 Statistics of Modules Inspected

The survey module details are summarized in Figures 2.3 through 2.10. Figure 2.3 shows the distribution of technology of the modules surveyed. Most of the modules inspected are crystalline silicon modules, about evenly distributed between mono crystalline silicon (mono c-Si) and multi crystalline silicon (multi c-Si). Apart from crystalline silicon modules, we have a good representation of amorphous silicon (a-Si) and cadmium telluride (CdTe), as well as a few CIGS and HIT. Figure 2.4 shows the histogram of the age of the modules, and it is seen that a majority of the modules (about 70%) fall in the young age group of 0 to 5 years, although we also have more than 350 modules in the older age categories. Figure 2.5 shows that the name-plate power ratings of the inspected modules mostly belong to the 0-100 Wp and 200-300 Wp categories. The maximum number of modules was surveyed in the Warm & Humid (W&H) zone, followed by the Composite (Comp) zone, but the other climatic zones were also well represented, as evident from Fig. 2.6. Figure 2.7 shows the biasing condition of the modules. Figure 2.8 shows the statistics with regard to the packaging materials used in the modules, at the front and back. A majority of the modules had glass cover on top (front) and polymer backsheet, as evident from Fig. 2.8. A few of the modules had polymer on the front instead of glass. Almost all of the systems surveyed had either only an inverter (grid-tied systems), or both inverter and battery (refer to Fig. 2.9). In Fig. 2.10, we have provided statistics regarding the various characterization tests performed during the survey. The major characterization tests like current-voltage (*I-V*) characterization (in daylight), infrared (IR) thermography, visual inspection, insulation resistance and interconnect breakage test were performed on all inspected modules at each site. Further, based on these characterization tests, some of the modules were selected for further testing, and were subjected to dark current-voltage (dark *I-V*) characterization, dark IR thermography, and electroluminescence (EL) testing.

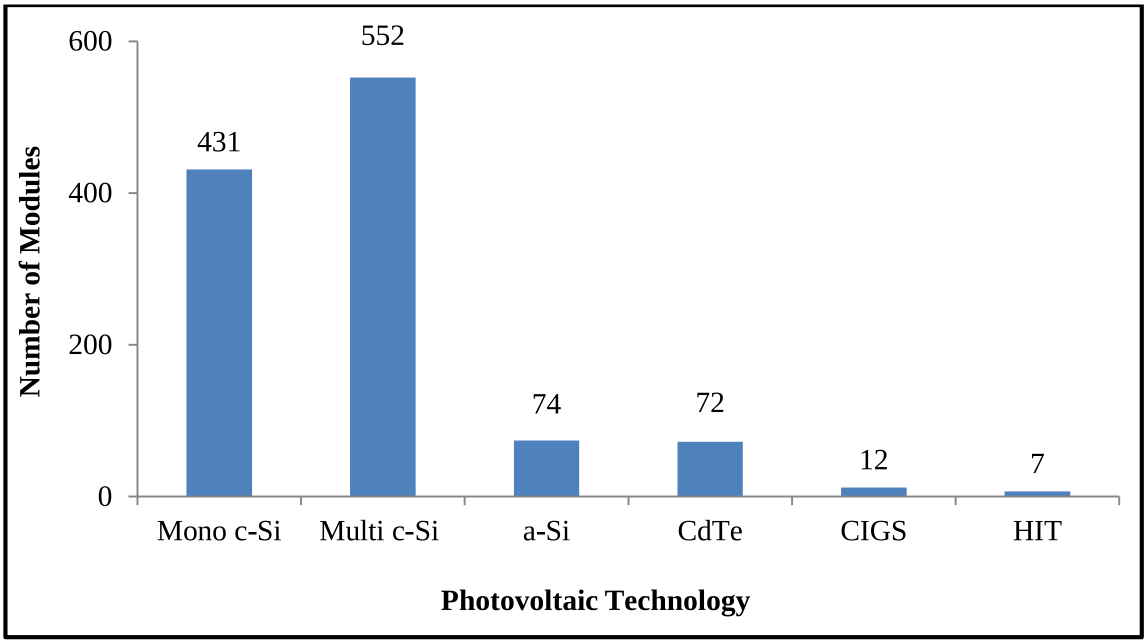

Fig. 2.3: Technology-wise distribution of inspected modules

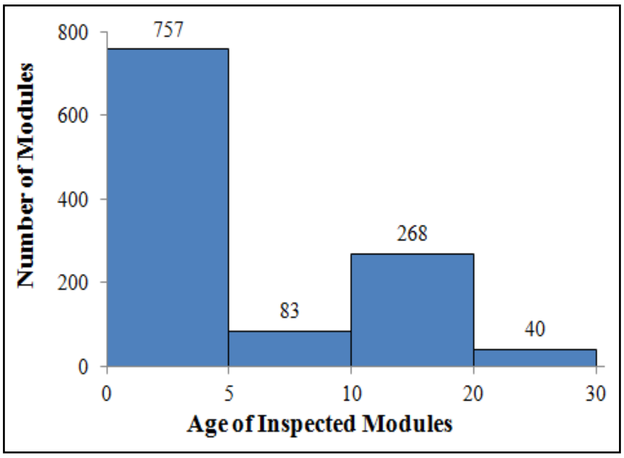

Fig. 2.4: Age-wise distribution of inspected modules

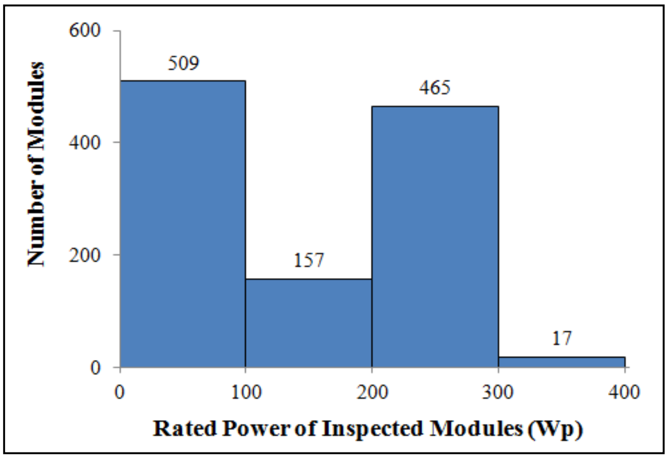

Fig. 2.5: Rated power distribution of inspected modules

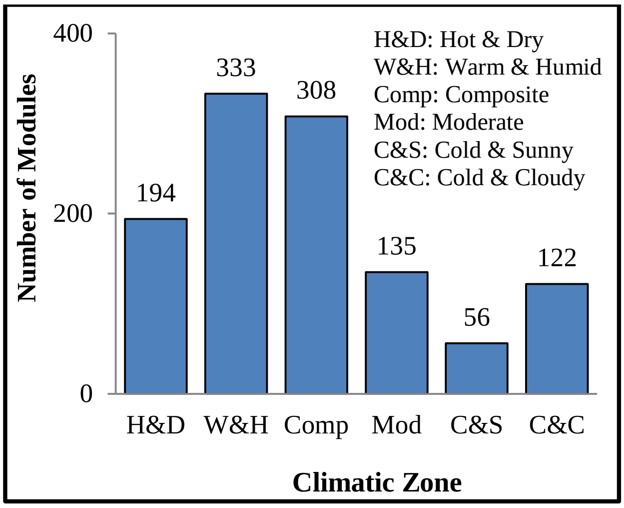

Fig. 2.6: Climatic zone-wise distribution of the modules

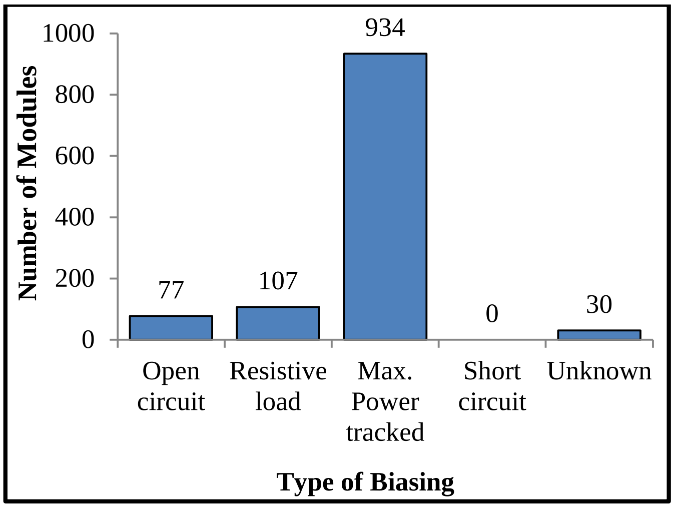

Fig. 2.7: Type of biasing of the inspected modules

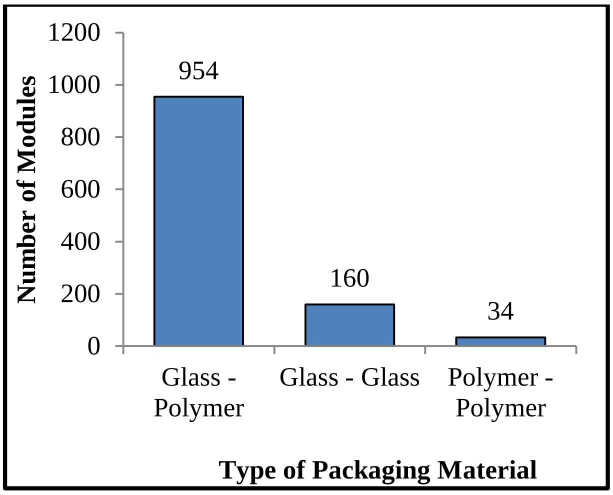

Fig. 2.8: Packaging material of inspected modules

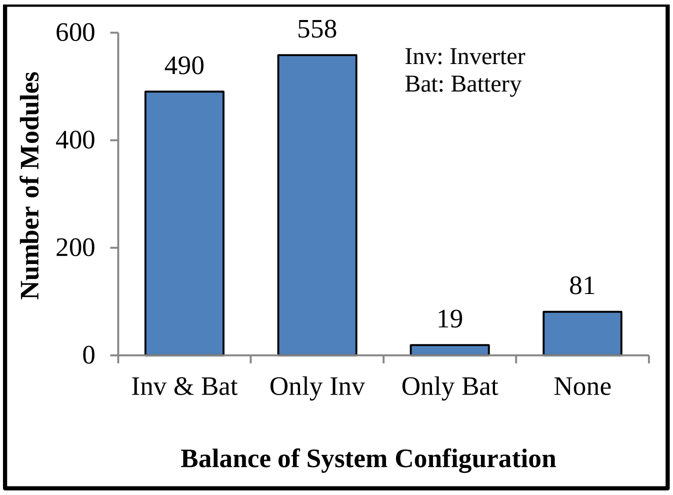

Fig. 2.9: Balance of system configuration

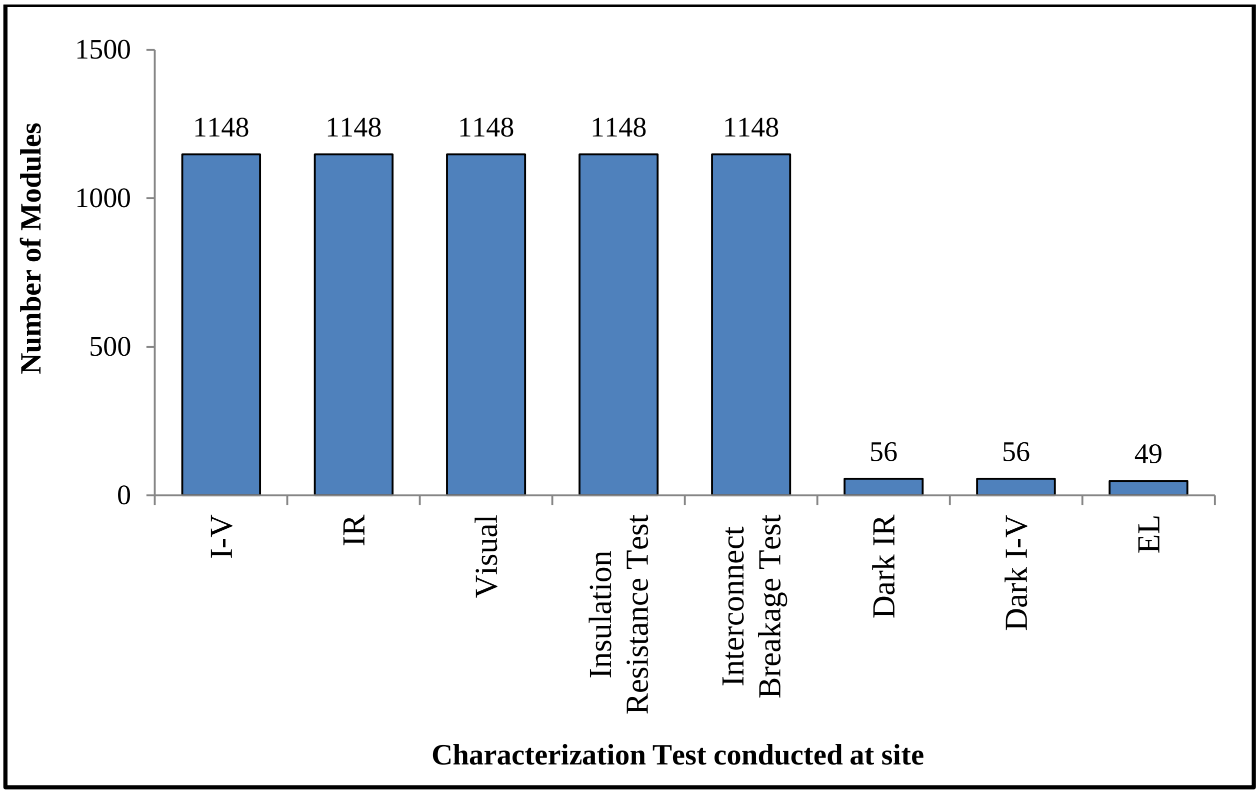

Fig. 2.10: Characterization tests conducted at the site

2.4 Summary

This chapter gives an overview of the surveyed modules in terms of various categories of site size, age, technology, climatic zone and other important aspects. It is seen that the 1148 modules inspected during the 2014 Survey are quite well represented in most of these categories. In particular, we generally have large enough numbers (barring a few cases) to arrive at reasonable statistical analyses. The following chapters will deal with the analysis of the electrical performance of the inspected modules, and correlate them with the visual and non-visual defects observed in these modules.

3. Analysis and Corrections Applied to Survey Data

3.1 Introduction

In the field, *I-V* data of the surveyed modules were naturally measured under varying conditions of module temperature and irradiance. To assess their performance it was necessary to translate the measured *I-V* data to a standard condition. The International Electrotechnical Commission (IEC) has defined the Standard Test Condition (STC) for PV modules as 1000 W/m^2 irradiance with AM 1.5G spectrum and 25^{o}C module temperature. Further, IEC 60891 defines the standard correction procedure for translating measured *I-V* data between different irradiance and temperature values. In our case, we have utilized a modified version of IEC 60891 correction procedure 1 [70] for translating the survey data. In this chapter we discuss the correction procedure and the associated errors introduced due to use of modified version of IEC 60891 especially when translating from low irradiance. We also discuss the errors associated with the measurement itself and the uncertainty in maximum power rating of the module. We will use the mean or average values to analyze and compare the data in this report, and we provide here the justification for choosing the mean over the median. Finally we explain the data plotting format with different error bars. The software package developed in Matlab to perform such *I-V* translations is also described briefly in this chapter.

3.2 IEC 60891 Correction Procedure

The IEC 60891 standard defines a procedure that helps to translate the measured *I-V* characteristics of photovoltaic devices to standard test condition (STC) i.e. 1000W/m^2 irradiance and 25^{o}C module temperature. In order to compare the performance of different modules, *I-V* data measured at different conditions of temperature and irradiance need to be translated to STC. IEC 60891 has three different procedures for translating the measured *I-V* characteristics to other conditions of temperature and irradiance (such as STC).The first procedure utilizes two equations, one for correcting current and the other for voltage; hence it corrects each point of the entire *I-V* curve. For better results in case of large irradiance corrections (>20%) the second correction procedure, involving an alternative algebraic method, can be used. In both these procedures, correction parameters must be determined prior to the correction; whereas the third correction procedure, which is an interpolation method, does not require any correction parameters. A comprehensive review of all the three correction procedure has been presented in the report of the All India Survey of Photovoltaic Module Degradation 2013 [1], and elsewhere, and the interested reader is referred to that.

3.3 Correction Procedure Adopted for Survey Data

IEC 60891 correction procedure 1 was used for translating the *I-V* data measured during the survey to the STC condition. This procedure involves four correction parameters for translating the entire *I-V* curve. These are: α (temperature coefficient for current), β (temperature coefficient for voltage), R_s (internal series resistance of the test specimen) and k (curve correction factor). Though the accuracy of the procedure using all four parameters is obviously better, the determination of R_s and k requires measurements of the temperature and irradiance dependency of the current and voltage. We explore whether these can be neglected without much loss of accuracy.

3.3.1 Correction Procedure 1a

The value of R_s of a module is determined by using three *I-V* curves at constant temperature but different irradiances, whereas in order to determine the value of k, we need three *I-V* curves at constant irradiance but different temperatures. Since enough field data is often not available to determine the values of R_s and k, we have considered only two parameters i.e. α (temperature coefficient for current) and β (temperature coefficient for voltage) while keeping R_s and k equal to zero. Furthermore, we use the 'typical' values of temperature coefficients obtained from literature [71], since the actual values for the particular module being evaluated are often not available. Hence, the equations of Correction Procedure 1 will get modified as follows:

$$I_2 = I_1 + I_{sc} * \left(\frac{G_2}{G_1} - 1\right) + \alpha * (T_2 - T_1) \quad .... (3.1)$$

$$V_2 = V_1 + \beta(T_2 - T_1) \quad .... (3.2)$$

The above two equations have been used for correcting the measured *I-V* curve to the STC condition. We call this procedure as Correction Procedure 1a. A MATLAB code was written in order to do this in an automated way.

In order to assess the level of accuracy of Correction Procedure 1a, we performed an exhaustive set of experiments which is described in detail in Appendix D. Results from these detailed experiments show that the error incurred if we use only the literature α and β varies between 1.4% and 5.4%. We deem this to be sufficiently small that for our survey we have consistently used Correction Procedure 1a with values of α and β reported in the literature.

3.3.2 Low Irradiance Correction

As per IEC 60891, translation procedures can be applied only for 20% variation in the irradiance, that is, the irradiance should lie between 800 W/m^2 and 1200 W/m^2 for translation to STC. This is a very demanding condition for a field survey. In our case, though most of the *I-V* data were taken around 700 – 800 W/m^2, some of the data were measured at much lower irradiances (around 500 W/m^2) due to overcast or smoggy weather. In order to ascertain whether we can include these data in our analysis, we experimentally determined the error in translating *I-V* data measured at low irradiances (down to 500 W/m^2) to STC using Correction Procedure 1a.

In order to estimate this error, we have performed an exhaustive experiment as described in Appendix E. The results of these experiments are shown in Table 3.1, which shows the error associated with translation from a particular temperature & irradiance combination to STC. The shaded cells in the table indicate irradiance and temperature conditions not encountered during the survey. It can be noticed that we can indeed use Correction Procedure 1a with literature values of α and β for irradiances as low as 500 W/m^2 without exceeding an error limit of 5%.

Table 3.1: Error in P_{max} value at STC obtained by translating using Procedure 1a

ΔP_{max} (%)	**Temperature (Deg. C)**									
Irradiance (W/m^2)	**25**	**30**	**35**	**40**	**45**	**50**	**55**	**60**	**65**	**70**
500	4.59	4.12	4.05	4.10	4.37	4.59	4.90	5.08	5.41	5.91
550	4.09	3.58	3.48	3.51	3.74	3.93	4.22	4.37	4.69	5.17
600	3.69	3.17	3.03	3.07	3.25	3.37	3.65	3.78	4.07	4.51
650	3.08	2.61	1.78	1.57	1.38	1.29	1.20	1.07	0.94	0.84
700	2.62	2.16	1.30	1.04	0.82	0.72	0.60	0.44	0.27	0.16
750	2.22	1.72	0.82	0.52	0.28	0.13	-0.01	-0.19	-0.39	-0.51
800	1.70	1.18	0.96	0.94	1.03	1.19	1.25	1.32	1.00	1.28
850	1.25	0.72	0.44	0.39	0.49	0.60	0.63	0.66	0.35	0.40
900	0.86	0.29	0.00	-0.07	-0.03	0.07	0.07	0.07	-0.29	-0.28
950	0.37	-0.37	-0.94	-1.24	-1.56	-1.67	-2.00	-2.47	-2.73	-2.90
1000	0.00	-0.60	-1.40	-1.75	-2.10	-2.24	-2.59	-3.08	-3.36	-3.58

3.4 Choice of Mean versus Median

In order to make meaningful inferences, we need to present overall trends in the measurements from the huge set of data collected in our survey. We have two choices, to use the mean of various parameters, or alternatively the median. In this section, we discuss the choice of mean versus median. In our 2013 survey analysis [1] we preferred median over mean to represent our data set because in that survey the sample size of the data was very small, and the mean could be significantly affected by outliers as compared to the median.

In the 2014 survey, however, we have a total sample size of 1148 modules which can be considered to be statistically significant. Even for different climatic zones, age groups, and technology types, we have fairly large numbers. For such a large sample size, the mean can serve as a good estimator of the central tendency provided the data is close to normal distribution. According to George and Mallery [72], a distribution can be considered to be normal if the values for asymmetry (skew) and kurtosis are between –2 and +2. Figure 3.1 shows the P_{max} degradation rate distribution of our data collected in the Composite climate. The skew and kurtosis for this data set are 0.55 and -1.21 which lie well within the range specified. Hence the mean can be used to represent the central tendencies of the data sets. Furthermore, some of the important statistical parameters like confidence interval (CI), as given in Eq. 3.3 below, are defined based on the mean values. We therefore use the mean or average values in most of the analyses which follow.

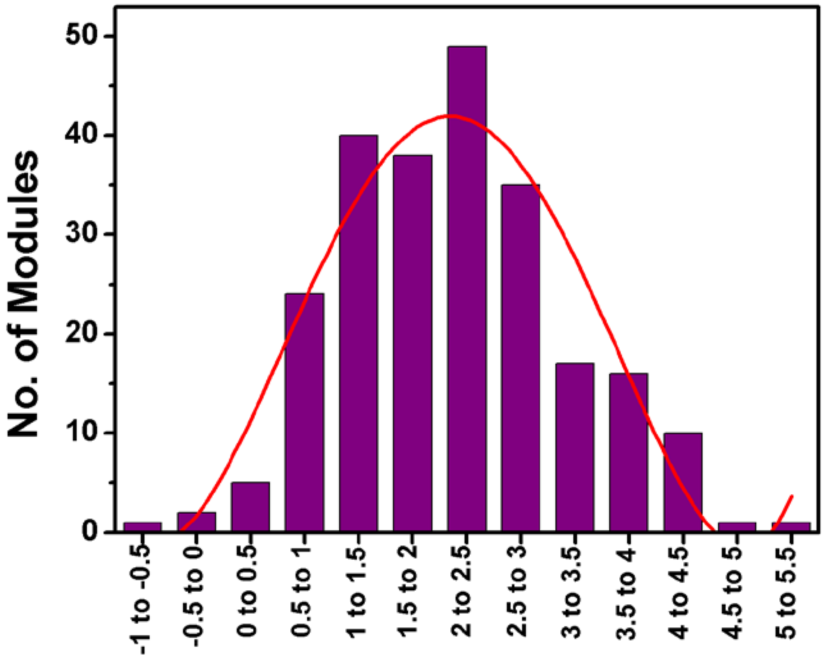

Fig. 3.1: P_{max} degradation rate distribution of our data collected in the Composite climate

$$x - 1.96 * \frac{s}{\sqrt{n}} < \mathrm{CI} < x + 1.96 * \frac{s}{\sqrt{n}} \qquad \text{..... (3.3)}$$

where:

x: Mean of the sample
s: Standard deviation of the sample
n: Number of data points in the sample
CI 95% confidence interval

3.5 Uncertainty in Degradation Rate Calculation

The *I-V* parameters at STC are derived from the field measurement followed by the Correction Procedure 1a. Hence any uncertainty in the STC data of a particular module depends on the uncertainty introduced by the correction procedure plus the uncertainties or errors due to the measurement equipment (refer Fig. 3.2).

3.5.1 Uncertainties in Measurements

We have used the Solmetric PVA-1000S portable *I-V* curve measurement tool during the survey. It has a K-type thermocouple as the temperature sensor, and a silicon photodiode as the irradiance sensor. The typical uncertainties of measured irradiance are stability, temperature coefficient, data acquisition and spectral mismatch. As per the manufacturer's datasheet, measurement uncertainty is ±2% for irradiance measurement, and ±2°C for temperature measurement. The manufacturer datasheet specifies the maximum measurement uncertainty in both voltage and current as ±0.5%.

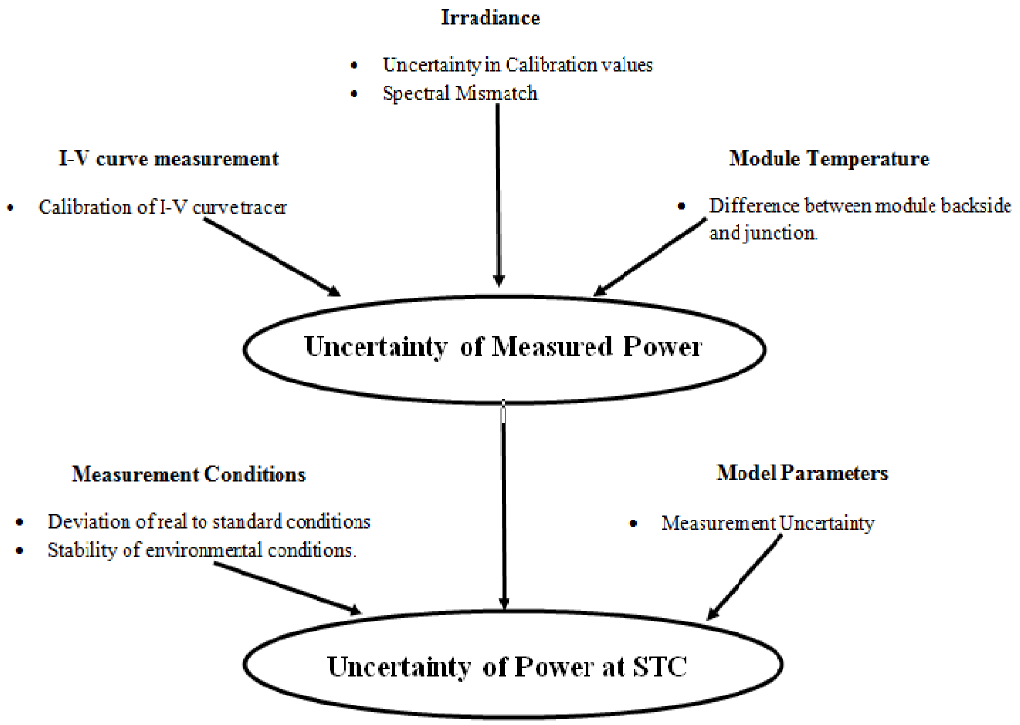

Fig. 3.2: Major influences on the combined uncertainty of power at STC [73]

In order to calculate the errors caused by the instrument on the *I-V* parameters at STC, we did a detailed error analysis, which is described in Appendix F. The outcome of the error analysis is presented in Table 3.2 and it can be seen that the maximum possible error caused by the instrument on the P_{max} value at STC is 4.05%.

Table 3.2: Error caused by the instrument on P_{max} at STC

ΔP_{max} (%)	Temperature (Deg. C)									
Irradiance (W/m^2)	**25**	**30**	**35**	**40**	**45**	**50**	**55**	**60**	**65**	**70**
500	4.05	4.05	4.04	4.03	4.01	4.00	3.99	3.97	3.96	3.93
550	4.05	4.05	4.03	4.03	3.97	3.95	3.94	3.91	3.90	3.88
600	4.05	4.05	4.04	4.03	3.97	3.95	3.94	3.92	3.91	3.88
650	4.05	4.05	4.01	3.99	3.97	3.95	3.93	3.92	3.90	3.89
700	4.04	4.04	4.01	3.99	3.97	3.95	3.93	3.92	3.91	3.89
750	4.04	4.05	4.00	3.99	3.97	3.95	3.93	3.92	3.90	3.89
800	4.04	4.04	3.99	3.97	3.96	3.94	3.92	3.91	3.89	3.88
850	4.04	4.04	4.00	3.98	3.96	3.94	3.93	3.91	3.90	3.89
900	4.03	4.03	4.00	3.98	3.97	3.95	3.93	3.92	3.91	3.89
950	4.03	4.03	4.01	3.99	3.98	3.96	3.95	3.94	3.93	3.88
1000	4.03	4.03	4.00	3.99	3.98	3.96	3.95	3.94	3.93	3.92

3.5.2 Uncertainties in Power at STC

The uncertainty in the corrected P_{max} is the combination of uncertainties in the measurement of the *I-V* data, temperature and irradiance in the field, and also due to the uncertainties in the temperature coefficients which are used in the translation equations. Table 3.3 shows the worst case error in the corrected P_{max} will be 8.64% for crystalline silicon modules, taking into account all the errors and uncertainties.

Table 3.3: Total error caused by instrument and Correction Procedure 1a on P_{max} at STC

ΔP_{max} (%)	Temperature (Deg. C)									
Irradiance (W/m^2)	**25**	**30**	**35**	**40**	**45**	**50**	**55**	**60**	**65**	**70**
500	8.64	8.17	8.09	8.13	8.38	8.59	8.89	9.05	9.37	10.44
550	8.14	7.63	7.51	7.54	7.71	7.88	8.16	8.28	8.59	9.05
600	7.74	7.22	7.07	7.1	7.22	7.32	7.59	7.7	7.98	8.39
650	7.13	6.66	5.96	5.73	5.63	5.64	5.63	5.3	5.12	4.83
700	6.66	6.2	5.48	5.25	5.12	5.1	5.06	4.83	4.52	4.18
750	6.27	5.77	5.02	4.76	4.6	4.55	4.5	4.12	3.89	3.54
800	5.74	5.22	4.95	4.91	4.99	5.13	5.22	5.33	5.54	5.83
850	5.3	4.76	4.44	4.43	4.52	4.7	4.77	4.86	5.06	5.33
900	4.92	4.32	4	3.93	4.03	4.16	4.21	4.28	4.45	4.68
950	4.43	3.66	3.99	4.13	4.33	4.67	4.73	5.05	5.35	5.56
1000	4.03	3.43	3.55	3.66	3.85	4.15	4.21	4.51	4.75	5.01

3.5.3 Uncertainties in Nameplate Data

In a field survey like ours, it is usually not feasible to get the initial performance data of the module when it was first installed, so the nameplate data has to be used instead. Therefore, an additional uncertainty in the degradation rate is created by the tolerance band provided by the module manufacturers in the nameplate power ratings of the modules (usually +/– 3% but also, in a few cases –0% / +5%). Hence the actual initial power rating could have been anything within the tolerance band. In order to estimate the error due to the name plate uncertainty, we were able to obtain actual initial STC data of 45 CdTe modules from a PV power plant. Figure 3.3 shows the distribution of the power output of these 45 modules. The nameplate rating of these modules was 85 W (–0%/ +5%), but as we can see the modules were evenly distributed around a mean value of 86.5 W. If we consider the higher end value (nameplate power plus tolerance) in the above calculation, then the calculated degradation rate will be higher compared to the degradation rate obtained using the lower end value (nameplate power minus tolerance). This would create a discrepancy in the calculated degradation rate which we have tried to avoid by defining the 'nominal' value of the electrical parameters. These nominal electrical parameters are calculated by taking average of the higher and lower end values of the electrical parameters. Obviously, when the module is rated at, say, +/– 3%, the nominal value is the nameplate value, but this is not the case when the rating is –0% / +5%. We have used these nominal values for the calculation of the degradation rates of the electrical parameters. Uncertainty in the nameplate value is referred to as the error due to nameplate, which can make up a significant fraction of the total error in the degradation rates for younger modules (but its effect fades as the modules' age increases). This fact is demonstrated graphically in Fig.3.4.

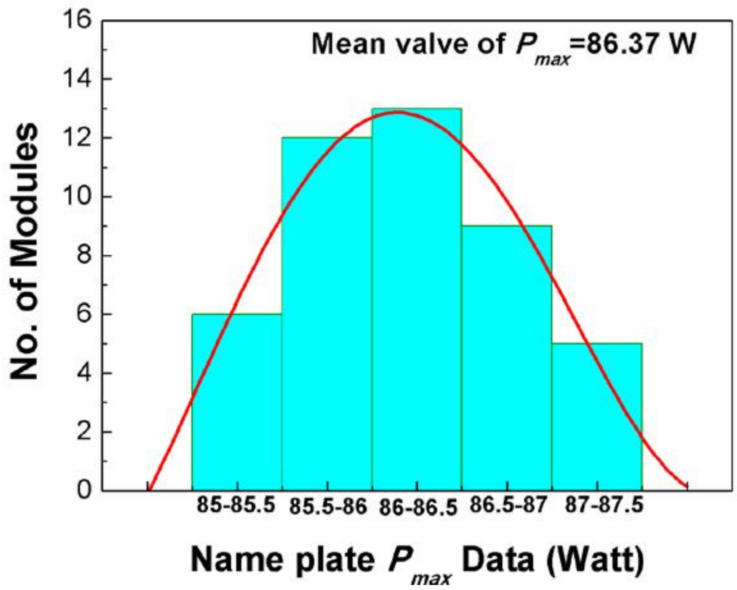

Fig. 3.3: Distribution of name plate P_{max} data of 45 number of CdTe modules.

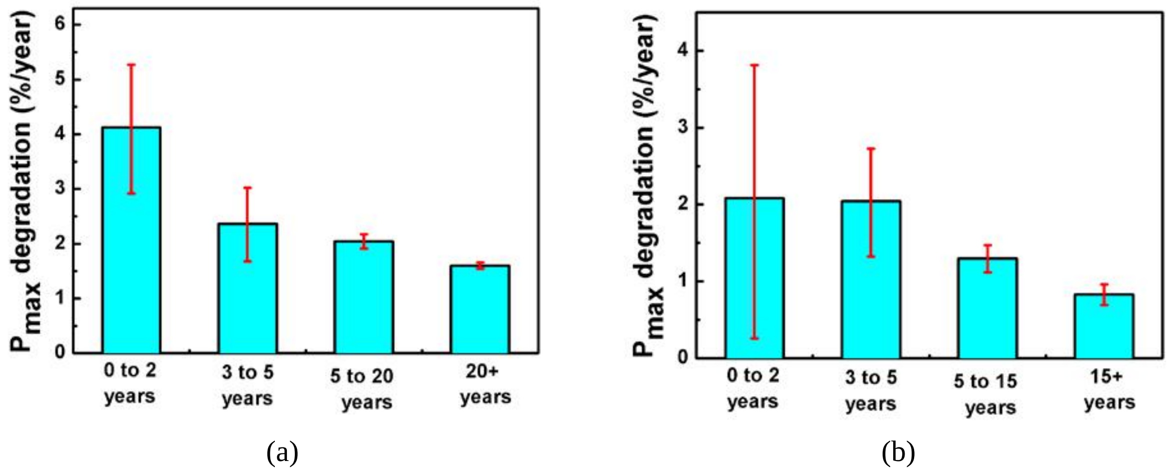

Fig. 3.4: Error due to nameplate uncertainty of ±2.5% (a) Hot zone, (b) Non hot zone

3.6 Graph Template

Figure 3.5 shows the template which will be followed for most of the graphs in this report (the values presented in this figure are indicative only). All the data points are shown clustered and usually overlapping. As already discussed, we shall use the mean value to represent the overall behaviour of the group. So each graph will show the mean value (red horizontal line), along with the associated 95% confidence interval (red diamond). As the mean and median values for most of the data sets are quite close, only the mean will be shown, except for a few exceptional cases where the median deviates from the mean by more than 30%, in which the median will also be indicated in the plot by a green horizontal line. The number in parentheses above the data points represents the number of modules or data points. We have consistently used inverted triangle symbol for data representing Indian climatic zones, diamond for the international classification and circles for the Hot and Non-Hot zone classification. Also, wherever applicable, we use hollow symbols for data points for modules of age less than 5 years, and solid symbols for age more than 5 years. Further, wherever it is deemed relevant, the following errors will be marked for each group:

a) Error due to measurement and STC correction (on right side of the plotted data, in green)

b) Error due to uncertainty in nameplate (on left side of the plotted data, in pink)

Graphs with a single data point per group (see the example of Fig. 3.6) will show the errors (a) and (b) as indicated above (i.e. error due to measurement and STC correction in green, and error due to uncertainty in nameplate in pink), but there would be no mean value or confidence interval.

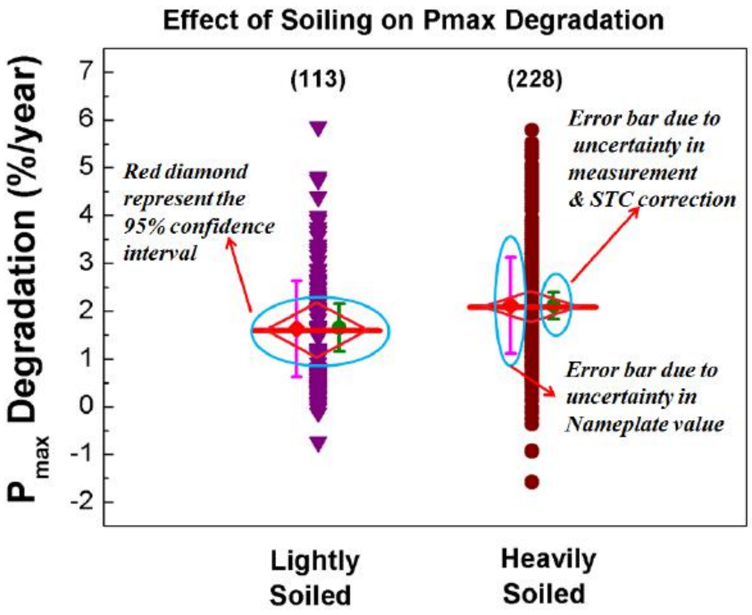

Fig. 3.5: Graph template showing various uncertainties for group of data

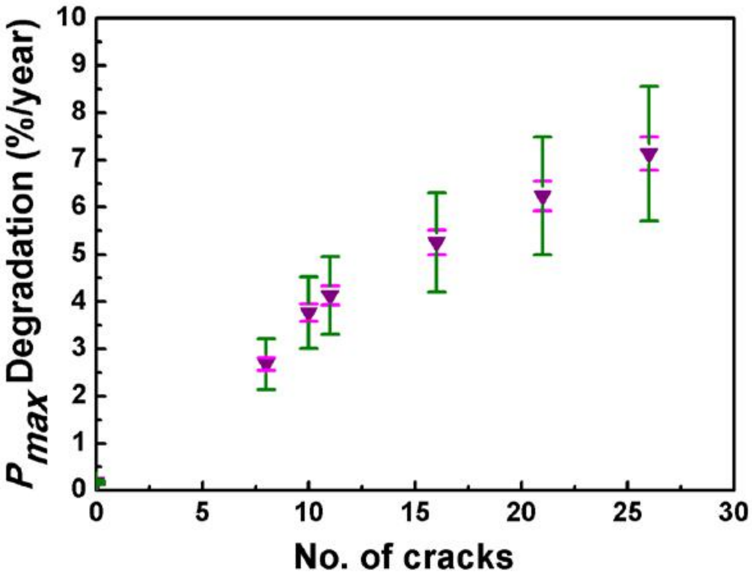

Fig. 3.6: Graph template showing various uncertainties for a single point data

3.7 Summary

We have used the STC Correction Procedure 1a (a modified version of IEC 60891 Correction Procedure 1) to translate measured field data to STC, and estimated errors due to this procedure. We have also assessed various errors originating from measurement uncertainties. The measurement and STC translation procedures together have been assessed and total error in P_{max} degradation rate has been found to be within 9% for crystalline silicon modules measured above 500 W/m^2. A further error arises due to uncertainty in nameplate rating. We have defined the ‘nominal’ power rating of the module, which will be used in place of the rated nameplate power rating (though they are often the same), for the calculation of the power degradation rates. We have laid a lot of emphasis on the errors involved, as the degradation rates calculated and presented in succeeding chapters need to be appropriately qualified.

4. Analysis of Electrical Degradation

4.1 Introduction

In recent years, the deployment of photovoltaic modules has increased significantly and hence an accurate prediction of power generated over the course of time is of vital importance. To get a good estimate of this, it is important to know the average degradation rate of the module, in terms of % power reduction per year, which quantifies the power decline with respect to time.

As explained in Chapter 3, the field measured *I-V* data of various modules is translated to standard test conditions (STC) using Procedure 1a. The extrapolated STC *I-V* data of the module enable us to compare its present-day performance with its initial performance at the time of installation (based on nameplate values), and thus calculate the percentage degradation rates of not only the maximum output power (P_{max}), but also other important electrical parameters like short-circuit current (I_{sc}), open circuit voltage (V_{oc}) and fill factor (*FF*). For those modules whose initial performance was unavailable we have used the nominal values of the electrical parameters (average of the higher and lower end nameplate values, as defined in section 3.5.3). In many cases, we have also calculated the series resistance and shunt resistance from the *I-V* curves.

The first step taken in the analysis of the electrical data is to separate out the data that is likely to have high error. Accordingly, data gathered under low irradiance conditions, below 500 W/m^2, have been removed from the electrical analysis. During our exhaustive data analysis we found that there is a wide variance in the degradation rate, and as described below in Section 4.2, it was desirable to separate out the surveyed sites into different categories – Group X, Group Y – based on their average degradation rates to draw any meaningful conclusions.

In this chapter, we present the degradation of the electrical parameters (P_{max}, I_{sc}, V_{oc}, *and FF*) with respect to climate and technology. We also present the age dependence of the P_{max} degradation rate to understand the causes behind the degradation of power in young (age less than 5years) and old (age more than 5 years) modules. Finally, we present the P_{max} degradation rate with respect to the system size in order to capture the difference in performance for large plants (more than 100kW) and small-to-medium sized installations (less than 100 kW).

4.2 Overall P_{max} Performance and Classification of Modules into Group X and Group Y

Out of the 1148 modules inspected during the survey, the *I-V* data for 161 modules were discarded due to low irradiance. From the remaining 987 modules, 221 modules (about 22 %) showed very high degradation rates in P_{max} above 6%/year, and these modules, termed 'outliers', were not taken up for further analysis as there appeared to be serious quality and other extraneous issues, such as over-rating, associated with them. Their performance is discussed separately in Appendix G. The histogram of the remaining modules showing degradation rate in P_{max} within 6%/year is shown in Fig. 4.1. There are total of 766 modules fulfilling this criterion, and the average (mean) degradation rate of P_{max} of these modules is 2.07%/year with a median value of 1.96%/year. However, it can be seen that there is a wide variability in the degradation rates. Almost 20% of the inspected modules show a degradation rate below 1%/year, and the most frequently occurring degradation rate (mode of the histogram) is 1.2%/year which is reasonably good, even though it exceeds the normal warranty (20% degradation in 25 years implying a linear degradation rate in P_{max} of 0.8%/year). It can also be seen that a significant number of modules show degradation rates which are quite high – greater that 3%/year. These observations lead us to conclude that the quality of the modules and/or installation procedures vary widely. There are 'good' sites, and there are 'problematic' ones. (Note that we cannot *a priori* distinguish between poor quality of modules used and poor transportation/installation procedures, both of which could lead to higher degradation rates.) If we wish to study, for example, the climatic dependence it would be appropriate to confine attention to the 'good' sites, so that climatic variation rather than some other extraneous parameter is captured in the analysis. This is described in detail below, which leads us to separate out the sites into Group X and Group Y sites.

To start with, we analyse the climatic variation of the 766 modules of Fig. 4.1. Figure 4.2 shows the P_{max} degradation rate in different climatic zones. From this figure we can see that there is a large variability in the performance of the modules within each climatic zone. There is no clearly discernible climatic variation, and surprisingly, we notice that the Cold & Cloudy zone shows the highest degradation rate. To understand these data better, we have plotted them separately for each module manufacturer and site, as shown in Fig. 4.3. In this figure, the x-axis represents the manufacturers (code named from A to Z to preserve anonymity) and the different sites of these manufacturers (1, 2, 3, etc.) are also mentioned at the top. For example, modules of manufacturer A were found in 2 sites, manufacturer B in 3 sites, C in 5 sites, and so on. Further, the data is colour coded to represent the different climatic zones. It can be seen that some of the sites show tightly bound degradation rates, while others show a highly dispersed rate. Further the average degradation rate of modules at a particular site varies a lot from site to site. The red horizontal bar indicates the average P_{max} degradation rate of each particular site. We therefore decided to divide the sites into two categories – Group X (sites where average degradation rate of the modules measured is less than 2%/year) and Group Y (sites where average degradation rate of the modules is more than 2%/year). The "2%/year" criterion has been chosen somewhat arbitrarily, but was guided by the fact that the average degradation rate of all modules is 2%/year, as seen in Fig. 4.1. The demarcation arising from the 2% criterion is purely empirical and therefore unbiased (we have not invoked Tier ratings or reputation of the EPC), but, as will be seen later, leads to a good appreciation of the reasons for the wide variance, an understanding of the climatic variation, and receives support from other field observations such as visual, EL, IR, etc. So, essentially we have split the dataset into sites performing (on the average) better than the overall average (Group X), and sites performing worse than the overall average (Group Y).

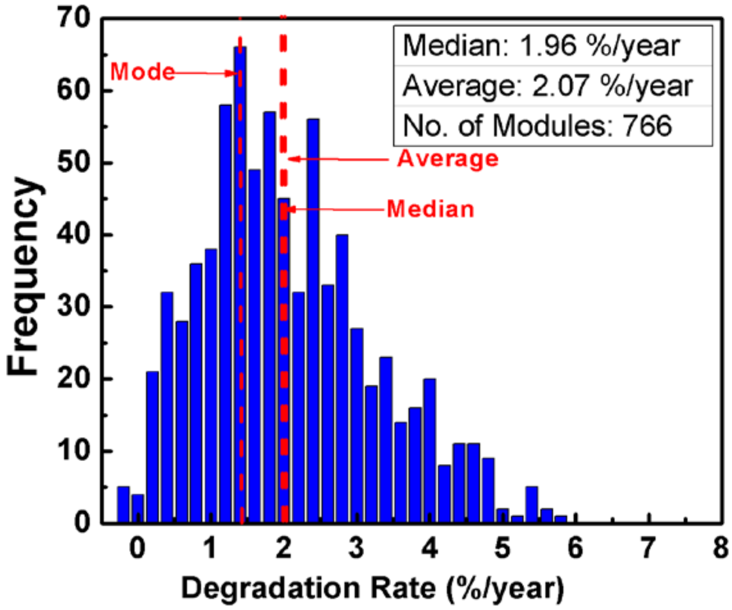

Fig. 4.1: Histogram of P_{max} degradation rate of survey data

Figure 4.4(a) shows the histogram of power degradation rate for modules in Group X sites. We can see that the average and median are equal to 1.33%/year and 1.32%/year respectively. Also, almost 85% of the modules have degradation rate below 2%/year. A total of 386 modules fall in this group, which represents 33% of all the surveyed modules, and about 50% of the 766 modules taken further for detailed electrical characterization. On the other hand, Fig. 4.4(b) shows the histogram of the power degradation rate for modules in Group Y sites, where we can see that the average and median degradation rates are about 2.75%/year with almost 25% of the modules showing degradation rate above 4%/year. This group of sites shows relatively poorer performance, and the possible reasons may be poor quality of raw materials used, poor manufacturing process, poor transportation, poor installation practices and/or other issues. (Many of these aspects will be explored further in subsequent chapters.) Since the modules from Group X sites show less variation, and further we believe that these are modules from 'good' sites, it is appropriate to perform a climatic variation for these modules, since other extraneous factors like manufacturing quality and installation procedures will tend to get factored out. On the other hand, the climatic variations of modules in Group Y sites are unlikely to capture the intrinsic effect of climate. We have performed technology and age variation analysis for both modules in Group X sites as well as 'All' modules (that is, modules in Group X plus Group Y). Similarly, in subsequent chapters, we look at 'All' modules or only Group-wise modules as deemed appropriate. We will often refer to modules in Group X sites as 'Group X modules', and modules in Group Y sites as 'Group Y modules' for brevity.

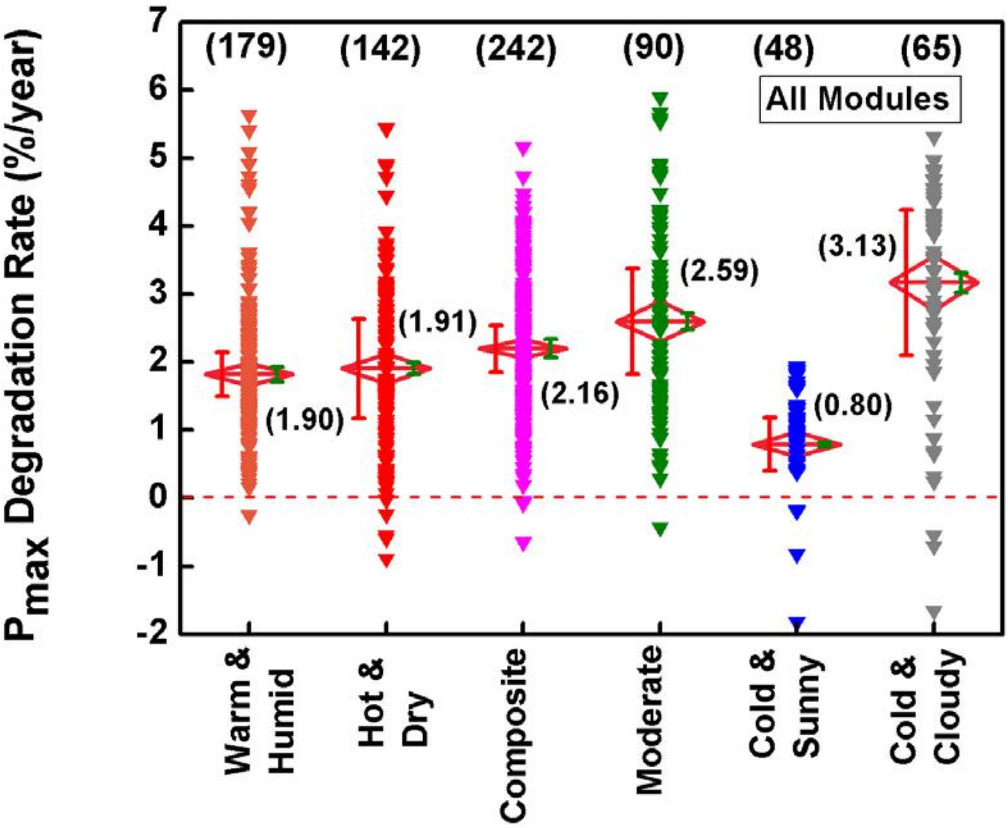

Fig. 4.2: Comparison of P_{max} degradation rate of survey data in different climatic zone

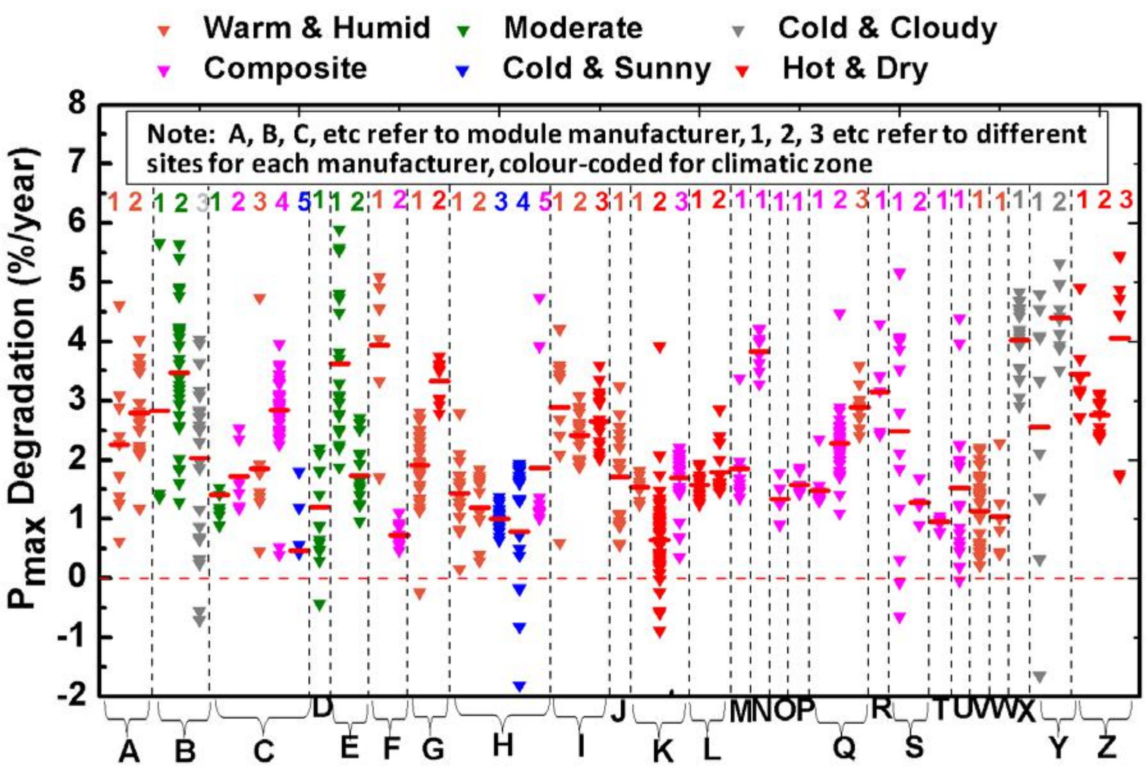

Fig. 4.3: Manufacturer wise and site wise P_{max} degradation rates

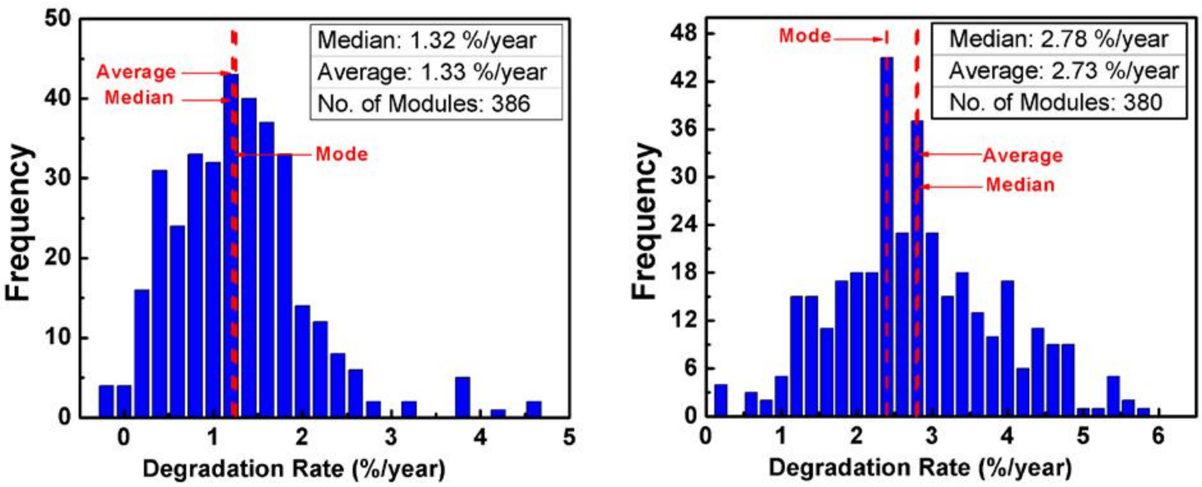

(a) (b)

Fig. 4.4: Histogram of P_{max} degradation rate of (a) Group X modules and (b) Group Y modules

4.3 Climatic Zone Variation

Since the degradation behaviour of PV module is heavily dependent on the climate [1], we shall first discuss the degradation rates of *I-V* parameters with respect to the climatic zone. As mentioned previously, we will focus on the climatic variation analysis for Group X modules. Initially, we present the P_{max} degradation rate with respect to the six-zone classification system of India suggested by Bansal and Minke [69]. We have colour-coded these six climatic zones, using orange for Hot & Humid, red for Hot & Dry, green for Composite, magenta for Moderate, blue for Cold & Sunny and grey for Cold & Cloudy. In order to understand the effect of high climatic temperatures on the P_{max} degradation rate, we have sometimes clubbed together Warm & Humid, Hot & Dry and Composite zones into 'Hot' zones and Cold & Sunny, Cold & Cloudy and Moderate zones into 'Non-Hot' zones. We shall therefore also present the P_{max} degradation rate with respect to Hot and Non-Hot climatic zones. Finally, for completeness, we also show the P_{max} degradation rate with respect to the internationally accepted Koppen-Geiger climate classification system. Besides the P_{max} degradation rate, we also present the various other *I-V* parameter degradation rates as a function of climate zone.

In all the figures shown in these sections we have used the mean (or average) to represent our data set which is shown by a red horizontal line. Furthermore, error due to measurement and STC correction (green error bar on right side) and error due to uncertainty in name plate (pink error bar on left side) have been shown. The red diamond represents the 95% confidence interval. The numbers in parentheses at the top are the number of data points (modules) in that category. We have consistently used inverted triangle symbol for data representing Indian climatic zones, diamond for the international classification and circles for the Hot and Non-Hot zones. We have used hollow symbols for modules whose age is less than 5 years and solid symbols for age more than 5 years.

4.3.1 Influence of Climate on P_{max} Degradation

The power degradation rate (%/year) of the Group X modules with respect to the six-zone climatic classification system has been shown in Fig. 4.5. It is seen that the degradation in power is highest in Warm & Humid climate and least in Cold climate. The reason may be that discoloration, delamination and corrosion of interconnects, which are all important causes of degradation in power, are accelerated at higher temperatures and humidity. Also, compared to Fig. 4.2, it is seen that the P_{max} degradation rate data are more tightly bunched for the Group X modules, and this lends confidence to our assertion that climatic variations are well captured by Group X. For comparison, we show also the climatic variation of Group Y modules (see Fig. 4.6), where no clear trend emerges, and it does appear as though climatic variations are masked by other variations which also lead to high dispersion within each climatic zone.

Figure 4.7 shows the power degradation rate of the Group X modules with respect to Hot and Non-Hot zones. From this figure we again see (in a more succinct manner) that modules in the Hot zones are degrading at a faster rate than the modules deployed in the Non-Hot zones. This is in agreement with the results of Tamizhmani [17] who has shown similar trends for hot zones versus other climatic zones in USA. Figure 4.8 shows the power degradation rate of the Group X modules with respect to Koppen-Geiger climate classification system. We can see that modules in Tropical Dry winter followed by Arid Hot steppe shows higher values of P_{max} degradation rate, which again highlights the fact that the modules in the hot climates are degrading at a faster rate.

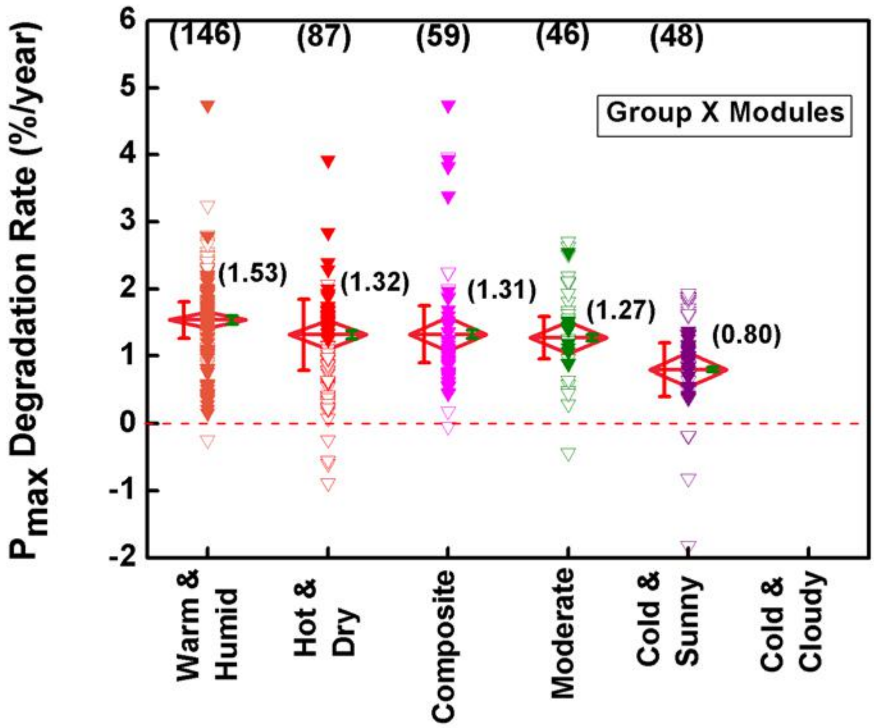

Fig. 4.5: Comparison of P_{max} degradation rate with respect to six-zone classification system for modules in Group X sites

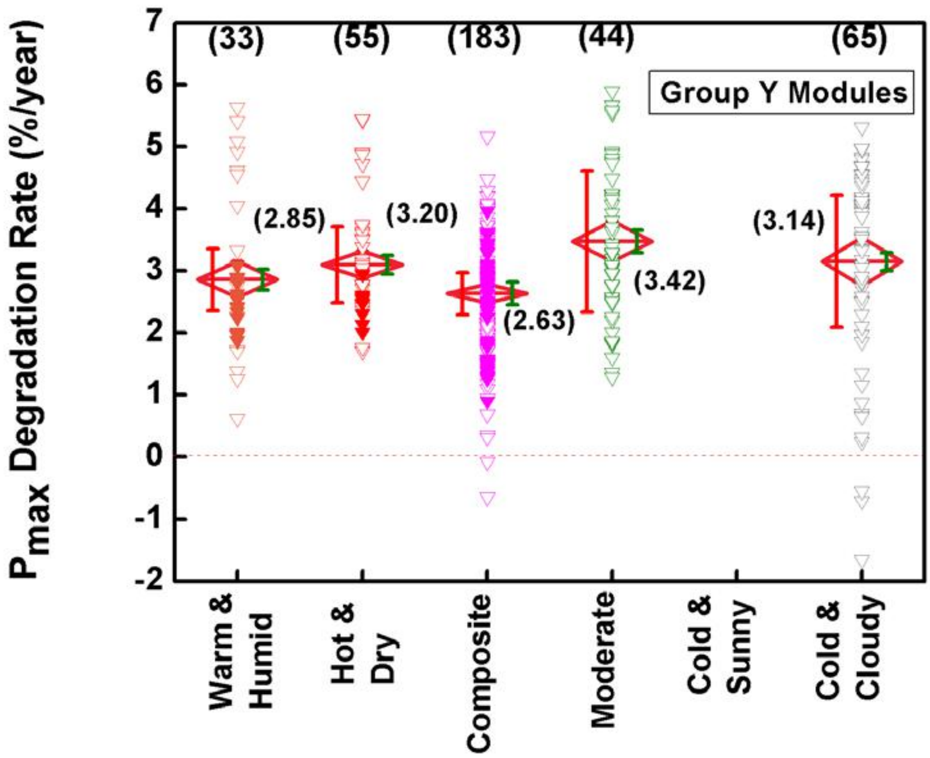

Fig. 4.6: Comparison of P_{max} degradation rate with respect to six-zone classification system for modules in Group Y sites

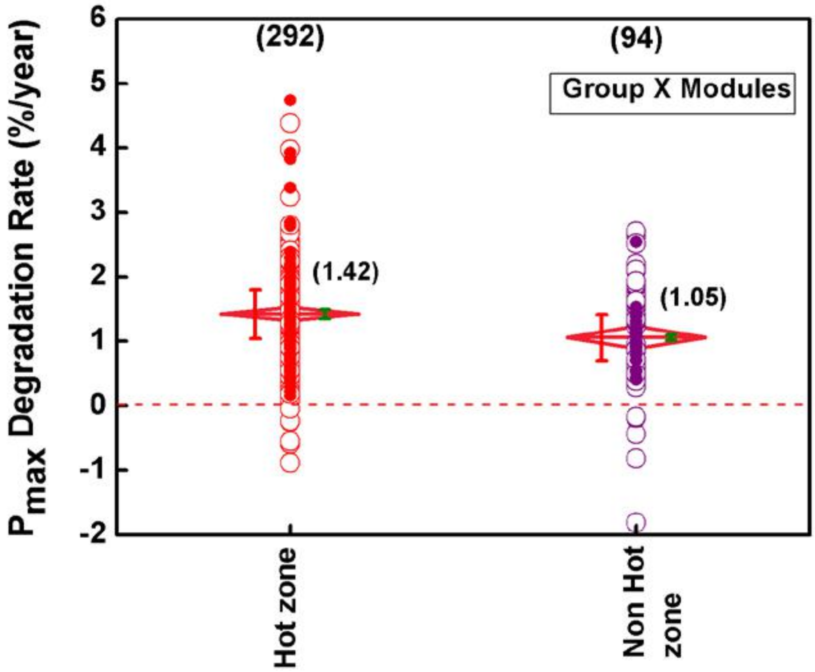

Fig. 4.7: Comparison of P_{max} degradation rate with respect to Hot and Non-Hot zones for Group X modules

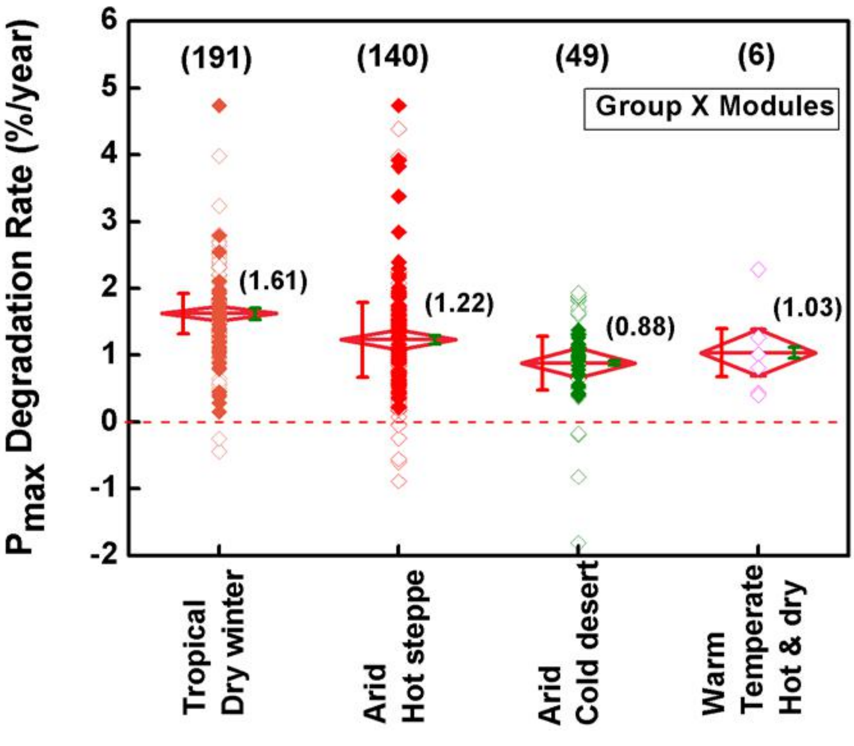

Fig. 4.8: Comparison of P_{max} degradation rate with respect to Koppen-Geiger climate classification for Group X modules

4.3.2 Influence of Climate on *I-V* Parameters (I_{sc}, V_{oc} & *FF*)

The climatic-zone distribution of degradation rates for the various *I-V* parameters (P_{max}, I_{sc}, V_{oc} and *FF*) for Group X modules is shown in Fig. 4.9. For most climate zones I_{sc} degradation is the largest contributor to P_{max} degradation. It is clearly seen that the I_{sc} degradation rate for all Hot zones is high. This is likely due to the high temperatures seen in these zones, leading to increased EVA browning which manifests itself in high I_{sc} degradation. In the Warm & Humid zone, the major contributor to P_{max} degradation is increase in *FF*, probably due to increased series resistance caused by metal corrosion. These correlations are described in detail in Chapter 6.

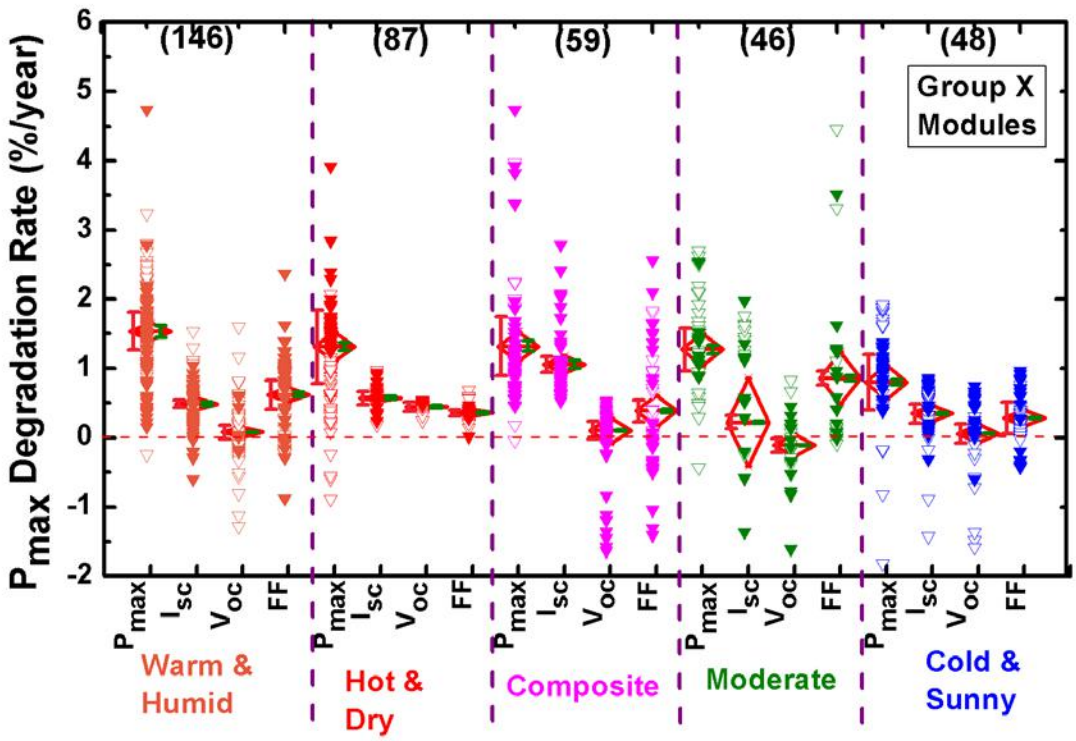

Fig. 4.9: *I-V* parameter degradation distribution with respect to six-zone classification system for Group X modules

4.4 Technology Based Variation

4.4.1 Influence of Technology on P_{max} Degradation

Figure 4.10 shows the P_{max} degradation rate per year for different technologies for Group X modules. From the figure we can see that multi crystalline silicon is degrading slightly faster than mono crystalline silicon modules. Among the thin-film modules, we note that CdTe modules are degrading least. Among all technologies, we see that HIT modules are performing the best, though the number of HIT modules surveyed is too small to assert this conclusively. Figure 4.11 shows the P_{max} degradation per year for different technologies for 'All' modules (including both Group X and Group Y). (Note that we have not used colours here since the technologies are not differentiated by climatic zone, though of course, it begs the question whether a preponderance of some technology in a particular climatic zone is skewing the data.)

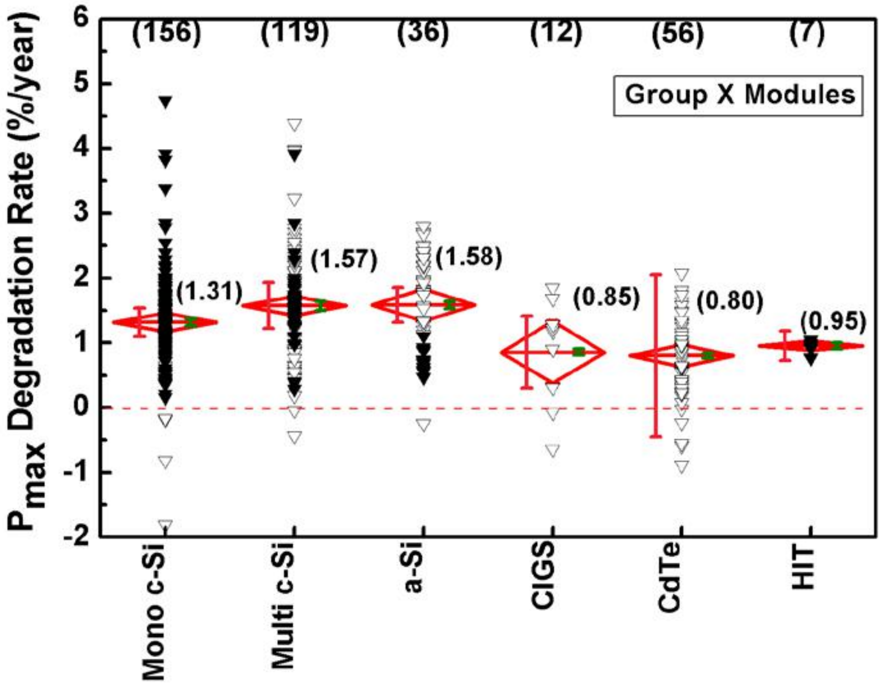

Fig. 4.10: P_{max} degradation per year for different technologies for Group X modules

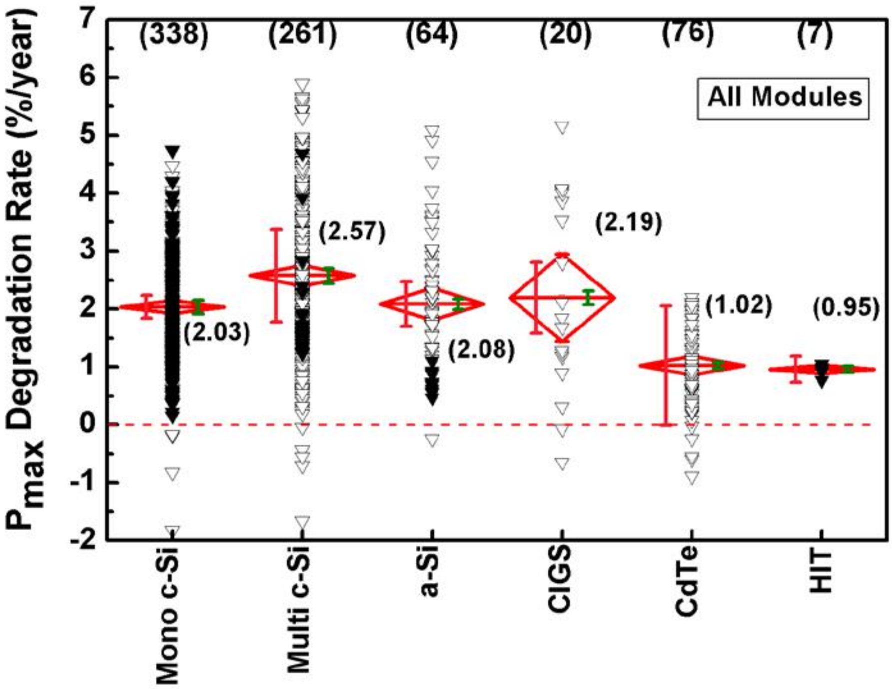

Fig. 4.11: P_{max} degradation per year of different technologies for 'All' modules

4.4.2 Influence of Technology on *I-V* Parameters (I_{sc}, V_{oc} and *FF*)

Also of interest is to understand how *I-V* parameter degradation differs by technology. Figure 4.12 shows P_{max}, I_{sc}, V_{oc} and *FF* degradation for c-Si and thin-film categories for Group X modules. From the figure it is quite evident that for crystalline silicon modules P_{max} degradation is mainly due to degradation in I_{sc}, followed by *FF*. On the other hand, the for the thin film modules, P_{max} degradation is mostly associated with the degradation in *FF* followed by I_{sc}. For both cases, V_{oc} contributes very little. These points will be discussed later in Chapter 6. Figure 4.13 shows P_{max}, I_{sc}, V_{oc} and *FF* degradation for c-Si and thin-film modules in 'All' categories, which yields similar conclusions.

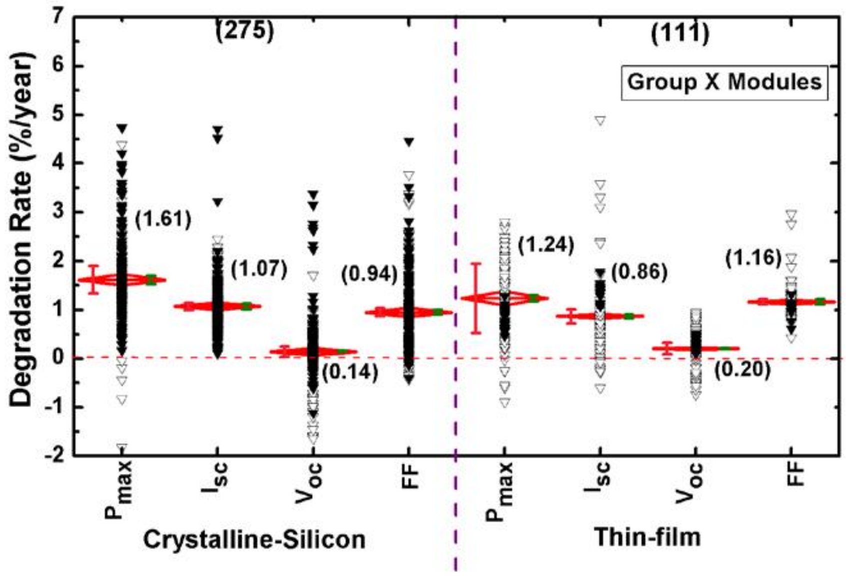

Fig. 4.12: P_{max}, I_{sc}, V_{oc} and *FF* degradation of different technologies for Group X modules

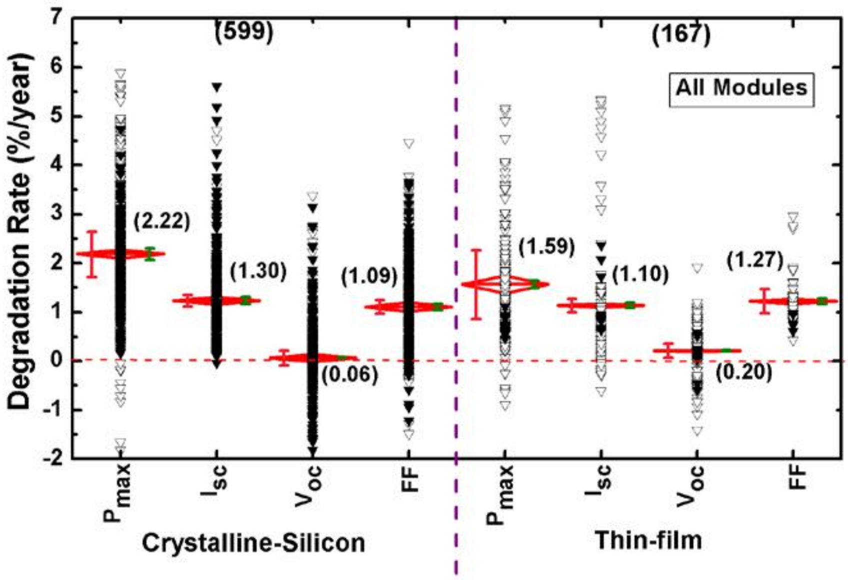

Fig. 4.13: P_{max}, I_{sc}, V_{oc} and *FF* degradation of different technologies for 'All' modules

4.5 Age Based Variation

In order to ascertain the effect of age on the P_{max} degradation rate (% per year), we separated out the modules into young (< 5 years old) and old (> 5 years old) categories. Since we had very few thin film modules in the old age category, we have confined our analysis of age variation only to crystalline silicon modules. Figure 4.14 shows the effect of age of module on the degradation of the *I-V* parameters of the crystalline silicon modules from Group X sites. From the figure we can say that the young modules are degrading slower than the old modules. This perhaps reflects the improvements in technology over the years. Also, it is seen from the figure that the degradation in power for young modules is more due to degradation in fill factor (*FF*), followed by degradation in short circuit current (I_{sc}). However, for the old modules, the degradation in P_{max} is more due to degradation in I_{sc}, than *FF*. This is an interesting distinction, which seems to point to the fact that old modules appear to degrade mainly due to EVA browning which reduces I_{sc}, whereas young modules degrade due to increase in *FF*, possibly caused by cracks generated during installation.

Figure 4.15 shows the effect of age on the degradation of the *I-V* parameters of 'All' (Group X plus Group Y) crystalline silicon modules. Here, in clear contrast to the observation for Group X modules, the degradation in P_{max} is *higher* for young modules. Again we can notice that degradation in power for young modules is due to fill factor (*FF*), whereas for old modules, degradation in I_{sc} dominates. *FF* degradation can be ascribed to cracks caused by poor installation. The picture which emerges is that for the 'good' Group X modules, improvements in technology are resulting in lower degradation rates for young modules compared to old modules, even though we do see a problem in *FF* due to cracks. When "All" modules are considered, young modules are seen to degrade faster than old modules. While this may be due to the well-known higher initial degradation, rates, the contrast with Group X modules also seems to point to poor quality and/or installation of the young modules (due to aggressive pricing and rush to meet installation targets). One may also notice the larger dispersion in young modules compared to old modules in Fig. 4.15, which again suggests quality issues.

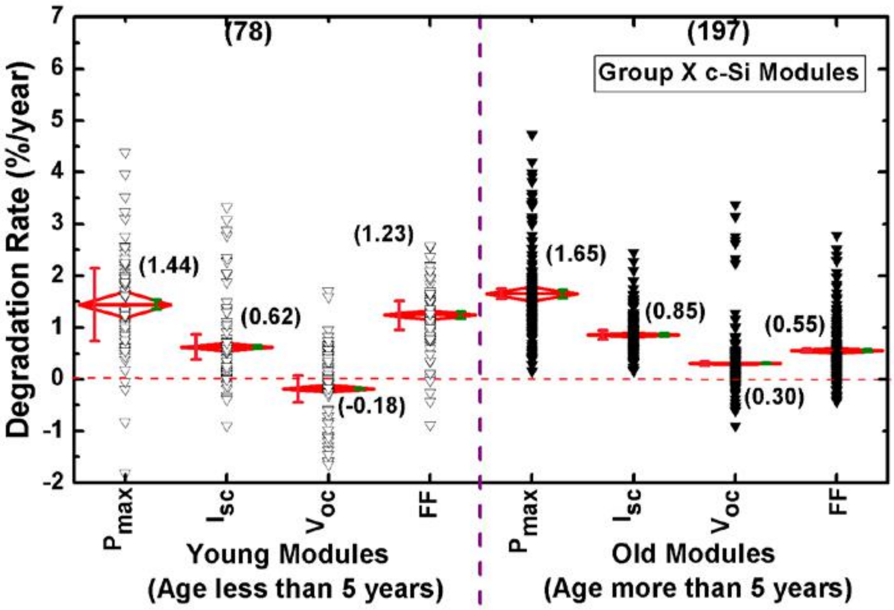

Fig. 4.14: Age variation on P_{max}, I_{sc}, V_{oc} and *FF* degradation for crystalline silicon of Group X modules

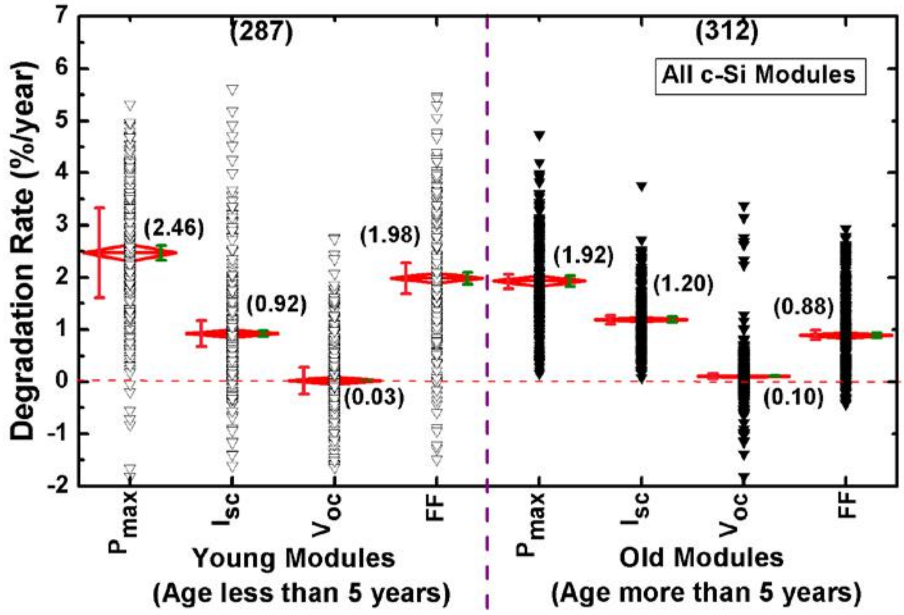

Fig. 4.15: Age variation on P_{max}, I_{sc}, V_{oc} and *FF* degradation for crystalline silicon of 'All' modules

4.6 System Size and Installation Based Variation

In order to understand the effect of the type and size of the PV installation on the P_{max} degradation rate of the modules, we separated out the sites surveyed into two categories – small/medium size (less than or equal to 100 kW) and large size (greater than 100 kW capacity). The reason for choosing 100 kW as a demarcation can be explained from Fig 4.16, which shows the average P_{max} degradation rate for different sites of 'All' modules with respect to respective system size. From the figure we notice that the data is concentrated on either side of 100 kW, which makes this value a suitable demarcation line for the analysis.

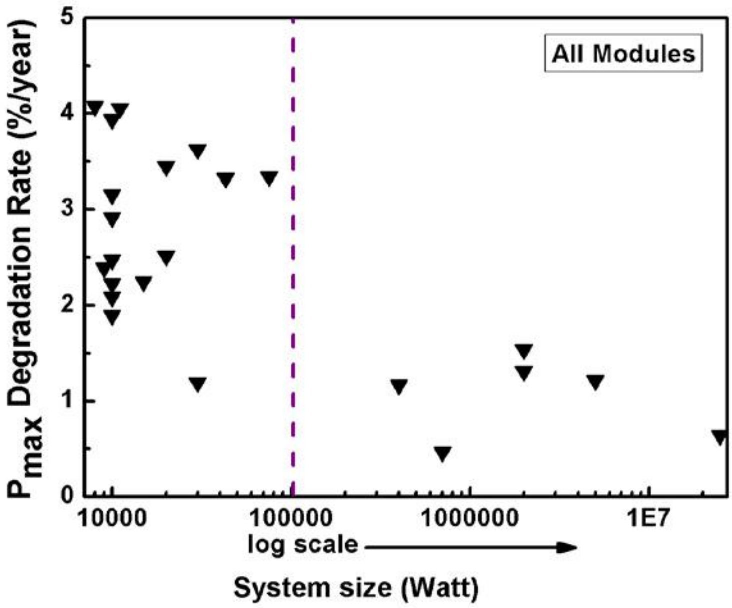

Fig. 4.16: Average P_{max} degradation rate of 'All' modules with respect to system size

Figure 4.17 shows the P_{max} degradation rate for these categories. From the figure, we can clearly say that modules installed in large PV systems (including large MW scale plants) are performing much better, and degrading at a much lower rate than the modules in the smaller installations. The 0.97%/year value seen for the large installations is near international norms. Another important point to note is that all the large systems fall in the Group X category. We have also tried to capture the effect of roof mounted versus ground mounted installations on the P_{max} degradation rate. Figure 4.18 shows the P_{max} degradation rate for roof and ground mounted modules, and from the figure it is seen that ground mounted modules are degrading at a lower rate than the roof mounted panels for the small/medium size category (we do not have any roof mounted large installation in our survey). This is not unexpected, and may be due to the fact that roof mounted modules tend to run hotter than ground mounted modules.

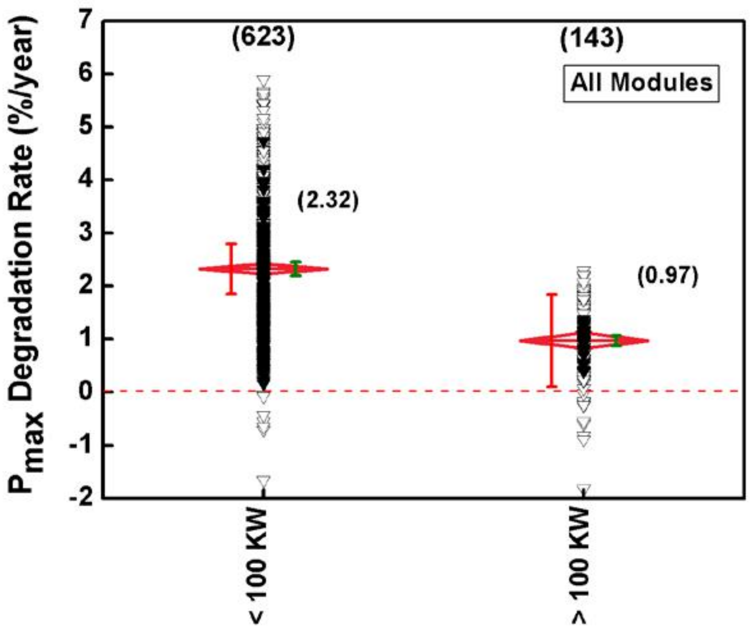

Fig. 4.17: Effect of system size on P_{max} degradation for 'All' modules

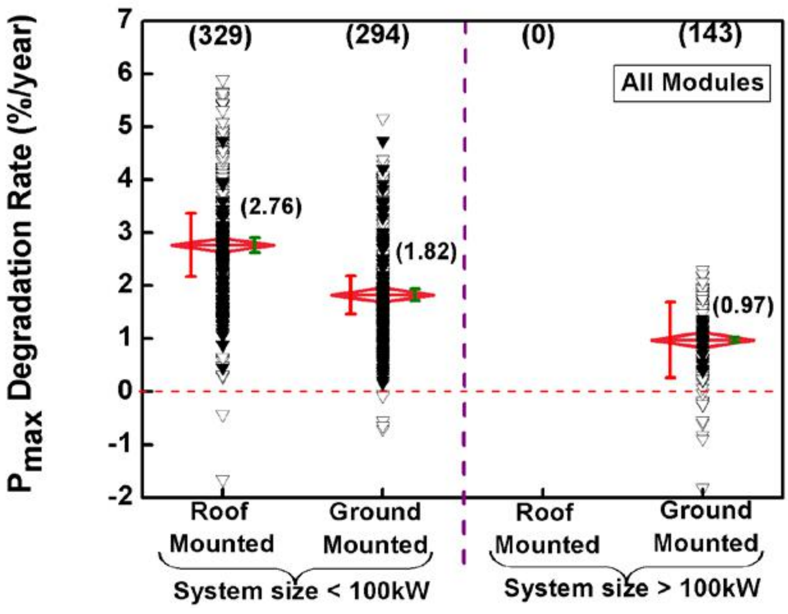

Fig. 4.18: Effect of installation type on P_{max} degradation for 'All' modules

It is comforting to know that the large ground mounted installations (which includes MW scale plants) have good performance and are all Group X sites. However, since 40% of India's 100 GW target is to be met by rooftop installations (which will often be small), there would appear to be a need to exercise care in this segment going forward.

4.7 Summary

From the electrical degradation analysis we can draw the following conclusions:

- There is a lot of variability in performance. Some modules (Group X) are performing well, whereas others (Group Y) are not. Some sites show excellent international-level performance, whereas some show grave problems. These observations point to issues regarding module quality and/or installation procedures.
- Modules in Hot zones (Hot & Dry, Warm & Humid and Composite) show higher degradation rates than the modules in Non-Hot zones (Moderate, Cold & Cloudy and Cold & Sunny). This warrants more attention to understanding the hot climate degradation modes, as well as accelerated testing and appropriate certification for these climates.
- In Group X, young modules (age <5 years) show a lower degradation rate than old modules (age >5 years). However, if 'All' modules are considered, young modules show a higher degradation rate than old modules. This indicates that young modules seem to suffer a significant problem in quality of modules and/or installation.
- In old crystalline silicon modules the main contributor to the P_{max} degradation is I_{sc} followed by *FF*, whereas in the case of young crystalline silicon modules the main contributor to the P_{max} degradation is *FF* followed by I_{sc}.
- For thin-film modules *FF* is the main contributor to the P_{max} degradation followed by I_{sc}, whereas for crystalline silicon modules, it is the other way around.
- Modules installed in large systems (size more than 100 kW) are degrading at a much lower rate (~ 1%/year) than modules installed in small systems of size less than 100 kW. All large systems fall in the 'good' Group X category.
- Roof mounted modules suffer from a higher degradation rate as compared to ground mounted modules. This needs special attention as 40 GW are planned to be installed on rooftops.
- Overall variability of module and installation quality is a cause for concern.

5. Analysis of Dark *I-V*, Insulation Resistance and Interconnect Breakage Data

5.1 Introduction

For assessment of the degradation of components of the PV modules, some additional tests have been performed like dark *I-V*, insulation resistance test, and interconnect breakage test have been performed. Dark *I-V* is one of the commonly used characterization tools for assessment of degradation in the semiconductor device (solar cell). It provides a good insight into the quality of the solar cell, and also about the contacts, series resistance and shunt resistance. High insulation resistance is an important safety criterion for PV modules, particularly in high voltage systems like in PV power plants. Interconnect breakage test provides information about the discontinuity in the cell or string interconnects which may be caused by corrosion or thermal fatigue in the module.

In this chapter, we will present the analysis of the dark *I-V* data, in terms of degradation in the ideality factor of the solar cell, with respect to age and climatic zone. We shall also correlate the P_{max} degradation with degradation in the ideality factor. We will then present the analysis of the insulation resistance with respect to Group X and Group Y modules and also with respect to small/medium and large systems. Finally we shall present the correlation of series resistance and P_{max} degradation with the number and extent of interconnect breakage in the PV modules.

5.2 Analysis of Dark *I-V* Data

Dark *I-V* characterization was done in the field by covering the module by with a black cloth and then sweeping the voltage from zero to the open circuit voltage and measuring the output current. The dark *I-V* of the module thus obtained was converted into the dark *I-V* of an equivalent solar cell by dividing the voltage (at each *I-V* data point) by the number of cells in the module [25]. Figure 5.1 graphically demonstrates the concept of dark *I-V* of the equivalent cell. The advantage of applying this technique is that it enables us to directly use the one diode model to obtain the dark *I-V* parameters such as ideality factor (n) and reverse leakage current (J_o) [22]. This technique to obtain the dark *I-V* parameters has been examined in detail and discussed separately in Appendix H.

5.2.1 Correlation of Ideality Factor with Age

The ideality factor n of the equivalent cell is calculated at the maximum power point. Figure 5.2 shows the variation in ideality factor with age. From the plot, we can see that the ideality factor n increases with increase in age of the module. This indicates that the solar cell or the effective series resistance (which will affect n) degrade over the years. This increase in ideality factor n is a reasonable expectation because as the age of the diode increases, its characteristics degrade and/or the series resistance increases, and hence its ideality factor increases. From Fig 5.3 (a) we can see that the series resistance for the modules (calculated as described later in Section 5.4.2) also increases with age in a manner similar to that of n, so it is likely that at least a part of the reason is indeed increase in series resistance. Fig. 5.3 (b) shows the relation between series resistance and ideality factor n.

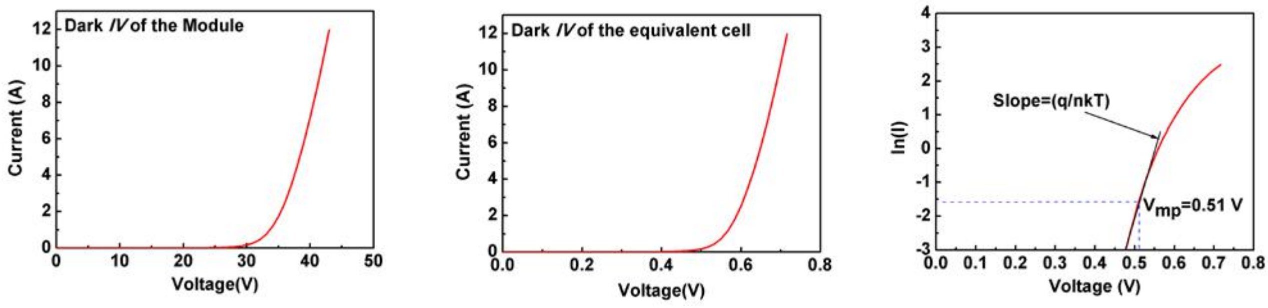

(a) (b) (c)

Fig. 5.1: (a) Measured dark *I-V* of the module and, (b) dark *I-V* of the equivalent cell obtained by dividing the module *I-V* voltages by number of cells (here 60), (c) ln(*I*) vs. voltage plot, showing also the tangent at V_{mp}, from which *n* can be found.

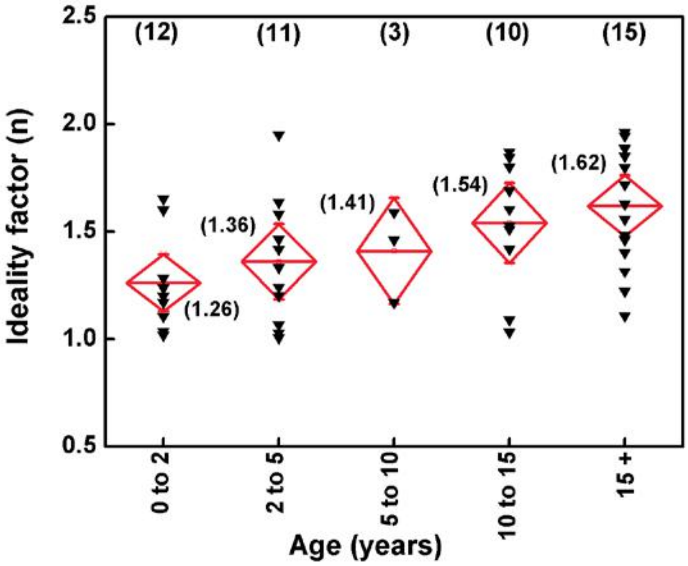

Fig. 5.2: Correlation of ideality factor *n* with age. The red diamond represents the 95% confidence interval.

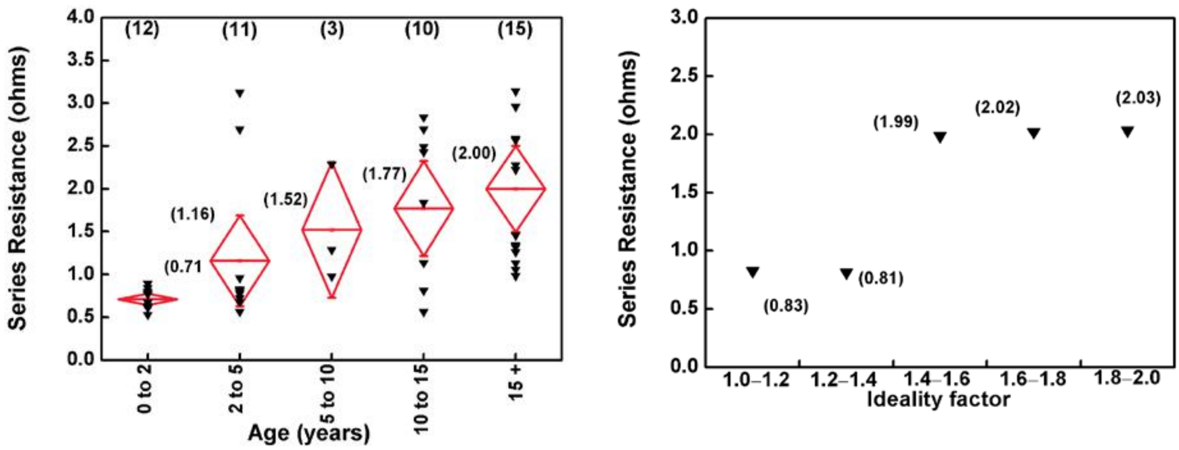

(a) (b)

Fig. 5.3: Correlation of (a) series resistance with age and (b) series resistance with ideality factor. The red diamond represents the 95% confidence interval.

5.2.2 Variation of Ideality Factor with Climate

Figure 5.4 shows how the age-averaged ideality factor *n* varies with respect to Hot and Non-Hot Zones. It is evident from the figure that the modules in the Hot zones have a slightly higher value of *n* as compared to modules in Non-Hot zones. A possible reason for the slightly higher ideality factor in the Hot zones may be that higher operating temperatures accelerate device degradation or increase the series resistance due to enhanced corrosion. The high value of ideality factor causes decrease in the value of the *FF* and eventually results in the degradation in P_{max} [23]. However, it should be noted that our data set for *n* is small, so reaching a definitive conclusion for climatic zone variation is difficult.

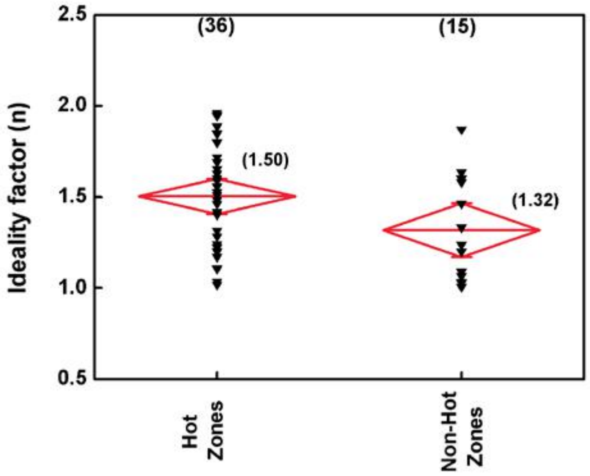

Fig. 5.4: Correlation of ideality factor with respect to Hot and Non-Hot zones. The ideality factor is averaged over all ages. The red diamond represents the 95% confidence interval.

5.2.3 Correlation of Ideality Factor with P_{max} Degradation

Figure 5.5 shows the correlation between the ideality factor *n* and the (total) percentage P_{max} degradation for 'All' (Group X and Group Y) modules. An increase in *n* causes a decrease in the *FF* value which finally decreases the power output of the module. Hence it clearly correlates the power output of the module with the quality of the semiconductor device and/or series resistance.

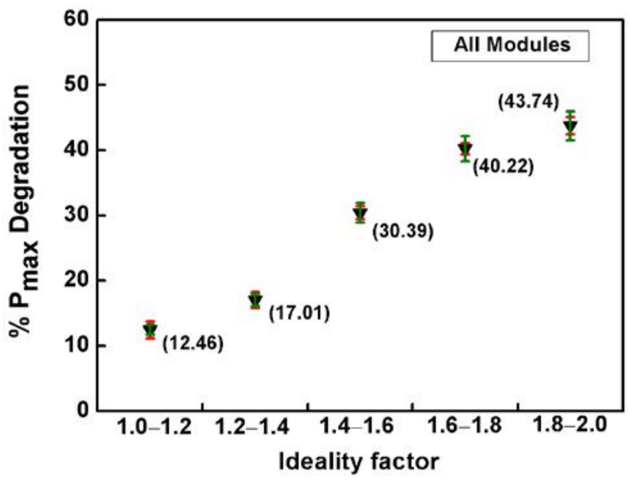

Fig. 5.5: Correlation of ideality factor *n* with the percentage P_{max} degradation.

5.3 Analysis of Insulation Resistance Data

Insulation resistance of the PV modules was measured by using a Fluke Insulation Tester. The output terminals of the module were shorted and connected to the positive terminal of the instrument, while the negative terminal of the instrument was connected to the frame of the module. The dry insulation resistance was measured in this manner. For the wet insulation resistance, the top glass of the module was fully covered by a wet cloth. This procedure for the wet insulation test differs from the IEC prescribed method which is used for indoor testing and certification of modules. In the IEC 61215 test procedure, the wet insulation resistance is measured by submerging the module in water. Since our wet insulation resistance measurement is not as per the IEC procedure, the analysis of the data can give us only qualitative information (which may not be comparable to the IEC standard).

5.3.1 Analysis of Dry Insulation Resistance

As per the IEC 61215 standard, the criterion for passing the dry or wet insulation test is that the product of insulation resistance and area of the module be more than 40 MΩ m^2 (for module area more than 0.1 m^2). From Fig. 5.6(a), we can say that 95% of the surveyed modules in all the categories (All, Group X and Group Y) have passed the dry insulation test. Also, from Fig. 5.6(b) we notice that more than 90% of both the young and old modules have passed the dry insulation resistance test. However, a higher percentage of young modules in 'not-so-good' Group Y have failed in this test as compared to the 'good' Group X.

5.3.2 Analysis of Wet Insulation Resistance

In the field we have also measured the wet insulation resistance value of the modules by putting a wet cloth over the PV modules. From the analysis, we have noticed that more than one-third of the modules have failed the wet insulation resistance test in all the categories (All, Group X and Group Y) and in all the age groups, if we use the same criteria as IEC 61215. However, as stated earlier, it must be noted that our wet insulation resistance measurement by covering the module with wet cloth is not as per the IEC procedure (which requires measuring insulation resistance by submersing the modules in the water tub). Hence, we would not like to project any definitive conclusion based on our wet insulation test results.

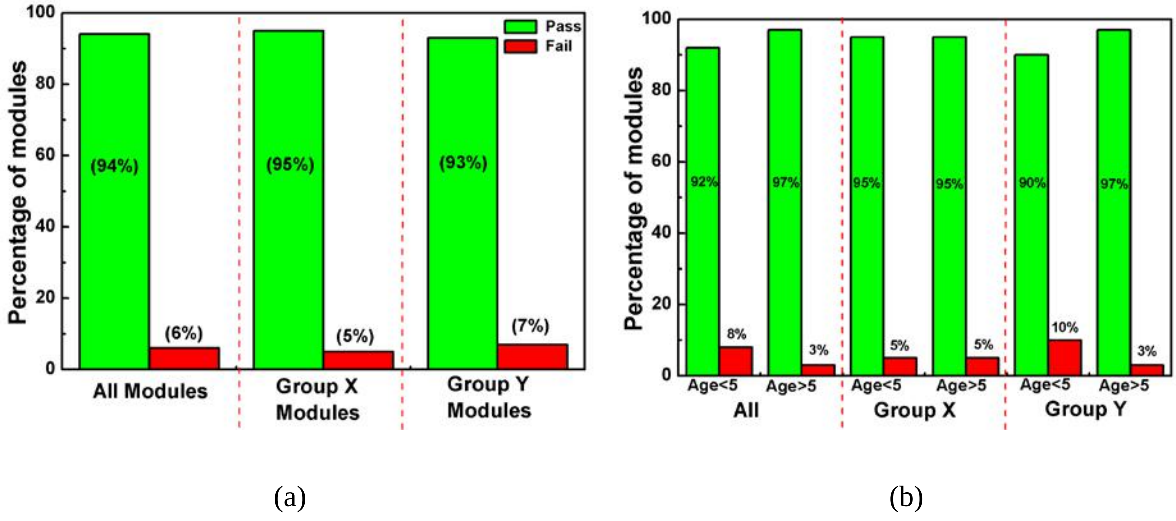

Fig. 5.6: (a) Percentage of modules passed or failed in the dry insulation resistance test for different groups – All, Group X, and Group Y, and (b) percentage of modules passed or failed in dry insulation resistance test for 'All', Group X, and Group Y modules for young and old category

5.3.3 Analysis of Insulation Resistance with respect to System Size

Figure 5.7 shows the percentage of modules passed or failed in the dry insulation resistance test for small/medium systems (size less than 100 kW) and large systems (size more than 100 kW). It is evident that the modules in large installations are performing better than small/medium installations, and 100% of the modules in the large installations have passed the dry installation test, which is indeed good news. From the analysis of the wet insulation test data, we have found that 37% of the modules in the small/medium installations have "wet cloth insulation resistance" lower than 40 $M\Omega m^2$ while only 14% of the modules in the large installations have this problem. Thus modules in large installations are, in general, better as compared to small/medium installations vis-à-vis insulation resistance.

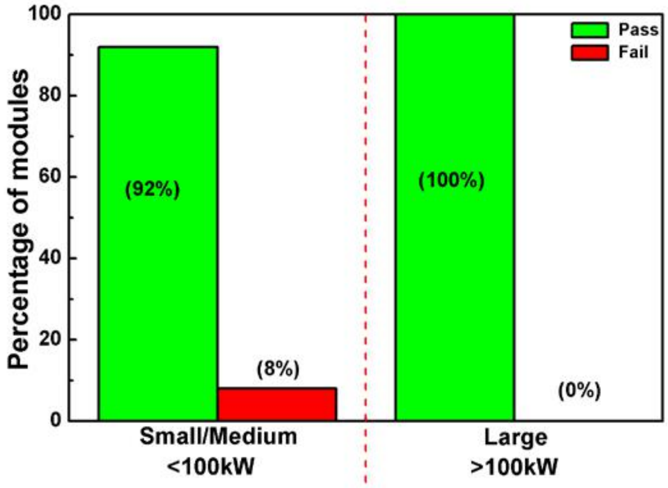

Fig. 5.7: Percentage of module passed or failed dry insulation resistance test for small/medium and large installation

5.3.4 Correlation of P_{max} Degradation with Insulation Resistance

Figure 5.8 shows that the P_{max} degradation rate (%/year) increases with decrease with dry insulation resistance for 'All' modules. This clearly indicates the correlation of the output power degradation of the PV modules with the material quality. Also, obviously, poor insulation resistance may result in safety related issues.

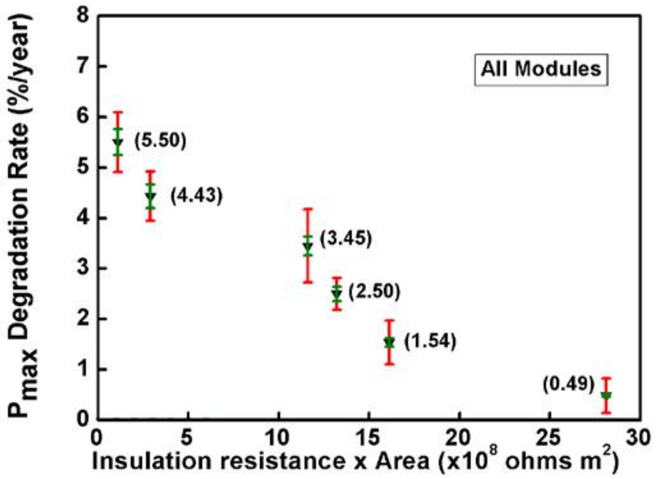

Fig. 5.8: Correlation of P_{max} degradation rate (%/year) with insulation resistance for 'All' modules.

5.4 Analysis of Interconnect Breakage Data

Interconnects provide electrical connection between the cells and conduct the electrical power to the external load from the cells in the PV module. Usually there are 2 or 3 interconnects in each cell, which provide necessary redundancy in case of breakage in any part of the interconnect. However, if there is a breakage even in one interconnect, the whole cell's current would have to be conducted by the other interconnects in the cell, leading to current crowding, which increases the series resistance of the module, thereby degrading the fill factor and the power output. During the survey, interconnect breakage has been tested using the Togami Cell Line Checker. The point where the interconnect breakage was obtained was marked with a red marker pen on the module. If the breakage is at a single point, then it is termed as point breakage, and if it continues over a length of the busbar then it is termed as line breakage. Figure 5.9 shows some examples of point breakage and line breakage. Severity in interconnect breakage is defined as the ratio of number of cells affected by the interconnect breakage to the total number of cells in the module.

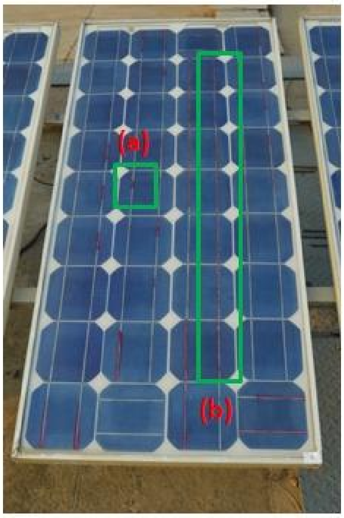

Fig. 5.9: (a) Point breakage and, (b) line breakage

5.4.1 <u>Analysis of Interconnect Breakage with respect to Climatic Zone</u>

Table 5.1 shows the percentage of modules affected by interconnect breakage in different climatic zone in all age categories. This table has been colour coded for ease of understanding, where green is used for low values (percentage of affected modules is less than 33%), orange for medium values (affected modules between 33% to 66%) and red for high values (more than 66% modules affected). From the table we can see that modules in Warm & Humid zone are affected the most as compared to the other climatic zones. The reason for high interconnect failure in this climatic zone is likely to be due to corrosion in interconnect which is accelerated in humid environments. Also, the percentage of modules affected by interconnect failure in young modules is relatively high even in the Hot & Dry climatic zone. Thermal cycling could be the probable reason for this. From this table we can conclude that the percentage of modules having interconnect breakages is more in Hot zones as compared to the Non-Hot zones.

Table 5.1: Percentage of modules affected by interconnect breakage in different climatic zones and age groups

Climatic Zone	Age Group				
	0-5 Years	5-10 Years	10-20 Years	20+ Years	All Ages
Hot & Dry	23% (52)	0% (10)	50% (36)	18% (44)	27% (142)
Warm & Humid	19% (42)	68% (28)	80% (51)	42% (33)	53% (154)
Composite	11% (46)	NA	47% (66)	21% (57)	28% (169)
Moderate	6% (89)	11% (19)	0% (10)	0% (17)	5% (135)
Cold & Sunny	10% (31)	NA	16% (25)	NA	13% (56)
Cold & Cloudy	NA	NA	NA	NA	NA

5.4.2 Correlation of Interconnect Breakage with Series Resistance

The series resistance of the module is calculated by taking the inverse of slope of the lighted *I-V* curve near the open circuit voltage point (where current is nearly zero). Figure 5.10 shows the correlation of series resistance with the 'severity' of the interconnect breakage. It can be clearly seen that as the severity of the interconnect breakage increases, the series resistance also increases which reduces the *FF* and consequently decreases the P_{max}. In section 5.4.1, we have seen that percentage of modules having interconnect breakage is more in Hot zones, which explains why modules in Hot zones have higher degradation rates as compared to the Non-Hot zones. This may also be the reason for the variation in the ideality factor *n* with climatic zone.

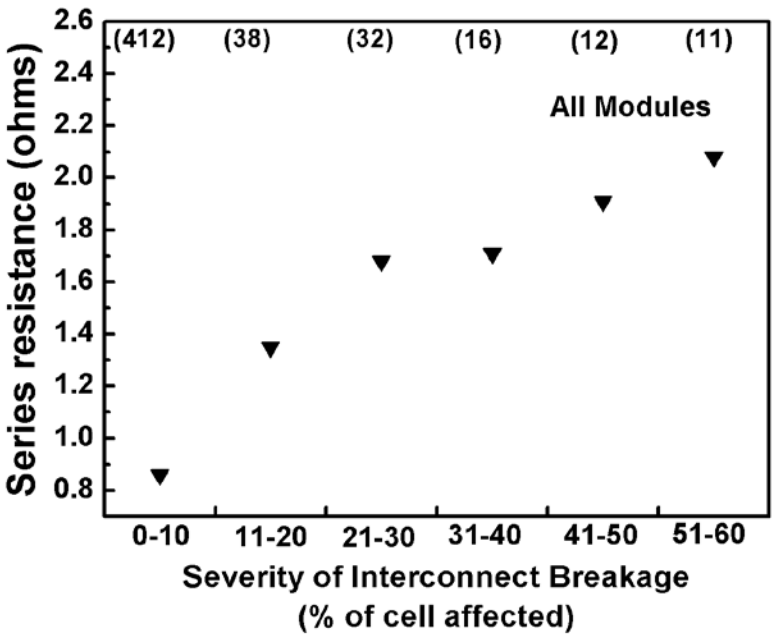

Fig. 5.10: Correlation of average value of series resistance with severity of interconnect breakage (numbers on top represent the number of modules in each category).

5.4.3 Correlation of Interconnect Breakage with P_{max} Degradation

Figure 5.11 shows the correlation of P_{max} degradation rate (%/year) with severity of interconnect breakage for Group X modules. It can be clearly seen that the output power degradation rate increases with the increase in the severity of interconnect breakage.

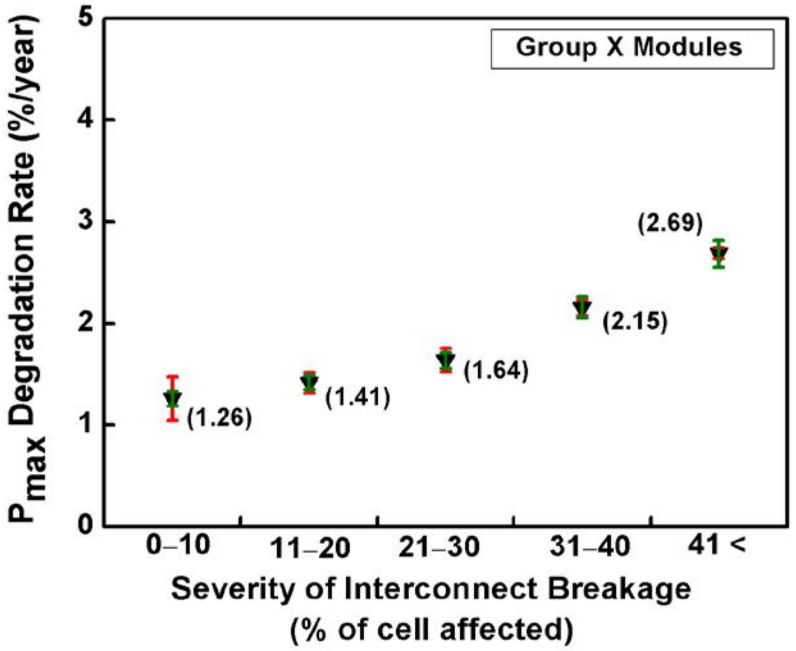

Fig. 5.11: Correlation of P_{max} degradation (%/year) with severity of interconnect breakage for Group X modules.

5.5 Summary

From the analysis of the dark *I-V*, insulation resistance and interconnect breakage data, we can reach the following conclusions:

- Ideality factor *n* of the module increases with the increase in the age of the module. This shows that the quality of the cells, the series resistance and/or the shunt resistance degrade as the age of the module increases. Correlation with other data indicates that series resistance is certainly one of the contributing factors.

- The ideality factor *n* is slightly higher in the Hot zones as compared to the Non-Hot zones and it has good correlation to the percentage power degradation.

- Analysis of insulation resistance shows that more than 90% of the modules have passed the dry insulation resistance test. Also, 100% modules installed in the large system category have passed the dry insulation test which shows that large power plants are doing well with respect to the safety and quality of the PV modules. Also, P_{max} degradation increases with decrease in the insulation resistance value.

- Modules in the Hot zones have shown larger percentage of interconnect failure as compared to the Non-Hot zones. Also the series resistance of the module increases with the increase in the severity of the interconnect failure which eventually reduces the power output of the module.

6. Analysis of Visual Degradation

6.1 Introduction

The degradation in the material components of PV modules often becomes visually evident even before there is any noticeable reduction in the electrical performance and often serves as a precursor marker to module degradation. Analysis of the visual degradation is useful in order to determine the root cause behind the degradation of the electrical parameters like short circuit current, fill factor etc. In the following sub-sections, the various visual degradation modes observed (using an enhanced NREL Visual Inspection checklist) during the survey are analyzed based on technology, age, climatic zone and size of installation. The degradation in the crystalline silicon modules and the thin film modules has been analyzed separately. The data will be presented first for 'All' modules, and then separately for Group X and Group Y, in order to bring out the differences. When presenting the data in the tables, they will be colour coded for ease of understanding, with green indicating low values, orange indicating medium values, and red indicating high values.

6.2 Visual Degradation Observed in Crystalline Silicon Modules

Different components of the PV module degrade in different ways – the encapsulant starts yellowing or browning upon long-term exposure to sunlight and high temperature, the metallization starts to corrode on being exposed to humidity and high temperatures, the encapsulant loses adhesion and delaminates due to humidity, and so on [74]. The major degradation modes observed for crystalline silicon modules are discussed in the following sections.

6.2.1 Influence of Climatic Zone and Age Group on Visual Degradation Modes

a) *Discoloration of Encapsulant*

Discoloration of encapsulant is one of the major reasons behind reduction in short-circuit current (I_{sc}) and consequently power output (P_{max}) of field-aged PV modules. Research in the late 1990s showed that discoloration of the EVA encapsulant occurs due to certain additives and it is possible to slow down and/or avoid this discoloration by a proper choice of the additives [31]. However, discoloration still occurs in field-aged modules, as shown in Fig. 6.1 and Table 6.1. In this table, each cell provides the percentage of modules affected in the respective climatic zone and age group, followed by the number of samples (in brackets). The values are colour-coded, with green for frequency of occurrence less than 33%, orange for 33-66% and red above 66%. Categories without any module samples are indicated by "NA". We can see from the table that discoloration of encapsulant is not frequently seen in the young modules, but is much more common in field-aged modules after about 5 years of exposure. In a few exceptional cases, like at a site in the Composite zone, about 35 "Young" modules of a particular batch and make were found to have extensive discoloration within 2 years of field exposure. Modules in both Hot zones (Hot & Dry, Warm & Humid, Composite) and the Non-Hot zones (Moderate, Cold & Sunny and Cold & Cloudy) show discoloration upon aging. Some glass-glass modules were inspected in the Hot & Dry zone which had been in the field for 27 years, but showed no discoloration of the encapsulant. Based on the age of these modules, it is suspected that the encapsulant used may not be EVA (which is presently used by almost all manufacturers) and these modules have been excluded from this discoloration analysis (as such types of modules were not found in other age groups and climatic zones).

In Chapter 4, it has been shown that there are some "good" sites (having average P_{max} degradation rate less than 2%/year, referred to as Group X) and some "not-so-good" sites (having average P_{max} degradation rate greater than 2%/year, referred to as Group Y). We deemed it useful to also analyze visual degradation separately for the Groups, as this may give some pointers to why modules in some sites are performing better than others. Table 6.2 provides the discoloration statistics (percentage of affected modules) for Groups X and Y. P_{max} degradation has not been calculated for modules in some of the sites (due to inadequate data, like *I-V* taken under irradiances less than 500 W/m^2), so the sum of modules reported in Table 6.2 for Groups X and Y may be lower than the total sample size reported in Table 6.1. In the last row of Table 6.2, comparative data is given by summing up data for all climatic zones, for which samples exist for both Groups X and Y (highlighted with blue shading). We can see that the percentage of discolored modules is comparable for Groups X and Y in age groups above 5 years i.e. old modules, but for the young modules, the percentage of affected modules is double in case of Group Y as compared to Group X, which points to the fact that the material quality (encapsulant) is poorer in the younger Group Y modules. Further, the fact that discoloration has started in a few young modules even in the so-called "good" sites, raises questions regarding the quality of materials being used by the manufacturers.

(a) Discolored cells in a young module in Composite zone

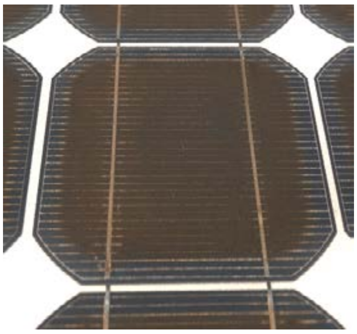

(b) Discolored cells in an old module in Warm & Humid zone

Fig. 6.1: Discoloration observed during the survey

Table 6.1: Percentage of c-Si modules of 'All' surveyed sites affected by discoloration in different climatic zones and age groups (total number of samples is given in brackets).

Climatic Zone	Age Groups				Total
	0-5 Years	5-10 Years	10-20 Years	20+ Years	
Hot & Dry	4% (74)	NA	100% (30)	NA*	32% (104)*
Warm & Humid	8% (93)	89% (72)	94% (105)	100% (2)	63% (272)
Composite	30% (133)**	0% (7)	65% (116)	NA	45% (256)
Moderate	0% (123)	NA	92% (12)	NA	8% (135)
Cold & Sunny	0% (34)	NA	77% (22)	NA	30% (56)
Cold & Cloudy	0% (112)	NA	NA	NA	0% (112)

* Excluding 38 nos. glass-glass modules that have shown no discoloration.
** All surveyed modules of a particular make and batch are showing discoloration.

Table 6.2: Comparison of Groups X and Y for discoloration in different climatic zones and age groups (total number of samples is given in brackets).

Climatic Zone	Age Groups			
	0-5 Years	**5-10 Years**	**10-20 Years**	**20+ Years**
Hot & Dry	X: NA Y: 4% (74)	NA	X: 100% (8) Y: 100% (22)	X: 100% (3) Y: NA
Warm & Humid	X: 22% (32) Y: 0% (61)	X: 82% (28) Y: 98% (40)	X: 93% (84) Y: 100% (21)	NA
Composite	X: 0% (19) Y: 61% (66)	X: 0% (7) Y: NA	X: 96% (28) Y: 81% (52)	NA
Moderate	X: 0% (31) Y: 0% (92)	NA	X: 92% (12) Y: NA	NA
Cold & Sunny	X: 0% (33) Y: NA	NA	X: 77% (22) Y: NA	NA
Cold & Cloudy	X: NA Y: 0% (76)	NA	NA	NA
All Climates (comparative)	X: 9% (82) **Y: 18% (219)**	X: 82% (28) **Y: 98% (40)**	**X: 94% (120)** Y: 90% (95)	No data for comparison

We have quantified the severity of discoloration in a module in order to correlate the visual degradation with the electrical degradation. In the field, the discolored modules have been found to have discoloration on all cells, except for a few cases where some of the cells had slightly higher discoloration (or other defects like delamination). Since in most modules manufactured today, the solar cells are in series (without any parallel connection), it is reasonable to think that the worst affected cell would limit the short circuit current of the module (and hence the power output). Hence, for defining the module's discoloration index, the *most* visually degraded cell has been identified in the module and its degree of discoloration (light or dark) and fractional discolored cell area (ranging from 0 to 1) are noted down (based on the NREL visual inspection checklist [30]). Based on these data, the module's discoloration index DI is defined by us using the formula:

$$\text{Discoloration Index (DI)} = \frac{\text{Degree of discoloration x Affected area of cell}}{\text{Maximum value of numerator}} \quad \text{…. (6.1)}$$

where, degree of discoloration = 1 for light/ yellow discoloration,

= 2 for dark/ brown discoloration

Affected cell area can range between 0 to 1, so the maximum value of numerator is 2, and the calculated value of discoloration index DI can vary between 0 (indicating "no discoloration") to 1 (indicating "dark brown discoloration over a full cell"). An important implication of the above method is that light discoloration on 100% cell area will give same discoloration index for the module as dark discoloration on 50% cell area.

Based on the discoloration index, the modules can be categorized into 5 categories with discoloration severity ranging from "Nil" to "Very High" as shown in Table 6.3.

Table 6.3: Discoloration category based on Discoloration Index

Discoloration Index	0	0 – 0.25	0.25 – 0.5	0.5 – 0.75	0.75 – 1
Discoloration Category	Nil	Low	Medium	High	Very High

Table 6.4(a) gives the average discoloration category for Group X modules in different age groups and climatic zones. As discussed in Chapter 4, the climatic influence can be best ascertained from the performance of the Group X modules. In the 10-20 years age group, modules in the Hot & Dry zone have the highest discoloration, followed by Warm & Humid zone and then the other zones. Hence it is reasonable to conclude that the encapsulant is degrading faster in the Hot zones as compared to the other zones in the long term. We can further see that there is "low" discoloration in the young age group i.e. 0-5 years age, which should be ideally "Nil" in case of young modules. This means that discoloration has started in the modules within 5 years of installation, which again raises concerns with regard to the quality of the encapsulant used in manufacturing the modules. Table 6.4(b) presents the above data in a concise manner by clubbing the climatic zones into Hot and Non-Hot categories. Hot climates are causing higher discoloration in the modules than Non-Hot climates, especially in the older age group of 10-20 years. Table 6.4(c) provides the average discoloration statistics for group Y modules, which shows that many modules show high discoloration within 10 years of operation, but there are some modules which show only "medium" discoloration even after 10 years (module manufacturers are different for the two age categories, so this result is not illogical). Thus, modules of some manufacturers in Group Y are discoloring very fast, which is not seen in group X modules, which suggests that quality of the encapsulating material and/or manufacturing process is not properly maintained by some manufacturers in Group Y.

Table 6.4 (a). Average extent of discoloration in Group X modules in different climatic zones and age groups (number of samples is given in brackets).

Climatic Zone	Age Groups			
	0-5 Years	5-10 Years	10-20 Years	20+ Years
Hot & Dry	NA	NA	Very High (8)	NA*
Warm & Humid	Low (32)	Medium (28)	High (84)	NA
Composite	Nil (19)	Nil (7)	Medium (28)	NA
Moderate	Low (31)	NA	Medium (12)	NA
Cold & Sunny	Low (33)	NA	Medium (22)	NA
Cold & Cloudy	NA	NA	NA	NA
* Excluding glass-glass modules from one particular manufacturer which have shown almost no discoloration even after 27 years in the field in Hot & Dry zone.				

Table 6.4 (b). Average extent of discoloration in Group X modules in Hot and Non-Hot climates for different age groups (number of samples is given in brackets).

Climatic Zone	Age Groups			
	0-5 Years	5-10 Years	10-20 Years	20+ Years
Hot Zones	Low (51)	Low (35)	High (120)	NA*
Non-Hot Zones	Low (64)	NA	Medium (34)	NA
* Excluding glass-glass modules from one particular manufacturer which have shown almost no discoloration even after 27 years in the field in Hot & Dry zone.				

Table 6.4(c): Average extent of discoloration in Group Y modules in Hot and Non-Hot climates for different age groups (number of samples is given in brackets).

Climatic Zone	Age Groups			
	0-5 Years	5-10 Years	10-20 Years	20+ Years
Hot Zones	Low (201)	Very High (40)	Medium (95)	NA
Non-Hot Zones	Nil (168)	NA	NA	NA

Table 6.5 compares the average extent of discoloration for small installations (less than 100 KWp rating) and large installations in the Hot and Non-Hot zones. It seems from the data that modules in large installations have lower discoloration than modules in the small installations, but a definite conclusion cannot be reached since the number of samples for large installations is very few.

Table 6.5: Average extent of discoloration in 'All' modules for small and large installations in the Hot and Non-Hot climatic zones and various age groups (number of samples is given in brackets).

Size of Installation	Climatic Zone	Age Groups			
		0-5 Years	5-10 Years	10-20 Years	20+ Years
Small	**Hot**	Low (280)	High (79)	Medium (251)	High (2)*
	Non-Hot	Low (239)	NA	Medium (29)	NA
Large	**Hot**	Low (20)	NA	NA	NA
	Non-Hot	Low (30)	NA	Nil (5)	NA
* Excluding glass-glass modules from one particular manufacturer which have shown almost no discoloration even after 27 years in the field in Hot & Dry zone.					

Based on the above, we conclude that the Hot & Dry and Warm & Humid zone are the harshest climates for the encapsulant. Further, modules of some manufacturers in Group Y show high discoloration within a short period of time in the field, which hints at the poor quality of materials being used by these manufacturers.

b) Front-side Delamination

Delamination refers to the loss of adhesion between any two layers of the module laminate. If delamination occurs on the front-side, on top of the solar cells, it increases the reflection losses, and thereby reduces the short-circuit current I_{sc} and power output P_{max} of the module. Examples of front-side delamination are shown in Fig. 6.2. Table 6.6 provides the statistics of front-side delamination in the surveyed modules. Delamination is rarely seen to occur in young modules, except for a few modules in Moderate climate, in which case the delamination has occurred mainly along snail tracks, and covered less than 5% of the affected solar cells. Among the older modules (more than 5 years old), delamination is seen more in the Hot & Dry and Warm & Humid zones, with around 30% of the modules affected in these zones. Modules in the cold zone seem to be least affected by delamination, indicating that temperature plays a role in the delamination process. This is consistent with theory, since high temperatures tend to reduce the adhesive property in polymers. In Table 6.7, Groups X and Y have been compared with regard to delamination, and we can see that Group Y has higher percentage of affected modules compared to Group X, in most age categories.

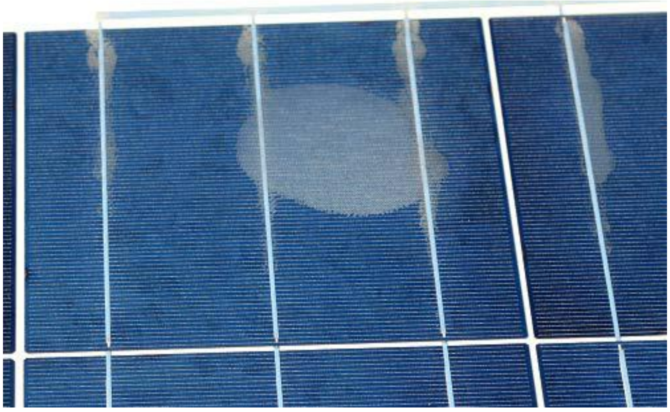

(a) Front-side delamination over cells in a young module in Composite zone

(b) Front-side delamination over cells in an old module in Warm & Humid zone (lighter in colour)

Fig. 6.2: Delamination observed during the survey

Table 6.6: Percentage of 'All' modules affected by delamination in different climatic zones and age groups (number of samples is given in brackets).

Climatic Zone	Age Groups				Total
	0-5 Years	5-10 Years	10-20 Years	20+ Years	
Hot & Dry	8% (74)	NA	24% (30)	82% (38)	31% (142)
Warm & Humid	0% (93)	56% (72)	45% (105)	100% (2)	33% (272)
Composite	11% (133)	0% (7)	17% (116)	NA	13% (256)
Moderate	28% (123)	NA	17% (12)	NA	27% (135)
Cold & Sunny	0% (34)	NA	0% (22)	NA	0% (56)
Cold & Cloudy	2% (112)	NA	NA	NA	2% (112)

As in the case of discoloration, quantification of the extent of delamination in a module is defined by us, which can then be compared with the degradation in electrical performance. It is important to note that even if one cell in a module is affected by delamination, the whole module's output reduces since all the cells are in series. Hence, the *most* visually degraded cell in terms of delamination has been identified and its delamination index has been quantified based on its delaminated area:

Delamination Index = Fractional delaminated area of the worst affected cell …. (6.2)

The delamination index may vary between 0 (indicating no delamination) to 1 (indicating whole cell delaminated). Based on the delamination index, the modules can be categorized into 5 categories with delamination severity ranging from "Nil" to "Very High" as shown in Table 6.8.

Table 6.7: Comparison of Groups X and Y for delamination in different climatic zones and age groups (number of samples is given in brackets).

Climatic Zone	Age Groups			
	0-5 Years	**5-10 Years**	**10-20 Years**	**20+ Years**
Hot & Dry	X: NA Y: 8% (74)	NA	X: 100% (8) Y: 0% (22)	X: 79% (38) Y: NA
Warm & Humid	X: 0% (32) Y: 0% (61)	X: 25% (28) Y: 80% (40)	X: 35% (84) Y: 86% (21)	NA
Composite	X: 0% (19) Y: 12% (66)	X: 0% (7) Y: NA	X: 21% (28) Y: 19% (52)	NA
Moderate	X: 23% (31) Y: 29% (92)	NA	X: 17% (12) Y: NA	NA
Cold & Sunny	X: 0% (33) Y: NA	NA	X: 0% (22) Y: NA	NA
Cold & Cloudy	X: NA Y: 3% (76)	NA	NA	NA
All Climates (comparative)	X: 9% (82) **Y: 16% (219)**	X: 25% (28) **Y: 80% (40)**	**X: 33% (120)** Y: 28% (95)	No data for comparison

Table 6.8: Delamination category based on Delamination Index

Delamination Index	0	0 – 0.25	0.25 – 0.5	0.5 – 0.75	0.75 – 1
Delamination Category	Nil	Low	Medium	High	Very High

Table 6.9 (a) gives the average delamination category for Group X modules in different age groups and climatic zones. Average delamination extent is “Low” (i.e. area affected does not exceed 25% of affected cell’s area) even after 20 years of field exposure, though in some of the modules the delamination can become “Very High” (like in the module shown in Fig. 6.2 (b)). The climatic zones are clubbed into Hot and Non-Hot zones in Table 6.9 (b). The data for 10-20 years age group shows that extent of delamination is higher in the Hot zone than the Non-Hot zone.

Table 6.9 (a): Average extent of delamination in Group X modules in different climatic zones and age groups (number of samples is given in brackets).

Climatic Zone	Age Groups			
	0-5 Years	**5-10 Years**	**10-20 Years**	**20+ Years**
Hot & Dry	NA	NA	Low (8)	Low (38)
Warm & Humid	Nil (32)	Low (28)	Low (84)	NA
Composite	Nil (19)	Nil (7)	Low (28)	NA
Moderate	Low (31)	NA	Nil (12)	NA
Cold & Sunny	Nil (33)	NA	Nil (22)	NA
Cold & Cloudy	NA	NA	NA	NA

Table 6.9 (b): Average extent of delamination in Group X modules in Hot and Non-Hot climates for different age groups (number of samples is given in brackets).

Climatic Zone	Age Groups			
	0-5 Years	5-10 Years	10-20 Years	20+ Years
Hot Zone	Nil (51)	Low (35)	Low (120)	Low (38)
Non-Hot Zone	Low (64)	NA	Nil (34)	NA

The extent of delamination is compared for modules in Groups X and Y for the Hot & Dry and Warm & Humid climates in Table 6.9 (c). This shows that the Warm & Humid zone appears to be slightly harsher than the Hot & Dry zone from the delamination point of view. Also, Group Y modules show slightly more delamination than Group X modules, in the long term.

Table 6.9(c): Average extent of delamination in Group X and Group Y modules in Warm & Humid climate and Hot & Dry climate, for different age groups (number of samples is given in brackets).

Climatic Zone	Group	Age Groups			
		0-5 Years	5-10 Years	10-20 Years	20+ Years
Warm & Humid	**Group X**	Nil (32)	Low (28)	Low (84)	NA
	Group Y	Nil (61)	Low (40)	Medium (21)	NA
Hot & Dry	**Group X**	NA	NA	Low (8)	Low (38)
	Group Y	Low (74)	NA	Nil (20)	NA

Table 6.10 shows the statistics for small installations versus large installations. Modules used in large installations have a lower delamination index as compared to modules in small installations, but since the number of samples in the large installation category is few, no definite conclusion can be reached.

Table 6.10: Average extent of delamination in 'All' modules for small and large installations in the Hot and Non-Hot climatic zones and various age groups (number of samples is given in brackets).

Size of Installation	Climatic Zone	Age Groups			
		0-5 Years	5-10 Years	10-20 Years	20+ Years
Small	**Hot**	Low (280)	Low (79)	Low (251)	Low (40)
	Non-Hot	Low (239)	NA	Low (29)	NA
Large	**Hot**	Nil (20)	NA	NA	NA
	Non-Hot	Nil (30)	NA	Nil (5)	NA

Based on the above discussion, it can be concluded that modules of Group Y sites are showing higher delamination in the long term as compared to modules in Group X sites, and the Warm & Humid zone is the harshest climate from delamination point of view.

c) Snail Trails

Snail trails (or snail tracks) are a relatively recent phenomena which have come to the fore in recent years [75]. They refer to curved black lines on top of solar cells, often looking similar to tracks made by snails (Fig. 6.3). Table 6.11 provides the statistics for snail trails in crystalline silicon modules observed by us. It can be seen that mostly the younger modules are affected by snail trails. This seems to indicate issues in material quality, transportation and/or installation. A high percentage of modules in the Non-Hot climatic zones (Moderate, Cold & Sunny and Cold & Cloudy) are affected which may be due to the higher probability of condensation of moisture at these sites (due to significantly low night time temperatures compared to day time temperatures). Table 6.12 shows the data for Groups X and Y. Both Group X and Group Y modules in the young age category are affected by snail trails.

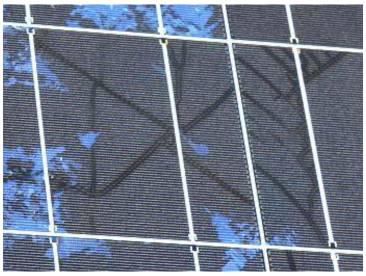

(a) Snail tracks in a young module in Warm & Humid zone

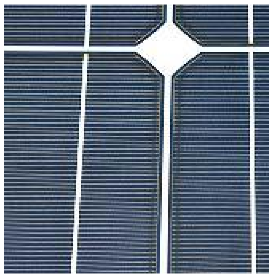

(b) Framing type snail trail in a young module in Moderate zone

Fig. 6.3: Snail Tracks observed during the survey

Table 6.11: Percentage of 'All' modules affected by snail trails in different climatic zones and age groups (number of samples is given in brackets).

Climatic Zone	Age Groups				Total
	0-5 Years	5-10 Years	10-20 Years	20+ Years	
Hot & Dry	35% (74)	NA	0% (30)	0% (38)	18% (142)
Warm & Humid	19% (93)	0% (72)	0% (105)	0% (2)	6% (263)
Composite	6% (133)	0% (7)	0% (116)	NA	3% (256)
Moderate	57% (123)	NA	8% (12)	NA	53% (135)
Cold & Sunny	50% (34)	NA	0% (22)	NA	30% (56)
Cold & Cloudy	45% (112)	NA	NA	NA	45% (112)

Table 6.12: Comparison of Groups X and Y for snail tracks in different climatic zones and age groups (number of samples is given in brackets).

Climatic Zone	Age Groups			
	0-5 Years	5-10 Years	10-20 Years	20+ Years
Hot & Dry	X: NA Y: 35% (74)	NA	X: 0% (8) Y: 0 % (22)	X: 0% (38) Y: NA
Warm & Humid	X: 44% (32) Y: 3% (61)	X: 0% (28) Y: 0% (40)	X: 0% (84) Y: 0% (21)	NA
Composite	X: 0% (19) Y: 0% (66)	X: 0% (7) Y: NA	X: 0% (28) Y: 0% (52)	NA
Moderate	X: 48% (31) Y: 60% (92)	NA	X: 8% (12) Y: NA	NA
Cold & Sunny	X: 52% (33) Y: NA	NA	X: 0% (22) Y: NA	NA
Cold & Cloudy	X: NA Y: 49% (76)	NA	NA	NA
All Climates (comparative)	**X: 35% (82)** Y: 26% (219)	X: 0% (28) Y: 0% (40)	X: 0% (120) Y: 0% (95)	No data for comparison

The severity of snail tracks in a module can be quantified based on the percentage of cells affected in the module, and on this basis the categorization has been done as follows:

Table 6.13: Snail Trail category based on percentage of affected solar cells

% of cells affected by Snail Trail	0	0 – 10%	10% - 25%	25% - 50%	>50%
Snail Trail Category	Nil	Low	Medium	High	Very High

Table 6.14 gives the Snail trail category for young modules in different climatic zones, and we can see that modules in the humid climates (Warm & Humid and Cold & Cloudy) have higher percentage of affected cells than the dry climates. This supports the theory that moisture assists the formation of snail trails [76].

Table 6.14: Average extent of snail tracks in young modules in different climatic zones (number of samples is given in brackets).

Climatic Zone	**Hot & Dry**	**Warm & Humid**	**Composite**	**Moderate**	**Cold & Sunny**	**Cold & Cloudy**
Snail Trail Category for "All" modules	Low (74)	Medium (93)	Low (133)	Low (123)	Low (34)	High (112)
Snail Trail Category for Group X modules	NA	High (32)	Nil (19)	Low (31)	Low (33)	NA

Table 6.15 shows the statistics for the snail trails in young modules installed in small and large installations, and it seems that the modules in the large installation are showing more snail trails than modules in the smaller installations. It should be noted that the snail trails observed in the large installation site are mostly of the framing type (not associated with cell cracks), but for the small sites, the snail trails are of the non-framing type (which have been shown to be associated with cell cracks in Chapter 7). Further, the number of samples for the large installations is too few to reach a definitive conclusion.

Table 6.15: Average extent of snail trails in 'All' modules in the young age category for small and large installations in the Hot and Non-Hot climatic zones (number of samples is given in brackets).

Size of Installation	**Climatic Zone**	**Extent of Snail Trails in Young Modules**
Small	**Hot**	Low (280)
	Non-Hot	Medium (239)
Large	**Hot**	High (20)*
	Non-Hot	Low (30)
*Modules in the large installation in Hot zone possessed framing type snail trails in most of the modules, whereas modules in the other categories had both the framing and non-framing types.		

Based on above discussion, we may conclude that the snail trails are occurring in the young modules in both Group X and Group Y sites, irrespective of the size of the installation, and its severity is higher in the humid climates.

d) *Discoloration on Metallization*

Metallization on top of the solar cells (fingers and busbars), and the interconnect ribbons conduct the current generated in the PV module to the terminal box at the backside of the module. Discoloration of the metallization can occur due to corrosion and also sometimes due to improper manufacturing practices (like deposition of solder flux leading to brown discoloration on the cell interconnect ribbon). Examples are shown in Fig. 6.4. Table 6.16 captures the statistics for the metallization (including interconnect) discoloration for the different age groups and climatic zones. The discoloration of metallization in the young modules (0-5 years age category) is predominantly due to non-corrosion issues (like deposition of solder flux etc.) whereas in the older modules, corrosion is the predominant reason behind such discoloration. This table highlights some manufacturing issues in the young modules and also shows that among the older modules, corrosion is occurring in all climatic zones. Table 6.17 shows that percentage of modules affected are similar in Groups X and Y.

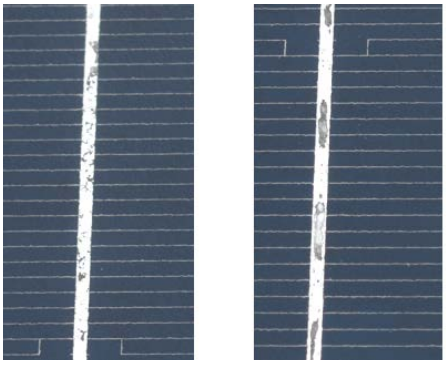

(a) Discoloration in cell interconnects observed in young modules

(b) Corrosion in cell interconnects and string interconnects observed in old modules

Fig. 6.4: Metallization discoloration observed during the survey

Table 6.16: Percentage of modules affected by discoloration in metallization in different climatic zones and age groups (number of samples is given in brackets).

Climatic Zone	Age Groups				Total
	0-5 Years	5-10 Years	10-20 Years	20-30 Years	
Hot & Dry	35% (74)	NA	97% (30)	100% (38)	65% (142)
Warm & Humid	34% (93)	96% (72)	92% (105)	100% (2)	73% (273)
Composite	41% (128)*	0% (7)	100% (116)	NA	67% (251)
Moderate	54% (123)	NA	100% (12)	NA	59% (135)
Cold & Sunny	79% (34)**	NA	86% (22)	NA	82% (56)
Cold & Cloudy	16% (112)	NA	NA	NA	16% (112)

*All back-contact type modules excluded as metallization is not externally visible.
** Due to non-corrosion issues (like deposition of solder flux etc.)

Table 6.17: Comparison of Groups X and Y for discoloration in metallization in different climatic zones and age groups (number of samples is given in brackets).

Climatic Zone	Age Groups			
	0-5 Years	**5-10 Years**	**10-20 Years**	**20+ Years**
Hot & Dry	X: NA Y: 35% (74)	NA	X: 100% (8) Y: 95% (22)	X: 100% (38) Y: NA
Warm & Humid	X: 47% (32) Y: 28% (61)	X: 89% (28) Y: 100% (40)	X: 89% (84) Y: 100% (21)	NA
Composite	X: 0% (19) Y: 77% (61)	X: 0% (7) Y: NA	X: 100% (28) Y: 100% (52)	NA
Moderate	X: 52% (31) Y: 55% (92)	NA	X: 100% (12) Y: NA	NA
Cold & Sunny	X: 79% (33) Y: NA	NA	X: 86% (22) Y: NA	NA
Cold & Cloudy	X: NA Y: 23% (76)	NA	NA	NA
All Climates (comparative)	X: 38% (82) **Y: 54% (214)**	X: 89% (28) **Y: 100% (40)**	X: 90% (120) **Y: 99% (95)**	No data for comparison

The extent of discoloration in the metallization has also been estimated from the visual images of the modules to define a Metallization Discoloration Index (MDI). Unlike the case of discoloration and delamination, the effect of corrosion on electrical behavior (series resistance) is additive in nature from cell to cell i.e. the total corrosion in different parts of the module will increase the series resistance of the module, thereby degrading the fill factor and the power output. Hence, for calculating the MDI value, the discoloration in different metallic current-carrying components of the module like fingers, busbars, interconnects, and output terminals have been summed up by using the following formula:

$$\text{MDI} = \frac{\sum_{i=1}^{n}(\text{degree of discoloration of "i"th component x fractional area affected of the component})}{\text{Maximum possible value of the numerator i.e. } 2n} \quad .... (6.3)$$

where, Degree of discoloration = 1 (for light discoloration),

= 2 (for dark discoloration)

The index i indicates a visible metallization component like fingers, busbars, interconnects, and output terminals etc. Its value can vary from 1 to the total number of visible metallization components (denoted by n). For example, for the standard c-Si modules available in the market, i =1 will represent the fingers, i =2 will represent the busbars and cell interconnects, i =3 will represent the string interconnects, i =4 will represent the output terminals, and in such a case n is equal to 4. The value of n can vary depending on the module design; for example, in some modules, string interconnects are not visible externally, so total number of visible metallization components n becomes 3. Further, in some module designs, there may be no visible metallization at all, in which case this method cannot be applied.

Based on above index, the modules have been grouped into 5 categories as follows:

Table 6.18: Metallization discoloration category based on the Metallization Discoloration Index

Metallization Discoloration Index	0	0 – 0.25	0.25 – 0.5	0.5 – 0.75	0.75 – 1
Metallization Discoloration Category	Nil	Low	Medium	High	Very High

The metallization discoloration data for Group X and Group Y modules are shown in Table 6.19. It is evident from the data for the 10-20 years age group that discoloration of metallization (which is mainly due to corrosion in these old modules) is more severe in the Warm & Humid and Composite zones as compared to the other climatic zones.

Table 6.19 (a): Average extent of discoloration in metallization in Group X modules in different climatic zones and age groups (number of samples is given in brackets).

Climatic Zone	Age Groups			
	0-5 Years	**5-10 Years**	**10-20 Years**	**20+ Years**
Hot & Dry	NA	NA	Medium (8)	Medium (38)
Warm & Humid	Low (32)	Low (28)	Medium (84)	NA
Composite	Low (14)	Nil (7)	Medium (28)	NA
Moderate	Low (31)	NA	Low (12)	NA
Cold & Sunny	Low (33)	NA	Low (22)	NA
Cold & Cloudy	NA	NA	NA	NA

Table 6.19 (b): Average extent of discoloration in metallization in Group Y modules in different climatic zones and age groups (number of samples is given in brackets).

Climatic Zone	Age Groups			
	0-5 Years	**5-10 Years**	**10-20 Years**	**20+ Years**
Hot & Dry	Low (74)	NA	Low (22)	NA
Warm & Humid	Low (61)	Low (40)	Medium (21)	NA
Composite	Low (61)	NA	Medium (52)	NA
Moderate	Low (92)	NA	NA	NA
Cold & Sunny	NA	NA	NA	NA
Cold & Cloudy	Low (76)	NA	NA	NA

Table 6.20 gives the statistics for the modules in small and large installations, and it can be seen that there is no difference between these categories from the metallization point of view.

Table 6.20: Average extent of discoloration in metallization in 'All' modules for small and large installations in Hot and Non-Hot climatic zones and various age groups (number of samples in brackets).

Size of Installation	Climatic Zone	Age Groups			
		0-5 Years	**5-10 Years**	**10-20 Years**	**20+ Years**
Small	**Hot**	Low (275)	Low (79)	Medium (251)	Medium (40)
	Non-Hot	Low (239)	NA	Low (29)	NA
Large	**Hot**	Low (20)	NA	NA	NA
	Non-Hot	Low (30)	NA	Low (5)	NA

To summarize, discoloration of metallization is more intense in the Hot zone as compared to the Non-Hot zone. Further, there is no significant difference in metallization discoloration between the Small and Large installations, or between the Groups X and Y.

e) Backsheet Degradation

The backsheet is the outermost protective layer of the module, which serves to provide electrical insulation and prevent the ingress of moisture into the module. However, the backsheet can easily get scratched due to improper handling, can get burnt due to hot spots in the modules, can lose adhesion (causing bubbles and delamination) due to moisture ingress, and also degrade thermally leading to chalking. Some of these effects are shown in Fig. 6.5.

(a) (b) (c)

Fig. 6.5: Backsheet degradation observed during the survey. (a) Chalking, (b) Cracking, and (c) Burn marks, scratches and delamination

Table 6.21 provides the statistics of modules with backsheet damage (like chalking, discoloration, bubbles, scratches and cracking) observed during the survey. There is considerable degradation of the backsheet in all climates except the cold zones. More than 25% of the young modules also show problems of the backsheet which points towards use of poor quality materials in these modules, apart from improper handling and installation practices (which can lead to scratches in backsheet, in turn accelerating the degradation of such modules). Table 6.22 shows the comparison of modules in Groups X and Y, and it can be seen that modules in Group Y fare worse than modules in Group X in most climates and age groups.

Table 6.21: Percentage of 'All' modules affected by degradation of backsheet in different climatic zones and age groups (number of samples is given in brackets).

Climatic Zone	Age Groups				Total
	0-5 Years	5-10 Years	10-20 Years	20-30 Years	
Hot & Dry	26% (74)	NA	73% (30)	NA	39% (104)*
Warm & Humid	27% (93)	69% (72)	90% (105)	100% (2)	63% (272)
Composite	28% (133)	29% (7)	92% (116)	NA	60% (256)
Moderate	25% (123)	NA	83% (12)	NA	39% (135)
Cold & Sunny	9% (34)	NA	36% (22)	NA	20% (56)
Cold & Cloudy	17% (112)	NA	NA	NA	17% (112)
*Excluding modules with glass back-cover					

Table 6.22: Comparison of Groups X and Y for backsheet degradation in different climatic zones and age groups (number of samples is given in brackets).

Climatic Zone	**Age Groups**			
	0-5 Years	**5-10 Years**	**10-20 Years**	**20+ Years**
Hot & Dry	X: NA Y: 26% (74)	NA	X: 95% (19) Y: 64% (22)	X: 100% (1) Y: NA
Warm & Humid	X: 25% (32) Y: 28% (61)	X: 18% (14) Y: 95% (40)	X: 83% (95) Y: 100% (21)	NA
Composite	X: 0% (19) Y: 50% (66)	X: 29% (7) Y: NA	X: 86% (29) Y: 91% (77)	NA
Moderate	X: 42% (31) Y: 20% (92)	NA	X: 83% (12) Y: NA	NA
Cold & Sunny	X: 9% (33) Y: NA	NA	X: 36% (22) Y: NA	NA
Cold & Cloudy	X: NA Y: 24% (76)	NA	NA	NA
All Climates (comparative)	X: 26% (82) **Y: 31% (219)**	X: 18% (14) **Y: 95% (40)**	X: 86% (143) **Y: 88% (120)**	Comparison not possible

For quantifying the extent of backsheet degradation of a module, a Backsheet Degradation Index (BDI) has been developed based on the affected module area, which can be calculated as follows:

$$\text{Backsheet Degradation Index} = \frac{\text{severity of chalking} + \text{severity of burns} + \text{severity of bubbles} + \text{severity of cracks}}{\text{Maximum value of numerator}} \quad .... (6.4)$$

where, the severity of burns, bubbles and cracks is decided based on the affected module area as follows:

Table 6.23: Backsheet degradation severity category based on affected area of module

Affected area	0-5%	5-25%	25 – 50%	50 – 75%	>75%
Severity Category	1	2	3	4	5

Chalking of the backsheet has been measured in the survey in "qualitative" terms as slight or excessive. For maintaining the same maximum weightage for chalking as done for the other degradation modes, the severity for chalking is assumed as "5" in case of excessive chalking, and "2.5" for slight chalking. The maximum value of the numerator is 20, and the BDI can vary in the range of 0 to 1. Based on this backsheet degradation index, the modules have been binned into 5 categories as mentioned below.

Table 6.24: Backsheet degradation category based on Backsheet Degradation Index

Backsheet Degradation Index	0	0 – 0.1	0.1 – 0.25	0.25 – 0.5	>0.5
Backsheet Degradation Category	Nil	Low	Medium	High	Very High

Table 6.25 gives the average backsheet degradation index for different age groups and climatic zones, for Group X sites. It is evident that the Hot climates are most severe for the backsheet, while the Non-Hot

climates are less harsh. Further, there is an overall trend of increase in the backsheet degradation with age, which is expected. There does not seem to be any significant difference between the Group X and Group Y modules. Some of the young modules are showing degradation in the backsheet within 5 years of outdoor exposure, which may cause degradation in the module's performance in the long run, and hence is not a good sign for the long term reliability of the modules.

Table 6.25 (a): Average extent of backsheet degradation in Group X modules in different climatic zones and age groups (number of samples is given in brackets).

Climatic Zone	Age Groups			
	0-5 Years	5-10 Years	10-20 Years	20+ Years
Hot & Dry	NA	NA	High (8)	NA
Warm & Humid	Low (30)	Low (28)	Medium (84)	NA
Composite	Nil (19)	Low (7)	Medium (28)	NA
Moderate	Low (31)	NA	Medium (12)	NA
Cold & Sunny	Nil (33)	NA	Low (22)	NA
Cold & Cloudy	NA	NA	NA	NA

Table 6.25 (b). Average extent of backsheet degradation in Group X modules in Hot and Non-Hot climates for different age groups (number of samples is given in brackets).

Climatic Zone	Age Groups			
	0-5 Years	5-10 Years	10-20 Years	20+ Years
Hot Zones	Low (51)	Low (35)	Medium (120)	NA
Non-Hot Zones	Low (64)	NA	Low (34)	NA

Table 6.25 (c): Average extent of backsheet degradation in Group Y modules in Hot and Non-Hot climates for different age groups (number of samples is given in brackets).

Climatic Zone	Age Groups			
	0-5 Years	5-10 Years	10-20 Years	20+ Years
Hot Zones	Low (201)	Nil (40)	Medium (95)	NA
Non-Hot Zones	Low (168)	NA	NA	NA

Table 6.26 gives the statistics for the modules in small and large installations, and it seems that the modules in large installations are having lesser degradation in backsheet as compared to modules in small installations. However, again, before coming to any conclusion, it has to be kept in mind that the number of samples in the large installations is very few.

Table 6.26: Average extent of backsheet degradation in 'All' modules for small and large installations in the Hot and Non-Hot climatic zones and various age groups (number of samples is given in brackets).

Size of Installation	Climatic Zone	Age Groups			
		0-5 Years	**5-10 Years**	**10-20 Years**	**20+ Years**
Small	**Hot**	Low (280)	Low (68)	Medium (251)	Medium (2)
	Non-Hot	Low (239)	NA	Low (29)	NA
Large	**Hot**	Nil (20)	NA	NA	NA
	Non-Hot	Nil (30)	NA	Low (5)	NA

Based on the above discussion, it seems that the quality of backsheet being used in the young modules and the installation practices are of great concern. There is indication that modules in the large installations fare better than modules in the installations smaller than 100 KWp.

f) Glass Degradation

The front glass provides protection to the solar cells from outside environment while allowing light to pass unhindered to the solar cells underneath. However, improper handling and cleaning has been found to cause haziness in the glass, brown and white spots (paint marks), scratches, and even complete shattering (often caused by impact of hard objects falling on the glass) as shown in Fig. 6.6. Table 6.26 gives the statistics for the various degradation modes of front glass observed in the survey.

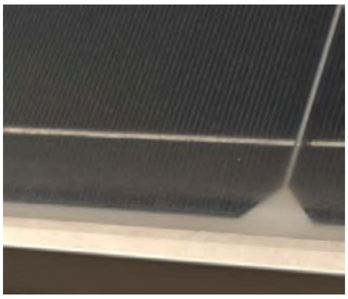

(a) Haziness in glass observed in old modules

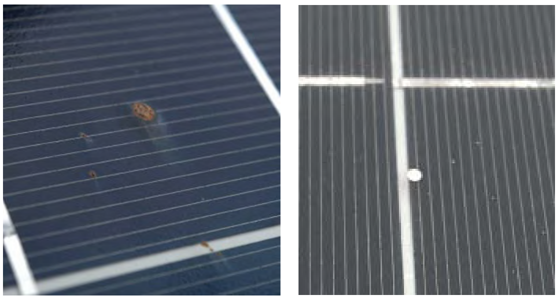

(b) Brown and white spots on front glass

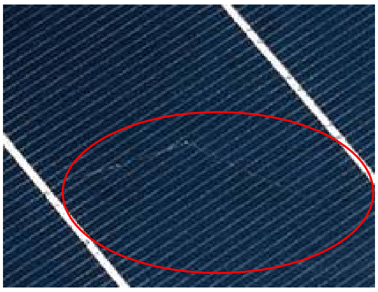

(c) Scratch on glass

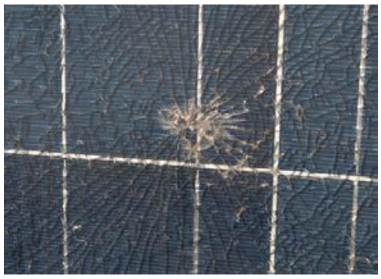

(d) Shattered glass

Fig. 6.6: Glass degradation observed during the survey

Table 6.27: Statistics of crystalline silicon modules affected by damage in front glass

Type of Damage	Percentage of Modules Affected	Additional Comments
Haziness in Glass	46%	In **8% of the modules**, the haziness extends over the solar cells, which can reduce the short circuit current of the module.
Scratches in Glass	3.7%	Percentage of young modules with scratches is **5 times higher** than the percentage of old modules with scratches which indicates improper handing during installation.
White Spots on Glass (paint marks)	2%	Percentage of young modules with white spots is **3 times higher** than the percentage of old modules which indicates improper maintenance at site.
Brown Spots on Glass	1.9%	Brown Spots have been observed only in the **young modules in Hot zone**.
Glass cracked/shattered	1.7%	Higher percentage of modules is shattered in **Hot zone** as compared to Non-Hot zone.

g) Frame Degradation

The frame provides mechanical strength and integrity to the module and keeps the various parts of the laminate together. It also serves to prevent moisture ingress into the module from the edges. However, improper handling during installation, poor maintenance and environmental stress can cause adverse impact on the frame, some examples of which are shown in Fig. 6.7. Table 6.28 shows the statistics of frame degradation.

(a) Algae growth (b) Corrosion (c) Scratches (d) Joint separation

Fig. 6.7: Degradation of frame observed during the survey

Table 6.28: Statistics of frame damage observed in the survey

Type of Damage	Percentage of Modules Affected	Additional Comments
Corrosion	33%	Minor corrosion in 32% cases, and major problems in 1% cases. Mostly the old modules are affected.
Bent	2%	3% of the young modules show cracks, joint separation or bend in the frame, while it is 5% for the old modules. Considering that young modules are installed less than 5 years ago, this 3% figure is also significant and points towards improper handling during installation.
Joints separated	3%	
Cracking	1%	
Scratches	5%	About 7% of the young modules show scratches in frame, while only 4% of the old modules show scratches, which again indicates poor handling and installation practices for the young modules.

h) Junction Box Degradation

The junction box provides protection to the output terminals of the PV module from the outside environment. Damage to the junction box will cause degradation in the output terminals, particularly corrosion due to humidity ingress, and this in turn will increase the series resistance and decrease the power output of the PV module. Table 6.29 shows the statistics.

Table 6.29: Statistics of junction box degradation observed in the survey

Type of damage	Percentage of modules affected	Additional Comments
Weathered or physically unsound	14%	Junction Box is damaged in 19% of the modules from the Hot zone, as compared to just 6% of the modules from the Non-Hot zone. However, no damage is seen in the young modules.
Poor attachment to module	3 %	Attachment is good in all young modules.
Lid missing	10%	Not found in young modules
Lid loose or cracked	3%	Not found in young modules
Poor sealing	21%	The seal has been found to be leaky in 4% of the young modules.
Corrosion of output terminals	14%	Output terminal corrosion is predominantly seen in the old modules in Hot zone (with 22% cases), but not in young modules and also not in Non-Hot zones.

6.2.2 Correlation of Visual Degradation with Electrical Performance Degradation

In this section, we correlate the visual degradation seen (quantified as described above) with the degradation in the electrical performance – I_{sc}, FF and P_{max}. This allows us to connect visual defects with module output.

a) Correlation with Short Circuit Current Degradation

The discoloration and delamination in the encapsulant can reduce the light reaching the solar cell and thereby decrease the short circuit current of the PV module. In order to correlate the discoloration and delamination observed in the surveyed modules to their electrical performance, the discoloration and delamination indices mentioned in previous section have been combined into a composite index, which we refer to as the Normalized Discoloration and Delamination Index (NDDI). NDDI is calculated using the following relation:

$$\text{NDDI} = \frac{\text{Degree of discoloration x Discolored cell area} + \text{Degree of delamination x Delaminated cell area}}{\text{Maximum value of numerator } (=4)} \quad \text{.... (6.5)}$$

where, Degree of discoloration = 1 for light discoloration,

= 2 for dark discoloration

Degree of Delamination = 2 (assuming same impact on cell's performance as dark discoloration)

The NDDI is derived from the discoloration index (defined in section 6.2.1(a)) and the delamination index (defined in section 6.2.1(b)), by combining these two indices for the worst affected cell in the module, with delamination given the same weightage as dark discoloration (i.e. degree of delamination taken as 2).

The Normalized Discoloration & Delamination Index (NDDI) value can vary between 0 and 1, with 1 representing the worst possible degradation (i.e. dark discoloration along with delamination on 100% cell area). Based on the NDDI value, the modules have been grouped into 5 categories, as follows:

Table 6.30: NDDI category based on the NDDI value

NDDI Value	0	0 – 0.25	0.25 – 0.5	0.5 – 0.75	0.75 – 1
NDDI Category	Nil	Low	Medium	High	Very High

Figure 6.8 shows examples of modules with Low, High and Very High NDDI values.

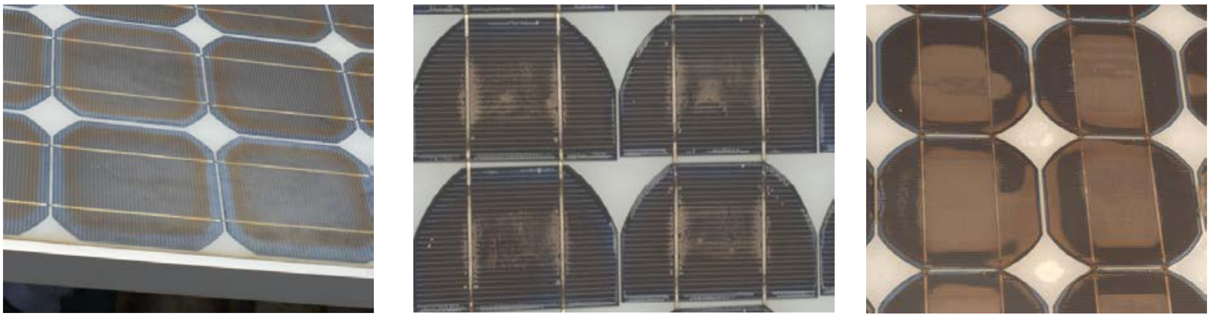

(a) (b) (c)

Fig. 6.8: Examples of the NDDI category (a) Medium degradation, (b) High degradation, (c) Very High degradation

Figure 6.9 shows the percentage reduction in short circuit current I_{SC} for different NDDI categories for Group X modules (note that this is the *total* reduction, not annual rate). The average values of I_{SC} degradation is indicated with the red horizontal bar and the red diamond indicates the 95% confidence interval for the average. The green vertical lines are the error bars due to uncertainty in measurement and STC correction, while the pink vertical lines on the left shows the error due to nameplate uncertainty (nameplate tolerance). It should be noted that there are multiple factors, apart from discoloration and delamination, which can reduce the I_{SC}, so there is a lot of scatter in the data points. The average is used as the estimator of central tendency. From the figure, we can see that the average I_{sc} reduction shows good correlation to the NDDI category (as it increases with increase in the NDDI category). It is however not possible to estimate the I_{sc} degradation based on the NDDI category, since there are many non-visual degradation modes which may also affect the short circuit current.

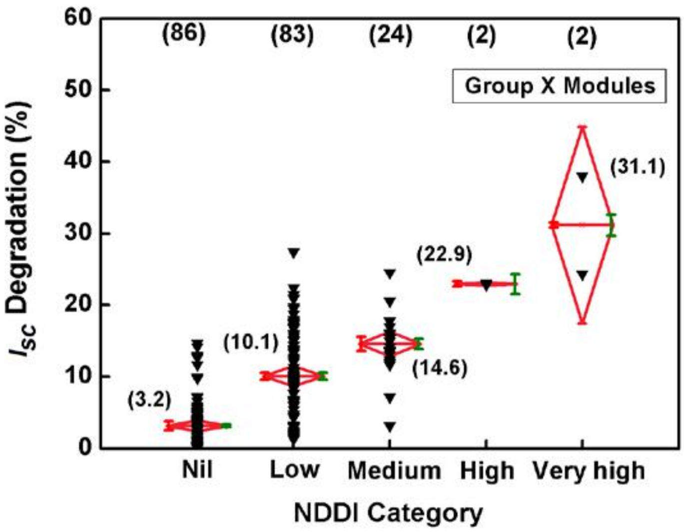

Fig. 6.9: Plot of short circuit current degradation versus extent of discoloration and delamination (NDDI category). Note that the y axis gives the *total* % reduction, not annual rate (%/year).

Further, the reduction in power output has been plotted for the different NDDI categories in Fig. 6.10 and found to be well correlated.

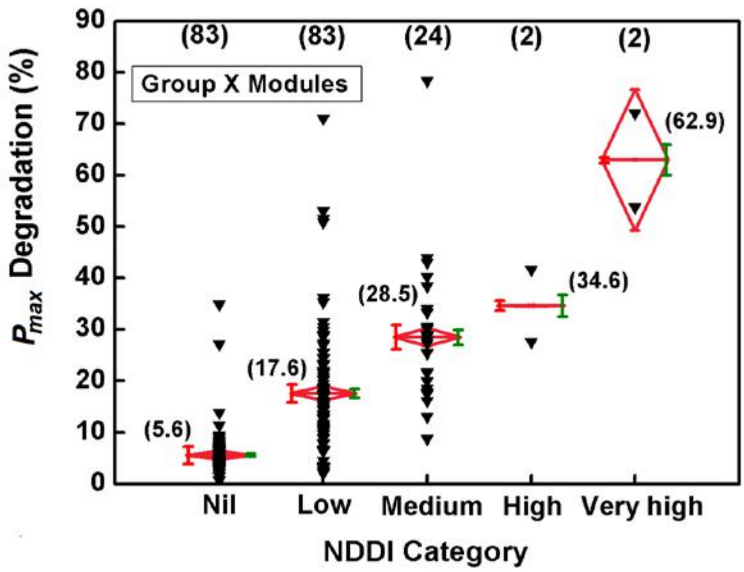

Fig. 6.10: Plot of output power degradation versus extent of discoloration and delamination (NDDI category). Note that the y axis gives the *total* % reduction, not annual rate (%/year).

b) Correlation with Fill Factor Degradation

Figure 6.11 shows the plot of the percentage fill factor degradation versus the metallization discoloration for modules of Group X. Metallization discoloration is mainly due to corrosion in the old modules, and hence it can be expected that as the discoloration increases over the years, there would be increase in series resistance, which would degrade the fill factor. In Fig. 6.11, it can be seen that the average total *FF* degradation (in %) increases with increase in the extent of metallization discoloration, thereby indicating a positive correlation between the two (as expected from theory).

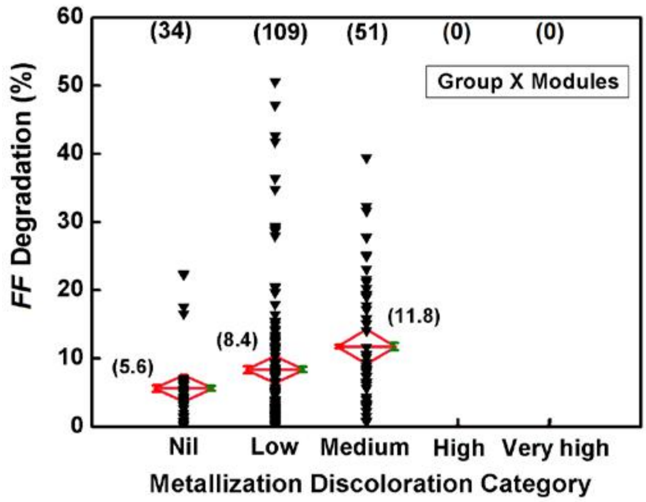

Fig. 6.11: Plot of *FF* degradation versus extent of metallization discoloration (MDI category). Note that the y axis gives the *total* % reduction, not annual rate (%/year).

c) Correlations with Total Power Degradation

Based on the discoloration, delamination and metallization discoloration (which is mainly due to corrosion in the old modules), a composite Visual Degradation Index (VDI) has been defined using the formula:

$$\mathrm{VDI} = \frac{\mathrm{NDDI} + \mathrm{MDI}}{2} \qquad \text{.... (6.6)}$$

Hence, VDI will also range between 0 (indicating no visual degradation) and 1 (indicating very high visual degradation). Again, based on the VDI, the modules can be grouped into 5 categories as before. Figure 6.12 shows the plot of the percentage degradation in output power for Group X modules for the different VDI categories. We can see that the degradation in power output increases with increase in the Visual Degradation Index, as expected. However, the visual degradation alone cannot fully explain the degradation in the power output (as indicated by the extent of scatter in the data). Various non-visual degradation modes are also active in the modules, like cracks in the solar cells, interconnect breakages, etc. which also contribute to the degradation in the power output.

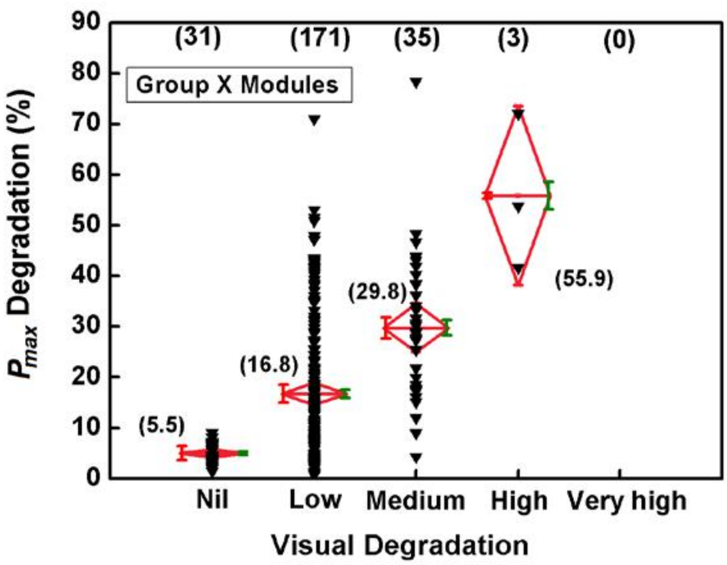

Fig. 6.12: Plot of output power degradation versus extent of visual degradation (VDI category)

d) Correlation of Snail Trails with Power Degradation Rate

Snail tracks have been observed in the young modules in all climatic zones, as discussed in Section 6.2.1(c). Figure 6.13 shows the plot of power degradation rate (in %/year) for modules with and without snail trails, and we can see that there is negligible difference in the average degradation rates of the two groups of modules. However, it may be mentioned here that snail trails are widely reported to be associated with module cracks and such cracks may become worse in the long run and lead to degradation in power output (which is discussed in Chapter 7).

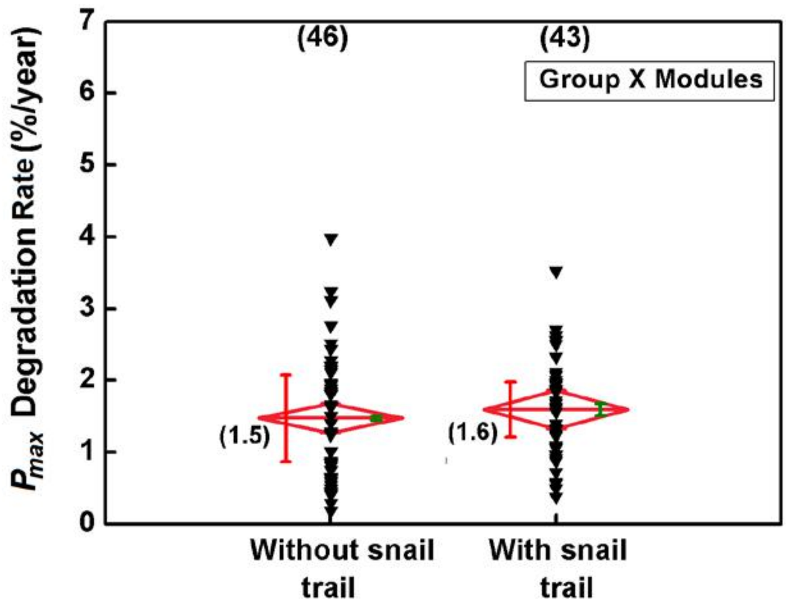

Fig. 6.13: Effect of snail trails on power degradation rate in PV modules

6.3 Visual Degradation Observed in Thin Film Modules

Thin Film modules have not been commonly used in India in the past, but have been increasingly deployed in recent years, due to their spectral response and temperature coefficients being better suited for Indian climatic conditions, and also various non-technical reasons. A total of 162 thin film modules were inspected in the field (excluding 7 HIT modules which have wafer-based cells and hence are not clubbed in the Thin Film category). All of these modules were in the young age group, and were spread across only the Hot climatic zones (Hot & Dry, Warm & Humid, and Composite zones). Table 6.31 shows the major degradation modes observed in the surveyed modules. White spots on the modules are a very commonly occurring phenomenon. These are visual indications of shunts in the module, created due to foreign particles embedded at the time of manufacturing and/or hot spots caused due to partial shading [44]. The second most prevalent degradation seen is delamination in the edge seal, which can lead to corrosion of the thin film active layer of the module due to moisture ingress into the module in the long run [77].

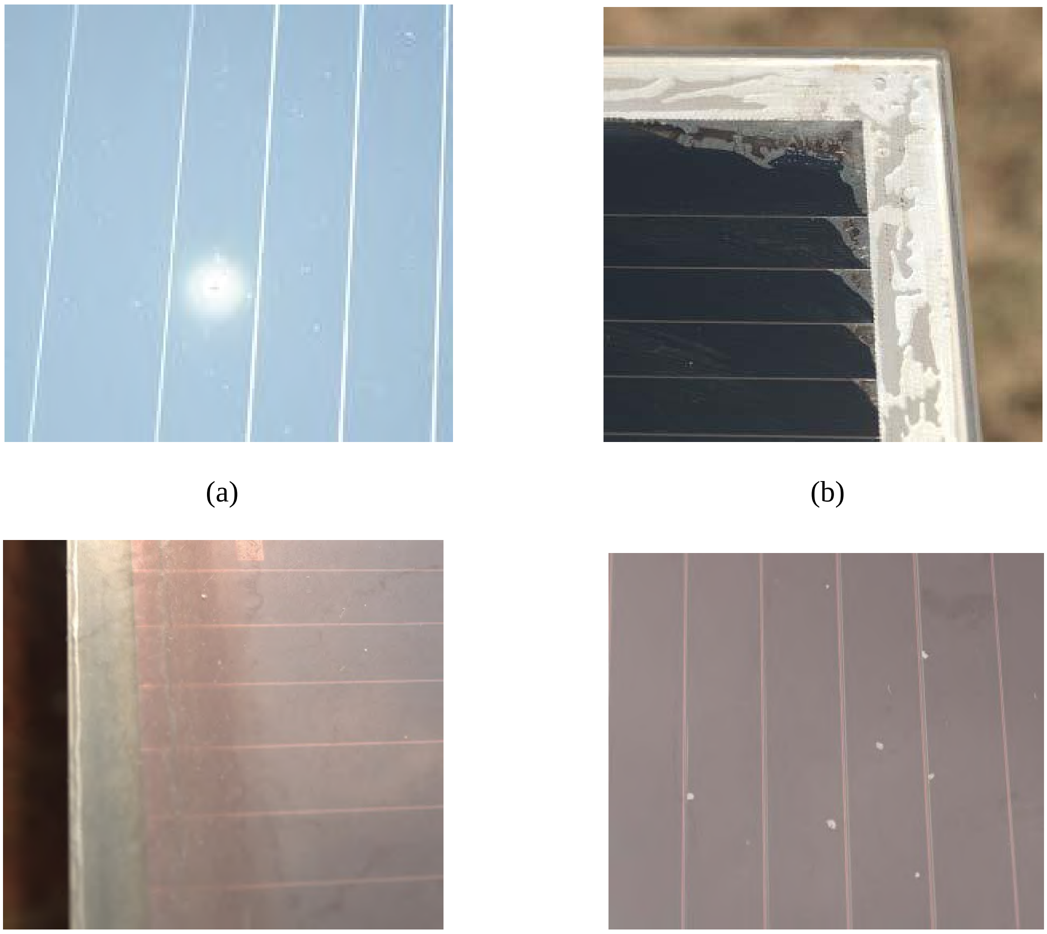

(a) (b) (c) (d)

Fig. 6.14. Degradation in Thin Film modules (a) White spot in CdTe module, (b) Delamination of edge seal and inside cells (bar graph corrosion) in CdTe module, (c) haziness in a-Si module, (d) White spots (debonding) in a-Si modules

Table 6.31: Statistics of thin film modules affected by various degradation modes

Technology	Total No. of Modules	Percentage of Modules Affected				
		White Spots	Cracked Glass	Non-Crack Damages	Cell Delamination	Edge Seal Delamination
Amorphous Silicon	74	77%	12%	22%	10%	NA
Cadmium Telluride	76	99%	4%	25%	9%	73%
Copper Indium Gallium Selenide	12	100%	0%	21%	29%	50%

The effect of white spots (created due to debonding) in amorphous silicon modules on their electrical performance is shown in Fig. 6.15. It can be seen that the modules with white spots show higher degradation rate for power, which seems to be mostly attributable to higher degradation rate of fill factor (*FF*). This is reasonable as white spots are related to shunts in the module, and shunts reduce the fill factor.

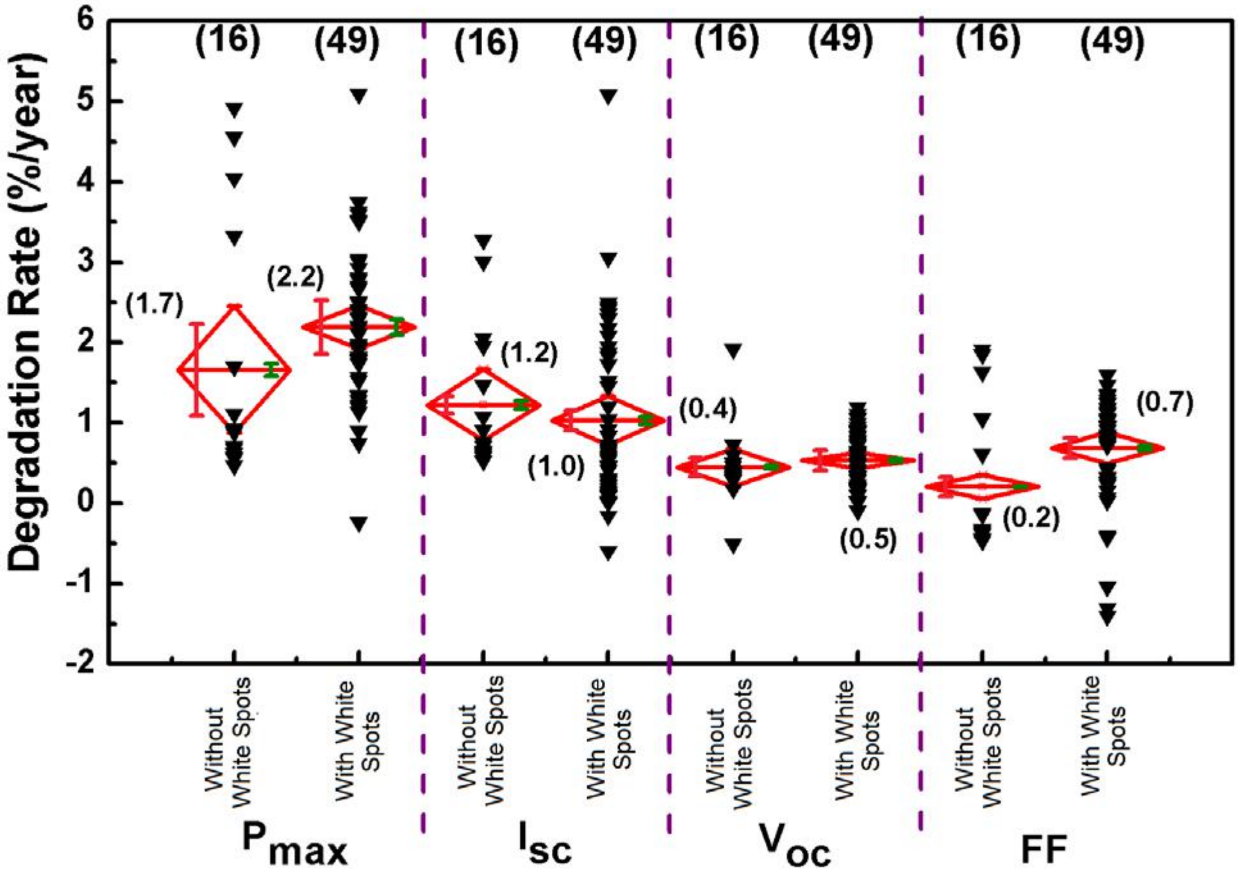

Fig. 6.15: Effect of white spots (debonding) in amorphous silicon modules on their electrical performance parameters

6.4 Summary

Visual degradation observed in the surveyed modules provides us useful insights into the current state of PV modules deployed in India, and leads us to the following conclusions:

- Encapsulant discoloration has been observed in all climatic zones and tends to occur in most modules which are in operation for more than 10 years. Modules in Hot zones discolor faster as compared to modules in Non-Hot zones. Among the young modules, discoloration is twice as common in Group Y modules as compared to the Group X modules, which raises concerns about the quality of the materials and the manufacturing process. Some 27 year old modules having glass-glass construction have been found to be free from discoloration in spite of operation in the Hot & Dry climate of Rajasthan.

- Front-side delamination is most commonly observed in the old modules in Warm & Humid zone, followed by the Hot & Dry zone. Delamination is more frequently detected (and is also more severe) in the Group Y modules, as compared to Group X modules. Discoloration and delamination have been found to correlate well with the decrease in the short circuit current of the modules, and the consequent power loss.

- Higher discoloration and delamination which result in power loss is likely to be one of the reasons why the Group Y modules show higher degradation rates.

- Metallization discoloration is observed not only in the old modules, but even in young modules, which hints towards poor material quality and manufacturing processes. Metallization discoloration is observed in all climatic zones but its severity is highest in the Warm & Humid zone. It has been found to correlate well with the degradation in the fill factor of the module.

- Snail Trails have been observed in all climatic zones, but are more severe in the humid zones – Warm & Humid and Cold & Cloudy. Snail trails do not seem to affect the present-day electrical performance of the modules.

- Backsheet has been found to degrade in both young and old modules, but there is indication that modules in the large installations are better off than the small installations.

- The quality of encapsulant appears to be an important differentiating factor between modules of Group X sites (which show average degradation rate within 2%/year) and Group Y sites (which show average degradation above 2%/year).

- Haze is the most commonly observed degradation mode in the front glass, and in about 8% cases, it has extended to the top of the bottom row solar cells, thereby creating partial shading in these modules. Scratches in the front glass and frame are 2 to 5 times more in young modules as compared to old modules, which indicate mishandling during transportation and/or installation of the young modules. Junction box damage and corrosion of output terminals is predominantly seen in the old modules of the Hot zone.

- White spots are the most commonly observed defect in thin film modules. Amorphous silicon modules having white spots degrade at a much faster rate as compared to modules without the white spots. This degradation is mainly observed in the fill factor, which in turn reduces the power output.

7. Analysis of EL and IR Data

7.1 Introduction

Electroluminescence (EL) and Infra-red (IR) imaging techniques are very commonly used characterization tools for PV modules. However, while IR imaging is predominantly used for outdoor characterization, EL is mostly used for indoor characterization, but as described below, we have used a special technique for outdoor field characterization. EL imaging provides insight into the quality and condition of the semiconductor material and helps us to identify inactive regions and cracks in the solar cells [78]. IR thermography shows the distribution of temperature in the module, and helps to identify the hot spots.

7.2 Analysis of Electroluminescence Data

EL imaging was done in the field using an image difference technique developed by us for the purpose of our field survey [65], which enabled us to obtain the EL images in the presence of ambient light. Two consecutive images of the selected module were taken using a silicon CCD camera – one image with the module in open circuit, and another image with the module under bias (passing 1.3 times the rated short circuit current of the PV module). The actual EL image was then obtained by subtracting the open circuit image from the image under bias. EL images of a total of 49 modules (39 crystalline silicon and 10 thin film) were taken in the field during the survey. Figures 7.1 and 7.2 show some of the EL images taken during the survey for both Group X and Group Y modules. There are some dark patches in Figs. 7.1 (a) and (b) which indicate inactive areas of the solar cells. In Fig. 7.1 (c), dark areas are present along some of the busbars, with very bright areas crowding near the opposite busbars. This is an indication of interconnect breakage. In Fig. 7.1 (d), lots of thin dark lines are visible, which are micro-cracks in the cells. In Fig. 7.2, we can notice lots of dark patches in these modules from Group Y sites. A general observation that can be made from these images is that the group Y modules show higher number of cracks in the solar cells as compared to group X modules. The higher number of cracks may be due to poor transportation or installation practices. It would have been interesting to see whether there are significant differences in terms of cell cracks between small and large installations, but the data are unfortunately too less to attempt such a comparison.

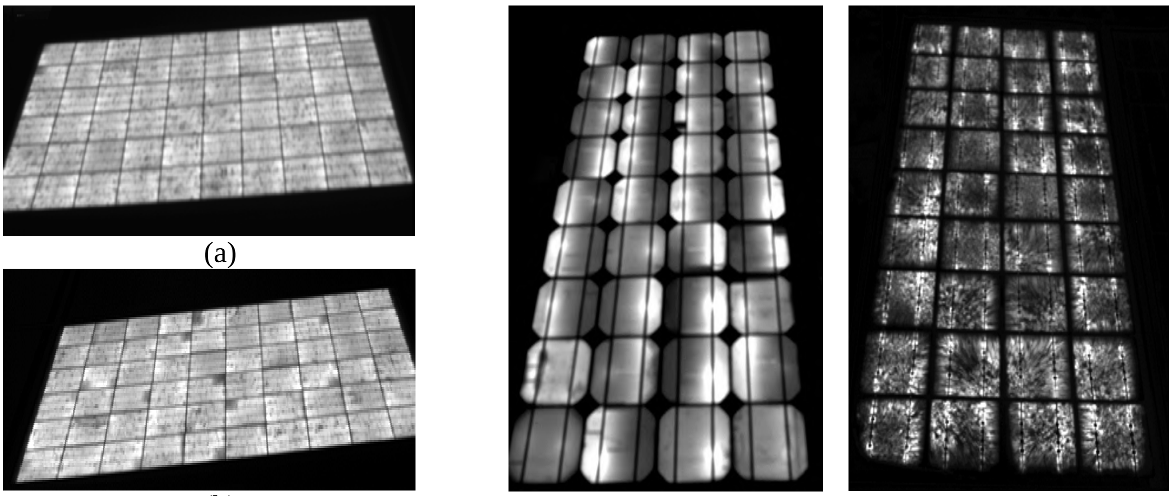

(a) (b) (c) (d)

Fig. 7.1: EL images of some Group X modules taken in the field

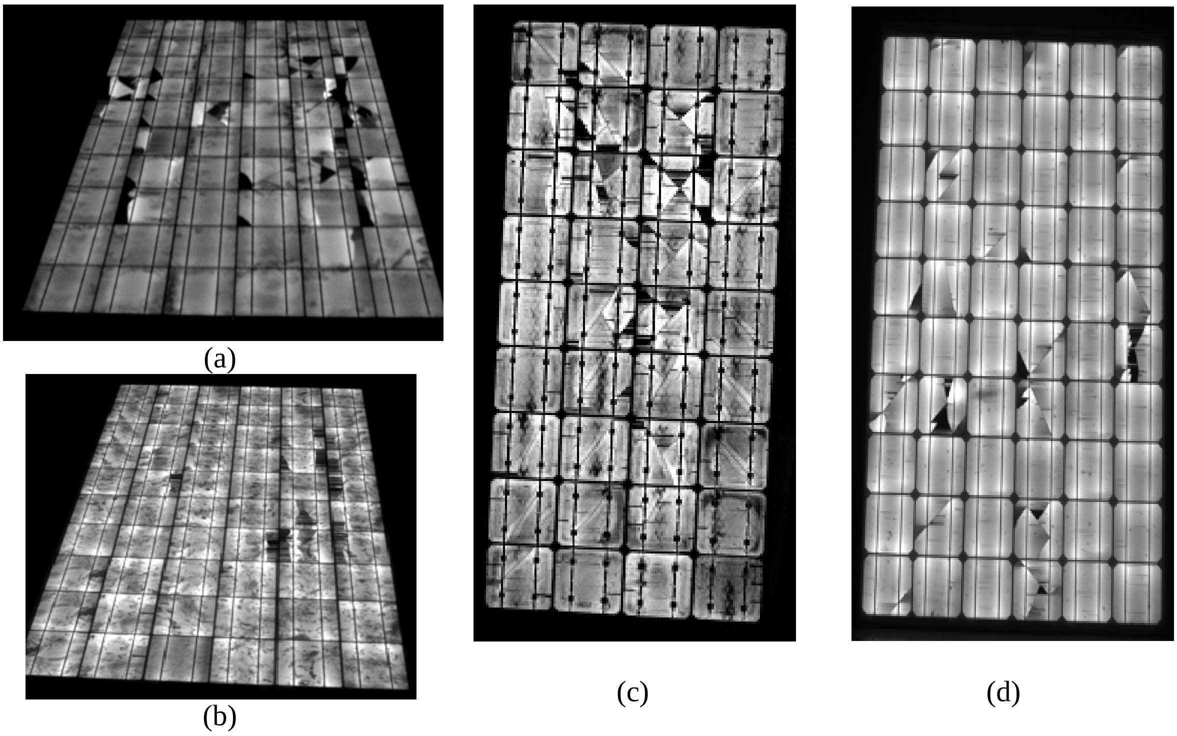

Fig. 7.2: EL images of some Group Y modules taken in the field

7.2.1 Classification of Cracks

Kontges *et al.* [79] have classified cracks into 3 categories based on the area affected by the crack as visible in the EL image:

a) Mode A cracks which are basically hair-line cracks, not associated with any dark area,
b) Mode B cracks which are associated with a grey (not very dark) area in the cell,
c) Mode C cracks which are associated with a dark area in the cell.

Figure 7.3 shows the EL image of a section of PV module with the 3 types of cracks labelled in the image. While mode A crack will not lead to any loss in short circuit current, mode B and mode C cracks can be expected to reduce the short circuit current, since the associated grey/dark area signifies that electrical connection to that area of the solar cell has been broken, and hence the charge carriers generated in that area of the solar cell are not collected and sent to the external load.

From the EL images taken during the survey, the number of cracks of different categories has been counted and the statistics are shown in Table 7.1, wherein we can see that modules in Group Y have a larger number of cracks as compared to Group X modules. Hence, cracks in the cells are likely to be one of the reasons behind the higher degradation rate observed in group Y modules. Table 7.2 shows the statistics for the young and old modules. Percentage of cracked cells in young modules is more than that in old modules, which suggests that the transportation and/or installation practices for young modules are hasty or improper.

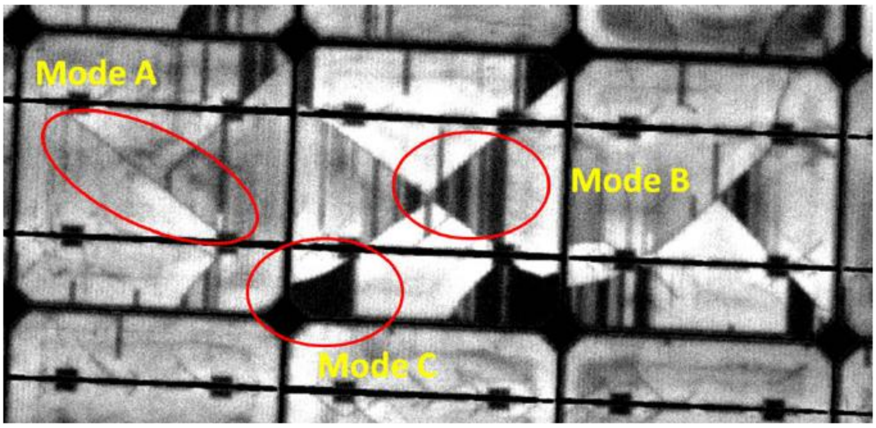

Fig. 7.3: Different types of cracks as visible in EL images

Table 7.1: Percentage of cells affected by different types of cracks in Group X and Group Y modules

	Percentage of cells affected by different types of cracks			Total no. of cells
	Mode A cracks	Mode B cracks	Mode C cracks	
Group X modules	2.4%	14.1%	3.2%	972
Group Y modules	29.7%	42.3%	14.2%	444

Table 7.2: Percentage of cells affected by different types of cracks in young and old modules

	Percentage of cells affected by different types of cracks			Total no. of cells
	Mode A cracks	Mode B cracks	Mode C cracks	
Young modules	37.9%	14.9%	12.2%	408
Old modules	0%	26.2%	4.4%	1008

7.2.2 Correlation of Snail Trails with Electroluminescence Images

Snail trails have been observed in the young modules during the survey, and these have been described in Chapter 6. The snail trails appear as black or brown curved lines running across the solar cells, and sometimes bordering them (like a frame). EL images of these modules show cracks in the solar cells, as shown in Figs. 7.4 and 7.5. These cracks are often not visible underneath the snail trail in the visual image and in some cases the snail trails are also not easily visible. EL imaging is a useful tool for detection of cracks in modules. Figure 7.4 shows the visible and EL images of a module in the Composite climatic zone. In Fig. 7.4 (b), the snail trails are clearly visible as dark lines criss-crossing the solar cells, and Fig. 7.4 (d) shows the EL image of the same section of the module, making it clear that snail trails (of the non-framing type) are associated with cracks in the solar cells. Figure 7.5 shows the snail trails observed in a module in Warm & Humid zone, and the corresponding EL image. The cracks enable the ingress of moisture to the top surface of the solar cells, where the moisture aids in the migration of the silver from the fingers into the front encapsulant to form silver nano-particles, resulting in snail trails, as mentioned in the literature [80] .

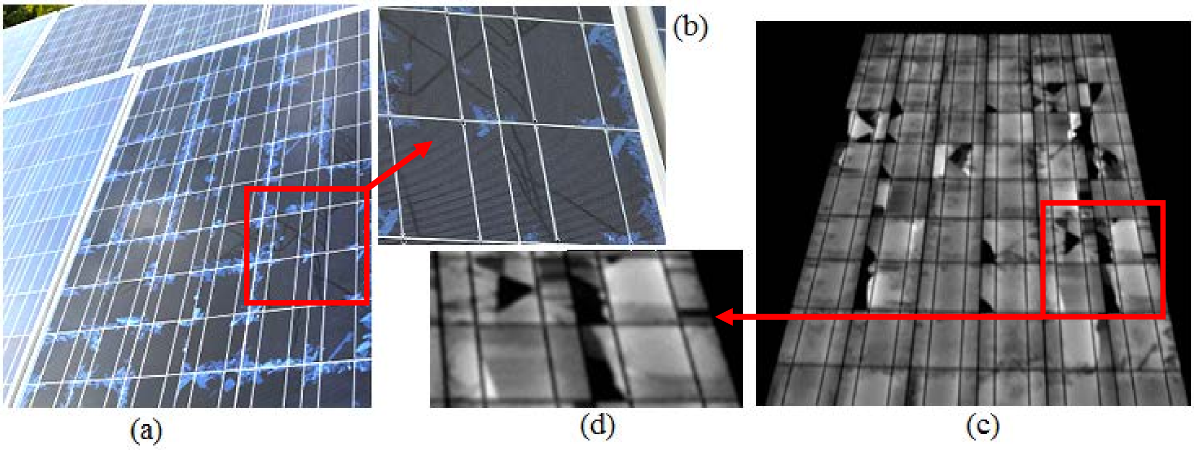

Fig. 7.4: (a) Snail trails observed in a PV module in Composite climatic zone, (b) blown-up image of the snail trails, (c) EL image of the same module showing the cell cracks and (d) blown-up section of the EL image showing the cracks corresponding to the snail trails visible in (b).

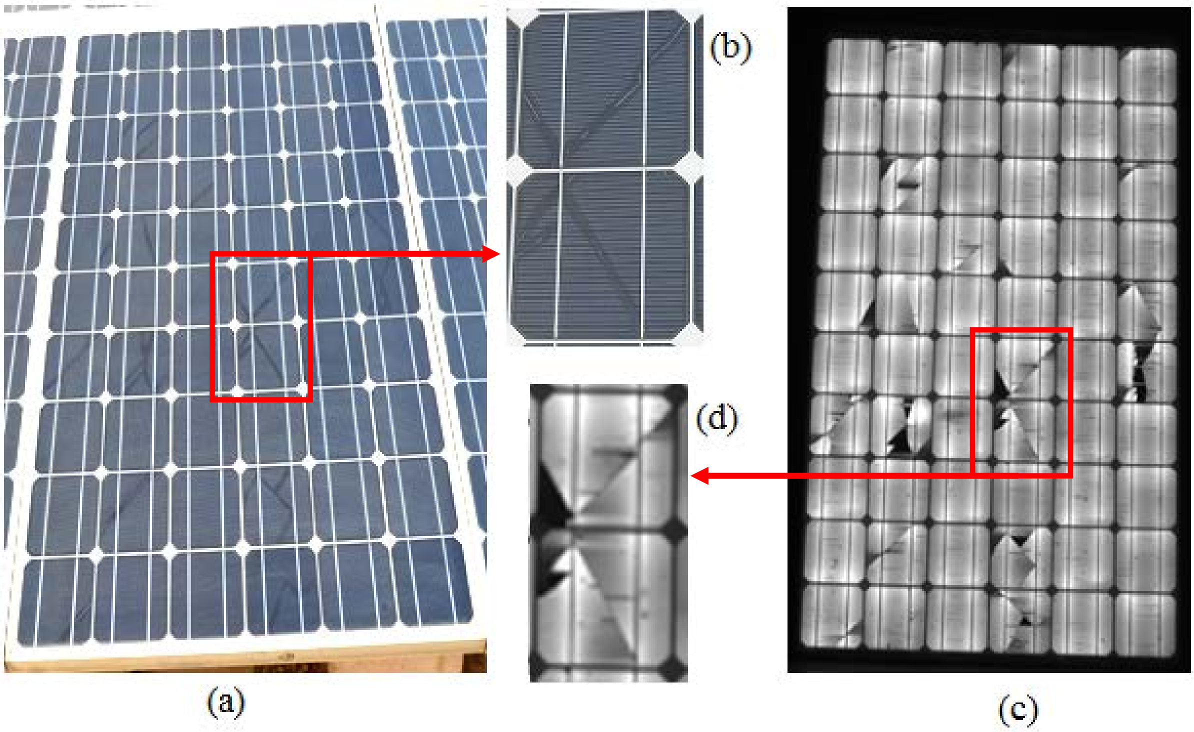

Fig. 7.5: (a) Snail trails observed in a PV module in Warm & Humid zone, (b) blown-up image of the snail trails, (c) EL image of the same module showing the cell cracks and (d) blown-up section of the EL image showing the cracks corresponding to the snail trails visible in (b).

7.2.3 Correlation of Interconnect Breakage with Electroluminescence Images

Interconnects provide electrical connection between the cells and conduct the electrical power to the external load from the cells in the PV module. Usually there are 2 or 3 interconnects in each cell, which provides necessary redundancy in case of breakage in any part of the interconnect. However, if there is a breakage even in one interconnect, the whole cell's current would have to be conducted by the other interconnects in the cell, leading to current crowding, which increases the series resistance of the module, thereby degrading the fill factor and the power output.

During the survey, interconnect breakage has been tested using the Togami Cell Line Checker, which has also been verified in some cases using EL imaging. In Figure 7.6 (a) we can see an interconnect breakage on the busbar (marked in red) which corresponds to the dark region in Fig. 7.6 (b). Similarly in Fig. 7.7 (a), several long interconnect breakages correspond to the dark regions in Fig. 7.7 (b). These interconnect breakages increase the series resistance of the module, which eventually reduce the power output. Also, in some cases they can cause catastrophic failure due to the complete breakage of the interconnect busbar.

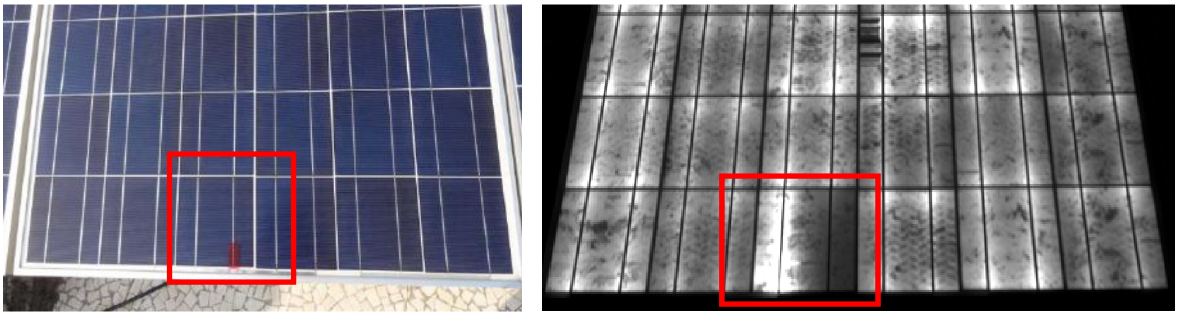

(a) (b)

Fig. 7.6: (a) Interconnect breakage in a PV module, detected using Togami Cell Line checker (marked red on the cell interconnect), and (b) the EL image of the corresponding section.

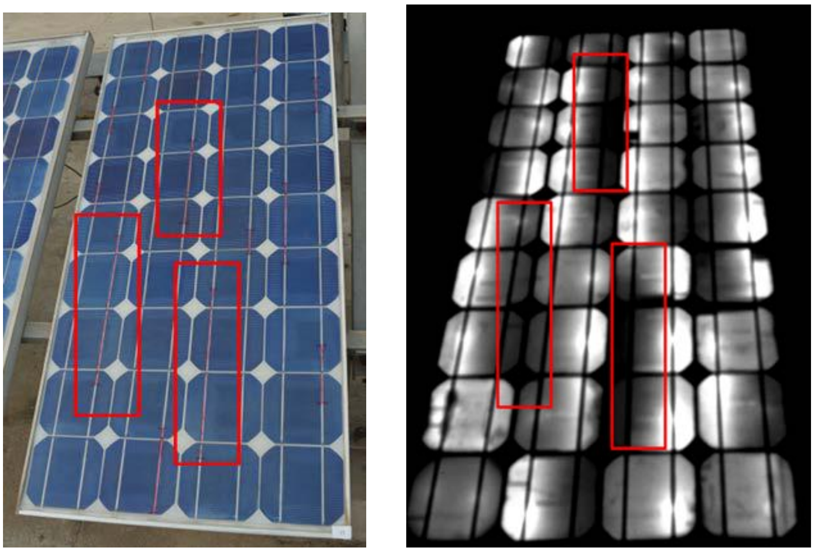

(a) (b)

Fig. 7.7: (a) Interconnect breakages in a PV module, detected using Togami Cell Line checker (marked red on the cell interconnects), and (b) the EL image of the same module

7.2.4 Correlation of Cracks with Location

The location of the cracks in the module can provide us information regarding the possible causes of such cracks. For analysing the location of the crack, each module is divided into 3 sections – the central zone, the intermediate zone, and the periphery. Figures 7.8 (a) and (b) show the percentage of modules affected by cracks in these 3 zones, with the total number of module samples being indicated in brackets. Cracks are mostly happening in the cells along the periphery of the modules, which suggests poor handling of the modules during transportation and/or installation (since these cracks may arise when the edges of the module strikes a hard object). Figure 7.8 (c) provides the percentage of cells cracked at each cell position for the 60-cell modules, and we can see that the bottom corner is the most vulnerable position.

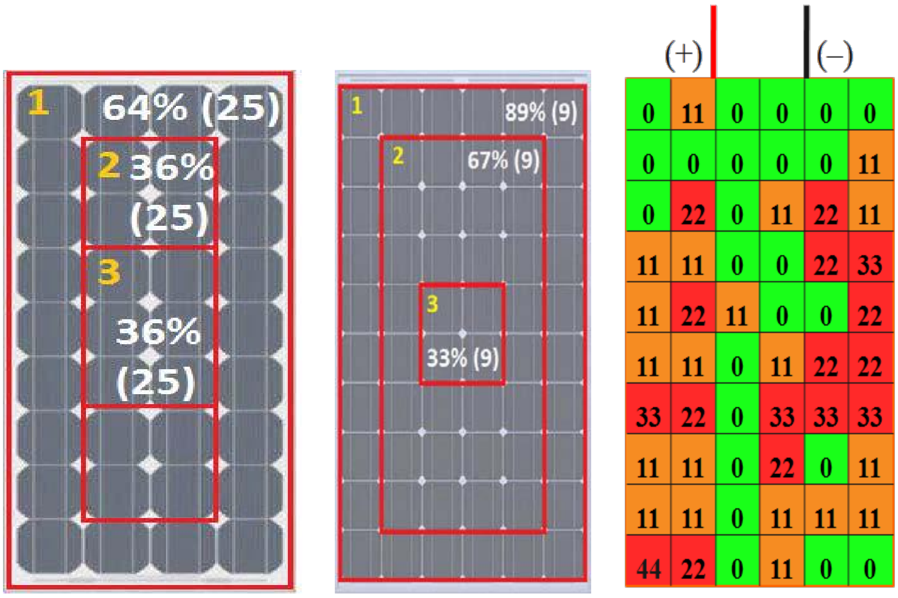

(a) (b) (c)

Fig. 7.8: (a) Percentage of modules affected by cracks in the 3 zones for the 36-cell modules (b) Percentage of modules affected by cracks in the 3 zones for the 60-cell modules (c) Percentage of cells cracked at each cell position for the 60-cell modules

7.2.5 Correlation of I_{sc} degradation with Percentage Dark Area of the Worst Cell

Cracks in the solar cells can cause reduction in the short circuit current, particularly in case of mode B and mode C cracks [79]. Since the cells in a module are in series, the affected area of just one cell will impact the overall output of the whole module. Figure 7.9 shows the plot of the percentage reduction in short circuit current I_{sc} of the module against the percentage dark area of the worst affected cell in the module (note that the *total* reduction not annual rate is being plotted). We can see that there is an increase in the short circuit current degradation with increase in the affected cell area. The percentage I_{sc} degradation is higher in the old modules as compared to the young modules because the old modules also suffer from encapsulant discoloration (which is not present in the young modules).

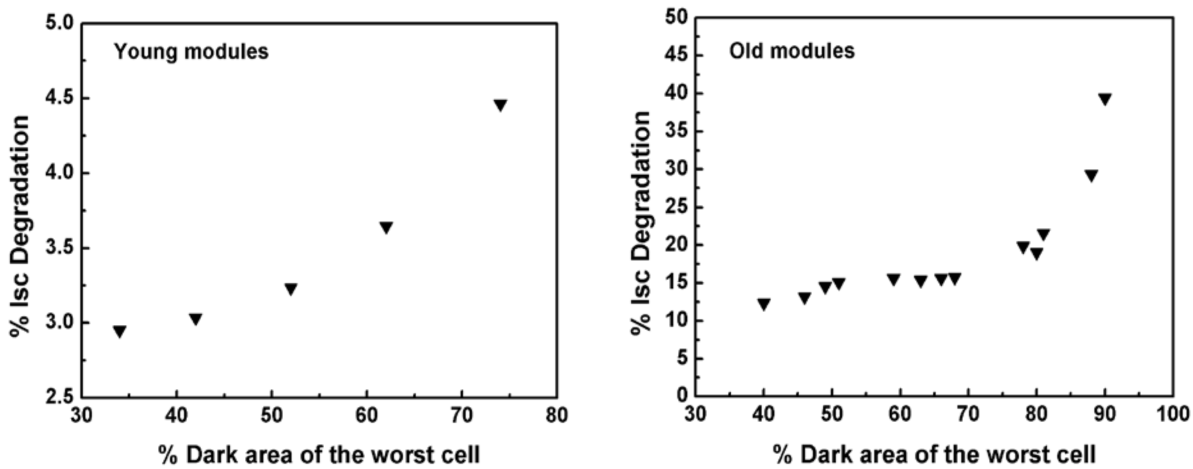

Fig. 7.9: Percentage reduction in short circuit current versus the affected cell area of cracked cell in young modules (left image) and old modules (right image)

7.2.6 Correlation of P_{max} Degradation with Number of Cracks

Figure 7.10 shows the plot of the power degradation rate (% per year) versus the total number of cracks in the module, and it can be seen that the degradation rate increases with increase in the number of cracks in the module. Furthermore, from the figure we can see the distinction between old and young modules, which again indicates the likelihood of poor installation for the young modules, or possibly the use of thinner – and more fragile – Si wafers.

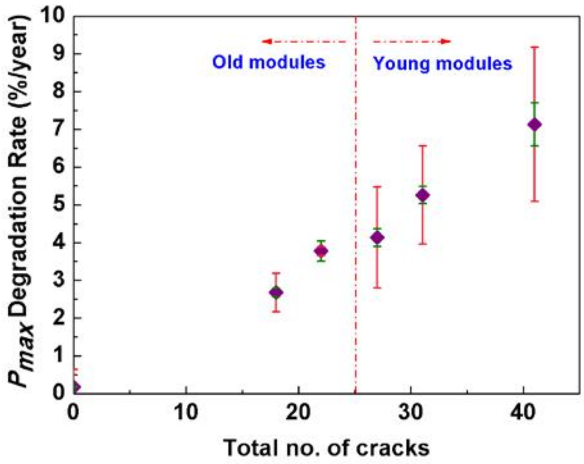

Fig. 7.10: P_{max} degradation rate (%/year) versus the total number of cracks in the module. The green and red bars indicate the instrument/STC correction error and nameplate error respectively.

7.2.7 Correlation of Dark IR Images with Electroluminescence Images

Dark IR thermography has been performed on a selected set of modules during the survey. The module is covered from the front using an opaque cover, and forward biased by a DC power supply at its rated short circuit current. The IR image of the module is captured from the backside of the module using a FLIR E60 infra-red camera. In Fig. 7.11, the EL image (left) shows a badly damaged solar cell with a significant inactive (dark) area, highlighted with the red box. The dark IR image on the right also shows this inactive area as dark (the IR image is taken from the backside while the EL image is taken from the front, and hence the features appear to be mirrored).

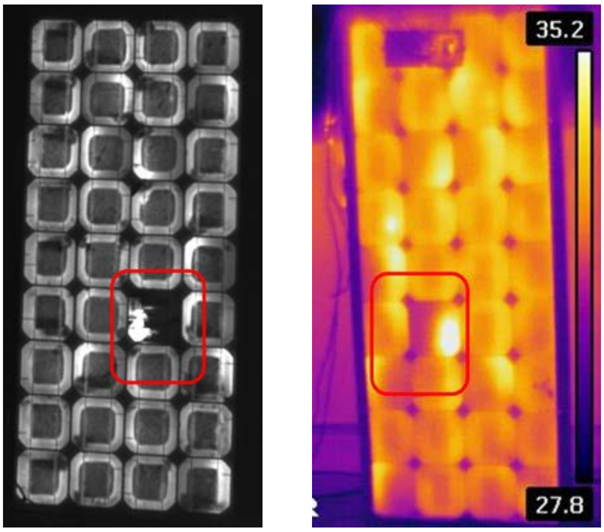

Fig. 7.11: Comparison of the EL image with the Dark IR image of an old module.

7.3 Analysis of Illuminated IR Data

During the survey, the IR image of each PV module under normal operating (illuminated) condition was taken from the back-side (wherever possible, otherwise taken from front), by short-circuiting the modules' terminals. The module was kept short circuited for at least 5 minutes before taking the IR image using a FLIR E60 camera. The hot spots so obtained can be regarded as the worst case scenario, as under normal operation of the module at maximum power point (MPPT), the hot spots are expected to be much less severe (since the module at MPPT would not be dissipating the total input energy as heat, as would happen in the case of the short-circuited module). Figure 7.12 shows the temperature histogram of a 2 year old module installed in Warm & Humid climate. The modal temperature of the histogram is considered to be the representative temperature of the PV module since it is the most frequently occurring temperature in the module IR. This modal value was found to be quite close to the median but far from the average, since the average temperature (obtained from the histogram) is influenced by the temperature of the frame and support structure (and sometimes the sky), which inevitably appear in the IR images. The highest temperature in the histogram is the maximum cell temperature, which is noted down for further analysis.

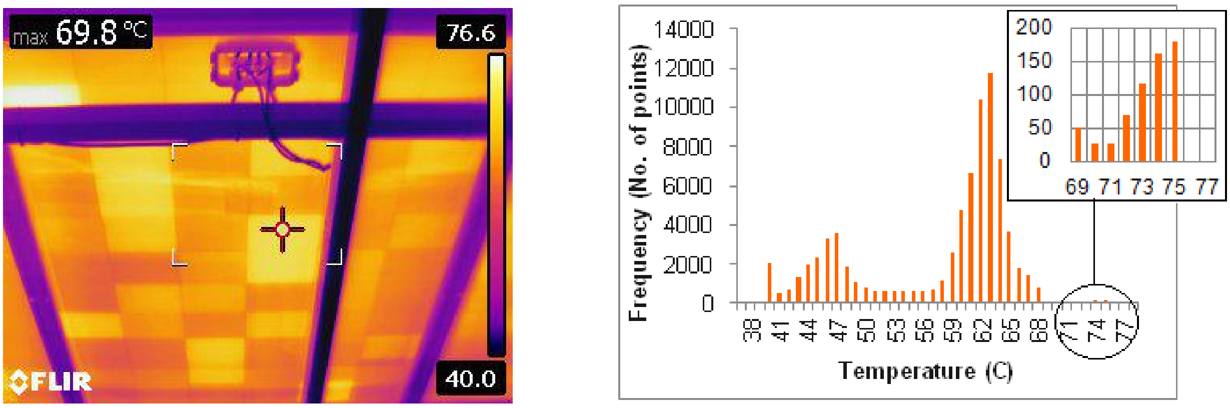

Fig. 7.12: (a) IR image of a 2 year old PV module installed in Warm & Humid climate, and (b) its temperature histogram extracted from the IR image. The highest temperature in this module is 75°C (shown in inset), and the representative temperature of the module is 63°C (modal value of histogram).

Figure 7.13 shows the histogram of the module temperature of 'All' modules (Groups X and Y) inspected in the survey, and the histogram of the maximum cell temperatures is given in Fig. 7.14. The lowest module temperature recorded was 15ºC (in Ladakh) while the highest was 70.3ºC (in Rajasthan), with the average around 44ºC. The highest cell temperature recorded for any module in the survey was 161ºC, and temperatures exceeding 100 ºC were observed in 9 modules. It is important to note that these readings were taken in the early winter season, with variable irradiance and ambient temperatures.

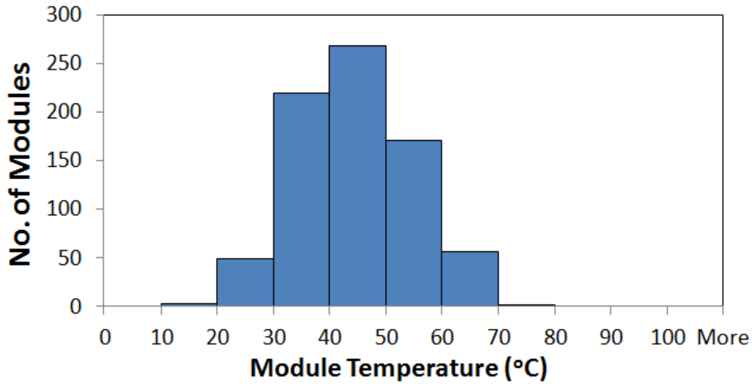

Fig. 7.13: Histogram of module temperature of 'All' modules inspected in the survey

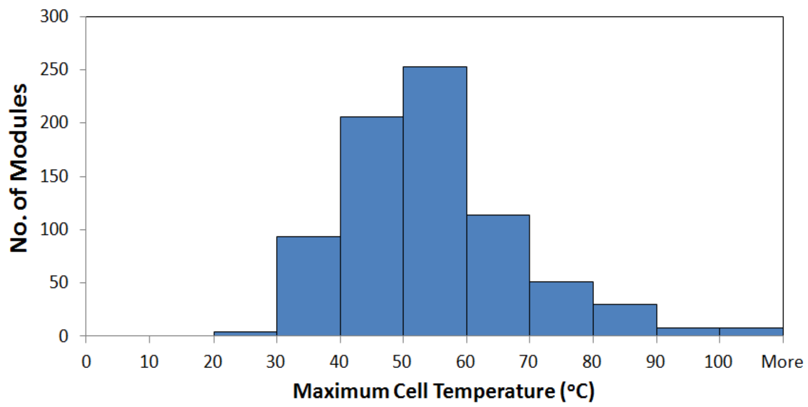

Fig. 7.14: Histogram of maximum cell temperatures of 'All' modules inspected in the survey

7.3.1 Normalization of IR Data

Since the IR images were taken for different modules at different times of the day, and on different days and sites, ambient conditions have varied greatly between the images. It is necessary to translate (normalize) the measured temperature to a reference condition so that comparisons can be made between the data collected during the survey. Based on the work of Moreton *et al.* [36] and Oh *et al.* [81], the temperatures were normalized to the reference condition of 1000 W/m^2 and 40°C, using the relation:

$$T_{normalized} = 40 + \frac{(T_{measured} - T_{ambient}) \text{ x } 1000}{\text{Irradiance}} \quad \text{.... (7.1)}$$

where,

$T_{normalized}$ = translated (normalized) temperature

$T_{measured}$ = module temperature (obtained from IR image)

$T_{ambient}$ = ambient temperature measured at site

Further, we define

$$\text{Module } \Delta T = T_{maxcell,norm} - T_{module,norm} \quad \text{....}$$

(7.2)

where,

$T_{maxcell,norm}$= Normalized maximum cell temperature of the module

$T_{module,norm}$ = Normalized modal temperature of the module

The module ΔT represents the extent of mismatch between the temperatures in different cells of the module. Vodermayer *et al.* [82] have reported that a single hot cell, running 9°C hotter than the surrounding cells, is associated with a decrease of almost 20% in I_{mp} (maximum power point current), with corresponding decrease in power output of 15%. Hence, we have considered modules with normalized module ΔT above 10°C as modules with 'Hot Cells'.

7.3.2 Analysis of Normalized IR Data

a) Effect of Hot Cells on Electrical Degradation Rate

The data has been screened for IR images taken above 700 W/m^2 (since translation accuracy will suffer at low irradiances and hence should be avoided, according to [36]). Since we want to compare the results with electrical degradation, it was also necessary that *I-V* of the module was recorded at irradiance above 500 W/m^2 (during the survey, the *I-V* and IR were often taken at different times, hence the different irradiance bars). The above screening process has unfortunately reduced the applicable sample size for the correlation. The influence of Hot Cells on the power degradation rates for group X modules is evident from Table 7.3. The power degradation rate for modules without Hot Cells in both Hot and Non-Hot zones is very similar in this table, though in fact the modules in the Hot zone for the larger sample size are degrading faster, as seen in Chapter 4. The sample size in this table is too low to provide us definitive degradation rates for the various zones, but the trend is important. We can see that modules with Hot Cells degrade much faster than modules without Hot Cells, in both Hot and Non-Hot climates. The Hot climate seems to further accelerate the degradation of the modules with Hot Cells.

Table 7.3: Effect of Hot Cells on power degradation rate of PV modules

Parameter (average of many samples)	**Hot zone**		**Non-Hot zone**	
	without Hot Cells	**with Hot Cells**	**without Hot Cells**	**with Hot Cells**
Power degradation rate (%/year)	1.39	2.02	1.39	1.70
Normalized *module* Δ*T* (°C)	6.8	24.7	5.7	18.9
Normalized maximum cell temperature (°C)	68.8	86.1	50.3	58.6
No. of Samples	10	18	14	17

Figure 7.15 shows the correlation between the average power degradation rate and the normalized Module Δ*T*, for the four categories of modules given in Table 7.3. Further investigation shows that the open circuit voltage and to some extent the fill factor, show a positive correlation with normalized module Δ*T* (see Fig. 7.16), but no such correlation is observed for short circuit current. In Fig. 7.16(b), the *FF* degradation rate for modules without Hot Cells in Non-Hot zones is coming disproportionately high with regard to its module Δ*T*, the reason for which is not known. Hence Hot Cells suffer from degradation in both the open circuit voltage and the fill factor.

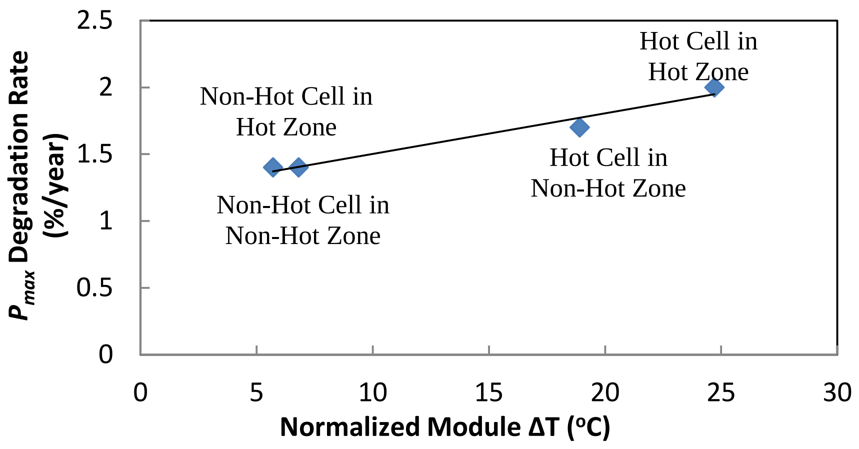

Fig. 7.15: Correlation of power degradation rate with normalized module ΔT

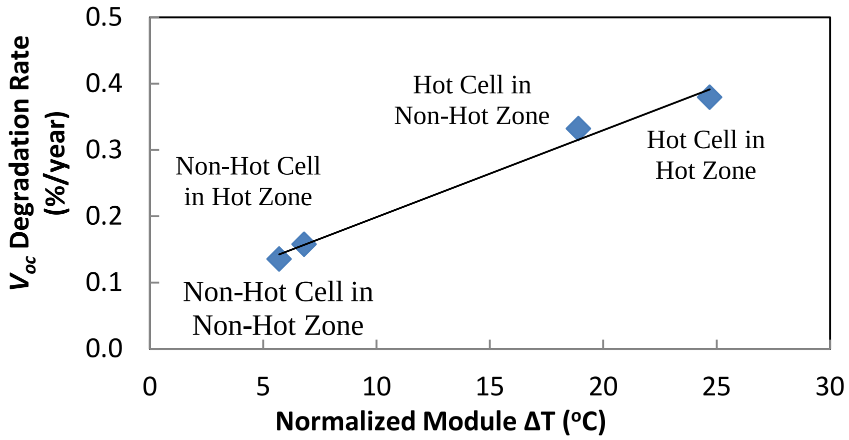

Fig. 7.16(a): Correlation of V_{oc} degradation rate with normalized module ΔT

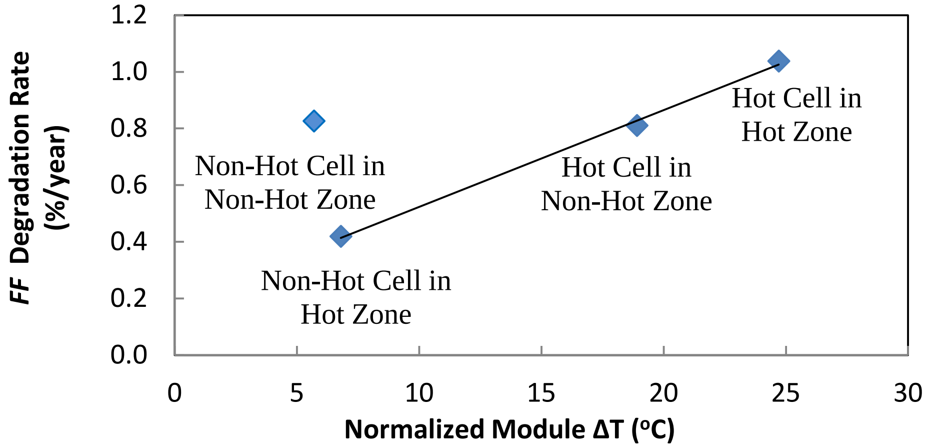

Fig. 7.16(b): Correlation of *FF* degradation rate with normalized module Δ*T*

b) *Effect of Mounting Location on Module Temperature*

The average normalized module temperature for different mounting locations (roof or ground) has been compared in Table 7.4. We can see that the roof-mounted modules in the Hot zone are running around 5 ºC hotter than ground-mounted modules, while the module temperatures are similar in the Non-Hot zone for both roof-mounted and ground-mounted systems. The second row gives the 95% confidence interval (CI) which shows the possible variability in the calculated average temperature.

Table 7.4: Effect of mounting location on normalized module temperature

	Hot Zones		Non-Hot Zones	
	Roof	**Ground**	**Roof**	**Ground**
Average Temperature (ºC)	65.52	59.75	46.14	45.76
95% CI (ºC)	1.35	1.77	1.91	2.40
No. of Samples	37	37	40	18

Based on the above data, it can be concluded that modules with Hot Cells in the Hot zone are degrading at high rates. The power degradation rate seems to correlate well with the extent of mismatch between the cell temperatures in a module. Since most of the country falls in the Hot zone category, the hot cell issue is a major cause of concern. Further, roof-mounted modules are seen to run hotter than ground-mounted ones in Hot zones, exacerbating the issue. These factors should be considered while designing module reliability test standards for hot climates.

7.4 Summary

From the analysis of the electroluminescence and IR images, we can reach the following conclusions:

- Modules in Group Y have a higher percentage of cracked cells than modules in Group X, which indicates poor handling of the modules during manufacturing, transportation and/or installation for Group Y sites. This conclusion is also supported by the higher percentage of mode A and mode C cracks observed in the young modules as compared to the old modules. Thus cracks in modules appear to be one of the contributing factors to the poorer performance of modules in Group Y sites.

- The cells at the edge and corner of the module show more cracks than the central portion of the module. Improper handling of the modules at the time of installation can be one of the reasons behind this.

- There is a good correlation between the total number of cracks in the module and the power degradation of the module. The affected area of the cells correlates well with I_{sc} degradation observed in the module.

- EL images are helpful in detecting cracked cells and broken interconnects in the module. Modules with snail trails have been found to have cracks in the corresponding cells.

- Modules with Hot Cells degrade much faster than other modules, and this gets worse in Hot climates. Out of the modules admissible for the IR analysis, almost 60% fall in the hot cell category, which is high, and calls for attention to the hot cell problem to avoid the long-term fallout of high power degradation rates. High degree of mismatch in cell temperatures can lead to faster degradation in module’s output power.

- Modules installed on rooftops in the Hot zone are running hotter than modules installed on the ground.

8. Risk Priority Number (RPN) Analysis of PV Modules in India

8.1 Introduction

Quantification of reliability of any technology is the most important aspect of its application, and is needed for successfully implementing the technology. IEC 60812 standard provides useful method for analysing and rating reliability and durability of a developing technology through the concept of Risk Priority Numbers (RPN). The probabilistic risk associated with particular PV modules due to design, operation and maintenance of photovoltaic systems needs to be analysed in terms of quality, reliability & maintainability. At present, similar risk analysis concepts are used in the production process of semiconductor industry. Researchers are already using RPN analysis in the field of PV cell manufacturing, and also in long-term outdoor performance assessment of PV technologies [18] [83]. Long-term field reliability study of PV modules is vital to safety and estimation of Levelized Cost of Energy (LCOE) under the given set of environmental conditions experienced in a climatic zone. Failure Mode, Effect, and Criticality Analysis (FMECA) is an excellent statistical tool to study criticality of a failure mode or a defect or both. In the present chapter, an in-depth qualitative analysis as per FMECA of c-Si PV modules is carried out for different climatic zones of India, by listing out all failure modes or defects found during the survey, including their causes and effects on module performance. There are two types of probabilistic risk analysis procedures available as per IEC 60812 standard. These are explained below.

8.1.1 Failure Mode Effective Analysis (FMEA)

According to IEC 60812, Failure Mode Effective Analysis (FMEA) is a systematic procedure for the analysis of any system to identify the potential failure modes, their causes and effects on system performance of the immediate assembly, and the entire system or process. It is a structured, bottom-up approach that starts with known potential failure modes at one level and investigates their effect on the next subsystem level. In 1963 NASA first proposed the FMEA as a formal design methodology for their obvious reliability requirements. It has been extensively used for safety and reliability of nuclear, aerospace and automotive sectors.

8.1.2 Failure Modes, Effects and Criticality Analysis (FMECA)

FMECA (Failure Modes, Effects and Criticality Analysis) is an extension to FMEA to include a means of ranking the severity of the failure modes for analysis purpose. This is done by combining the severity measurement and frequency of occurrence to produce a matrix called 'Criticality'. Criticality means the impact or importance of a failure mode that would demand it to be addressed and mitigated. The purpose is to quantify the relative magnitude of each failure effect, with a combination of criticality and severity, so that action should be taken to minimize the effect of certain failures on priority basis. Traditionally, criticality or risk analysis is done in two ways – by calculating a criticality number (CN) or by developing a Risk Priority Number (RPN).

a) Criticality Number (CN)

For the failure modes of items, if failure rates are determined under environmental and operational conditions similar to those assumed for the system being analysed, the event frequencies for the effects can be added directly to the FMECA. Usually failure rates are available for items, for different environmental or operating conditions. The failure rates of the failure modes need to be calculated. The following relation is used to calculate failure rate:

$$\lambda_i = \alpha_i \text{ x } \lambda_j \text{ x } \beta_i \qquad \text{.... (8.1)}$$

where λ_i denotes the estimate of failure rate for failure mode i, λ_j stands for the failure rate of the component j, α_i is the failure mode ratio of i^{th} failure mode, i.e. the probability that the item will have failure mode i, and β_i is the conditional probability of the failure effect for the failure mode i.

Then the criticality number is defined as

$$CN_i = \lambda_i \text{ x } t_j \qquad \text{.... (8.2)}$$

Where t_j is the time of component operation during the entire predetermined time used for FMECA, for which the probability is evaluated – time of active component operation. However, CN approach is not used for PV modules as 'Severity' clause is not defined in this approach.

b) *Risk priority Number (RPN)*

Among the identified failure mode and effects of a system on the basis of priority ranking, a critical analysis can be done by using a quantitative index, known as Risk Priority Number (RPN). RPN is given by

$$\text{RPN} = S \times O \times D \qquad \text{.... (8.3)}$$

where *S* is the severity, representing the impact of the failure mode; *O* is the occurrence, representing the probability of occurrence of the failure mode based on the feedback of field data; and *D* is the detection, represents the recognizing or spotting and removing or preventing of the failure mode. The analysis is done by identifying the failure modes, their respective causes, and immediate and final effects. Before doing the analysis, planning for the analysis should be done where the clear and specific definition of the purpose and expected results should be known. The information about the system structure in terms of their characteristics, performances, roles, functions and logical connections should be understood. The main important thing of probability analysis is defining of the system boundary. The system boundary forms the physical and functional interface between the system and its environment including other systems with which the analysed system interacts.

Failure mode determination of a particular system can be enhanced by the preparation of a list of failure modes. The most likely causes for each potential failure mode should be identified and described. Since a failure mode can have more than one cause, the most likely potential independent causes for each failure mode need to be identified and described. A failure effect is the consequence of a failure mode in terms of the operation, function or status of a system. A failure effect may be caused by one or more failure modes of one or more items. There may be two different types of failure effects: local failure effects and system level failure effects.

In this chapter, we will discuss only the Risk Priority Number (RPN) in detail and apply it for the c-Si technology to find out the failure mode which is most risky in the different climatic zones of India. For the calculation of RPN, different failure modes should be ranked based on its defined criteria. By using the RPN analysis, system owners can determine the state-of-health of their system. For project developers, RPN is very useful to select climate-resilient module designs, and for manufacturers, it can be used to take climate-specific corrective action on designs.

8.2 Methodology

The rating of different failure modes is analysed by using data mining technique of field data collected from different climatic zones. There are many ways a PV module or its component may fail. The potential failure mode estimation of a PV module depends on system components, environment, and past history of failures in similar systems. The techniques used for failure mode identification include careful inspection of the PV module, visually and/or using sophisticated instruments. Accumulating failure data for individual modules with reference to a failure mode/ defect with a significant number of statistical data for each climatic zone. As described by Kuitche *et al.* [18], the potential failure modes in PV modules are of two categories – safety and performance. The details are listed in Tables 8.1 and 8.2.

Table 8.1: Safety failure modes

<table>
<tr><th>Glass</th><th>Frame</th><th>Junction box</th></tr>
<tr><td>Front glass crack
Front glass shattered</td><td>Frame grounding severe corrosion
Frame joint separation
Frame cracking</td><td>Junction box crack
Junction box burn
Junction box loose
Junction box lid fell off
Junction box lid crack
Junction box sealing will leak</td></tr>
<tr><th>Backsheet</th><th>Wire</th><th>Insulation resistance</th></tr>
<tr><td rowspan="3">Backsheet peeling
Backsheet delamination
Backsheet crack/cut under cell
Backsheet crack/cut between cells</td><td rowspan="3">Wires burnt
Wires animal bite/marks
Wire insulation cracked</td><td>Lower insulation resistance</td></tr>
<tr><th>Cell</th></tr>
<tr><td>Hotspot above 20 ^{0}C
String interconnect arc tracks</td></tr>
</table>

Table 8.2: Performance failure modes

Glass	**Frame**	**Junction box**
Front glass lightly soiled	Major corrosion of frame	Junction box unsound
Front glass heavily soiled	Minor corrosion of frame	Junction box weathered
Front glass crazing	Frame bent	Junction box warped
Front glass chip	Frame degraded	Junction box adhesive
Front glass milky discoloration	Frame oozed	Junction box lid loose
	Frame adhesive missing	Junction box wire attachment loose
		Junction box wire attachment fallen off
		Junction box wire attachment arced
		Junction box wire attachment fire
Cell	**Encapsulant**	**Backsheet**
Fingers light discoloured	Encapsulant delamination over cell	Backsheet discoloration
Fingers dark discolored	Encapsulant delamination between cell	Backsheet chalking
Busbars light discolored	Encapsulant delamination corner	Bubbles in backsheet
Busbars dark discolored	Encapsulant delamination edge	Cracks in backsheet
Busbars obvious corrosion	Encapsulant delamination interconnect	Burn mark in backsheet
Busbars diffuse corrosion	Encapsulant delamination near junction box	
Busbars misalignment	Encapsulant discoloration	
Cell interconnect light discolored		
Cell interconnect dark discolored		
Cell obvious corrosion		
Cell burn		
Cell breakage		
Moisture in cell		
Foreign particle in cell		
Cell snail trails		
String light discolored		
String dark discolored		
String obvious corrosion		
String burn		
String breakage		
String arc		
Hot spot		
Edge seal	**Wires**	**Others**
Edge seal delamination	Wires pliable degraded	Solder bond fatigue/failure
Edge seal moisture ingression	Wires embrittled	
Edge seal discoloration	Wires corroded	
Edge seal squeezed out/ pinched out	Wires soiled	

For the analysis, data mining technique [84] is used to study the large and complex observational datasets of field failure data. A typical decision tree is designed based on information gain splitting rule by using 'divide and conquer' technique [84]. The identification of the effect of a particular failure mode is mainly depending on the severity; with high severity it is very easy to find out the effect. During the analysis of the data it has been observed that degradation rate of P_{max} and I_{sc} increases with the increase of defects in busbar, cell interconnecting ribbon and string interconnecting ribbon. Due to the increase in discoloration of busbar and interconnect ribbon, the series resistance will also increase, thus decreasing the current. Usually moisture and atmospheric gases ingress through the backsheet can cause corrosion of the metallization. However in case of the busbar, due to use of low quality of flux during soldering, sometimes a dark black layer is deposited in the busbar, and because of this the power level goes down. This is usually the case in industries where the PV modules are manufactured in manual mode, not using stringers. Due to de-lamination and bubble formation in the backsheet of the module, the thermal conductivity is reduced locally, resulting in an increase in the temperature of the solar cell [85]. The power decreases with the increase of bubbles as the temperature of the particular cell increases. This may cause hot spot formation. With the discoloration of EVA, the short circuit current decreases because the discoloration leads to low transmissivity of light. But the degradation in I_{sc} depends on position of discoloration of EVA, because if the discoloration happens over one cell in a string, then the total current of the module will go down. So there will not be much difference between discoloration of one cell and more cells. It is also observed that the discoloration does not significantly affect the fill factor and V_{oc}. Proper sealing and covering of junction box is needed to reduce the corrosion of output terminals which may happen due to ingression of moisture. Most of the modules surveyed have shown corroded output terminals and damage in the junction box. It has been observed that the pattern of degradation is not uniform with junction box detachment.

D. L. Meier *et al.* reported that series resistance is mainly dominated by the solder bond failure [86]. Kuitche *et al.* reported that large increase in the value of series resistance indicates solder bond failures [18]. So, change in series resistance with the exposure time is an indirect measurement of solder bond failure. Series resistance (R_S) increase of more than 1.5 times that of initial value is indicated as a solder bond defect. The formula given by Dobos *et al.* is used for the calculation of R_S [87]:

$$R_S = C_S \frac{V_{oc} - V_{mp}}{I_{mp}} \qquad \text{.... (8.4)}$$

where the constant C_S = 0.32 for mono-crystalline silicon and C_S = 0.34 for poly-crystalline silicon modules. There are no common guidelines for the rating of different failure modes. The ranking of RPN is a quantitative index for the estimation of the failure mode. The ranking of Severity, Detection and Occurrence of a PV module are given below.

8.2.1 Severity

Severity *S* of a failure mode is determined by using the safety and performance degradation of the PV modules, ranked from 1 to 5. Severity ranking of failure mode is done with respect to degradation rate per year which is having a particular failure mode as a dominant factor. It is very difficult to find out the severity ranking of a particular failure mode as the degradation of a module is not dependent only on an individual defect. In this analysis the severity numbers from 4-5 are related to safety issues. The numbers from 1-3 depend on the performance degradation. The severity ranking of the failure mode is done with respect to the degradation rate per year of the module which is having that particular failure mode as a dominant mode in inducing the degradation. For this data mining techniques are usually used.

8.2.2 Detection

Ranking of Detection *D* of each failure mode is done based on the criteria of detection with the monitoring system itself or with visual inspection or with sophisticated tools only possible in lab conditions. The ranking 1 is given if the monitor system i.e. field control mechanism detects the failure mode in the scheduled/regular maintenance or event-triggered inspections. In this study, detection rating corresponds to the likelihood that the detection method will detect the failure before the system reaches the end-user. The detection technique of failure modes are ranked with the accelerated stress tests designed to induce known field failure modes as reported by Wohlgemuth and Kurtz [88] [89] and Tamizhmani [90]. Basically, the number goes higher as different techniques are needed to detect the failure mode. If the failure mode is detected visually, the number 2 is given and if the failure mode is detected using a single or multiple tools, a number from 3-4 is given. If the failure mode is detectable only in the lab i.e. it is not possible to detect in the field, then the highest number 5 is given.

8.2.3 Occurrence

Occurrence *O* ranking is performed on the basis of field data. The frequency of occurrence of each failure mode has been calculated by plotting the histogram of number of modules for a particular defect. The number of module failures per thousand per year is calculated. This rating value corresponds to the estimated number of failures that could occur for a given cause over the operational life of the system. Failure modes are identified in terms of probability of occurrence, grouped into discrete levels. These levels establish the qualitative failure probability level. The cumulative number of module failures per thousand per year (CNF) is calculated by using the following formula:

$$\mathrm{CNF}/1000 = \frac{(\text{cumulative \% defects})/10}{\text{cumulative operating time}} = \frac{\sum_{\text{systems}}(\text{\% defects})/10}{\sum_{\text{system}}(\text{operating time})} \qquad \text{.... (8.5)}$$

Table 8.3 describes the scores for various conditions of Severity, Occurrence and Detection [1]:

Table 8.3: Rank determination of severity and detection [18]

Severity (*S*)	**Occurrence (*O*)**	**Detection (*D*)**	**Score**
Defect will cause module not to work and become a safety hazard	Defect frequent: fp > 0.20	Controls will not or cannot detect the existence of a deficiency or defect: 0% chance	5
Module might be safe, but non- functional: Change in P_{max}, ΔP_{max} > 20%	Defect probable: $0.10 < \text{fp} \leq 0.20$	Controls not likely to detect the existence of a deficiency or defect: chance < 50%	4
Module not meeting warranty requirement: Change in degradation rate, $\Delta R_d > 0.8\%$ & $\Delta P_{max} < 20\%$	Occasional probability of occurrence: $0.01 < \text{fp} \leq 0.10$	Controls are likely to detect the existence of a deficiency or defect: chance = 50%	3
Slight deterioration of part or system (long term concern): $\Delta R_d < 0.8\%$ & $\Delta P_{max} < 20\%$	Remote probability of occurrence: $0.001 < \text{fp} \leq 0.01$	Controls have a good chance of detecting the existence of a deficiency or defect: chance > 50%	2
No effect on performance: $\Delta P_{max} \leq 8\%$	A very unlikely probability of occurrence: $\text{fp} \leq 0.001$	Controls will almost certainly detect the existence of a deficiency or defect: chance = 100%	1

8.3 Failure Mode Analysis

All the modules are analysed as per the safety, reliability and durability failure using the definition stated by Shrestha *et al*. [91]. It is reported that defects with safety issues can be termed as safety failure; modules with degradation rate more than 1%/year (excluding the modules with safety issues) are termed as module with reliability failure; and modules with degradation rate less than 1%/year (excluding the module with safety issues) but having other defects are termed as module with durability failure.

Figure 8.1 shows the pie chart of safety, reliability and durability failure in crystalline silicon PV module for different climatic zones. For this analysis modules are divided into two age groups – young (less than 5 years of exposure) and old (more than 5 years of exposure). It has been observed that for young modules, percentage of modules with reliability failure is more. For old modules, percentage of modules with safety failure is more. For a systematic analysis, it is very necessary to separate out the safety and performance issues of PV module.

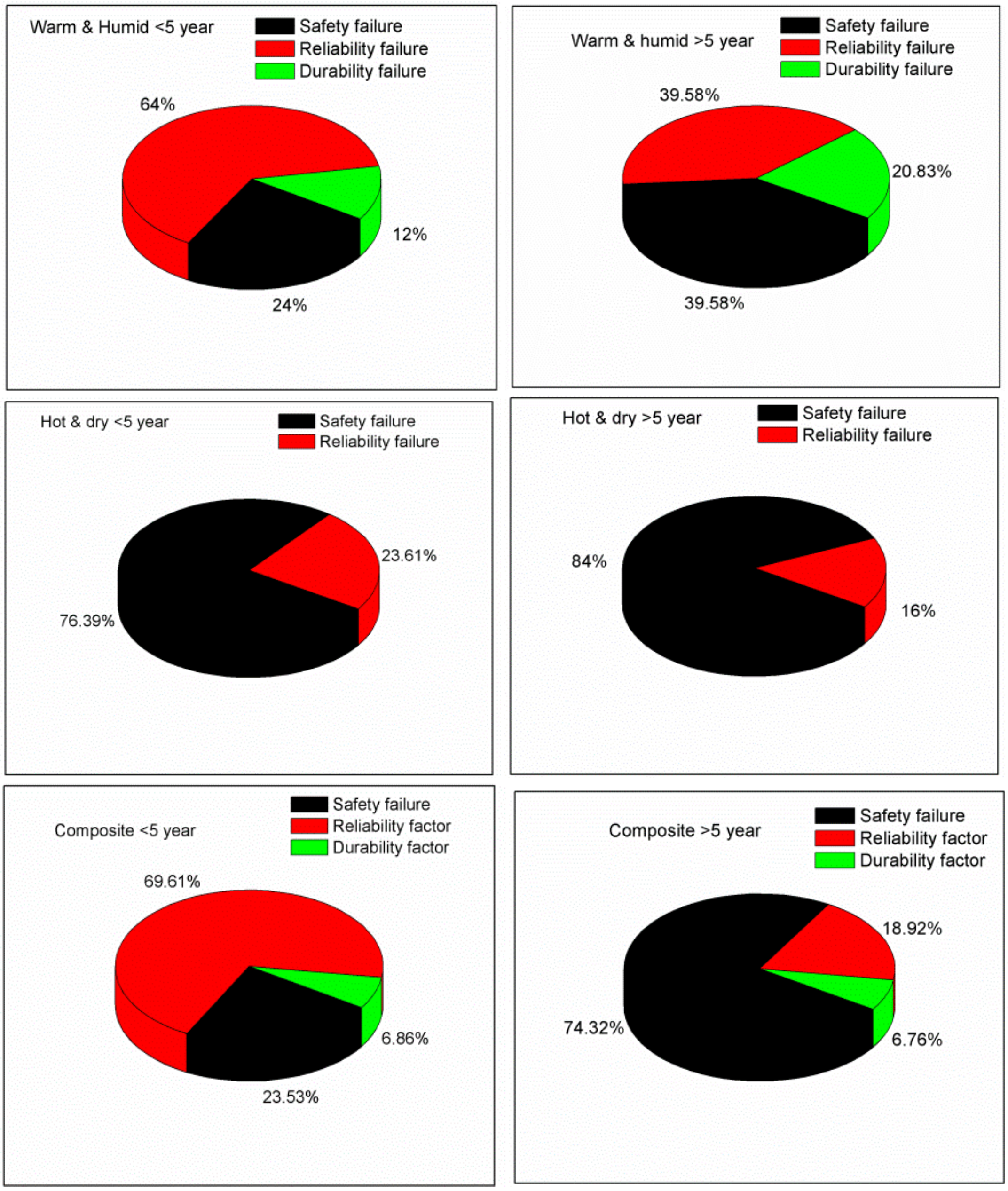

Fig. 8.1(a): Safety failure, Reliability failure and Durability failure for modules of different years of exposure for the Hot zones - Warm & Humid, Hot & Dry, and Composite.

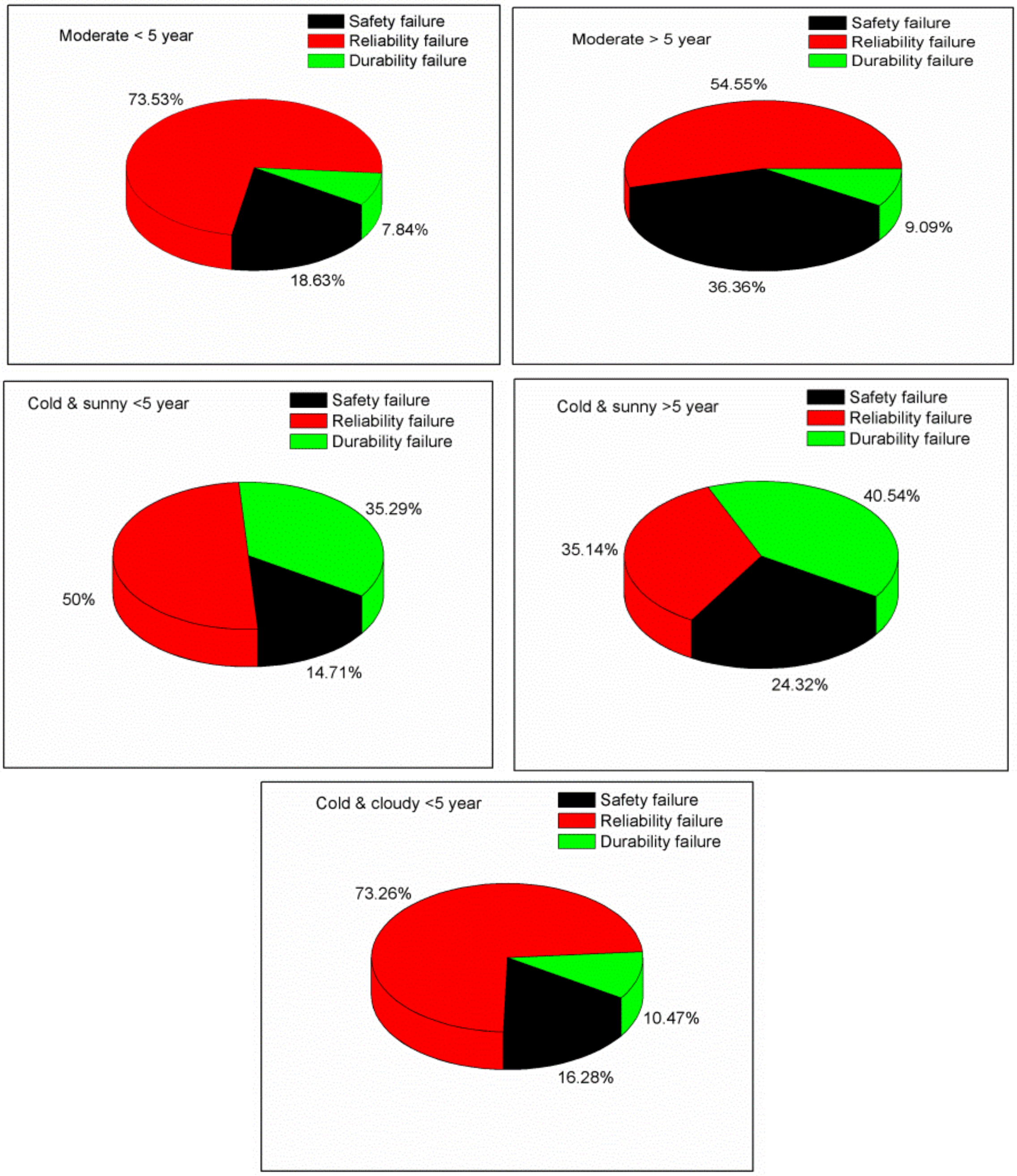

Fig. 8.1(b): Safety failure, Reliability failure and Durability failure for modules of different years of exposure for Non-Hot zones – Moderate, Cold & Sunny and Cold & Cloudy

8.4 Estimation of RPN

The failure mode is divided into two parts: safety and performance issues. Tables 8.4 and 8.5 show the severity and detection of different failure mode as per safety and performance issues.

Table 8.4: Severity and detection ranking of failure mode with safety issues

Failure mode	Severity rank	Detection
Front glass crack	5	3
Front glass shattered	5	3
Frame grounding severe corrosion	5	2
Frame joint separation	5	1
Frame cracking	5	1
Junction box crack	5	2
Junction box burn	5	2
Junction box loose	5	2
Junction box lid fell off	5	1
Junction box lid crack	5	1
Junction box sealing will leak	5	2
Wires burnt	5	2
Wires animal bite/marks	5	1
Backsheet peeling	5	5
Backsheet delamination	5	5
Backsheet crack/cut under cell	5	5
Backsheet crack/cut between cell	5	5
Insulation resistance	5	5

Table 8.5: Severity and detection of failure mode with performance issues

Failure mode	Severity	Detection	Failure mode	Severity	Detection
Front glass crazing	1	3	Cell dark discolored	3	5
Front glass chip	1	3	Cell obvious corrosion	3	5
Front glass milky discoloration	2	3	Cell burn	1	2
Major corrosion of frame	1	1	Cell breakage	1	1
Minor corrosion of frame	1	1	Moisture in cell	1	1
Frame bent	1	1	Foreign particles	1	1
Frame degraded	1	1	Cell snail trails	1	1
Frame oozed	2	1	String light discolored	3	3
Junction box loose	3	2	String dark discolored	3	3
Junction box weathered	2	2	String obvious corrosion	3	3
Junction box warped	2	2	String burn	3	3
Junction box adhesive	2	2	String breakage	3	3

Junction box lid loose	1	1	String arc	3	3
Junction box wire attachment loose	2	1	Hot spot	2	3
Fingers discolored	3	3	Encapsulant delamination corner	1	1
Busbars light discolored	3	3	Encapsulant delamination edge	1	1
Busbars dark discolored	3	3	Encapsulant delamination interconnect	1	1
Busbars obvious corrosion	3	3	Encapsulant delamination near junction box	1	1
Busbars diffuse	3	3	Encapsulant discoloration	3	5
Busbars misalignment	3	3	Back sheet discoloration	3	5
Cell intercon-nect discolored	3	5	Back sheet chalking	3	5
Edge seal moisture ingression	2	2	Bubbles in back sheet	3	5
Wires pliable degraded	2	2	Cracks in back sheet	3	5
Wires embrittled	1	2	Wires corroded	1	2
Solder bond fatigue/failure	5	4	Wires soiled	1	1

Figures 8.2 and 8.3 shows the plot between RPN and safety failure modes for young and old modules for different climatic zones. It can be observed that in case of safety RPN of young modules (less than 5 years exposure), backsheet peeling and backsheet delamination are the dominant failure modes. Insulation resistance (dry & wet), and problem of junction box are seen to be more significant safety issues. For old modules (greater than 5 years of exposure), safety RPN is highest for failure modes due to back-sheet peeling, back-sheet crack, and junction box loose, which are observed in all the climatic zones. However, frame grounding due to corrosion in the grounding wire is one of the significant safety issues in Hot & Dry climatic zones. Due to backsheet problem, the current carrying circuit may be exposed to the ambient, and this may create electric shock hazard to the maintenance personal. Significant bypass diode failures are not observed and hence not included in the safety failure estimation. Some modules showed lower insulation resistance (dry & wet); they may cause a problem of leakage current to the frame based on the system voltage and climatic conditions. Problems due to open (without cover), detached and corroded junction box are observed and are major safety issues. These also observed to create problems of moisture ingression and electrical shock hazard.

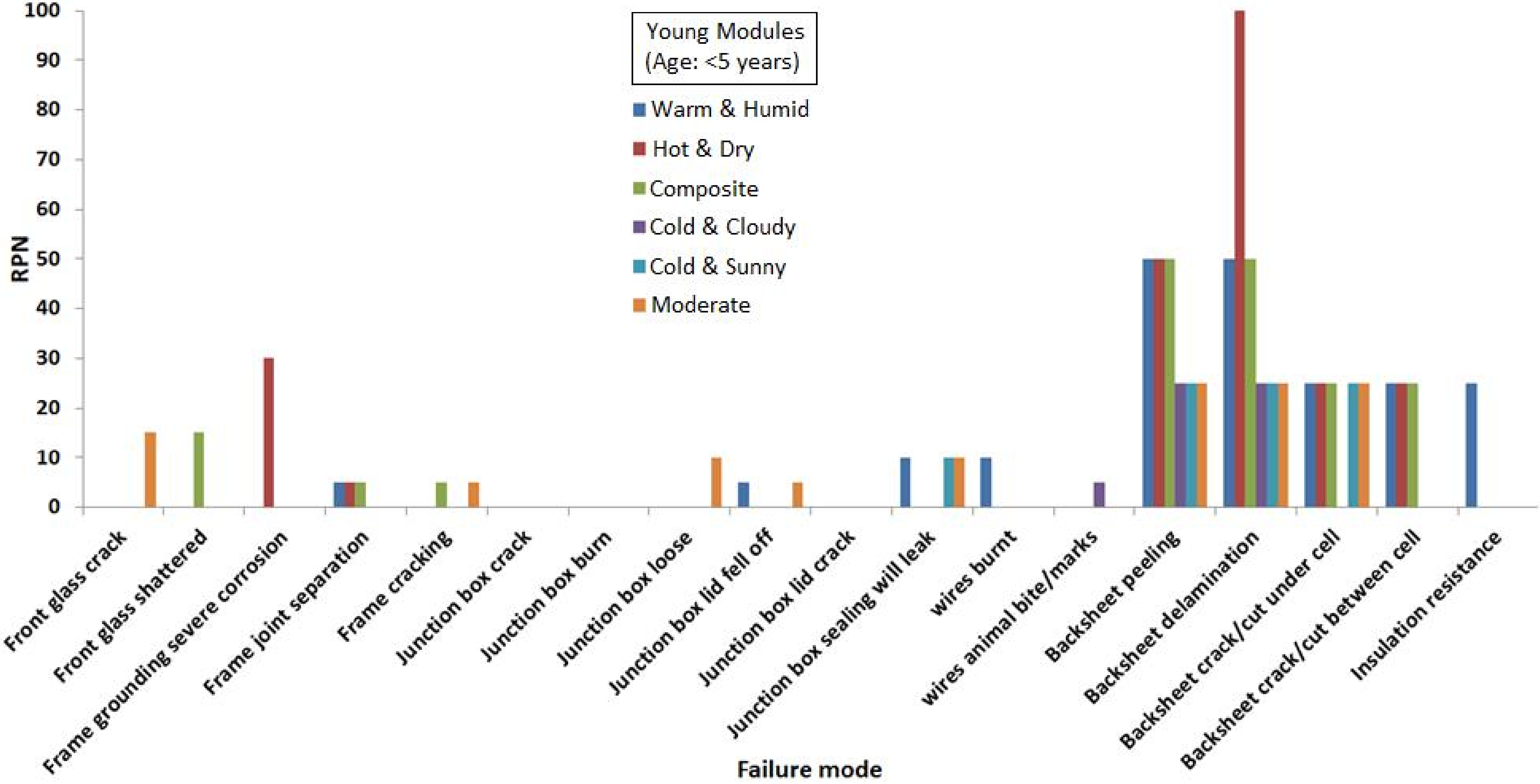

Fig. 8.2: RPN for various safety failure modes of young modules in different climatic zones

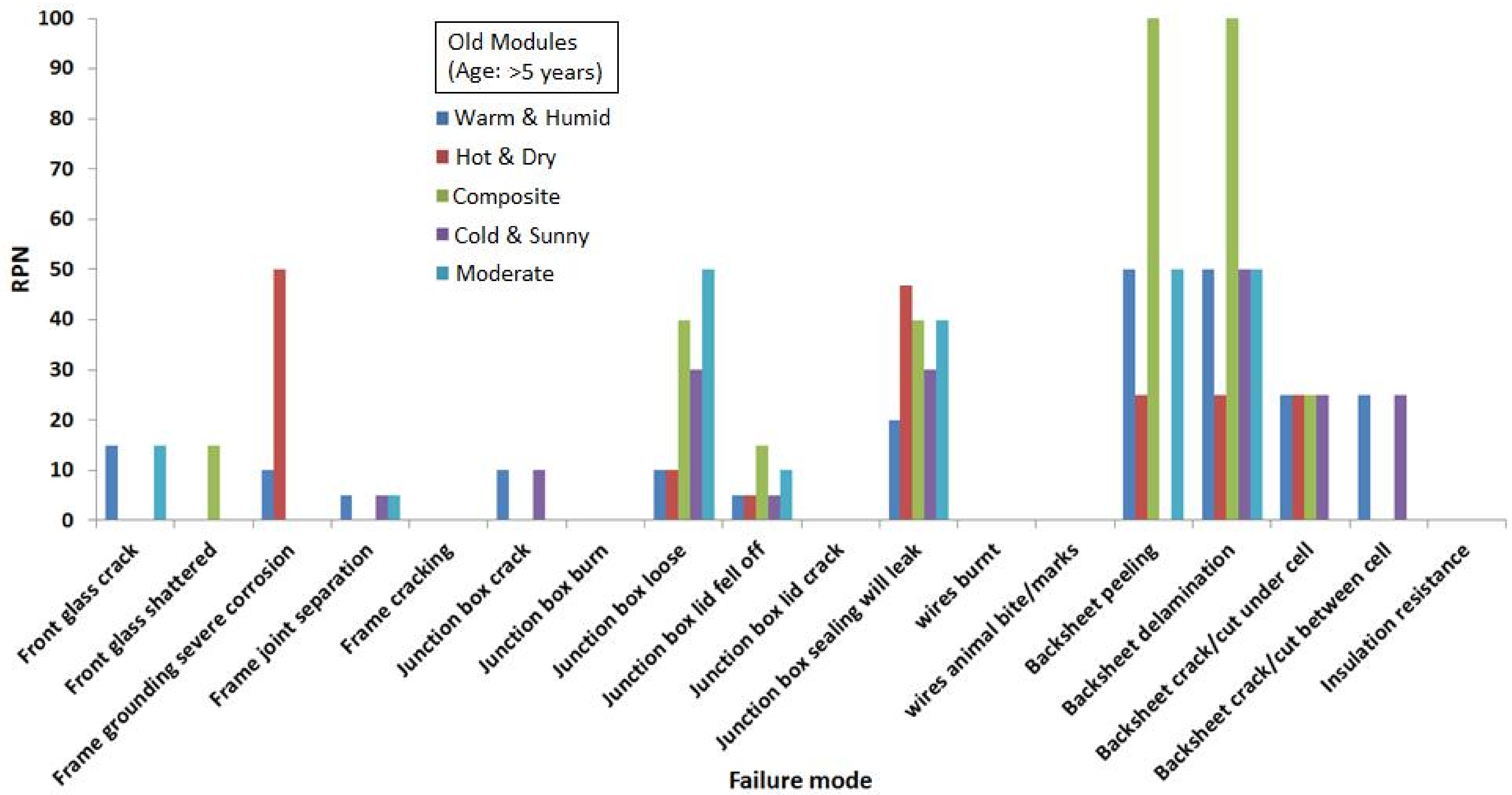

Fig. 8.3: RPN for various safety failure modes of old modules in different climatic zones

Figures 8.4 and 8.5 shows the plot between RPN and performance failure modes observed for young and old modules respectively for different climatic zones. It can be observed that in case of performance RPN of young modules, encapsulant discoloration is the main defect for almost all the climatic zones, except Cold & Cloudy zone. Solar cell discoloration is also another common defect in the module. All modules studied in this section were EVA based and other designs are not available. Literature on discoloration of EVA has been discussed in Chapter 1. The discoloration of encapsulant reduces the optical transmission, power output, and service life of PV modules. Hot spot is also a problem in Composite and Moderate zone for this category of modules. A hot spot with localized temperature rising more 20˚C compared to other cells of the module is a fire hazard and a major safety issue. Hot spots can reduce the power output severely. In case of performance RPN of old modules, encapsulant discoloration is the most common defect. The solder bond fatigue/failure is the most severe defect with the highest RPN value for the Hot & Dry zone. This problem is severe in Warm & Humid, and Composite zone also. The solder bond fatigue/failures analyzed in this section reflects the relative increases of series resistance. The main cause of this failure is the thermal cycling due to exposure to the outdoor conditions. With the increase of series resistance the power output decreases. Finger, busbar, and string discoloration; chalking of backsheets are also common types of defect observed in the modules installed in all the climatic zones. The likely reasons for these defects are explained in the previous chapters of this report.

8.5 Summary

The quantification of reliability of PV modules has been analysed by using IEC 60812 standard. The analysis of dominant failure mode of c-Si PV module(s) in the different climate zones of India is carried-out by using FMECA and data mining techniques. In case of safety issues, problems in backsheet and loose junction boxes are the main defects in almost all climatic zones. Solder bond failure and encapsulant discoloration are the main failure modes in case of performance RPN for Warm & Humid, Composite and Hot & Dry climatic zones.

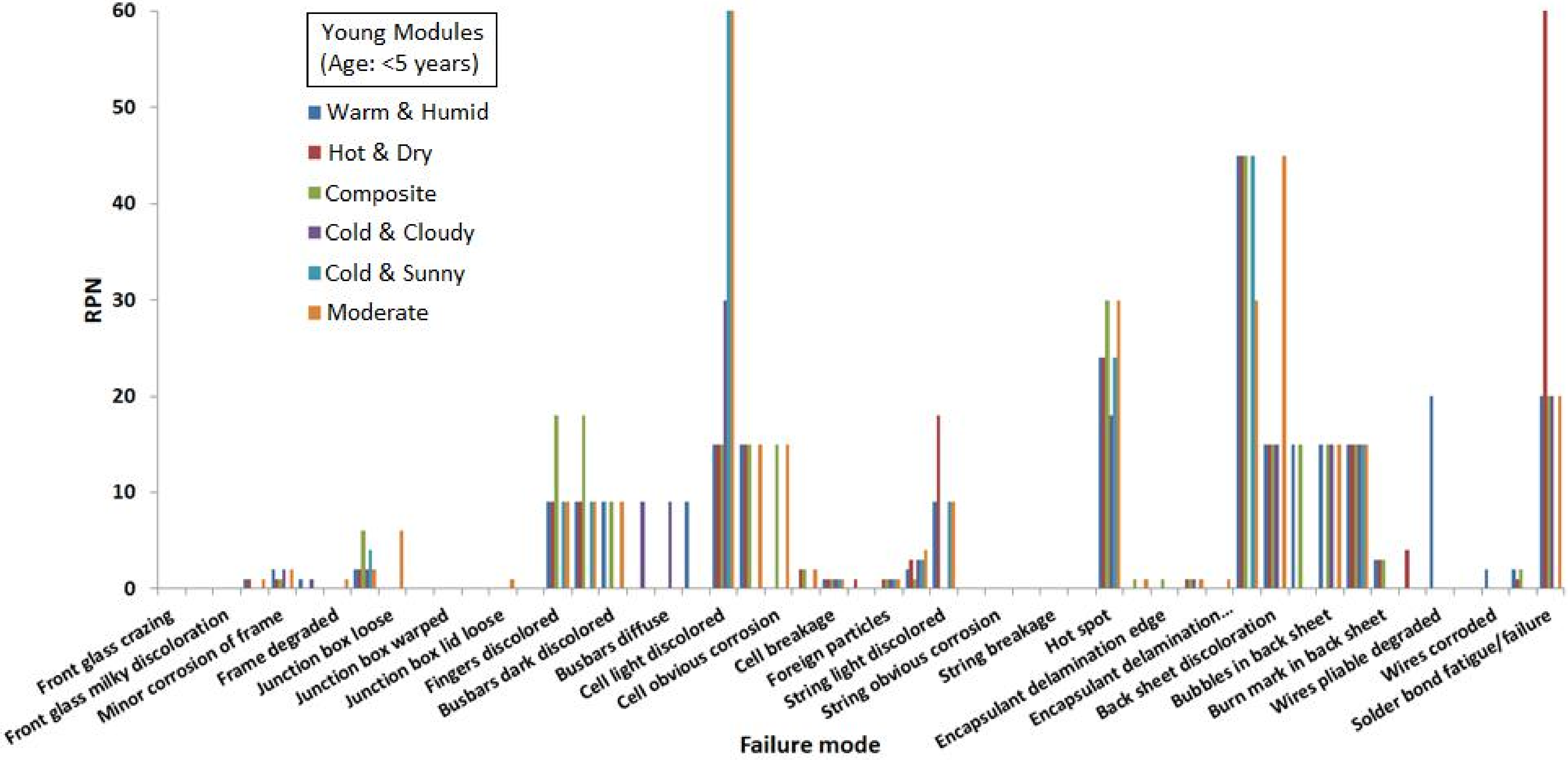

Fig. 8.4: RPN for various performance failure modes of young modules in different climatic zones

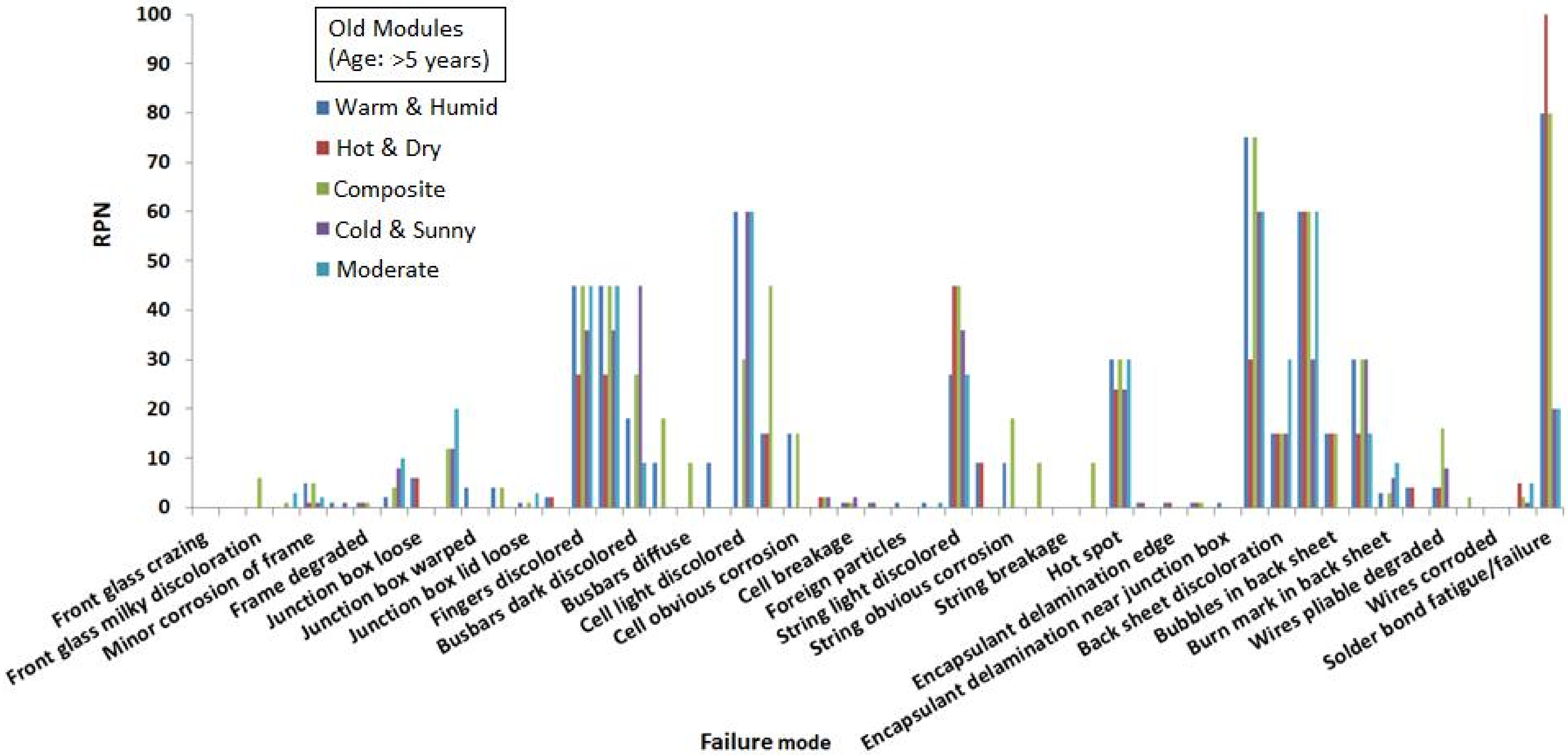

Fig. 8.5: RPN for various performance failure modes of old modules in different climatic zones

9. Socio Economic Aspects Affecting PV System Performance

9.1 Introduction

Degradation, underperformance and even failure of PV systems due to improper installation and lack of maintenance are often reported in literature [46]. In a dynamic PV market like India's, it is important to understand how the performance and degradation of PV systems are influenced by the socio-economic and behavioural aspects of the system owners. Solar PV technology has reached a good level of maturity in India during the past 10 years, but how far the society has been enabled to receive the technology is a matter of concern. The paper by Jafar *et al.* [48] states that the nature of maintenance support and the expenses on maintenance can be studied effectively by categorising the installations based on their ownership. A detailed study by Cust *et al.* [56] provides adequate inputs for designing a framework for analysing renewable energy based rural electrification projects based on the ownership of assets of generation and distribution and end use of the generated power. Based on the insights from the above literature as well as a few other case studies [57], [58], [59], [61], [62], we have developed an analysis framework to capture the complex relationship between society, technology, policy and other market drivers, with data coming from the present survey.

The framework categorises the surveyed systems into different groups, first based on the size of the system and then based on the nature of ownership of the systems. Appropriateness in installation (technical design, use of proper support structure, consideration for shading, proper orientation and tilt angle for modules, etc.) and system maintenance activities (frequency of module cleaning, scope of routine checks, skill level of technicians doing the maintenance, etc.) were studied across these different categories. The results from the above analysis was further scrutinised along with more information such as sources of finance for installation and maintenance, and the 'true' motivation or need behind the installation of the systems.

9.2 Selection of Sites for Analysis

The team surveyed 51 different PV installation sites during the three months of survey. Based on the size of the PV arrays installed, we can categorise the systems into small/medium scale installations and large installations. The categorisation is already explained in Section 2.2. Most of the sites had small or medium scale installations where the installed PV array size was less than 100 kW_p. Only six sites had large scale installations greater than $100kW_p$ capacity (large power plants).

Again, if we consider the design of the PV systems, we can categorise them as 'off-grid' systems and 'grid connected' systems. Many systems surveyed were 'off-grid' systems with battery-based energy storage. By categorizing a system as 'off-grid', it basically means the PV modules are primarily used to charge a battery bank and the loads use this stored energy. In some sites, charging the batteries from the grid was also possible. When the battery banks are drained below a critical level and the primary source, PV, is not able to generate enough energy to recharge them, the batteries are charged from the grid supply. This functionality is available in most of the power conditioning units (PCU) used in off-grid PV system designs. The grid connected systems directly feed the power into the grid and the size of typical grid connected 'rooftop' system we had surveyed ranged from 10 to 500 kW.

A third categorisation of systems can be based on the application or the use of power form the PV system. Most of the small/medium scale systems were used to run various domestic or office electrical appliances. Some of them had battery backup while some of them were in grid-tied mode. Another major application of small scale off-grid systems was water pumping. Some installations were done only for research purpose. Power from large installations was mainly fed to the grid, as per the power purchase agreement between the power plant developer and the utility company. Figure 9.1(a) shows the number of surveyed installations under grid-tied and off-grid categories. Figure 9.1(b) shows further sub categories within off-grid systems. Out of the 16 grid tied systems surveyed, three were MW scale power plants and rest of them were large rooftop power plants.

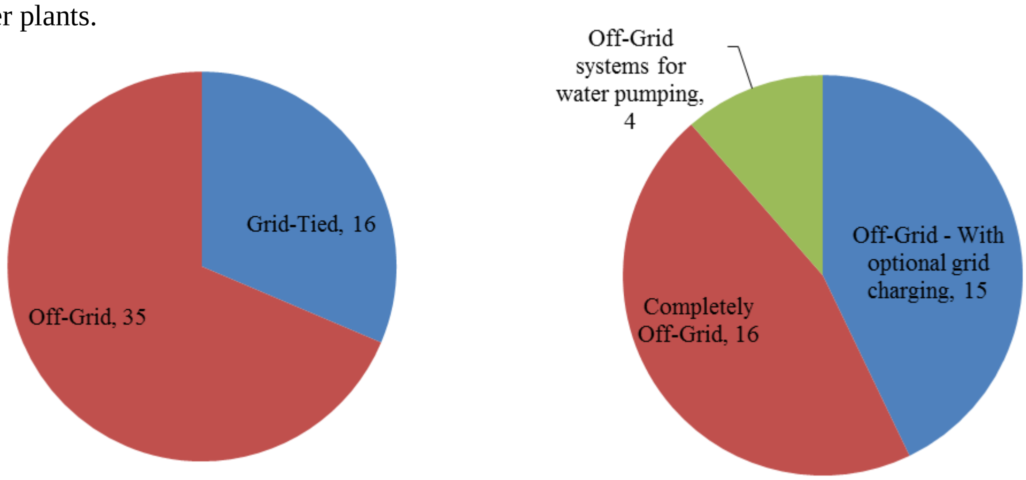

(a) (b)

Fig. 9.1: Different categories of systems surveyed (a) Number of installations under grid-tied and off-grid categories and (b) Number of installations under sub categories of off-grid systems

Analysis of the degradation rate of P_{max} in Section 4.6 shows that the modules from small/medium sized power plants degrade faster than the ones in the large power plants. Most of the large power plants are designed, commissioned and maintained by professional EPC companies. Hence it is expected that they have given enough care for the selection of components, design and execution of the project. There is not expected to be much variability in terms of the skill levels, design methodology, maintenance practices etc. among these power plants, though, as we have seen, there do appear to be differences installation practices. So, when it came to the choice of sites suitable for analysis of socio-economic and behavioural aspects of system owners, it was decided that the main focus should be given on small/medium scale installations, where the variability of the above mentioned parameters is likely to be more. The systems were categorised into two categories at a first level based on system size ('small/medium' sized systems and 'large' systems as explained in Chapter 2 and Chapter 4), and at second level, they were classified based on the ownership types (as explained below in Section 9.3.1).

Whenever multiple power plants owned by a same owner were visited in a location, we have considered only one site from this group for analysis. All these plants were designed, installed and maintained in a similar way by the same team of engineers. Hence they do not contribute three different data sets; rather we should consider only one of the sites to compare the performance parameters with other systems.

We have neglected the small PV systems installed in research institutions in this analysis. In order to evaluate the appropriateness of installation and maintenance, we have used certain criteria such as appropriate tilt angle, proper installation without shading, frequent cleaning cycle etc. to assign points for each installation. In research institutes, the modules were sometimes intentionally installed at various tilt angles, kept without cleaning, kept at open circuit condition for long time as a part of experiments to study various degradation modes. Hence we could not accommodate them in our common framework for comparison of systems.

Out of the 51 sites surveyed, we identified 35 unique sites for analysis based on the criteria mentioned above. To summarize, various issues were studied based on the data from 31 small/medium scale installations (less than 100kW$_p$ installed capacity) and on 4 large power plants separately.

9.3 Analysis of Small/Medium Scale Installations

This section explains the framework used to analyse and compare the appropriateness of installation and maintenance of small and medium scale systems. The systems were grouped into four categories, based on the ownership and later they were compared based on their financial models and motivation for installation.

9.3.1 Classification of Surveyed Systems based on Ownership

There were 4 major system ownership models observed during the 2014 All-India Survey and they are categorized as follows.

- *Systems owned by private institutions/organizations:* This category includes private institutions like private engineering colleges, hotels, corporate offices, etc.
- *Systems owned or installed and maintained by 'not for profit' institutions/organizations:* These are systems owned or operated by non-governmental organisations (NGOs) and trusts, which work on a not-for-profit basis. Most of these installations are funded by domestic and/or foreign charities.
- *Systems owned by a user group or a community:* These are generally systems with a few kW capacity installed and operated by a group of individuals for a common use. Examples are the community water pumping system by farmers, community street light system in a village, rooftop systems powering the common loads of a housing society, etc.
- *Installations owned by Government and Semi-government Institutions:* These are typically the systems installed by government or semi-government organisations as a part of some scheme of policy decision.

9.3.2 Various Financial Models for PV Systems Identified in the Survey

There were basically 4 financial models found in the different installation sites we have surveyed.

- *Self-financed systems without government incentives:* These are systems where individuals or communities have paid 100% of the initial investment as well as the maintenance charges. In some cases they have obtained loans from banks to bear the initial cost of the project.
- *Self-financed with capital subsidy from the government:* These are installations which have availed a capital subsidy (varying between 30 - 70%) from the central/state governments, and are self-financing the maintenance charges.
- *Government/ External funded capital and users bearing the Operation and Maintenance (O&M) charges:* Here the government (state or central) has given 100% investment of capital and are trying for cost recovery through monthly charges for the users. This model was found especially in projects where PV is considered as better option than grid extension and the government invests in PV to provide basic electricity requirements of the society.
- *Government funded capital investment and O&M:* These are the cases where the local, state or central government has invested in PV systems mainly for promotion of technology through demonstration projects. Typical examples are the systems installed on government offices and public buildings as a part of some scheme or policy decision to promote PV (and to achieve some installation targets).

9.3.3 Motivation for Installation of the PV Systems Covered in the Survey

The basic motivation or end purpose for the installation of the surveyed PV systems were analysed and are categorised as below.

- *Necessity:* These are installations which are absolutely necessary in their given context. The proper functioning of the system is essential for meeting some urgent needs of the installer.
- *Optional/Back-up power:* These are installations where the installer has an alternate option for power. PV is an optional or back-up option to meet emergency situations when grid is not available.
- *Income generation/Savings:* There are installations where the major driving force was income generation (like agriculture) or saving money on electricity bills or diesel. The savings could also be in terms of tax holidays and 'accelerated depreciation' benefits on investments made on PV systems.
- *Promotion of Green Energy:* Here the basic motivation for installing a PV system is to promote green energy. Some of them are installed as a part of government schemes (with some installation target to be achieved) and some are projects initiated by NGOs to demonstrate the viability of PV systems. Some systems are installed by the interests of the owners to project themselves as 'pro-green' organisations.

9.3.4 Comparison of Small/Medium Scale Installation: Results

a) Motivation for Adopting PV

Figure 9.2 shows the various reasons which were reported as the 'motivation' for installing the PV system, by different system owners. Analysis of the figure shows that private institutions have opted for PV mainly for two reasons: either the systems support income generation or savings (through reduction in energy bills or savings in tax) or they want to project themselves as a 'pro-green' organisation supporting solar PV technology. In 6 out of 7 sites surveyed under this ownership category, the motivation was reported to be either 'income generation/saving' or 'promotion of green energy'. Government institutions have mainly installed PV as a part of some schemes and programmes to promote PV. NGOs have played a major role in promoting PV in areas where they are absolute necessities, like home lighting systems in rural areas and power in remote hospitals. Four out of 8 installations owned and operated by NGOs are installed mainly to meet some 'necessities'. Community-owned micro-grids and water pumping systems are examples for systems with regular income generation or saving. They save considerable amount of money which was otherwise spent on diesel.

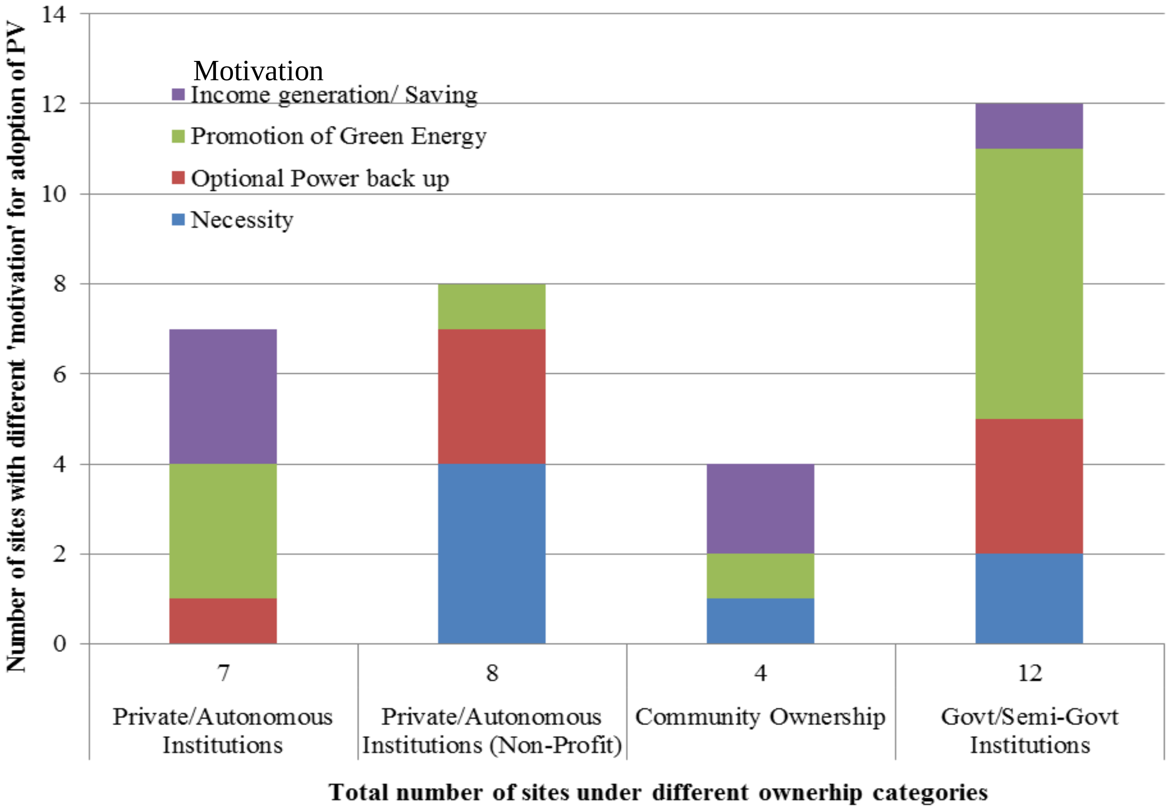

Fig. 9.2: Motivation for adopting PV for different ownership categories

b) *Mode of Implementation of the Project*

Who installed the system is an important factor which will affect the quality of design, installation and maintenance of PV systems. Figure 9.3 shows that most of the government and private institutions as well as community-based user groups have approached EPC contractors for the design and completion of their projects. This shows that institutionalisation of ownership of system can result in a proper procedure for identifying and entrusting the responsibilities of system design and installation to a professional company. Especially, the presence of a documented ‘technical specification’ and ‘functional requirements’ of the PV system will be ensured and proper tendering procedures will be followed if the ownership of the system is with an institution. Studies conducted as early as the 1980s have concluded that village energy centres are technically and economically more viable than individual rooftop systems. Better maintenance, superior load management and better security are some of the advantages of centralised systems [54]. Our results also point towards the positive side of the ‘centralisation’ or ‘institutionalisation of ownership’ of the PV projects at a regional level. It was noted that the NGOs are mostly dependent on the local electricians for the design and implementation of the projects, but it was also revealed in the survey that these were professionally trained local electricians under the institutional umbrella of the NGOs.

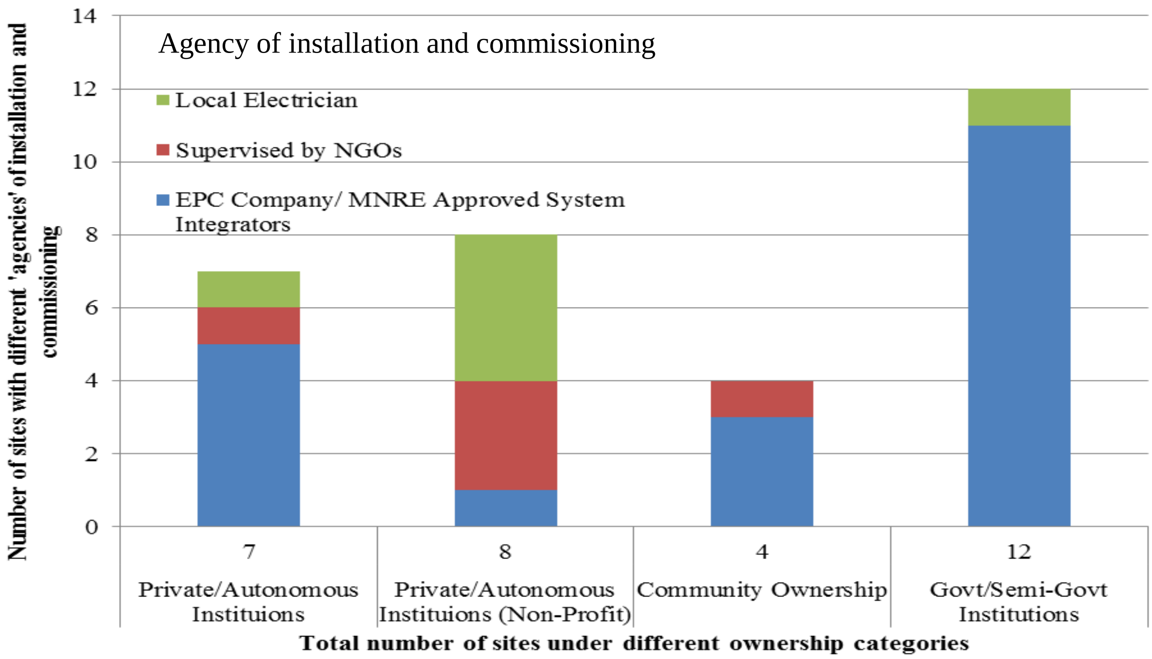

Fig. 9.3: Agency installing and commissioning PV systems for different ownership categories

c) *Financial Facilitation for Different Types of Owners*

Lack of financial facilitation is often reported as a barrier for penetration of PV into society. Figure 9.4 shows the various sources from which the projects were funded at various sites we have surveyed. The figure shows that that most of the institutional consumers have availed loans and government support for PV installation. Some of them were able to get both government and external funding. All the community-owned systems and a few private institutions have adopted PV even without any financial facilitation from the government. Motivation behind installing such systems was mostly income generation or tax saving. This shows that people are willing to invest in PV if they are convinced about the economic advantage resulting from the system. The service offered by some NGOs in availing loans and external aids for solar projects and community-owned PV systems is often useful.

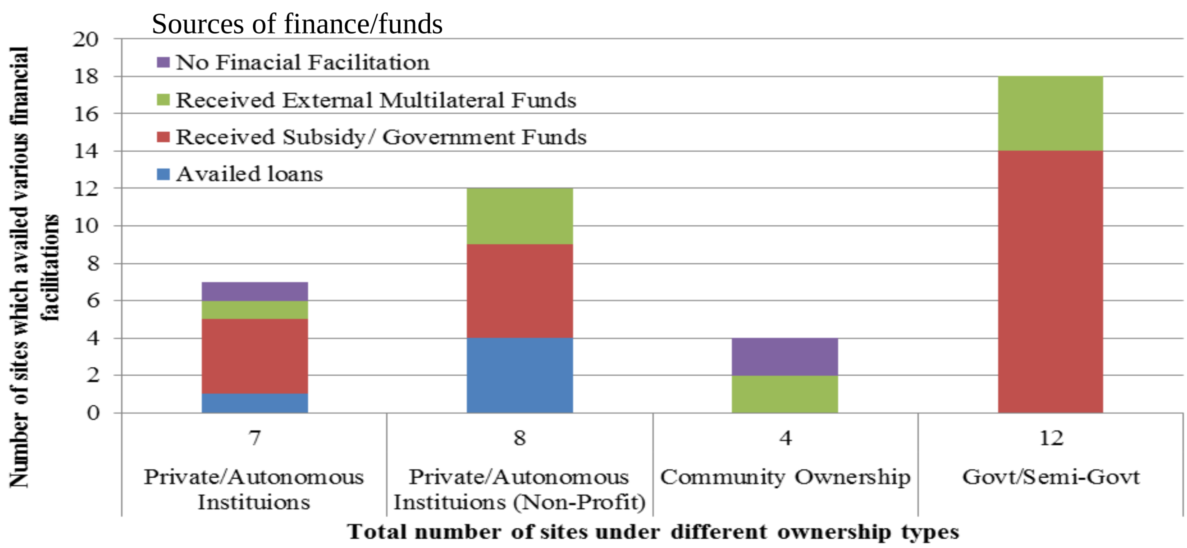

Fig. 9.4: Access to financial facilitation for different ownership categories

d) Nature of System Maintenance

Whether the systems are maintained on a preventive basis or on a remedial basis is a good indication of the system owner's concern towards system performance. The frequency at which routine check-ups are done and modules are cleaned also indicates the appropriateness of maintenance.

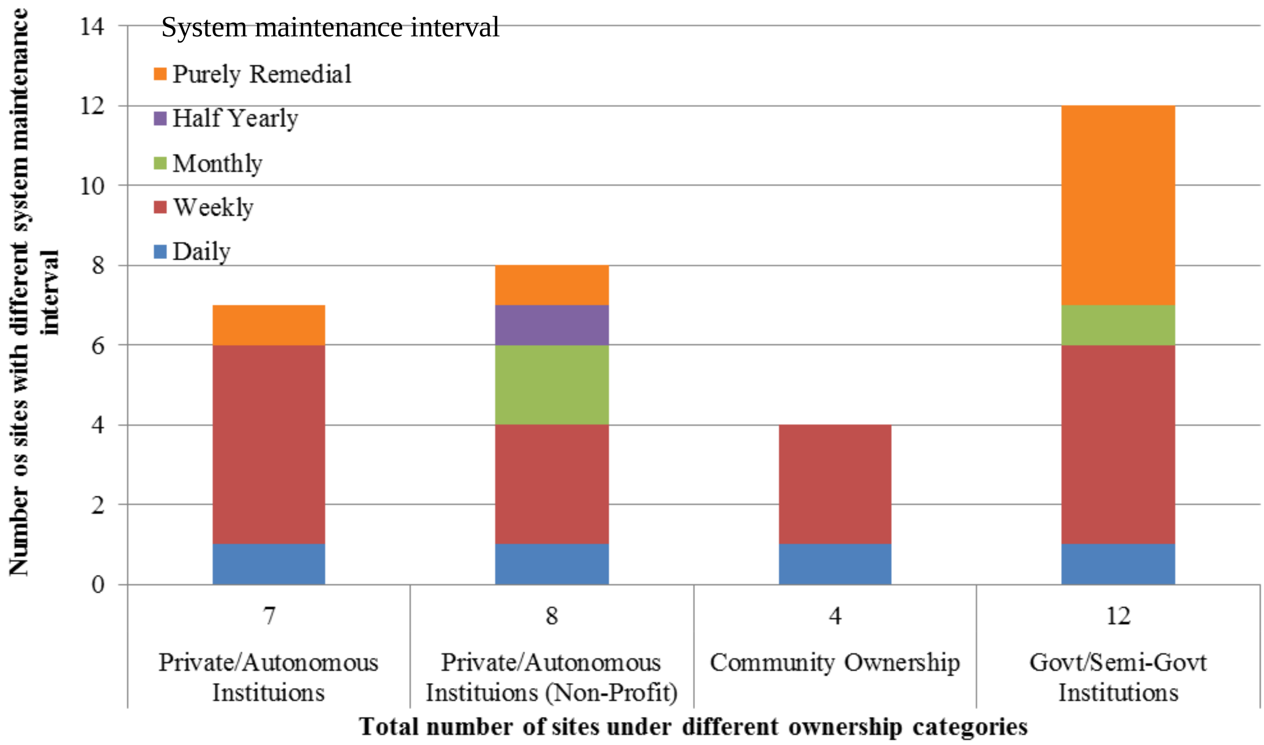

Fig. 9.5: Frequency and nature of system maintenance for different ownership categories

Figure 9.5 shows that most of the private institutions, NGO and community owned systems are maintained on a preventive basis and are checked regularly on a weekly or monthly basis, whereas negligence in system maintenance is seen from government institutions and some NGOs. It may be noted that most of the latter systems are installed at the expense of public money or through aid. Since the end-users have not spent anything, there appears to be a lack of 'ownership' that leads to the negligence.

The importance of installing the modules at an easily accessible place has been emphasised in a case study by El-Shobokshy *et al.* [51] in their paper dealing with the degradation of solar cells due to accumulation of dust. The importance of regular cleaning of modules is also highlighted in a study from Algeria [52]. Similarly, shading of single-module based rooftop home lighting PV systems was found to be a serious issue resulting from improper installation location [53]. Though the frequency for module cleaning depends on the nature and amount of dust getting accumulated, it is a good practice to clean the modules regularly. But this has not been observed to be a general practice across all types of ownerships. Figure 9.6 shows that among all types of system owners, the cleaning cycle of the modules are on a monthly basis or not regular for at least 50% of the sites. Ignorance of the deleterious effect of dust on yield reduction may be a reason.

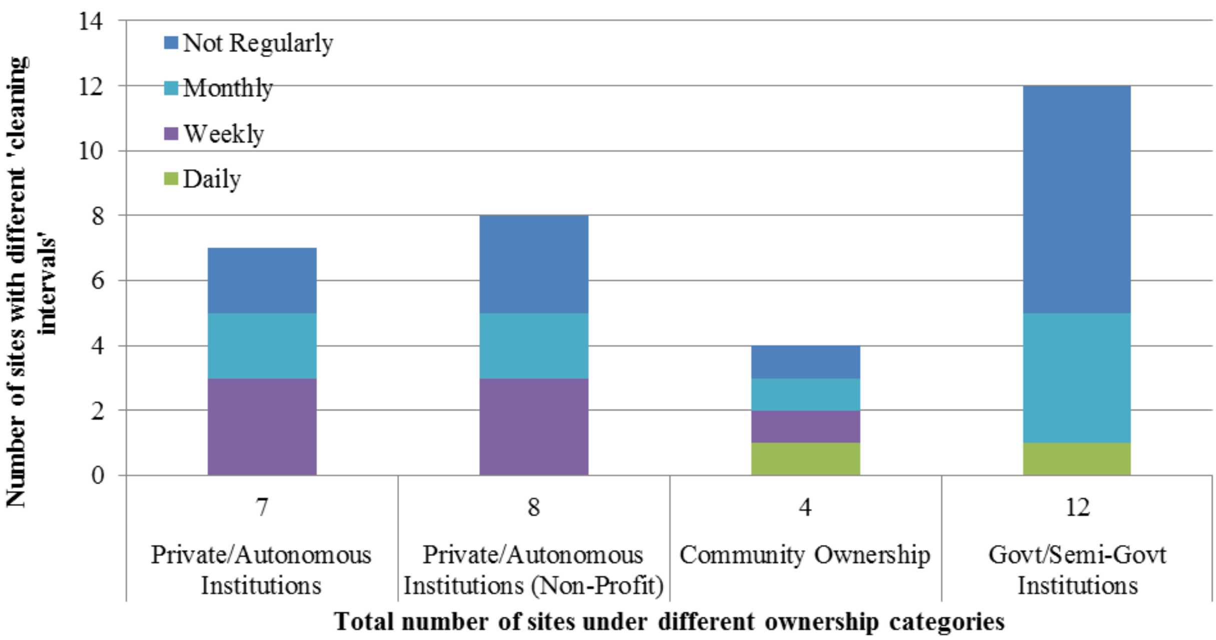

Fig. 9.6: Frequency of module cleaning for different ownership categories

Figure 9.7 shows that there is some correlation between the frequency of module cleaning and the P_{max} degradation rate of the modules. More regularly cleaned modules are degrading at a lesser rate.

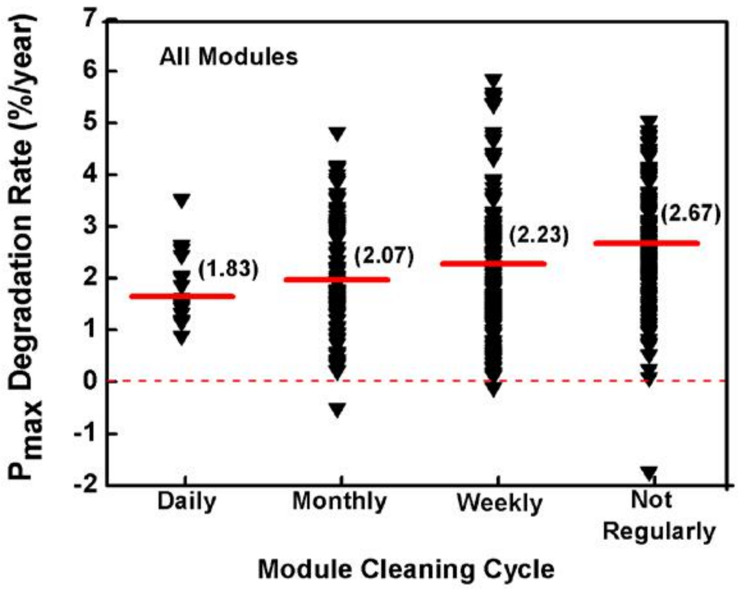

Fig. 9.7: Frequency of module cleaning and its correlation with P_{max} degradation

During visual inspection, the modules were classified into lightly soiled and heavily soiled modules. Lightly soiled modules were the ones with negligible thin layer of dust which can be easily removed by rubbing with a dry cloth, whereas the heavily soiled modules were having considerable amount of dust deposited on it, due to improper cleaning. Most of the times the removal of the dust was possible by using wet cloth, and with little pressure on the glass. Heavily soiled modules were having haziness near the bottom frame, as explained in Section 6.2.1. Figure 9.8 shows that lightly soiled modules degrade at a lesser rate than the heavily soiled modules. This is another indication for the need of regular module cleaning.

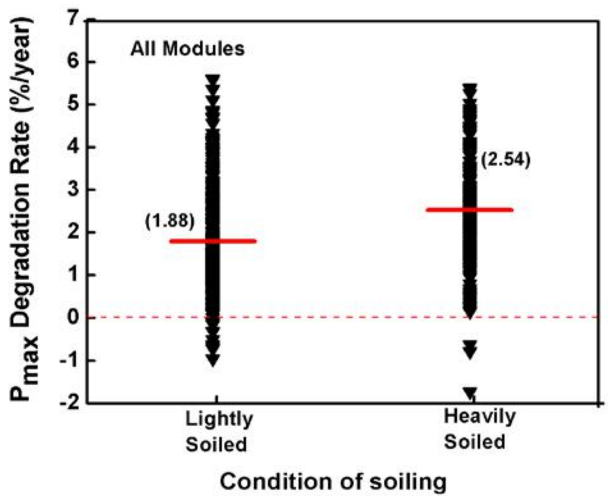

Fig. 9.8: Condition of soiling on module and its correlation with P_{max} degradation

Similarly, shading of modules by buildings and trees was observed in many of the smaller sites. Figure 9.9 shows that the mean value of P_{max} degradation of modules from sites which do not have the problem of shading are better when compared to the modules from systems which are shaded by surrounding trees and buildings. Hence enough care must be given in the selection of installation site and layout of the modules. It is clear that besides the obvious loss of power due to shading, there is also a long-term deleterious effect of shading in terms of increased degradation rate. Shading analysis of the installation site, especially for rooftop projects, is very important for better performance of the system.

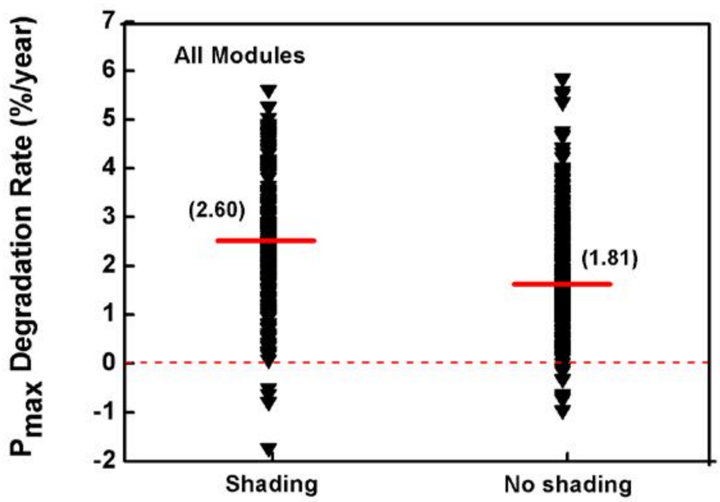

Fig. 9.9: Correlation between shaded systems and degradation: modules from systems which have shading have higher degradation rates compared to modules from unshaded sites

e) Availability of Skilled Local Technicians

After spending a substantial amount on PV systems, people often expect them to work without failure. Even a small down time of the system can cause dissatisfaction for the owner and create a negative impact on PV technology's popularity. The availability of a local technician who is trained and capable of fixing system failures becomes very important. A better practice for smaller systems is to train the system owner to do the basic trouble-shooting and repairing. Analysis shows that around 25-30% system owners are self-trained for basic trouble shooting in the government, community-owned and NGO sectors.

Figures 9.10 and 9.11show that the NGO's played an important role in promoting PV through proper training of local technicians. The overall statistics show that 48% of site owners resort to trained technicians for major repairs, but the rest depend on technicians who are not formally trained in PV. If we keep apart the 'trained' aspect, 45% systems are maintained by local technicians and the rest are by out-station technicians. Another statistics shows that 49% of the technicians are diploma or degree holders or ITI (Industrial Training Institutes) graduates. This shows the importance and need for including PV related training content in the syllabus of ITIs and polytechnics through government initiatives.

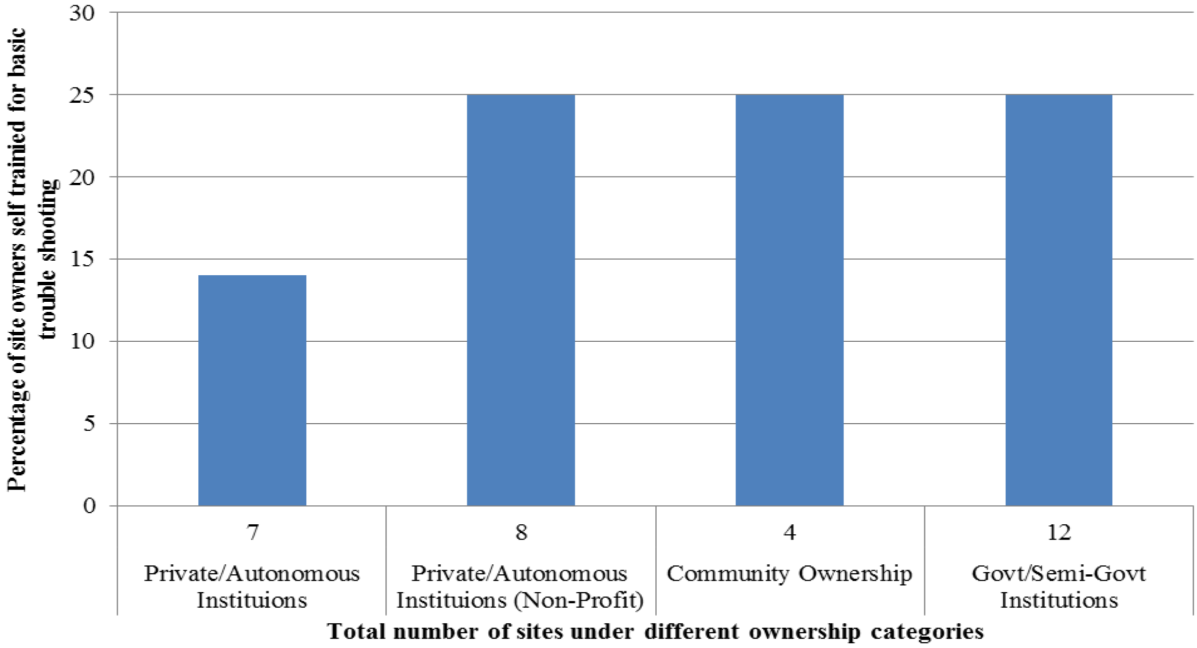

Fig. 9.10: Percentage of system owners self-trained for basic trouble shooting of PV systems

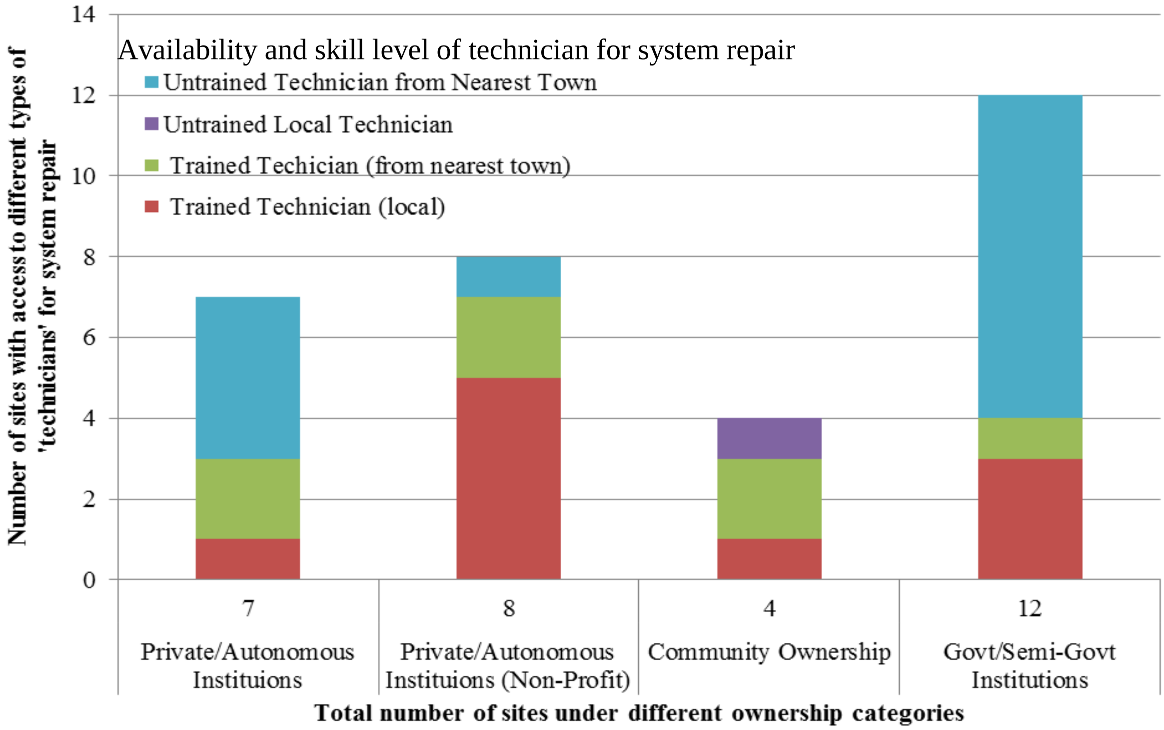

Fig. 9.11: Human resources available for system repair for major faults: technicianavailability and skill level of technician for system repair

Figure 9.12 shows the mean degradation in P_{max} of the modules from various systems installed and maintained by trained and untrained technicians. The data show that in those sites where the work is done by trained technicians, modules have degraded less. There may be various other reasons for degradation, but the care given in the execution of the project can be one reason for better performance. As explained in Section 7.2, a lot of cracks can be induced in the modules if they are not handled properly at the site and this can lead to P_{max} degradation. Data from the EL images of modules were taken, and grouped into two categories, based on whether the project was executed by trained technicians or not. Table 9.1 shows that the percentage of cells affected with mode A and B cracks in sites which are installed by trained technicians is less when compared to the sites installed by untrained technicians.

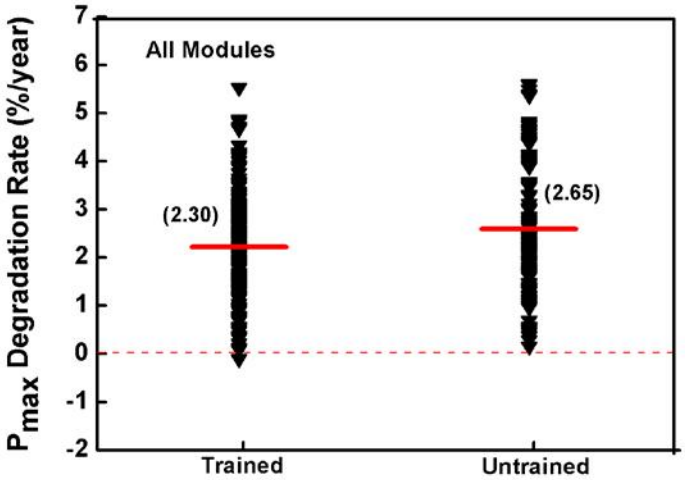

Fig. 9.12: Comparison of P_{max} degradation of modules from sites installed and maintained by trained and untrained technicians

Table 9.1: Correlation between cracks in modules and the skill level of technician handling the modules

	Percentage of cells affected by different types of cracks			**Total no. of cells**
	Mode A cracks	**Mode B cracks**	**Mode C cracks**	
Trained	9.2%	15.9%	4.4%	900
Untrained	16.2%	26.1%	3.1%	444

f) Flaws in the Design Philosophy: Over Sizing the Inverters

In many of the off-grid systems, the size (power rating) of the inverters has not been chosen based on proper load estimation. In many cases, the inverter ratings were chosen based on the installed PV 'array capacity', rather than on the load it has to drive. Due to this, most of the times, the inverters run on low loads and at poor efficiency. The reason why the higher size inverters were chosen was mainly because they have to handle higher PV array size in the battery charging circuit. Size of the PV array is basically decided by the energy requirement per day. Most of the off-grid inverters come with an integrated solar charge controller. The PV power handling capacity of this charge controller is usually proportional or close to the load handling capacity of the inverter. This results in the selection of larger kVA rating of inverters for handling larger PV power (but actually driving lower loads). In such a situation, a better cost-effective solution is to isolate the battery charging circuit with an external charge controller and to drive the load using a lower rated inverter appropriate for the load. The expense of buying a higher kVA rated inverter is more than that of buying an additional charge controller along with a lower kVA rated inverter matching the load requirement [92]. Table 9.2 shows that the inverter load power capacity has been oversized in many of the sites surveyed and hence the efficiency at nominal operating conditions is much smaller than the full load efficiency and the full load itself is much smaller than the actual rated capacity of the inverter itself.

Table 9.2: Issue of inverter oversizing

Site	PV Array (kW)	Inverter Rating (kVA)	Full Load (kVA)	η-nominal load	η - full load	Inverter Oversized
Site A	15	15	3.25	71%	79%	Yes
Site B	0.9	2	0.375	77%	84%	Yes
Site C	30	30	15	90%	92%	Yes
Site D	4	3	1.5	90%	95%	Yes
Site E	20	10	2	NA	82%	Yes
Site F	2	2	0.1	NA	NA	Yes
Site G	4	4	1	NA	NA	Yes

g) *Overall Scores for System Owners*

From the previous sections, we could identify various factors affecting the system performance apart from the local climatic conditions. Some of them are the design, workmanship, shading of modules, cleaning cycles, frequency of preventive maintenance checks, skill level of technician etc. We tried to evaluate the systems on a 25-point scale by quantifying all the observations in the field. The criteria for points allocation is as shown in Table 9.3. The analysis shows that the systems owned by government institutions have low scores. Community owned systems were ranked at the top when considered for the appropriateness in system installation and maintenance practices. Table 9.4 shows the maximum, minimum and the average score achieved by different groups of sites categorised based on ownership.

Table 9.3: Criteria for quantifying the observations in the field for overall ranking

Criteria	Observation and associated points allotted
Overall system design and workmanship (Maximum 5 points)	Proper sizing of inverter based on load analysis – 2 Proper sizing and configuration of modules and battery bank – 1 Right selection of wiring thicknesses based on currents carried – 1 Good workmanship and finishing of work (including safety) – 1
Shading of modules (Maximum 3 points)	Modules are unshaded – 3, A few modules have shading issue – 1.5, Many modules are shaded – 0
Module orientation and tilt angle (Maximum 3 points)	Modules are facing true south – 1.5, Modules are mounted at a tilt angle equal to latitude angle – 1.5, Deviation in tilt angle from latitude (deviation < ± 25% of optimum – 1, < ± 50% – 0.5, > ± 50%– 0
Module mounting (Maximum 3 points)	Modules are mounted on proper structures which are in good condition – 3, Structures rusted – 2, Structure broken or bended – 1, No structure – 0
Module cleaning (Maximum 3 points)	Modules are clean – 3, Lightly soiled – 2 , Heavily soiled – 0
Maintenance checks (Maximum 3 points)	Daily/ Weekly – 3, Monthly – 2 , Half yearly – 1, Purely remedial maintenance – 0
Availability and skill of technicians (Maximum 2 points)	Trained technician available locally – 2, Untrained technician available locally – 1.5, Outstation trained technician – 0.5, Outstation untrained technician – 0
Self-training (Maximum 3 points)	System owner self-trained in basic trouble shooting and repair – 3 System owner unaware of trouble shooting system failures – 0

Table 9.4: Maximum, minimum and average overall score for systems owned by different categories

Ownership	Max. Score Achieved	Min. Score Achieved	Average Score	Rank
Private/Autonomous Institutions	18	14	15.71	2
Private Institutions (Non-Profit)	19	7	14.63	3
Community Ownership	18	15	16.86	1
Government/Semi-Government Institutions	19.5	6	12.38	4

When we compare the average scores obtained by different ownership models with the mean value of P_{max} degradation of the modules from these sites, it was seen that the private not-for-profit institutions are best in terms of lowest degradation rates, closely followed by community owned systems. Figure 9.13 shows the trend of P_{max} degradation of the systems under different ownership models. This result is a little different from the trend of the scores obtained in the previous section. Still the difference in the scores between the community-owned systems and the systems owned by NGOs were very less. Similarly the difference in the average degradation values of P_{max} from these categories of systems is also very small. The low scores obtained by the government institutions are compatible with the high degradation value seen in this category.

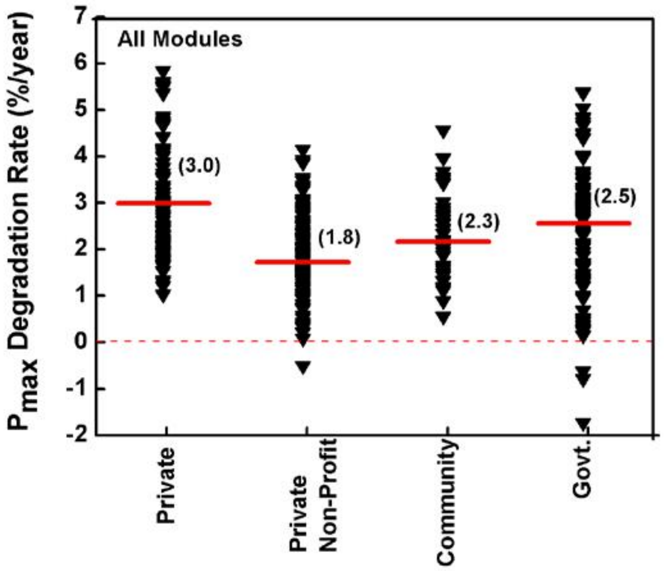

Fig. 9.13: Comparison of P_{max} degradation of modules from sites under different ownership categories

h) Group X and Group Y Sites Among the Different Ownership Categories

During the module power degradation analysis in Chapter 4, we had categorized the sites as Group X or Group Y. Basically Group X sites are the ones with an average annual degradation rate in P_{max} less than 2%/year and Group Y sites have a rate more than 2%/year. Figure 9.14 shows the number of Group X and Group Y sites under different ownership categories. Above 80% sites owned by private and government institutions are falling under Group Y sites. It was observed in Section 9.3.4.a that most of the systems under these ownership categories were installed by professional EPC companies and MNRE approved system integrator companies. In spite of this, the degradation rates are very high in these categories of systems.

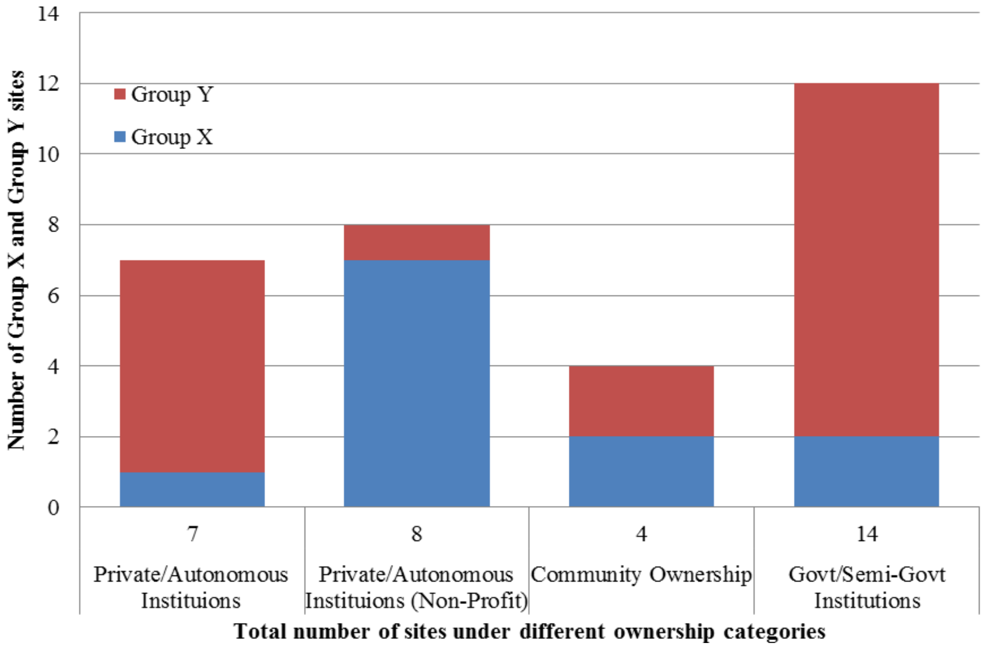

Fig. 9.14: Number of Group X and Group Y sites under different ownership categories

9.4 Analysis of Large Installations

As mentioned in Section 9.2, four unique samples were available for the analysis and comparison of performance of large power plants. The average P_{max} degradation value from these power plants was found to be 0.97%/year and is much lower than the average value of small and medium scale power installations. The motivation for installation of these power plants was basically income generation through sale of electricity or savings in the cost of diesel used for running a generator (one of them was an off grid power plant). The comparison of some of the parameters of these power plants is summarized in Table 9.5. As expected, there were no issues regarding shading and the workmanship and safety measures were quite good in all the power plants. If we try to quantify the power plants as per the criteria given in Table 9.3, then all of them have very good scores above 20 (out of 25).

Table 9.5: Observations made in the large power plants

Parameters	Power Plant 1	Power Plant 2	Power Plant 3	Power Plant 4
Mode of implementation	By EPC	By EPC	By EPC	By EPC
System Maintenance	Monthly	Weekly	Weekly	Daily
Module cleaning cycle	Monthly	Weekly	Monthly	Bi-Monthly
Availability of skilled labour	Site engineer and maintenance staff stationed at the power plant , 24x7	Site engineer and maintenance staff stationed at the power plant , 24x7	Site engineer and maintenance staff stationed at the power plant , 24x7	Site engineer and maintenance staff stationed at the power plant , 24x7
Overall Score out of 25	23	25	24	21

All the sites fall under Group X and the module degradation rates are less than 2%. Hence it can be concluded that the large scale power plants are generally well designed, installed and maintained.

9.5 Summary

- Major motivation for private installations under institutional ownership and community users is income generation, saving in electricity bills or saving of taxes. Many of them have invested in PV even if they have not availed capital subsidies from the government.
- Many of the government funded installations are for promoting green energy, but in many cases they are not properly maintained.
- From a financial facilitation perspective, institutional system owners are finding it easier to get access to loans, government and external funds.
- Generally, government and private institutions get the design, installation and commissioning work of PV systems done by EPC contractors. NGOs, individuals and community owners resort to local electricians for getting their work done.
- NGOs have played a major role in ‘localizing’ PV technology by training the local electricians on PV technology.
- Community owned PV systems are having better maintenance practices in the field, especially when the systems help in meeting the necessities or provide an income source to the community. Unfortunately the degradation rates of modules in such systems are seen to be high, may be because of the selection of poor quality modules.
- A large number of technicians who actually undertake system installation and maintenance are either high school or diploma school graduates. There is a huge need of trained local electricians to maintain the PV systems.
- Inverter over-sizing in off grid systems was found to be a major design flaw, even among the systems designed by the so called ‘knowledgeable’ EPC contractors.
- Improper orientation, tilt angle, poor support structure, soiling, shading etc. are some of the problems in the site which give rise to degradation and failure of PV systems.
- More regularly cleaned modules were having lesser P_{max} degradation rate and those modules which were observed as heavily soiled in the field were having higher P_{max} degradation rate.
- Mean value of P_{max} degradation of shaded modules was higher by 0.8%/year than the unshaded modules, showing the evidence of long-term deteriorating effect of shading in module output power.
- The number of mode A and B cracks appearing in the modules is more in the installations done by untrained technicians, possibly due to improper handling of modules. This has resulted in higher P_{max} degradation rate in such sites.

10. Conclusions and Recommendations

10.1 Conclusions

We present below the major conclusions of the 2014 All-India Survey of Photovoltaic Module Reliability conducted mostly during September-November 2016. The survey covered 1148 modules in 51 sites in all 6 climatic zones of India. The age of the modules ranged from 1 year to more than 25 years, and included 6 technologies, though the majority were crystalline silicon. The modules were located mainly in small/medium installations, but also in large installations.

- The performance of PV modules surveyed is found to vary widely. Annual degradation rates vary from less than 0.6%/year to more than 4%/year. Degradation observed through visual, IR, EL and other means also varies significantly.
- In order to analyse the performance critically, we have separated the sites into two groups – Group X and Group Y. Group X sites have *average* module power degradation rate less than 2%/year, and are the so-called ‘good’ sites. Group Y sites have *average* module power degradation rate more than 2%/year, and are the so-called ‘problematic’ sites. The overall average degradation rate for *all* Group X modules is 1.33%/year, which is somewhat higher than the internationally reported degradation rates. Overall average degradation rate for *all* Group Y modules is 2.73%/year.
- When sites are separated based on their size, the large installations (>100 kW) show a good average degradation rate of 0.97%/year compared to the small/medium sites (<100 kW) which show a much higher average degradation rate of 2.32%/year. All large sites fall in the Group X category. This indicates that module quality and/or installation practices are much better for large power plant installations.
- A detailed climatic zone analysis for Group X modules was performed. This shows that modules in the ‘Hot’ climates (Hot & Dry, Warm & Humid, Composite) degrade at a faster rate of 1.42%/year than modules in ‘Non-Hot’ climates (Temperate, Cold & Sunny, Cold & Cloudy), which degrade at 1.05%/year. This is likely to be partly because of the higher percentage of interconnect failures and faster encapsulant discoloration observed in the ‘Hot’ climates.
- The Group X modules fare worst in the ‘Warm & Humid’ climate, degrading at 1.53%/year. The ‘Hot & Dry’ climate is the next worst. The most benign climate for the modules is the ‘Cold & Sunny’ climate, with the average degradation rate in this zone being only 0.8%/year.
- Overall, young modules (< 5 years) show a higher degradation rate than old modules (> 5 years old). This may reflect the higher initial degradation rate seen for many technologies. However, taken together with the fact that for only Group X modules, young modules degrade slower than old modules, the results also suggest that newer installations have poorer quality of modules and/or installation practices. For the young modules, the main contributor for P_{max} degradation is the fill factor (*FF*), whereas short circuit current (I_{sc}) degradation is the main factor in case of old modules.
- Roof-mounted modules suffer from a higher degradation rate as compared to ground-mounted modules. Infrared (IR) measurements show that modules installed on rooftops in the ‘Hot’ zones are running hotter than modules installed on the ground. Coupled with the higher degradation rate seen for small/medium systems (which are often roof-mounted), this means special attention is needed for the 40 GW rooftop target.
- Modules in Group Y have higher percentage of cracked cells than modules in Group X as seen by visual checking and electroluminescence (EL), which indicates poor handling of the modules during

manufacturing, transportation and/or installation for Group Y sites, many of which fall into the young category. A higher percentage of mode A and mode C cracks has been observed in the young modules as compared to the old modules. The cells at the edge and corner of the module show more cracks than the central portion of the module, which again may be caused by improper handling at the time of installation. There is a good correlation between the total number of cracks in the module and the power degradation of the module.

- The quality of encapsulant appears to be another differentiating factor between modules of Groups X and Group Y sites. Group Y modules of young age show significantly more discoloration than Group X modules. Also, delamination is more frequently detected (and is also more severe) in the Group Y modules, as compared to Group X modules. These observations, together with that of cracks in Group Y modules as mentioned above, point to poorer quality of materials used and improper or hasty installation practices for Group Y sites. These data also provide independent corroboration for the decision to separate the sites into Group X and Group Y sites.
- A large number of modules show hot cells in the field, which calls for attention to the hot cell problem. Modules which contain hot cells (detected by IR thermography) degrade faster than other modules. This problem gets worse in 'Hot' climates, where the modules containing hot cells show a much higher average module temperature, and degrade faster than their counterparts in 'Non-Hot' climates. High degree of mismatch in cell temperatures can lead to faster degradation in module's output power.
- Snail trails are mostly seen in the young modules and are more severe in the humid zones – 'Warm & Humid' and 'Cold & Cloudy'. However, snail trails do not seem to affect the present-day electrical performance of the modules. Modules with non-framing type of snail trails have been found to have cracks in the corresponding cells.
- Metallization discoloration is observed not only in the old modules, but even in young modules, which again hints at poor material quality and manufacturing processes. Metallization discoloration is observed in all climatic zones but its severity is highest in the Warm & Humid zone. It has been found to correlate well with the degradation in the fill factor (*FF*) of the module.
- Scratches in backsheet, front glass and frame have been found in the young modules, again indicating improper handling during installation. Backsheet has been found to degrade in both young and old modules, but modules in the large installations are better off than the small/medium installations.
- Ideality factor n for the modules has been found to increase with age, indicating the degradation in the solar cells or increase in series interconnect resistance with aging. It correlates well to the percentage power degradation.
- For thin-film modules *FF* is the main contributor to the P_{max} degradation followed by I_{sc}, whereas for crystalline silicon modules, it is the other way around. In the thin-film modules, white spots are the most prevalent degradation mode. White spots have been found to reduce the fill factor in amorphous silicon modules, thereby contributing to P_{max} degradation.
- More than 90% of the surveyed modules have passed the dry insulation test, with 100% passing in the large installations.
- Discoloration and delamination have been found to correlate well with the decrease in the short circuit current of the modules, and consequent power loss. Discoloration of metallization is most common in the 'Warm & Humid' climate and has been found to correlate well with the degradation of the fill factor. A Visual Degradation Index (VDI) has been developed based on the discoloration, delamination and metallization discoloration, and it correlates well with the overall power degradation in the modules.
- The 'Hot' climatic zones of India – 'Hot & Dry', 'Warm & Humid' and 'Composite', where most of the installations are likely to take place, present a challenging environment for PV modules. Problems encountered in these zones include higher annual degradation rates, greater incidence of hot cells, more discoloration and delamination, higher metal corrosion, and more interconnect breakage.

- The higher annual degradation rates seen in the ‘Hot’ climatic zones appear to be most likely due to the following mechanisms: enhanced discoloration and delamination (both of which reduce I_{sc}), enhanced metal corrosion (which increases series resistance and hence reduces *FF*), and enhanced interconnect breakage, possibly due to thermal cycling (which again increases series resistance and reduces *FF*). The fact that hot cells cause modules in the ‘Hot’ zones to run significantly hotter than modules in the ‘Non-Hot’ zones further exacerbates all the above degradation mechanisms.
- A detailed Risk Priority Number (RPN) analysis has been performed to assess what the main risks are in different climatic zones. In terms of the performance RPN, that is, the risk factor for degradation of performance, encapsulant discoloration and solder bond failure are the main culprits in the ‘Hot’ zones. This is understandable since encapsulant discoloration is accelerated by high temperatures, and high temperatures, high temperature cycling and humidity all lead to problems with solder bonds.
- The RPN analysis for safety, that is, the risk factor associated with safety of personnel, shows that problems in backsheet and loose junction boxes are the main culprits in all climatic zones.
- The socio-economic survey of the small/medium sites reveals several interesting points. Generally speaking, privately-owned installations are not as well installed as those owned by government or semi-government organizations, but they are usually much better maintained and cared for. A correlation has been seen between annual power degradation rate ΔP_{max} and installation procedure (lower ΔP_{max} when installed by trained personnel, lower ΔP_{max} and fewer cracks when installed properly in a shade-free area by trained personnel), and also with cleaning cycle (lower ΔP_{max} for more frequent cleaning).

10.2 Recommendations

Based on, and arising out of, the above conclusions, our recommendations for the photovoltaic community are as follows:

- Quality of modules can vary significantly, so due diligence should be exercised while selecting and procuring modules. This may include verifying the antecedents of the manufacturer, and independent checks on the quality of the module(s). Although most modules available in the market carry the IEC certification, it should be noted that the IEC certification is really a certification of the manufacturing process, and does not guarantee that the module will perform adequately through its intended life. This is especially important for the installation of small/medium sites, where this problem is seen to be most prevalent during this survey.
- Materials used in modules are important. EVA and backsheet particularly can be of different qualities, and should be specified by the manufacturer in the datasheet, and also in the tender for procurement.
- An independent audit of modules and installations by third party is recommended. This may include detailed testing of randomly selected modules before as well as after shipment.
- Some cases of ‘over-rating’ of modules have been detected during the survey, especially in small/medium sites. Owners and installers should be vigilant about this malpractice.
- Module manufacturers and installers should place more emphasis on proper packaging and handling of the modules during transportation since improper handling can induce cracks in the solar cells and lead to long-term degradation.
- Installation procedures and protocols are important, and standard procedures as recommended should be diligently followed. This calls for a well-trained workforce, and the need for a good certification programme. The many small/medium rooftop sites which are likely to come up also need to be installed by trained personnel.
- It is recommended that a field-based electroluminescence (EL) study be performed after receiving the modules at site and installation to reveal micro-cracks which may have been caused during the transport

and installation phases. Though this may not feasible at the smaller sites, it would be possible for the large sites.

- It has been noted that the 'Hot' climates present a harsh operating environment for PV modules. An intensive study of degradation phenomena in hot climates, which has not been emphasized sufficiently by the PV community so far, is needed. This is particularly important for India, since much of the 100 GW is expected to come up in the 'Hot' zones of the country.
- The IEC certification protocols (eg. 61215), and other standards, which are currently being updated, need to take into account the hot climate phenomena, and develop more aggressive test protocols going to higher temperatures. Indian R&D and industry involvement in PVQAT (International PV Quality Assurance Task Force) is highly recommended.
- Modules and sites perform very well in the 'Cold & Sunny' climate of Ladakh. Power plants set up in this region will enjoy not only low degradation rates, but also excellent irradiance.
- It is felt that some of the quality issues seen especially in the young modules are the result of aggressive pricing and improper handling/installation, especially in the small/medium sized sites.

References

[1] R. Dubey, S. Chattopadhyay, V. Kuthanazhi, J. John, C. S. Solanki, A. Kottantharayil, B. M. Arora, K. Narsimhan, J. Vasi, B. Bora, Y. Singh and O.S. Sastry, "All-India Survey of Photovoltaic Module Degradation 2013," NCPRE, Mumbai, 2014.

[2] E. Christensen, "Flat-Plate Solar Array Project of the US Department of Energy's National Photovoltaics Program: 10 Years of Progress," NASA, 1985.

[3] *Crystalline Silicon Terrestrial Photovoltaic Modules - Design Qualification and Type Approval*, IEC 61215 Ed. 2, 2005.

[4] Canadian Solar, "www.solarsouthwestflorida.com," [Online]. Available: http://www.solarsouthwestflorida.com/wp-content/uploads/2012/01/PV-Module-Warranty-and-Warranty-Insurance-Comparisons-White-Paper-Sept.-2011.pdf.

[5] D. C. Jordan, J. H. Wohlgemuth and S. R. Kurtz, "Technology and Climate Trends in PV Module Degradation," in *27th European Photovoltaic Specialists Conference and Exhibition*, Frankfurt, 2012, pp. 3118-3124.

[6] D. C. Jordan, S. R. Kurtz, K. VanSant and J. Newmiller, "Compendium of Photovoltaic Degradation Rates," *Progress in Photovoltaics: Research and Applications*, 2016.

[7] A. Suleske, J. Singh, J. Kuitche and G. Tamizh-Mani, "Performance Degradation of Grid-Tied PV modules in a Hot-Dry Climatic Condition," *SPIE 8112: Reliability of Photovoltaic Cells, Modules, Components, and Systems IV*, 2011.

[8] O.S. Sastry, S. Saurabh, S. Shil, P. Pant, R. Kumar, A. Kumar and B. Bandopadhyay, "Performance analysis of field exposed single crystalline silicon modules," *Solar Energy Materials and Solar Cells*, vol. 94, pp. 1463-1468 , 2010.

[9] D. Magare, O.S. Sastry, R. Gupta and A. Kumar, “Data Logging Strategy of Photovoltaic (PV) Module Test beds,” in *27th European Photovoltaic Specialists Conference and Exhibition*, Frankfurt, 2012, pp. 3259-3262.

[10] V. Sharma, O.S. Sastry, A. Kumar, B. Bora and S. Chandel, “Degradation Analysis of a-Si, HIT and mono c-Si Solar Photovoltaic Technologies Under Outdoor Conditions,” *Energy*, vol. 72, pp. 536-546, 2014.

[11] B. Bora, O.S. Sastry, A. Kumar, Renu and M. Bangar, “Performance Modelling of three PV module technologies based on clearness index and air-mass using contour map,” in *42nd IEEE Photovoltaic Specialists Conference*, New Orleans, 2015, pp. 1-4.

[12] S. Rai, B.Bora, O.S.Sastry, M. Bangar, Y.K.Singh, A.Kumar, K.Yadav, M.Kumar, R.Singh, Renu and A. Kumar, “Modeling the performance of HIT Technology for composite climatic zone of India,” in *42nd IEEE Photovoltaic Specialists Conference*, New Orleans, 2015, pp. 1-5.

[13] V. Sharma, A. Kumar, O.S.Sastry and S.S.Chandel, “Performance assessment of different solar photovoltaic technologies under similar outdoor conditions,” *Energy*, pp. 1-8, 2013.

[14] R. Singh, B. Bora, K. Yadav, O.S. Sastry, M. Kumar, A. Kumar, Renu, A. Bangar, S. Rai and A. Kumar, “Effect of series resistance on degradation of Isc, Power output and Fill Factor of HIT Technology,” in *42nd IEEE Photovoltaic Specialists Conference*, New Orleans, 2015, pp. 1-5.

[15] D. B. Magare, O.S. Sastry, R. Gupta, T. Betts, R. Gottschalg, A. Kumar, B. Bora and Y. Singh, “Effect of seasonal spectral variations on performance of three different photovoltaic technologies in India,” *International Journal of Energy and Environmental Engineering*, vol. 7, pp. 93-103, 2014.

[16] M. Bangar, B. Bora, Renu, A. Kumar and O.S.Sastry, “Analysis of spectrum variations in different seasons in composite climatic zone of India,” in *42nd IEEE Photovoltaic Specialists Conference*, New Orleans, 2015, pp. 1-4.

[17] G. Tamizhmani, “Climate dependent degradation rates based on nation-wide onsite I-V measurements,” presented at *2016 PV Module Reliability Workshop*, Lakewood, CO, 2016.

[18] J. Kuitche, R. Pan and G. Tamizhmani, "Investigation of dominant failure modes for field-aged c-si modules in

desert climatic conditions," *IEEE Journal of Photovoltaics*, vol. 4, no. 3, pp. 814-826, 2014.

[19] J.-S. Jeong, N. Park and C. Han, "Field failure mechanism study of solder interconnection for crystalline silicon photovoltaic module," *Microelectronics Reliability*, vol. 52, no. 9-10, pp. 2326–2330, 2012.

[20] A. Kaminski, J. J. Marchand, A. Fave and A. Laugier, "New method of parameters extraction from dark I-V curve," in *26th IEEE Photovoltaic Specalists Conference*, Anaheim, CA, 1997.

[21] D. L. King, B. R. Hansen, J. A. Kratochvil and M. A. Quintana, "Dark current-voltage measurements on photovoltaic modules as a diagnostic or manufacturing tool," in *26th IEEE Photovoltaic Specalists Conference*, Anaheim, CA, 1997, pp. 1125-1128.

[22] K. Bouzidi, M. Chegaar and M. Aillerie, "Solar cells parameters evaluation from dark I–V characteristics," *Energy Procedia*, vol. 18, pp. 1601-1610, 2012.

[23] O. Breitenstein, P. Altermatt, K. Ramspeck, M. Green, J. Zhao and A. Schenk, "Interpretation of the commonly observed I–V characteristics of C-Si cells having ideality factor larger than two," in *IV World Conference on Photovoltaic Energy Conversion*, Waikaloa, Hawaii, 2006, pp. 879-884.

[24] J. Salinger, V. Benda, Z. Machacek, "Determination of recombination centres in c-Si solar cells from dark IV characteristics," in *27th International Conf. on IEEE Microelectronics (MIEL)*, 2010, pp. 149-151.

[25] S. V. Spataru, D. Sera, P. Hecke, T. Kerekes and R. Teodorescu, "Fault identification in crystalline silicon PV modules by complementary analysis of the light and dark current–voltage characteristics," *Progress in Photovoltaics: Resaerch and Applications*, 2015.

[26] A. Mansouri, M. Zettl, O. Mayer, M. Lynass, M. Bucher, O. Stern and R. Burhenne, "Defect detection in photovoltaic modules using electroluminescence imaging," in *27th European Photovoltaic Specialists Conference*, Frankfurt, Germany, 2012, pp. 3374-3378.

[27] T. Fuyuki, H. Kondo, T. Yamazaki, Y. Takahashi and Y. Uraoka, "Photographic surveying of minority carrier diffusion length in polycrystalline silicon solar cells by electroluminescence," *Applied Physics Letters*, vol. 86, p. 262108, 2005.

[28] Y. Kaji, Y. Takahashi, A. Ogane, Y. Uraoka and T. Fuyuki, "Characterization of polycrystalline silicon solar cells by electroluminescence," in *15th International Photovoltaic Science & Engineering Conference*, Shanghai, China, 2005.

[29] T. Fuyuki, H. Kondo, Y. Kaji, A. Ogane and Y. Takahashi, "Analytic findings in the electroluminescence characterization of crystalline silicon solar cells," *Journal of Applied Physics*, vol. 101, p. 023711, 2007.

[30] C. Packard, J. H. Wohlgemuth and S. R. Kurtz, "Development of a visual inspection data collection tool for evaluation of fielded PV Module condition," NREL, Technical Report no. NREL/TP-5200-56154, Golden, Colorado, 2012.

[31] W. Holley and S. Argo, "Advanced EVA Based Encapsulants : Final Report," NREL, Technical Report no. NREL/TP-5200-56154, Golden, USA, 1998.

[32] A. W. Czanderna and F. Pern, "Encapsulation of PV Modules using ethylene vinyl Acetate Co-polymer as a pottant : A Critical review," *Solar Energy Materials & Solar Cells*, vol. 43, pp. 101-181, 1996.

[33] C. Schmid, J. Chapon, G. Kinsey, J. Bokria and J. Woods, "Impact of High Light Transmission EVA basedv encapsulant on the performance of PV Modules," in *27th European Photovoltaic Specialists Conference and Exhibition*, 2012, pp. 3494-3498.

[34] N. Dhere and M. B. Pandit, "Study of delamination in acceleration tested PV Modules," in *17th European Photovoltaic Specialists Conference and Exhibition*, Munich, 2001.

[35] Tsuyoshi Shioda, "Delamination failures in long-term field-aged PV modules from point of view of encapsulants," in *Phootovoltaic Module reliabilioty Workshop*, Colorado USA, 2013.

[36] R. Moreton, E. Lorenzo, J. Leloux and J.M.Carrillo, "Dealing in Practice with Hot Spots," in *29th European Photovoltaic Solar Energy Conference and Exhibition*, Amsterdam, 2014, pp. 2722-2727.

[37] C. Buerhop, D. Schlegel, M. Niess, C. Vodermayer, R. Weißmann and C. Brabec, "Reliability of IR Imaging of PV Plants under operating conditions," *Solar Energfy Materials & Solar Cells*, vol. 107, pp. 154-164, 2012.

[38] M. Quintana, D. King, T.J.McMohan and C. Osterwald, "Commonly observed degradation in field-aged

photovoltaic modules," in *29th IEEE Photovoltaic Specalists Conference*, 2002, pp. 1436-1439.

[39] S. Ver-Bruggen, "Enduring to the End," PV Magazine, March 2014. [Online]. Available: http://www.pv-magazine.com/archive/articles/beitrag/enduring-to-the-end-_100014468/618/#axzz3tnvNRKKJ. [Accessed 6 12 2015].

[40] G. Oreski and G. Wallner, "Aging mechanisms for polymeric films for PV encapsulation," *Solar Energy*, vol. 79, pp. 612 – 617, 2005.

[41] William Gambogi, "Qualification of PV Materials," in *SPI Workshop*, 2013.

[42] S. Pingel, D. Koshnicharov, O. Frank, T. Geipel, Y. Zemen, B. Striner and J. Berghold, "Initial Degradation of Industrial Silicon Solar Cells in Solar Panels," in *25th European Photovoltaic Specialists Conference*, 2010.

[43] M. Goldstein and L. Dunn, "Light Soaking Effects on PV Modules: Overview and Literature Review," in *NREL PV Module Reliability Workshop*, Denver, 2011.

[44] M. Kontges, C. Packard, S. Kurtz, U. Jahn, K. A. Berger, K. Kato, T. Friesen, H. Liu, "Review of Failures of Photovoltaic Modules," International Energy Agency, Technical Report no. IEA-PVPS T13-01,2014.

[45] Sharp Corporation, "Installation Manual," [Online]. Available: http://www.beck-solar.de/fileadmin/user_upload/Datenblaetter/Sharp/InstallationManual_SHARP_NA_FxxxGK_KTA10007_Ver3-11.pdf.

[46] International Energy agency, "16 Case Studies on the Deployment of Photovoltaic Technology in Developing Countries," IEA, Technical Report no. IEA-PVPS T9-07, 2003.

[47] Simon Bawakyillenuo, "Deconstructing the dichotomies of solar photovoltaic (PV) dissemination trajectories in Ghana, Kenya and Zimbabwe from the 1960s to 2007," *Energy Policy*, vol. 49, pp. 410-421, 2012.

[48] M. Jafar, "Renewable Energy in the South Pacific—options and constraints," *Renewable Energy*, vol. 19, pp. 305-309, 2000.

[49] S. Ling, J. Twidell and B. Boardman, "Household photovoltaic market in Xining,Qinghai province, China: the role of local PV business," *Solar Energy* , vol. IV, no. 73, pp. 227-240, 2002.

[50] Yale University School of Management, "SELCO 2009: Determining a path forward," Yale University School of Management, 2009. [Online]. Available: http://nexus.som.yale.edu/design-selco/. [Accessed 4 October 2015].

[51] M. El-Shobokshy and F. Hussein, "Degradation of photovoltaic cell performance due to dust deposition on to its surface," *Renewable Energy*, vol. III, pp. 585-590, 1993.

[52] A. Benatiallah, R. Mostefaou and K. Bradja, "Performance of photovoltaic solar system in Algeria," *Desalination*, vol. III, no. 209, pp. 39-42, 2007.

[53] A. Ubisse and A. Sebitosi, "A new topology to mitigate the effect of shading for small photovoltaic installations in rural sub-Saharan Africa," *Energy Conversion and Management*, vol. 7, no. 50, pp. 1797-1801, 2009.

[54] H. Saha, "Design of a Photovoltaic electric power system for an Indian village," *Solar Energy*, vol. II, no. 27, pp. 103-107, 1981.

[55] G. S. Schmidt-Kuntzer, "Village power plants versus SHS," *SunWorld*, vol. III, no. 17, pp. 17-20, 1993.

[56] J. Cust, A. Singh and K. Neuhoff, "Rural Electrification in India:Economic and Institutional aspects of Renewables," in *EPRG*, Cambridge, 2007.

[57] K. Ulsrud, T. Winther, D. Palit, H. Rohracher and J. Sandgren, "The Solar Transitions research on solar mini-grids in India: Learning from local cases of innovative socio-technical systems," *Energy for Sustainable Development*, vol. 15, pp. 293-303, 2011.

[58] D. Palit, "Solar energy programs for rural electrification: Experiences and lessons from South Asia," *Energy for Sustainable Development*, vol. 17, pp. 270-279, 2013.

[59] D. Miller and C. Hope, "Learning to lend for off-grid solar power: policy lessons from World Bank loans to India, Indonesia, and Sri Lanka,," *Energy Policy*, vol. 28, pp. 87-105, 2000.

[60] P. Raman, J. Murali, D. Sakthivadivel and V. Vigneswaran, "Opportunities and challenges in setting up solar photo voltaic based micro grids for electrification in rural areas of India," *Renewable and Sustainable Energy Reviews*, vol. 16, pp. 3320– 3325 , 2012.

[61] M. Gandhi, "The real issues of solar energy in India," *Renewable Energy*, vol. VI, no. 3, pp. 191-206, 1995.

[62] A. Chaurey and T.C Kandpal, “Solar lanterns for domestic lighting in India:Viability of central charging,” *Energy Policy*, vol. 39, pp. 4910–4918,2009.

[63] C. A. Gueymard, "SMARTS2: A Simple Model of the Atmospheric Radiative Transfer of Sunshine: Algorithms and Performance Assessment," Florida Solar Energy Center Technical Report No. FSEC-PF-270-95, Florida, 1995.

[64] M. Kempe, M. Reese, A. Dameron and T. Moricone, "Types of Encapsulant Materials and Physical Differences Between Them," in *NREL Photovoltaic Module Reliability Workshop*, 2010.

[65] R. Dubey, S. Chattopadhyay, V. Kuthanazhi, J. John, C. S. Solanki, A. K., B. M. Arora, K. Narsimhan and J. Vasi, "Daylight Electroluminiscence Imaging of Photovoltaic Modules by Image Difference Technique," in *6th World Conference on Photovoltaic Energy Conversion*, Kyoto, 2014.

[66] G. Tamizhmani and J. Kuitche, "Failure and Degradation Modes of PV Modules in a Hot Dry Climate: Results after 12 to 26 years of field exposure," in *NREL PV Module Reliability Workshop*, 2013.

[67] N. G. Dhere, N. S. Shiradkar and E. Schneller, "Cell Line Checker Correlated to Infrared Thermography," in *US PVMC Infrared Thermography Workshop*, 2013.

[68] *National Building Code of India*, SP 7:2005, 2005.

[69] N. K. Bansal and G. Minke, *Climatic Zones and Rural Housing in India*, Julich: Forschungszentrum Julich GmbH, 1995.

[70] *Photovoltaic devices - Procedures for temperature and irradiance corrections to measured I-V characteristics*, IEC 60891, 2009.

[71] R. M. Smith, D. C. Jordan and S. R. Kurtz, "Outdoor PV Module Degradation of Current-Voltage Parameters," in *World Renwable Energy Forum*, Denver, 2012.

[72] D. George and P. Mallery, 2010.

[73] D. Dirnberger, J. Bartke, A. Steinhuser, K. Kiefer and F. Neuberger, "Uncertainty of Field I-V Curve Measurements in Large Scale PV Systems," in *25th European Photovoltaic Solar Energy Conference and Exhibition*, Valencia, Spain, 2010.

[74] J. Wohlgemuth, D. W. Cunningham, A. Nguyen, "Failure Modes of Crystalline Silicon Modules," in *NREL PV Reliability Workshop*, Denver, 2010.

[75] V. Kelkar, "Snail Trail in PV Modules," [Online]. Available: http://www.solarquarter.com/index.php/item/750-snail-trail-in-pv-modules. [Accessed 3 12 2015].

[76] M. Kontges, I. kunze, V. Naumann, S. Richter, C. Hagendorf, J. Berghold and M. Roericht, "Snail Tracks (Schneckenspuren), Worm marks & Cell Cracks," [Online]. Available: http://iea-pvps.org/index.php?id=223&eID=dam_frontend_push&docID=1272. [Accessed 3 12 2015].

[77] Sharp Corporation, "SHARP Installation Manual" [Online]. Available: http://www.beck-solar.de/fileadmin/user_upload/Datenblaetter/Sharp/InstallationManual_SHARP_NA_FxxxGK_KTA10007_Ver3-11.pdf

[78] A. Mansouri, M. Zettl, O. Mayer, M. Lynass, M. Bucher, O. Stern and R. Burhenne, "Defect detection in photovoltaic modules using electroluminescence imaging," in *27th European Photovoltaic Solar Energy Conference and Exhibition*, Frankfurt, 2012, pp. 3374-3378.

[79] M. Kontges, I. Kunze, S. Kajari-Schroder, X. Breitenmoser and B. Bjorneklett, "The risk of power loss in crystalline silicon based photovoltaic modules due to micro-cracks," *Solar Energy Materials & Solar Cells*, vol. 95, pp. 1131-1137, 2011.

[80] S. Meyer, S. Timmel, S. Richter, M. Werner, M. Gläser, S. Swatek, U. Braun and C. Hagendorf, "Silver nanoparticles cause snail trails in photovoltaic modules," *Solar Energy Materials and Solar Cells*, vol. 121, pp. 171-175, 2014.

[81] J. Oh and G. TamizhMani, "Temperature Testing and Analysis of PV modules per ANSI/UL 1703 and IEC 61730 standards," in *35th IEEE Photovoltaic Specialist Conference*, Honolulu, 2010, pp. 984-988.

[82] C. Vodermayer, M. Mayer, T. Müller, M. Nieß, G. Wotruba, G. Becker, M. Zehner and J. Schumacher, "First

Results – Correlations between IR images and Electrical Behaviour and Energy Yield of PV Modules," in *23rd European Photovoltaic Specialists Conference*, Valencia, Spain, 2008.

[83] O.S. Sastry, B. Bora, Y. K. Singh, M. Bangar, R. Singh, Renu, M. Kumar, K. Yadav, R. Singh, A. Kumar and S. Rai, "RPN Analysis of Field exposed mono crytalline silicon PV modules under composite climate of India," in *42nd IEEE Photovoltaic Specialists Conference,* New Orleans, 2015, pp. 1-3.

[84] M. H. Dunham, *Data Mining: Introductory and Advanced Topics*, Pearson Education, 2003.

[85] A. Sinha, O.S. Sastry and R. Gupta, "Detection and Characterization of Delamination in PV modules by Active Infrared Thermography," *Nondestructive Testing and Evaluation*, vol. 31, no. 1, 2016.

[86] D. L. Meier, E. A. Good, R. A. Garcia, B. L. Bingham, S. Yamanaka, V. Chandrasekaran and C. Bucher, "Determining components of series resistance from measurements on a finished cell," in *4th World Conference on Photovoltaic Energy Conversion*, Waikoloa, 2006.

[87] A. P. Dobos, "An improved coefficient calculator for the California energy commission 6 parameter photovoltaic module model," *Journal of Solar Energy Engineering,* vol. 134, 2012.

[88] J. Wohlgemuth and S. Kurtz, "Reliability Testing beyond Qualification as a Key Component in Photovoltaic's Progress toward Grid Parity," in *IEEE International Reliability Physics Symposium*, 2011.

[89] J. H. Wohlgemuth and S. Kurtz, "Using Accelerated Testing to Predict Module Reliability," in *37th IEEE Photovoltaic Specialists Conference* , Seattle, 2011, pp. 3601-3605.

[90] G. TamizhMani and J. Kuitche, "Accelerated lifetime testing of photovoltaic modules," Solar America Board of Codes and Standards, 2013.

[91] S. M. Shrestha, J. K. Mallineni, K. R. Yedidi, B. Knisely, S. Tatapudi, J. Kuitche and G. TamizhMani, "Determination of Dominant Failure Modes Using FMECA on the Field Deployed c-Si Modules Under Hot-Dry Desert Climate," *IEEE Journal of Photovoltaics,* vol. 5, no. 1, 2015.

[92] Urjakart, [Online]. Available: www.urjakart.com.

Appendix A
Survey Checklist

Site No.: ELECTRICAL CHECKLIST (GROUP – A)

A1. Module & System Information

Manufacturer _______________ Model # _______________ Serial # _______________

Installation Site/Facility Serial # ________________________________

Module Nameplate Data: ☐ Available ☐ Missing

P_{max} _____________ V_{oc} ____________ I_{sc} ___________________

Sys Volt_________ V_{max} __________ I_{max} ____________________

Bypass diode, I_f ____________ Series fuse ____________________________

Temperature Coefficients:

Voltage: _______________ Current : ________________ Power : ______________

System design: ☐ single module ☐ multiple modules (a) ☐ unknown

(a.) Multiple module system:
Module location/number in a series string (from negative) _____________
No of modules in series (string) _______ No of strings in parallel (array) _________
No of bypass diodes___________ Rating & Model No. of Bypass Diodes: ______________
No of modules per Blocking diode _________ Rating & Model No. of Bypass Diodes: ___________

System Bias: ☐ open circuit ☐ resistive load ☐ max. power tracked ☐ short circuit ☐ Unknown

System Grounding: ☐ grounded (a.) ☐ not grounded ☐ unknown

(a.) ☐ Negative ☐ positive ☐ center of string ☐ unknown

Comments: ____
____

Filed by: Page 1 Date:

Site No.: ELECTRICAL CHECKLIST (GROUP – A)

A2. I-V Characteristics (☐ Not applicable ☐ Applicable)

Tracer used ☐ Solmetric I-V Tracer ☐ Meco System Analyzer
☐ PVPM I-V curve tracer ☐ Amprobe I-V curve tracer

I-V Curve File number/name & Time: ____

Comments on I-V curve : ____

____

Cell Line Checker Experiments

A3. Bypass Diode Test (☐ Not applicable ☐ Applicable)

No. of Bypass Diodes: _______________

No. of solar cells per Bypass Diode: ___________________

No. of Diodes functioning properly: ___________________

If functioning properly: Signal strength (No. of LED glowing 1 to 10)_____________________

If Diode not functioning properly: Nos. Shorted_______________ Nos. Open_______________

A4. Interconnect Failure Test (☐ Not applicable ☐ Applicable)

Interconnect Failure Present: ☐ Yes (a) ☐ No (b)

(a) No. of interconnect failure sites: ___________________

(a) Visual Image File No. : __________________________

(b) Max signal strength (No. of LED glowing 1 to 10)________

Min signal strength (No. of LED glowing 1 to 10)________

(b) Visual Image File No. : __________________________

Comments: ____
____

Filed by: Page 2 Date:

Site No.:

SOCIO-ECONOMIC & SYSTEM LEVEL CHECKLIST (GROUP – B)

1. **Year and month of** Procurement: ______________ Installation______________ Commissioning: _______________
2. **System Ownership**

☐ Private Individual ☐ Private Institution ☐ Community Ownership ☐ Govt/Semi-Govt Institutions

3. **Implementation Model**

☐ EPC Company /System Integrators ☐Supervised by NGOs ☐Supervised by MNRE Nodal Agency ☐Self (local electrician)

4. **Financial Model: Capital Investment:** Rs ___________

Did you avail any loans from banks? ☐ Yes ☐ No Bank: __________________

Loan Amount: Rs ___________________ Interest rate =__%

☐ Availed capital subsidy from MNRE ☐ Availed capital subsidy from State Govt

☐ Pending ☐ Pending

Percentage/Amount: ________________ Percentage/Amount: _________________

Year Received: ____ Year Received: ____

☐ Received funds from Govt/CSRs/Foreign Aids/NGOs

Amount: ______________

Year Received: ____

5. **O&M Expenses**

☐ Self ☐ Receive funds from Govt/Foreign Aids

☐ Generated by pay for service model

☐ Can be met from the savings in electricity bills

☐ Can be met from the replacement cost of previous power source (kerosene etc.)

6. **System Maintenance**

☐ **Preventive** Comes from nearest town (___km away)

☐Daily ☐ Monthly ☐ Half Yearly ☐Yearly Other__________

Basic Trouble Shooting and Maintenance done by:

☐Self ☐Trained Technician Next Technician Visit Due on: ____________ After _________days/months/

☐ From same locality ☐Comes from nearest town (___km away)

☐ **Responsive**

No of times the system failed in a year: _____

Repair works when system is down done by

☐ Self (Owner is trained) ☐Trained Technician

☐ From same locality Response Time:_______________Mean repair time: __________

☐ Comes from nearest town (___km away), Response time: _____Mean repair time: _______

Average Expenses on operation and Maintenance: ___________Rs/ Year

7. **Skill Level of Technician**

☐High School ☐ Diploma ☐ Graduate ☐ Engineering Graduate ☐ Other: ________ ☐ Taken PV training at technical Institutes/ NGOs /Companies etc.

Years of Experience: __________

8. **What all maintenance services are done in a technician visit?**

Visual Inspection, Module Cleaning ☐ Checking the Junction boxes for tight wiring/ corrosion ☐Check battery terminal

☐ Check for shading issues ☐ Remove debris ☐ Adjust tilt ☐ Inspect mounting system ☐ Inspect Battery Enclosure

☐ Watering of battery ☐ Specific Gravity Measurement of electrolyte ☐Charge Equalization ☐ Load Testing

☐ Capacity Testing ☐ Thermal inspection of Electrical equipment ☐ Disconnects, Fuses, Circuit breakers

☐ Strains in Wiring, Insulation damage

Comments: ____

____

Filled By: Page: 1 Date:

Site No.:

SOCIO-ECONOMIC & SYSTEM LEVEL CHECKLIST (GROUP – B)

List of Equipment: ____

____

____

____

Level of trouble shooting: ☐ System Level ☐ Subsystem Level ☐ Component level ☐ Element level

Most frequently replaced part of the system: ____________________________

9. Motivation for installation of the system

☐ **Necessity:**

- ☐ ***Home Lighting System***
  - ***Impact of SHS:*** No of additional hours added to daily activities____
  - ☐ Entertainment and Information form TV/Radio
  - ☐ Extra income generation through small artisanal activities
  - ☐ Reduced indoor pollution (kerosene fumes)
  - ☐ Communication facility (Mobile phone charging)

☐ **Optional power back up**

- ☐ Grid is available, but high interruption rates
- ☐ Grid available, but with low interruption rates

☐ **PV for community**

- ☐ Provision of potable water
- ☐ Powering Health centers
- ☐ Powering of educational/community center
- ☐ Street lights
- ☐ Telecommunication (Towers/ Repeaters etc.)

☐ **Promotion of green energy**

- ☐ Even though the economies are not attractive, invested on PV for proving pro-green.
- ☐ Demonstrate the viability and scope (publicity)
- Others________________________________

____

☐ **Income generation/saving**

- ☐ ***Non-Agricultural productive Enterprises***
  - ☐ Cottage industry (by powering small tools)
  - ☐ Commercial Sector (Telephone Shops, Restaurant, Cinema etc.)
  - ☐ Service Sector (Charging station, hiring of lamps, Power supplier, Communication services etc.)
- ☐ ***Agricultural and Animal Husbandry***
  - ☐ Irrigation
  - ☐ Aeration for Aquaculture/Fishing
  - ☐ Electric Fencing
- ☐ ***Saving from electricity bill***/Previous electricity source, pay back in ____years
  - Cost of 1 unit of replaced electricity:______Rs/unit. LCOE of 1 unit of PV electricity: _____Rs/unit
- ☐ ***Income generation through sale of electricity***
  - ☐ To Grid Rate: _____Rs/unit REC mechanism utilized: ☐ Yes ☐ No Years of PPA:____
  - ☐ Microgrid Rate: _____Rs/unit REC mechanism utilized: ☐ Yes ☐ No Years of agreement:__
- ☐ **Tax Savings**: Accelerated depreciation of assets and associated tax savings, etc.

☐ **Research**

Comments: ____

____

Filled By: Page: 2 Date:

Site No.:

SOCIO-ECONOMIC & SYSTEM LEVEL CHECKLIST (GROUP – B)

10. Constrains faced while installation/ What delayed you getting into solar?

- ☐ High capital investment and Lack of Financial Model (Credit/ Soft loans/ EMIs/ FITs, PPAs)
- ☐ Lack of knowledge about technology (didn't get information about the possibilities of application of PV)
- ☐ Poor market infrastructure and supply chain (Didn't know where to buy and what to buy, quality assurance etc.)
- ☐ Lack of legal and regulatory framework, administrative delays
- ☐ Lack of standards, codes and certification for quality control
- ☐ Lack of trained man power/consultants
- ☐ Lack of infrastructure and grid connectivity

Inverter and Battery Bank

1. **Type of system:** ☐ Off Grid ☐ Grid tied, export ☐ Grid sharing (captive) ☐ Grid dependent (Battery+Grid)
2. **Inverter Details** **ϕ:** ☐ **1** ☐ **3** **Rated kVA ______**
   Max.Load:____ _ **Tripped at ______kVA**
   ☐ Connected ☐ Indoor ☐ Adequate ventilation ☐ Outdoor ☐ Vibration and Noise ☐ Properly Earthed
   MPPT available: ☐ Yes ☐ No
   MMPT Range: _______________V ___________________A
   IP Protection: ☐ 65 ☐ 64 ☐ Not Available
3. **Operation at maximum load**: **DC Side**: _____V, _____A , ____W
   AC Side: ____V, ____A, _____W Efficiency: ___%
   P.F=_____ T.H.D: ____% Operation Temperature:_____ Nominal Temperature:_____ Array Grounding:______
4. **Condition of Battery**
   ☐ Connected Manufacturer:________ Single Unit: ____V, ____Ah Price per unit: _______ Parallel:___, Series:____
   Terminals Corroded: ☐ Yes ☐ No Terminal Lugs: ☐ Tight ☐ Loose ☐ Sulphation Observed
   Electrolyte levels above critical: ☐ Yes ☐ No ☐ NA
   Electrolyte levels equal in all cells: ☐ Yes ☐ No ☐ NA
   Difference in specific gravity of electrolyte among different cells >±0.004: ☐ Yes ☐ No ☐ NA
   How often batteries are changed:____________________
5. Module Transportation related issues
   What are the precautions done during transportation of modules?

____

____

Mode of transport: ____________________

Place from where the modules were shipped in: ____

Comments: ____

____

Filled By: Page: 3 Date:

Site No.: SOCIO-ECONOMIC & SYSTEM LEVEL CHECKLIST (GROUP – B)

System Layout Diagram

Comments: ____

Filled By: Page: 4 Date:

Site No. : SOILING & IR CHECKLIST (GROUP – C)

C1. Surroundings:

Soiling

Appearance of Glass: ☐ clean ☐ lightly soiled ☐ heavily soiled

Location of soiling: ☐ locally soiled near frame:

☐ left ☐ right ☐ top ☐ bottom ☐ all sides

☐ locally soiled on glass /bird droppings

Soiling sample taken on glass slides ☐ yes ☐ no

Cleaning interval ____

Last cleaned on (date)____

Shading

Kind of shading: ☐ Building ☐ Trees

Any reflecting surface nearby ☐ Yes ☐ No

Debris ☐ Yes ☐ No

Solar Path Finder Details Camera used:

Corner 1	Corner 2	Corner 3	Corner 4
Pic No:	Pic No:	Pic No:	Pic No:

IR Images of system

IR Image before cleaning:

IR image after cleaning:

Filed By: Page 1 Date:

Site No. : SOILING & IR CHECKLIST (GROUP – C)

C2. IR Images

IR Camera used:

<table>
<tr><th>Mod. Id.</th><th>IR Image No. & Condition</th></tr>
<tr><td>1</td><td>Backside IR Images: Special IR Images:
<table><tr><td>Open Ckt.</td><td>Short Ckt.</td></tr><tr><td></td><td></td></tr></table>Remarks:

Hot Spot (Y/N):</td></tr>
<tr><td>2</td><td>Backside IR Images: Special IR Images:
<table><tr><td>Open Ckt.</td><td>Short Ckt.</td></tr><tr><td></td><td></td></tr></table>Remarks:

Hot Spot (Y/N):</td></tr>
<tr><td>3</td><td>Backside IR Images: Special IR Images:
<table><tr><td>Open Ckt.</td><td>Short Ckt.</td></tr><tr><td></td><td></td></tr></table>Remarks:

Hot Spot (Y/N):</td></tr>
</table>

Filed By: Page 2 Date:

Site No.: VISUAL CHECKLIST (GROUP – D)

Location: ………………………………………… Lat/Long: ……………………… Altitude: ……………….

Module Details: Manufacturer: …… Model No. & Sl. No. : …… Type of Module: *Mono-cSi / Multi-cSi / Thin Film (…..)* Certification : *IEC61215 / IEC61646 / IEC61730 / UL1703* Estimated deployment date: ……. No. of Cells: …… Dimension of Cells (cm): ……. x …… Dimension of Module (cm): ………….x …………. **Ref. photo no.:** ……	**Module Name Plate Available: Y/N** Name Plate Condition: *Like New / Discolored / Torn* Voc: ……….V Isc: ……….A Vmpp: ……….V Impp: ……..A Pmax: ……..W System Voltage Limit: …….. Series Fuse Rating: …….. By-pass Diode Model & Rating: …….. Temperature coefficients: Voltage: …… Current: …… Power: … **Ref. photo no.:** ……
Backsheet Applicable: Y/N Texture: *Like New / Wavy (Delam)/ Wavy (NoDelam.) / Dented* Damage: *None / Small Localized / Extensive* Discoloration: *Like New / Major / Minor* Chalking: *None / Slight / Significant* Delaminated area (%) : *<5 / 5-25 / 25-50 / 50-75 />75%* Fraction of cracks/scratches that exposes the circuit: *<5% / 5-25% / 25-50% / 50-75% />75%* Bubbles (nos., dimension): ……, *<5mm / 5-30mm / 30mm* Fraction of area with bubbles > 5mm: *<5% / 5-25% / 25-50% / 50-75% />75%* Cracks/scratches (nos. & location): ……,*random/over cells / between cells* Cracks location: *Only Near JB / Only near Nameplate / Other* Fraction of cracks/scratches that exposes the circuit: *<5% / 5-25% / 25-50% / 50-75% />75%* Burn Marks (nos. & area): ….., *<5% / 5-25% / 25-50% / 50-75% />75%* **Ref. photo nos.:** ……	**Rear-Side Glass Applicable: Y/N** Damage: *None/ Small Localized / Extensive* Crazing (or other non-crack damage): …… Shattered (tempered/non-tempered): …… Cracks: nos. : *1 / 2 / 3 / 4-10 / >10* Cracks start from: *mod. corner / mod. edge / cell / JB / foreign object impact spot* Chips: nos. : *1 / 2 / 3 / 4-10 / >10* Chipping location: *module corner / module edge* **Ref. photo nos.:** …… **Frameless Edge Seal Applicable: Y/N** Appearance: *Like New / discolored / Visibly degraded* Discoloration area : *<5% / 5-25% / 25-50% / 50-75% / >75%* Material Problems : *Squeezed Out / signs of moisture penetration* Delamination : *Localized / widespread* Delaminated area (%) : *<5 / 5-25 / 25-50 / 50-75 />75%* **Ref. photo nos.:** ……
Frame Applicable: Y/N **(Photos:** …..) Appearance: *Like New / damaged / Missing* Damage: *Corrosion (major or minor) / Bent/ Joints separated/ Cracking* Frame Adhesive : *Not visible / Like New / Degraded / oozed out / missing in some areas*	**Frame Grounding Present: Y/N** Original State : *No ground / Wired / Resistive/ Unknown* Corrosion : *Nil / Minor / Major* Functionality: *Well Grounded / No Connection* **Ref. photo nos.:** …..
Wires: *NA / Like New / pliable but degraded / embrittled / Cracked or disintegrated insulation / burnt / corroded / animal bites /soiled* **Ref. photo nos.:** …..	**Connectors**: *NA / MC3 or MC4 / Tyco / Others* Condition: *Like New / pliable but degraded / embrittled / Cracked or disintegrated insulation / burnt / corroded / animal bites / soiled* **Ref. photo nos.:** …..

Filed by: Page 1 Date:

Site No.:

VISUAL CHECKLIST (GROUP – D)

Front Cover : Glass / Polymer / Others

Features: *Smooth / slightly textured / pyramid texture / ARC*

Damage: *None / Small Localized / Extensive*

Shattered (tempered/non-tempered): ……

Cracks: nos. : *1 / 2 / 3 / 4-10 / >10*

Cracks start from: *mod. corner / mod. edge / cell / JB*

Chips: nos. : *1 / 2 / 3 / 4-10 / >10*

Chipping location: *module corner / module edge*

Damaged Area : *<5% / 5-25% / 25-50% / 50-75% / >75%*

Fraction of area affected by Haziness / milky discoloration: *NA / <5% / 5-25% / 25-50% / 50-75% / >75%*

Ref. photo nos.: ……

Metallization :

A1: < 5%, A2: 5-25%, A3: 25-50%, A4:50-75%, A5:>75%

Fingers: *NA / Like New / Discolored (Light / Dark, ……%)*

Busbars: *NA / Like New / Discolored (Light / Dark, ……%)/ Obvious Corrosion / Diffuse Burn Marks / Misalignment*

Cell Interconnect Ribbon: *NA / Like New / Discolored (Light / Dark, ……%)/ Obvious Corrosion / Burn Marks / Breakage*

String Interconnect: *NA / Like New / Discolored (Light / Dark, ……%) / Obvious Corrosion / Burn Marks / Breakage / Arc tracks (thin burns)*

Ref. photo nos.:

Crystalline Silicon Module : Y/N

Cells in each string(nos.): ……… Strings in parallel (nos.) : ……….

Spacing : Cell to cell = ……. mm

Frame to cell (mm) = …….(top), ……. (bottom), …….(left), …….(right)

Module Discoloration: *None / Light / Dark, (……% area)*

No. of cells discoloured: ……

Discoloration Location : *Overall / Module centre / Module edges / Cell Center / Cell edges / over fingers / over busbars / over tabbing / between cells / individual cells darker than others / partial cell discoloration*

Effect in JB area: *Same as elsewhere / more / less*

Effect in Name Plate area: *Same as elsewhere / more / less*

Damage : *Burn marks / Cracks / Moisture / Snail tracks / foreign particles embedded*

Burn marks (nos.): …… Cells cracked (nos.): ……

Cells with Snail Trails (nos.): ……

Area Delaminated: *Nil / Over cells (…%), Between cells (…%), uniform / from edges / at corners / near JB / near Interconnects (cell or string)*

Ref. photo nos.: ……

Thin Film Module : Y/N

Cells in each string (nos.): ……,

Strings in parallel (nos.): ……

Distance between frame and cell : …… mm

Module Discoloration: *None / Light / Dark, (…… % area)*

Discoloration Type : *White Spots/Haze /Other*

Discoloration Location : *overall / Module centre / Module edges / Cell Center / Cell edges / near cracks*

Damage : *No / Small Localized / Extensive*

Damage Type : Burn Marks / Cracking / Moisture / Foreign particles embedded

Delamination : *None / Small Localized / Extensive*

Delamination Location: *From edges / uniform / corners/ near junction box / near busbar / along scribe lines*

Delamination Type : *Absorber delamination/ AR Coating delamination/ Other*

Ref. photo nos.: ……

Junction Box (JB) Applicable : Y/N **Ref. photo nos.:** ……

Physical state : *Intact / unsound / weathered / cracked / burnt/ warped/ output terminals corroded*

Lid : *Intact(potted) / loose / fell off / cracked*

Attachment : *Well attached / loose / fallen off*

Wire attached in JB : *Well attached / Loose / Fell off/ arced / caused fire*

Seal : *Good sealing / will Leak*

Mounting Structure Details:

Material: ……

Condition of structure: *Good / rusted / bent / broken*

Installation Site : Roof top / Ground

Tilt Angle: …… Direction of PV Panels: ……

Ref. photo nos.: ……

Filed by: Page 2 Date:

Site No.:

Dark I-V, IR & EL CHECKLIST

<table>
<tr><td rowspan="3">1</td><td colspan="3">Module Tech. & Make: ______________________ Module Id No. : __________________</td></tr>
<tr><td>Module Dark I-V File Nos.:
a) Data : ________________
b) Graph: ________________

Diode I-V File Nos.:
a) Data : ________________
b) Graph: ________________</td><td>IR Image:
a) Initial Image No.: ________
a) Bias Voltage : _________
b) Bias Current: _____________
c) IR Image File Nos.:
(i) Computer : _________
(ii) Camera : ___________</td><td>EL Image:
a) No-bias Image No.:
____
b) Bias Voltage :
____
b) Bias Current:
____
c) EL Image File Nos.:
___________________</td></tr>
<tr><td colspan="3">Remarks:</td></tr>
<tr><td rowspan="3">2</td><td colspan="3">Module Tech. & Make: ______________________ Module Id No. : __________________</td></tr>
<tr><td>Module Dark I-V File Nos.:
a) Data : ________________
b) Graph: ________________

Diode I-V File Nos.:
a) Data : ________________
b) Graph: ________________</td><td>IR Image:
a) Initial Image No.: ________
a) Bias Voltage : _________
b) Bias Current: _____________
c) IR Image File Nos.:
(i) Computer : _________
(ii) Camera : ___________</td><td>EL Image:
a) No-bias Image No.:
____
b) Bias Voltage :
____
b) Bias Current:
____
c) EL Image File Nos.:
___________________</td></tr>
<tr><td colspan="3">Remarks:</td></tr>
</table>

Comments: ____
____

Filed by:

Appendix B
Koppen-Geiger Climate Classification

While the six-climate classification of Bansal and Minke [69] is being used throughout this report for the analysis of the survey data (as discussed in Chapter 1), we have presented some of the important climate-dependent analysis in Chapter 4 also in terms of internationally accepted Koppen-Geiger climate classification system [68]. This Appendix briefly describes the Koppen-Geiger system, and also lists the climatic zone of all sites visited as per this classification.

Unlike the six-climate classification system of Bansal and Minke, which uses temperature and relative humidity as the classification criteria, the Koppen-Geiger system uses temperature and precipitation [68]. The Koppen-Geiger classification system has 5 main groups – Tropical (type A), Arid (type B), Warm Temperate (type C), Continental (type D) and Polar (type E), out of which India has the first four climates. The criteria for determining these main groups are shown in Fig. B.1. Each of these groups is further sub-divided based on temperature and annual precipitation ranges. The climatic zone map of India as per the Koppen-Geiger classification system is shown in Fig. B.2. The Koppen-Geiger system uses 2 or 3 letters to designate the climatic zone of any location, which have been described in Tables B.1 and B.2.

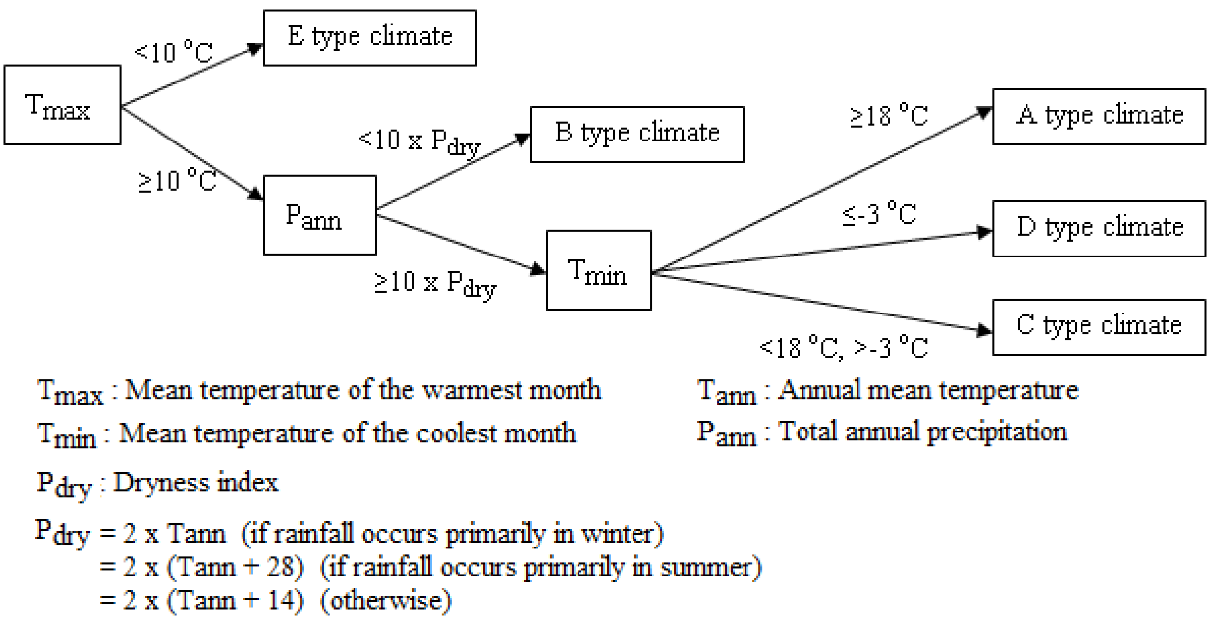

Fig. B.1: Criteria for determining the main climate types in Koppen-Geiger Climate classification system [68].

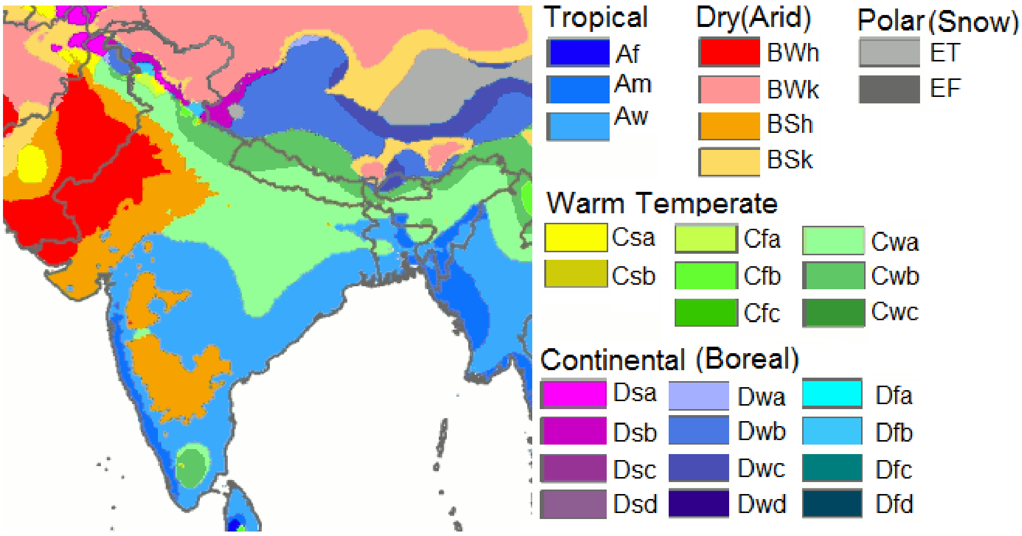

Fig. B.2: Koppen-Geiger Climate classification Map of India (based on [70])

Table B.1: Meaning of 2nd Letter in Koppen-Geiger classification [68]

Main Classes (1st Letter)	2nd Letter	Meaning
A,C,D	f	Missing dry period
	s	Dry period in summer
	w	Dry period in winter
B	S	Steppe
	W	Desert
E	T	Tundra
	F	Frost

Table B.2: Meaning of 3rd Letter in Koppen-Geiger classification [68]

Main Classes (1st Letter)	3nd Letter	Meaning
B	h	Hot
	k	Cold
C, D	a	Hot summer
	b	Warm summer
	c	Cool summer, cold winter
	d	Extremely continental

Table B.3 shows the climate classification of the survey sites according to the Bansal-Minke six-zone classification and also the Koppen-Geiger classification. As per the Koppen-Geiger classification, the survey sites can be grouped into the following categories: - (a) Tropical with dry winters, (b) Arid – hot steppe, (c) Arid – cold desert, (d) Warm temperate with hot & dry summer, (e) Warm temperate with dry winter and warm summer.

Table B.3: Climate classification of the survey sites

Survey Site Nos. (see Appendix C)	**Bansal-Minke Classification**	**Koppen-Geiger Classification**
1	Warm &Humid	Tropical – dry winter (Aw)
2, 3, 4, 5	Temperate	Tropical – dry winter (Aw)
6	Temperate	Tropical – dry winter (Aw)
7,8,9,10	Warm &Humid	Tropical – dry winter(Aw)
11	Warm &Humid	Tropical – dry winter (Aw)
12,13,14	Warm &Humid	Tropical – dry winter(Aw)
15	Warm &Humid	Tropical – dry winter(Aw)
16	Warm &Humid	Tropical – dry winter(Aw)
17	Warm &Humid	Arid – hot steppe (BSh)
18,19	Composite	Arid – hot steppe (BSh)
20	Hot & Dry	Arid – hot steppe (BSh)
21,22	Hot & Dry	Arid – hot steppe (BWh)
23,24,25	Hot & Dry	Arid – hot steppe (BSh)
26,27,28	Cold & Sunny	Arid – cold desert (BWk)
29	Cold & Cloudy	Warm Temperate – hot & dry summer (Csa)
30,31,32,33,34	Composite	Arid – hot steppe (BSh)
35	Composite	Arid – hot steppe (BSh)
36,37	Composite	Warm Temperate – hot & dry summer (Csa)
38,39,40,41,42	Warm & Humid	Tropical – dry winter(Aw)
43	Cold & Cloudy	Tropical – dry winter (Aw)
44,45	Cold & Cloudy	Warm Temperate – dry winter & warm summer (CWb)
46,47,48,49	Cold & Cloudy	Warm Temperate – hot summer (Cfa)
50,51	Cold & Cloudy	Warm Temperate – hot & dry summer (Csa)

Appendix C
Description of Sites Surveyed

DATE OF VISIT : 20th Sept. 2014

SITE NO. : 1

LOCATION : Maharashtra

CLIMATE : Warm & Humid

TYPE OF MODULES SURVEYED: Multi c-Si (22 nos.)

YEAR OF INSTALLATION: 2012

DATE OF VISIT : 22nd Sept. 2014

SITE NO. : 2

LOCATION : Karnataka

CLIMATE : Temperate

TYPE OF MODULES SURVEYED: Multi c-Si (16 nos.)

YEAR OF INSTALLATION: 2012

DATE OF VISIT : 24th Sept. 2014

SITE NO. : 3

LOCATION : Karnataka

CLIMATE : Temperate

TYPE OF MODULES SURVEYED: Mono c-Si (9 nos.), Multi c-Si (3 nos.)

YEAR OF INSTALLATION: 2002

DATE OF VISIT : 25th Sept. 2014

SITE NO. : 4

LOCATION : Karnataka

CLIMATE : Temperate

TYPE OF MODULES SURVEYED: Multi c-Si (35 nos.)

YEAR OF INSTALLATION: 2011

<table>
<tr>
<td>DATE OF VISIT : 26th Sept. 2014 SITE NO. : 5
LOCATION: Karnataka CLIMATE: Temperate

TYPE OF MODULES SURVEYED: Multi c-Si (15 nos.)
YEAR OF INSTALLATION: 2009</td>
<td>DATE OF VISIT : 27th Sept. 2014 SITE NO. : 6
LOCATION : Karnataka CLIMATE : Temperate

TYPE OF MODULES SURVEYED: Multi c-Si (41 nos.)
YEAR OF INSTALLATION: 2011</td>
</tr>
<tr>
<td>DATE OF VISIT : 28th Sept. 2014 SITE NO. : 7
LOCATION : Kerala CLIMATE: Temperate

TYPE OF MODULES SURVEYED: Multi c-Si (16 nos.)
YEAR OF INSTALLATION: 2012</td>
<td>DATE OF VISIT : 30th Sept. 2014 SITE NO. : 8
LOCATION : Kerala CLIMATE : Warm & Humid

TYPE OF MODULES SURVEYED: Multi c-Si (40 nos.)
YEAR OF INSTALLATION: 2011</td>
</tr>
</table>

DATE OF VISIT : 1st Oct. 2014

SITE NO. : 9

LOCATION: Kerala

CLIMATE: Warm & Humid

TYPE OF MODULES SURVEYED: Multi c-Si (2 nos.)

YEAR OF INSTALLATION: 2006

DATE OF VISIT : 1st Oct. 2014

SITE NO. : 10

LOCATION : Kerala

CLIMATE : Warm & Humid

TYPE OF MODULES SURVEYED: a-Si (8 nos.)

YEAR OF INSTALLATION: 2012

DATE OF VISIT : 4th Oct. 2014

SITE NO. : 11

LOCATION : Tamil Nadu

CLIMATE: Warm & Humid

TYPE OF MODULES SURVEYED (Nos.) : a-Si (36)

YEAR OF INSTALLATION: 2009

DATE OF VISIT : 6th Oct. 2014

SITE NO. : 12

LOCATION : Puducherry

CLIMATE: Warm & Humid

TYPE OF MODULES SURVEYED: Mono c-si (21), Multi c-Si (18)

YEAR OF INSTALLATION: 1994 (31 nos.), 2006 (8 nos.)

DATE OF VISIT : 7th Oct. 2014 SITE NO. : 13

LOCATION: Puducherry CLIMATE : Warm & Humid

TYPE OF MODULES SURVEYED: Mono c-Si (21)

YEAR OF INSTALLATION: 1994

DATE OF VISIT : 8th Oct. 2014 SITE NO. : 14

LOCATION: Puducherry CLIMATE : Warm & Humid

TYPE OF MODULES SURVEYED: Multi c-si (11)

YEAR OF INSTALLATION: 1996

DATE OF VISIT : 10th Oct. 2014 SITE NO. : 15

LOCATION: Tamil Nadu CLIMATE : Warm & Humid

TYPE OF MODULES SURVEYED: Multi c-Si (29 nos.)

YEAR OF INSTALLATION: 1994, 1999, 2004, 2012

DATE OF VISIT : 11th Oct. 2014 SITE NO. : 16

LOCATION: Andhra Pradesh CLIMATE : Warm & Humid

TYPE OF MODULES SURVEYED: CdTe (30 nos.), Multi c-Si (10 nos.)

YEAR OF INSTALLATION: 2010

DATE OF VISIT : 14th Oct. 2014

SITE NO. : 17

LOCATION: Andhra Pradesh

CLIMATE : Composite

TYPE OF MODULES SURVEYED: Multi c-Si (40 nos.)

YEAR OF INSTALLATION: 2013

DATE OF VISIT : 17th Oct. 2014

SITE NO. : 18

LOCATION: Maharashtra

CLIMATE : Hot & Dry

TYPE OF MODULES SURVEYED: Multi c-Si (20 nos.)

YEAR OF INSTALLATION: 2012

DATE OF VISIT : 17th Oct. 2014

SITE NO. : 19

LOCATION: Maharashtra

CLIMATE : Hot & Dry

TYPE OF MODULES SURVEYED: Mono c-Si (10 nos.)

YEAR OF INSTALLATION: 2009

DATE OF VISIT : 19th Oct. 2014

SITE NO. : 20

LOCATION: Gujarat

CLIMATE : Hot & Dry

TYPE OF MODULES SURVEYED: Multi c-Si (44 nos.)

YEAR OF INSTALLATION: 2012

DATE OF VISIT : 21st Oct. 2014 SITE NO. : 21

LOCATION: Rajasthan CLIMATE : Hot & Dry

TYPE OF MODULES SURVEYED: a-Si (12 nos.)

YEAR OF INSTALLATION: 2010

DATE OF VISIT : 22nd Oct. 2014 SITE NO. : 22

LOCATION: Rajasthan CLIMATE : Hot & Dry

TYPE OF MODULES SURVEYED: CdTe (40 nos.)

YEAR OF INSTALLATION: 2012

DATE OF VISIT : 24th Oct. 2014 SITE NO. : 23

LOCATION: Rajasthan CLIMATE : Hot & Dry

TYPE OF MODULES SURVEYED: Multi c-Si (32)

YEAR OF INSTALLATION: 1987

DATE OF VISIT : 25th Oct. 2014 SITE NO. : 24

LOCATION: Rajasthan CLIMATE : Hot & Dry

TYPE OF MODULES SURVEYED: Mono c-Si (26)

YEAR OF INSTALLATION: 1989

DATE OF VISIT : 26th Oct. 2014 SITE NO. : 25

LOCATION: Rajasthan CLIMATE : Hot & Dry

TYPE OF MODULES SURVEYED: Mono c-Si (10 nos.)

YEAR OF INSTALLATION: 1999

DATE OF VISIT : 28th Oct. 2014 SITE NO. : 26

LOCATION: Ladakh CLIMATE : Cold & Sunny

TYPE OF MODULES SURVEYED: Mono c-Si (20 nos.)

YEAR OF INSTALLATION: 1998

DATE OF VISIT : 30th Oct. 2014 SITE NO. : 27

LOCATION: Ladakh CLIMATE : Cold & Sunny

TYPE OF MODULES SURVEYED Multi c-Si (30 nos.)

YEAR OF INSTALLATION: 2012

DATE OF VISIT : 31st Oct. 2014 SITE NO. : 28

LOCATION: Ladakh CLIMATE : Cold & Sunny

TYPE OF MODULES SURVEYED Mono c-Si (5 nos.)

YEAR OF INSTALLATION: 1997

DATE OF VISIT: 4th Nov. 2014 SITE NO. : 29

LOCATION: Jammu & Kashmir CLIMATE : Cold & Cloudy

TYPE OF MODULES SURVEYED:

Multi c-Si (1 nos.)

YEAR OF INSTALLATION: 2009

DATE OF VISIT : 6th Nov. 2014 SITE NO. : 30

LOCATION: Haryana CLIMATE : Composite

TYPE OF MODULES SURVEYED:

Mono c-Si (43 nos.)

YEAR OF INSTALLATION: 1998

DATE OF VISIT : 7th Nov. 2014 SITE NO. : 31

LOCATION: Haryana CLIMATE : Composite

TYPE OF MODULES SURVEYED: Mono c-Si (64 nos.)

YEAR OF INSTALLATION: 1998

DATE OF VISIT : 9th Nov. 2014 SITE NO. : 32

LOCATION: Haryana CLIMATE : Composite

TYPE OF MODULES SURVEYED:

CIGS (19 nos.)

YEAR OF INSTALLATION: 2012

DATE OF VISIT : 9th Nov. 2014 SITE NO. : 33

LOCATION: Haryana CLIMATE : Composite

TYPE OF MODULES SURVEYED: HIT (12 nos.)

YEAR OF INSTALLATION: 2008

DATE OF VISIT : 10th Nov. 2014 SITE NO. : 34

LOCATION: Haryana CLIMATE : Composite

TYPE OF MODULES SURVEYED: Mono c-Si (50 nos.)

YEAR OF INSTALLATION: 1995

DATE OF VISIT : 11th Nov. 2014 SITE NO. : 35

LOCATION: Uttar Pradesh CLIMATE : Composite

TYPE OF MODULES SURVEYED: Multi c-Si (40 nos.)

YEAR OF INSTALLATION: 2010

DATE OF VISIT : 14th Nov. 2014 SITE NO. : 36

LOCATION: Bihar CLIMATE : Composite

TYPE OF MODULES SURVEYED: Multi c-Si (19 nos.)

YEAR OF INSTALLATION: 2010

DATE OF VISIT : 15th Nov. 2014 SITE NO. : 37

LOCATION: Bihar CLIMATE : Composite

TYPE OF MODULES SURVEYED: Multi c-Si (21 nos.)

YEAR OF INSTALLATION: 2010

DATE OF VISIT : 19th Nov. 2014 SITE NO. : 38

LOCATION: West Bengal CLIMATE : Warm & Humid

TYPE OF MODULES SURVEYED: Mono c-Si (40 nos.)

YEAR OF INSTALLATION: 2005

DATE OF VISIT : 20th Nov. 2014 SITE NO. : 39

LOCATION: West Bengal CLIMATE : Warm & Humid

TYPE OF MODULES SURVEYED: Mono c-Si (41 nos.)

YEAR OF INSTALLATION: 1994

DATE OF VISIT : 20th Nov. 2014 SITE NO. : 40

LOCATION: West Bengal CLIMATE : Warm & Humid

TYPE OF MODULES SURVEYED: Mono c-Si (2 nos.)

YEAR OF INSTALLATION: 2010

DATE OF VISIT : 21st Nov. 2014 SITE NO. : 41

LOCATION: West Bengal CLIMATE : Warm & Humid

TYPE OF MODULES SURVEYED: Multi c-Si (10 nos.)

YEAR OF INSTALLATION: 2011

DATE OF VISIT : 21st Nov. 2014 SITE NO. : 42

LOCATION: West Bengal CLIMATE :Warm & Humid

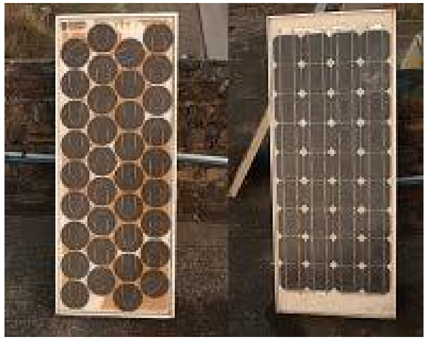

TYPE OF MODULES SURVEYED: Mono c-Si (2 nos.)

YEAR OF INSTALLATION: 1995

DATE OF VISIT : 10th Dec. 2014 SITE NO. : 43

LOCATION: Tamil Nadu CLIMATE : Cold & Cloudy

TYPE OF MODULES SURVEYED: Mono c-Si (5 nos.)

YEAR OF INSTALLATION: 2004

DATE OF VISIT: 13th Dec . 2014 SITE NO. : 44

LOCATION: Tamil Nadu CLIMATE : Cold & Cloudy

TYPE OF MODULES SURVEYED: Multi c-Si (24 nos.)

YEAR OF INSTALLATION: 2010

DATE OF VISIT : 14th Dec. 2014 SITE NO. : 45

LOCATION: Tamil Nadu CLIMATE : Cold & Cloudy

TYPE OF MODULES SURVEYED: Multi c-Si (20 nos.)

YEAR OF INSTALLATION: 2010

DATE OF VISIT : 21 Sept. 2015 SITE NO. : 46

LOCATION: Himachal Pradesh CLIMATE : Cold & Cloudy

TYPE OF MODULES SURVEYED: Multi c-Si (16 nos.)

YEAR OF INSTALLATION: 2013

DATE OF VISIT : 21 Sept. 2015 SITE NO. : 47

LOCATION: Himachal Pradesh CLIMATE : Cold & Cloudy

TYPE OF MODULES SURVEYED: Multi c-Si (4)

YEAR OF INSTALLATION: 2015

DATE OF VISIT : 24 Sept. 2015 SITE NO. : 48

LOCATION: Himachal Pradesh CLIMATE : Cold & Cloudy

TYPE OF MODULES SURVEYED: Multi c-Si (8)

YEAR OF INSTALLATION: 2015

DATE OF VISIT : 24 Sept. 2015 SITE NO. : 49

LOCATION: Himachal Pradesh CLIMATE : Cold & Cloudy

TYPE OF MODULES SURVEYED:
Multi c-Si (8 nos.)

YEAR OF INSTALLATION:
2015

DATE OF VISIT : 25 Sept. 2015 SITE NO. : 50

LOCATION: Himachal Pradesh CLIMATE : Cold & Cloudy

TYPE OF MODULES SURVEYED:
Multi c-Si (16 nos.)

YEAR OF INSTALLATION:
2013

DATE OF VISIT : 26 Sept. 2015 SITE NO. : 51

LOCATION: Himachal Pradesh CLIMATE : Cold & Cloudy

TYPE OF MODULES SURVEYED:
Multi c-Si (16 nos.)

YEAR OF INSTALLATION:
2013

Appendix D
Analysis of Correction Procedure 1a

In order to understand the level of accuracy of Correction Procedure 1a, we performed the following experiment. We measured the characteristics of a crystalline silicon module at STC condition on the Spire Solar Simulator Model 5600 SPL Blue in the laboratory IIT Bombay. This module was then taken outdoors and allowed to heat up in the sun. When the temperature of the module reached around 60°C, it was quickly brought back inside the laboratory. Since the laboratory temperature was set at 25°C, the module temperature started decreasing, and its *I-V* was taken at regular intervals on the Spire till the module reached room temperature. The simulator was set such that it could take *I-V* data at three different irradiance levels (1000 W/m^2, 800 W/m^2 and 600 W/m^2) in a single flash. The temperature coefficients of current (α) and voltage (β) were calculated by taking the slope of I_{sc} with temperature and V_{oc} with temperature respectively. The values of R_s and k were calculated as per the procedure described in IEC 60891 (since we had available three *I-V* curves at constant temperature but different irradiances and three *I-V* curves at constant irradiance but different temperatures). Then an *I-V* data set measured at 800 W/m^{2}and 47°C was translated to STC using four different parameter combinations: (a) using only α and β measured experimentally (R_s and k set to 0), (b) using only α and β obtained from literature (R_s and k set to 0), (c) using α, β and R_s measured experimentally (k set to 0) and (d) using α, β, R_s and k measured experimentally. Different *I-V* parameters such as P_{max}, V_{oc}, I_{sc} and *FF* were calculated. These data for one module are compared in Table D.1. It can be seen that not much error – about 1.5% in P_{max} – is made by using only α and β obtained from literature (i.e., Correction Procedure 1a).

Table D.1: Comparison of P_{max}, V_{oc}, I_{sc} and *FF* translated to STC using different parameters

Parameter	**STC Values measured directly on Spire**	**Translated from 800 W/m^2 and 47°C to STC using**			
		α, β (measured)	**α, β (from literature)**	**α, β & R (measured)**	**α, β, R, & k (measured)**
V_{oc} (Volts)	44.2	44.6	44.94	43.96	44.05
I_{sc} (Amp)	5.2	5.17	5.19	5.18	5.17
P_{max} (Watts)	170.1	171.2	172.7	167.6	169.6
***FF* (%)**	74.0	73.9	74.02	73.6	74.3

Similar data were taken on four other modules, and the full *I-V* curves are shown in Fig. D.1 for all 5 modules. From the figure we can see that the Spire-measured STC *I-V* data and the translated *I-V* data (measured at 800 W/m^{2}and 47°C) using only α and β obtained from literature (i.e., using Procedure 1a) match very well, and the RMS error is between 1.4% and 5.4%.

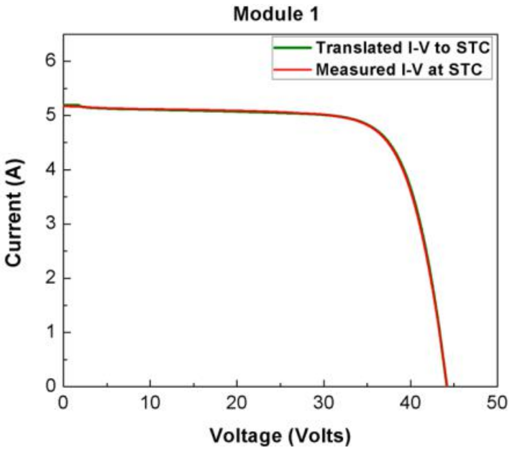

Error: 1.4%

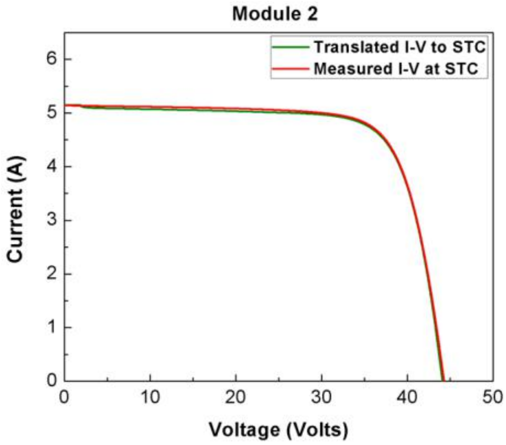

Error: 3.1%

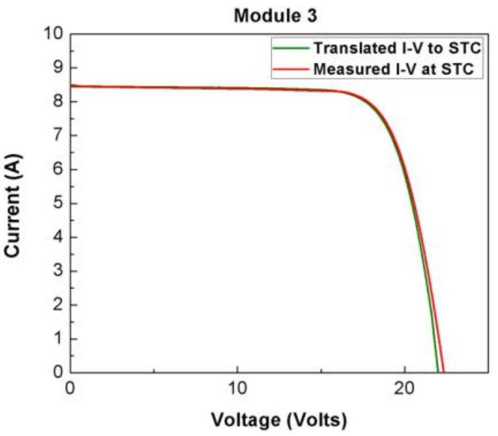

Error: 5.4%

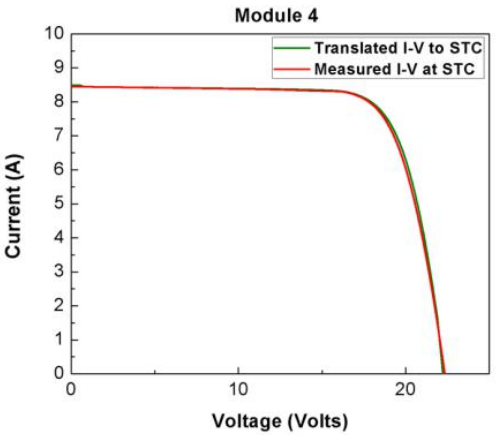

Error: 3.6%

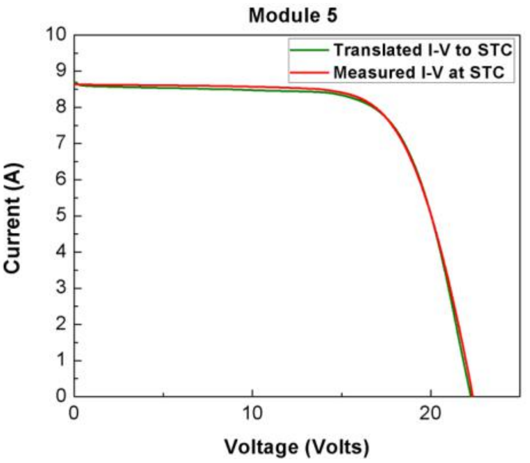

Error: 3.8%

Fig. D.1: Comparison of R.M.S error for the measured *I-V* data at STC and translated *I-V* using only α, β obtained from literature.

Appendix E
Error Analysis for Low Irradiance Correction

In order to estimate the error in translating *I-V* data measured at as low as 500 W/m^2 to STC using Correction Procedure 1a, we measured the *I-V* data of a crystalline silicon module on the Spire Solar Simulator Model 5600 SPL Blue at different values of irradiance ranging from 500 to 1000 W/m^2 and temperature ranging from 25°C to 70°C. These *I-V* data were then corrected to STC by using Correction Procedure 1a. Table E.1 shows the P_{max} value when translated to STC from the given set of irradiance and temperature for a crystalline silicon module. Table E.2 shows the percent error associated with P_{max} (error is estimated with respect to the P_{max} at STC) when translated to STC from the given set of irradiance and temperature. Table E.3 shows the number of surveyed modules which fall in different categories of irradiance and temperature. Using Table E.2 and Table E.3 we obtained a modified error Table E.4. The shaded region in this Table means that we do not have any field *I-V* data in these categories. Hence from Table E.4 we can conclude that the error in translation (using Procedure 1a) from irradiance of 500 W/m^2 or above is within 5% for crystalline silicon modules. This experiment was further repeated for 4 more modules and similar results were obtained. This important experiment and conclusion allows us to use data obtained at irradiance levels above 500 W/m^2 with reasonable accuracy. However, the errors in translation of the actual field data may be marginally higher than the 5% value mentioned above, since the spectral changes associated with overcast (low irradiance) conditions could not be simulated in our controlled laboratory experiment.

Table E.1: P_{max} value at STC obtained by translating using Procedure 1a

P_{max} (Watts)	Temperature (Deg. C)									
Irradiance (W/m^2)	**25**	**30**	**35**	**40**	**45**	**50**	**55**	**60**	**65**	**70**
500	150.43	149.74	149.64	149.72	150.11	150.42	150.86	151.12	151.59	152.32
550	149.70	148.97	148.83	148.87	149.20	149.47	149.89	150.11	150.56	151.25
600	149.12	148.37	148.18	148.24	148.49	148.67	149.06	149.25	149.67	150.31
650	148.25	147.58	146.38	146.08	145.81	145.68	145.55	145.36	145.17	145.03
700	147.59	146.92	145.69	145.32	144.99	144.86	144.67	144.45	144.21	144.05
750	147.01	146.29	144.99	144.56	144.22	144.01	143.80	143.54	143.26	143.08
800	146.27	145.51	145.21	145.16	145.30	145.53	145.62	145.71	145.26	145.66
850	145.62	144.86	144.45	144.38	144.53	144.68	144.73	144.77	144.32	144.39
900	145.06	144.24	143.81	143.71	143.77	143.91	143.92	143.92	143.40	143.41
950	144.35	143.28	142.46	142.03	141.57	141.41	140.94	140.27	139.89	139.65
1000	143.82	142.96	141.80	141.30	140.80	140.59	140.09	139.38	138.99	138.67

Table E.2: Percent error in P_{max} value at STC obtained by translating using Procedure 1a

ΔP_{max} (%)	**Temperature (Deg. C)**									
Irradiance (W/m^2)	**25**	**30**	**35**	**40**	**45**	**50**	**55**	**60**	**65**	**70**
500	4.59	4.12	4.05	4.10	4.37	4.59	4.90	5.08	5.41	5.91
550	4.09	3.58	3.48	3.51	3.74	3.93	4.22	4.37	4.69	5.17
600	3.69	3.17	3.03	3.07	3.25	3.37	3.65	3.78	4.07	4.51
650	3.08	2.61	1.78	1.57	1.38	1.29	1.20	1.07	0.94	0.84
700	2.62	2.16	1.30	1.04	0.82	0.72	0.60	0.44	0.27	0.16
750	2.22	1.72	0.82	0.52	0.28	0.13	-0.01	-0.19	-0.39	-0.51
800	1.70	1.18	0.96	0.94	1.03	1.19	1.25	1.32	1.00	1.28
850	1.25	0.72	0.44	0.39	0.49	0.60	0.63	0.66	0.35	0.40
900	0.86	0.29	0.00	-0.07	-0.03	0.07	0.07	0.07	-0.29	-0.28
950	0.37	-0.37	-0.94	-1.24	-1.56	-1.67	-2.00	-2.47	-2.73	-2.90
1000	0.00	-0.60	-1.40	-1.75	-2.10	-2.24	-2.59	-3.08	-3.36	-3.58

Table E.3: Number of surveyed modules in different categories of irradiance and temperature

# of Modules	**Temperature Range (Deg. C)**								
Irradiance (W/m^2)	**25 – 30**	**30 – 35**	**35 – 40**	**40 – 45**	**45 – 50**	**50 – 55**	**55 – 60**	**60 – 65**	**65 – 70**
500 – 550	2	16	7	17	13	4	0	0	0
550 – 600	0	2	4	22	14	13	0	0	0
600 – 650	0	1	6	26	34	13	0	0	0
650 – 700	1	4	3	14	30	8	1	1	0
700 – 750	2	0	4	16	20	12	3	3	2
750 – 800	0	1	4	14	32	19	4	3	6
800 – 850	0	3	1	7	25	22	23	8	1
850 – 900	0	0	1	8	25	25	37	21	0
900 – 950	0	0	3	8	10	21	47	66	8
950 – 1000	0	4	19	39	47	42	30	28	8

Table E.4: Percent error in P_{max} value at STC obtained by translating using Procedure 1a for actually surveyed modules (shaded boxes indicate that such field conditions were not encountered)

ΔP_{max} (%)	**Temperature (Deg. C)**									
Irradiance (W/m^2)	**25**	**30**	**35**	**40**	**45**	**50**	**55**	**60**	**65**	**70**
500	4.59	4.12	4.05	4.10	4.37	4.59	4.90	5.08	5.41	5.91
550	4.09	3.58	3.48	3.51	3.74	3.93	4.22	4.37	4.69	5.17
600	3.69	3.17	3.03	3.07	3.25	3.37	3.65	3.78	4.07	4.51
650	3.08	2.61	1.78	1.57	1.38	1.29	1.20	1.07	0.94	0.84
700	2.62	2.16	1.30	1.04	0.82	0.72	0.60	0.44	0.27	0.16
750	2.22	1.72	0.82	0.52	0.28	0.13	-0.01	-0.19	-0.39	-0.51
800	1.70	1.18	0.96	0.94	1.03	1.19	1.25	1.32	1.00	1.28
850	1.25	0.72	0.44	0.39	0.49	0.60	0.63	0.66	0.35	0.40
900	0.86	0.29	0.00	-0.07	-0.03	0.07	0.07	0.07	-0.29	-0.28
950	0.37	-0.37	-0.94	-1.24	-1.56	-1.67	-2.00	-2.47	-2.73	-2.90
1000	0.00	-0.60	-1.40	-1.75	-2.10	-2.24	-2.59	-3.08	-3.36	-3.58

Appendix F
Instrument Error Analysis

In order to calculate the errors caused by the instrument on the *I-V* parameters at STC we performed the following analysis. From the equations used for Correction Procedure 1a (reproduced below as Eqs. (F.1) and (F.2)), we can conclude from Eq. (F.1) that the maximum positive deviation in the translated current at STC (I_2) is obtained if there is maximum positive deviation in current measurement (I_1, I_{sc}), maximum negative deviation in irradiance measurement (G_1) and maximum negative deviation in temperature (T_1) measurement.

$$I_2 = I_1 + I_{sc} * \left(\frac{1000}{G_1} - 1\right) + \propto * (25 - T_1) \qquad \text{.... (F.1)}$$

Similarly, maximum positive deviation in voltage at STC (V_2) occurs if there is maximum positive deviation in voltage measurement (V_1) and maximum positive deviation in temperature (T_1) measurement (refer Eq. F.2, and note that β is negative).

$$V_2 = V_1 + \beta * 25 - \beta * T_1 \qquad \text{.... (F.2)}$$

The instrument error for temperature measurement is ±2°C. If we consider the maximum negative deviation of temperature (–2°C), then the maximum P_{max} error will be 2.81% but if we consider the maximum positive deviation of temperature (+2°C), then the maximum P_{max} error will be 3.81%. Considering all possible combinations of measurement error in voltage, current, irradiance, and temperature, the maximum possible error caused by the instrument in the P_{max} value at STC is shown in Table F.1 for different combinations of irradiance and temperature. The shaded boxes in the table again means that we do not have any field *I-V* data in these categories (refer Appendix E). Hence the maximum error caused by the instrument is 4.05%.

Table F.1: P_{max} Error caused by the instrument on P_{max} at STC

Error (%)	Temperature (Deg. C)									
Irradiance (W/m^2)	25	30	35	40	45	50	55	60	65	70
500	4.05	4.05	4.04	4.03	4.01	4.00	3.99	3.97	3.96	3.93
550	4.05	4.05	4.03	4.03	3.97	3.95	3.94	3.91	3.90	3.88
600	4.05	4.05	4.04	4.03	3.97	3.95	3.94	3.92	3.91	3.88
650	4.05	4.05	4.01	3.99	3.97	3.95	3.93	3.92	3.90	3.89
700	4.04	4.04	4.01	3.99	3.97	3.95	3.93	3.92	3.91	3.89
750	4.04	4.05	4.00	3.99	3.97	3.95	3.93	3.92	3.90	3.89
800	4.04	4.04	3.99	3.97	3.96	3.94	3.92	3.91	3.89	3.88
850	4.04	4.04	4.00	3.98	3.96	3.94	3.93	3.91	3.90	3.89
900	4.03	4.03	4.00	3.98	3.97	3.95	3.93	3.92	3.91	3.89
950	4.03	4.03	4.01	3.99	3.98	3.96	3.95	3.94	3.93	3.88
1000	4.03	4.03	4.00	3.99	3.98	3.96	3.95	3.94	3.93	3.92

Appendix G
Outliers

G.1 Introduction

From the analysis of the survey data, it has been found that about 200 modules, all of which belong to the small/medium installations, show power degradation rate above 6%/year, which is very high as compared to the warrantees given by module manufacturers. This Appendix deals with these 'outliers'. All the modules in the Outlier category are young modules, which have been in the field for less than 5 years, as evident from Fig. G.1. This fact raises concerns regarding the quality and nameplate rating of the modules, and installation practices, in the small/medium sites. In six sites, we found that the PV system has been installed more than a year ago but not connected to any load, and most of the modules in these sites fall in the Outlier category, showing very high degradation rates. This suggests carelessness of the system installer and/or the site owner, and it is possible that poor quality modules were selected by the installer. A deliberate 'over-rating' of the modules (that is, the actual power rating being significantly less than the nameplate value) is also possible in some cases.

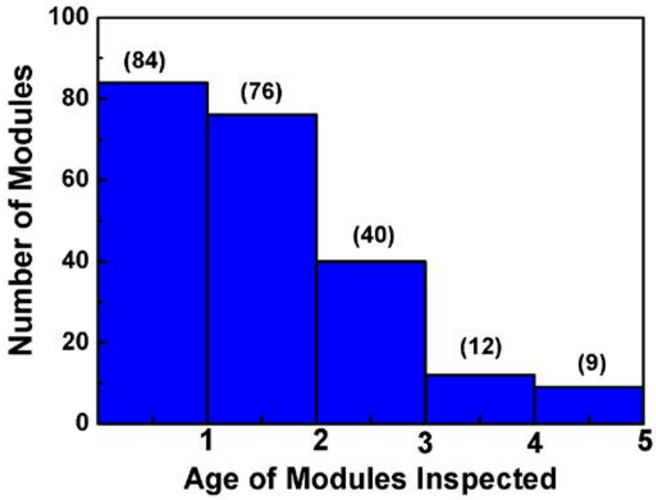

Fig. G.1: Age distribution of the Outlier modules

G.2 Electrical Degradation

The histogram of the P_{max} degradation rates for the Outlier modules is shown in Fig. G.2 and the degradation rates for various climatic zones are shown in Fig. G.3. The average degradation rate for these modules is 9.36%/year. The modules in the Hot zone are degrading at a slightly higher rate than modules in the Non-Hot zone, though climatic conditions do not seem to be the primary cause behind the high degradation rates. For some of the modules with degradation rate above 10%/year (mainly in the small sites), there is a suspicion that these modules have been over-rated.

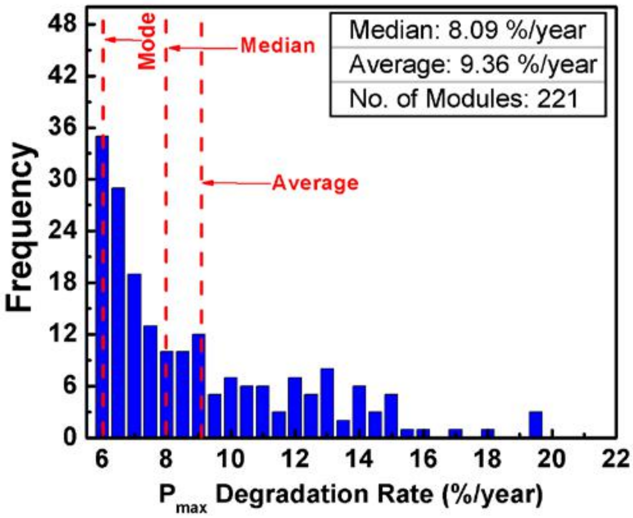

Fig. G.2: Histogram of P_{max} degradation rates of the modules in Outlier category

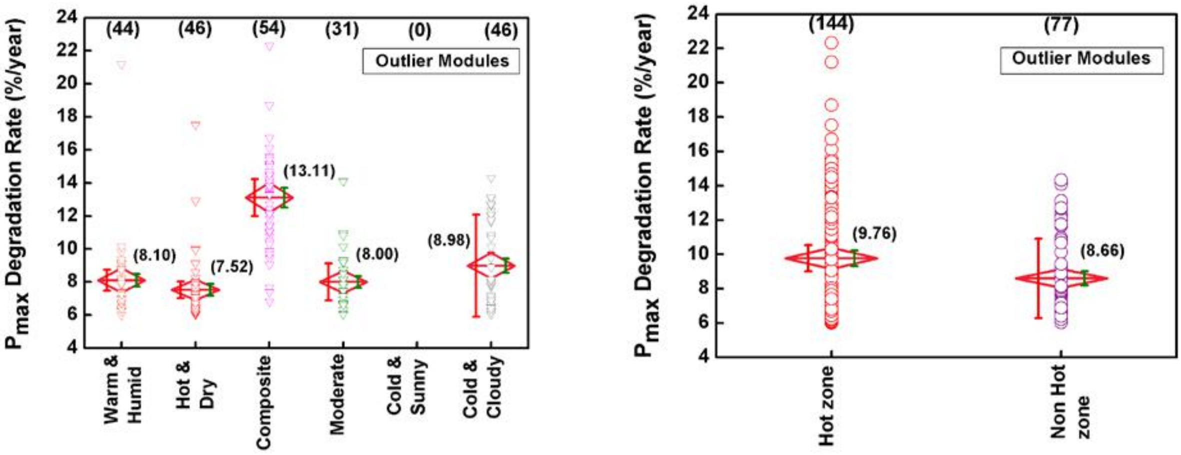

(a) (b)

Fig. G.3: Effect of climatic zone on P_{max} degradation rate of the Outlier modules – (a) as per six-zone classification (b) climatic zones clubbed into Hot and Non-Hot zones

G.3 Visual Degradation and Correlation to Electrical Degradation

The outliers are young modules which have been in the field for less than 5 years, and show very minor visual degradation. Table G.1 shows the percentage of the modules in the Outlier category which show some visual degradation. In some of these modules, discoloration has been observed in the front sticker, which is not considered relevant since the sticker is outside of the active cell area. Only the discoloration above the active cell area has been considered for our analysis. It also shows the average power degradation rate for modules with and without the specified visual degradation. From the data, it is evident that in most cases the visually unaffected modules have as high as or higher power degradation rate than the affected modules. Hence it is clear that visible degradation is not the underlying cause for the poor performance of these modules. This is in contrast to the modules described in the main body of the report, where we have been able to correlate, in many cases, visual degradation and electrical degradation rates.

Table G.1: Percentage of Outlier modules affected by various visual degradation modes and correlation to power degradation rate

Type of Visual Degradation	Percentage of Outlier modules affected	Power degradation rate for affected Outlier modules (%/year)	Power degradation rate for un-affected Outlier modules (%/year)
Encapsulant Discoloration	1 %	7.4	10.2
Delamination	6 %	10.1	9.3
Snail Tracks	29 %	7.3	9.7
Discoloration on Metallization	23 %	9.45	9.47
Backsheet Damage	21 %	8.5	9.6

G.4 IR thermography and Correlation with Electrical Degradation

From the IR images, using the criteria set in Chapter 7 for hot cells, it has been found that 56% of the Outlier modules showed hot cells. The average power degradation rate for the modules with hot cells and without hot cells is very close (9%/year and 9.5%/year). In some of these modules, we suspect that potential induced degradation is the primary cause behind the high degradation in power output. In the IR images of PID affected modules, usually the cells towards the edge of the module show hotter cells than the cells in the centre [44]. Fig. G.4 shows some IR images for Outlier modules at a particular site, which hints at PID in these modules.

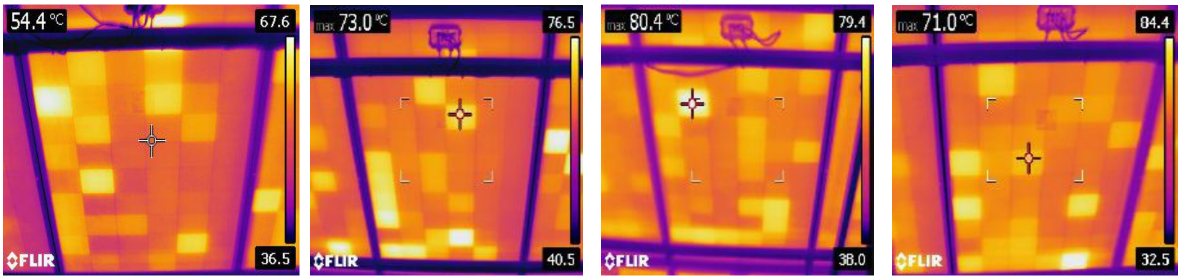

Fig. G.4: IR images of some Outlier modules in which PID is suspected.

G.5 Summary

A significant number of modules in the small/medium sites have shown degradation rates in excess of 6%/year. The exact causes for such high degradation cannot be ascertained without more detailed studies on these specific modules. Some of the possible reasons poor quality of modules, over-rating of modules (resulting in high apparent if not actual degradation rates), and PID. It would be advisable to analyze such modules and their antecedents in detail, as many modules are likely to be installed in small/medium sites as a part of India's 40 GW rooftop target.

Appendix H
Dark *I-V* Parameter Extraction Methodology

In order to calculate the dark *I-V* parameters of the module, we converted the dark *I-V* of the module into the dark *I-V* of an equivalent solar cell by dividing the voltage (at each *I-V* data point) by the number of (series) cells in the module. Figure H.1 graphically demonstrates the concept of dark *I-V* of the equivalent cell. It should be noted that the module's cell-to-cell interconnect resistance gets subsumed into an equivalent solar cell series resistance.

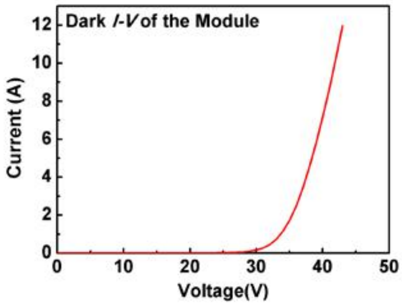

(a)

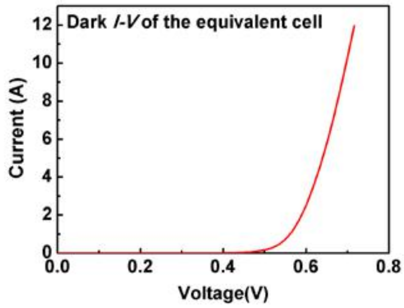

(b)

Fig. H.1: (a) Measured dark *I-V* of the module and, (b) dark *I-V* of an equivalent cell obtained by dividing the module *I-V* voltages by number of cells (here 60).

The ideality factor n of the equivalent solar cell diode is calculated from the slope obtained by drawing a tangent at the maximum power point voltage V_{mp}, (as shown in Fig. H.2). Figure H.3 shows an expanded version, with the slope calculated as 39.13 V^{-1}, and the intercept on the y-axis (at $V = 0$) as − 21.57. These values yield $n = 0.99$ (T is taken as 300K), and the diode leakage current $I_o = 4.3 \times 10^{-10}$ A.

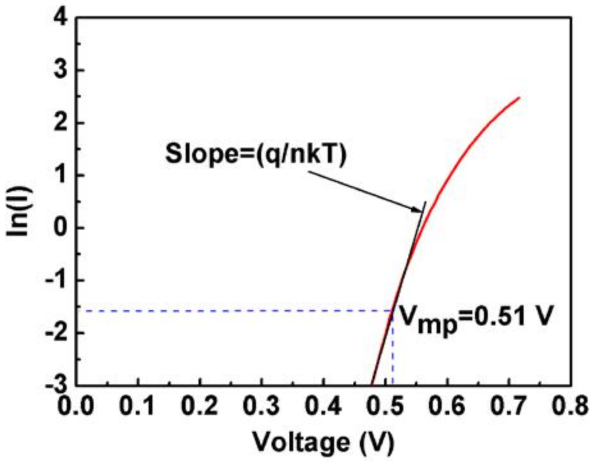

Fig. H.2: ln (I) vs. Voltage V plot, showing also the tangent at V_{mp}, from which n can be found.

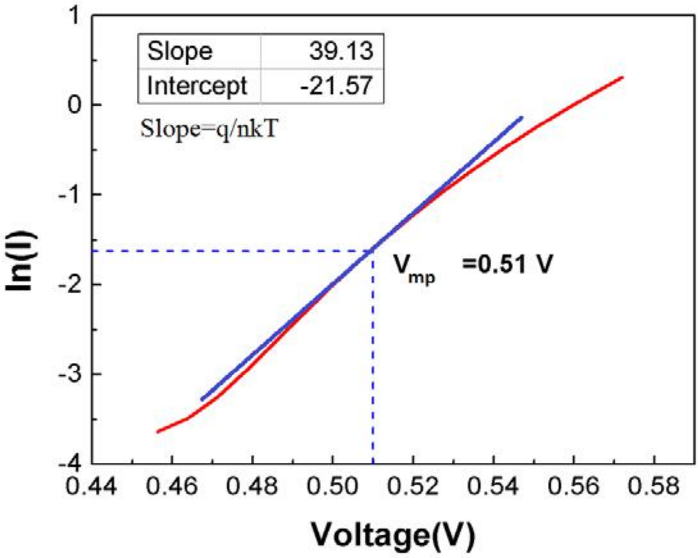

Fig. H.3: Enlarged plot of ln (I) vs. Voltage around V_{mp}, also showing the tangent at V_{mp}, from which n and I_o can be calculated.